USED FUEL DISPOSITION CAMPAIGN

Engineered Materials Performance: Gap Analysis and Status of Existing Work

Fuel Cycle Research & Development

Prepared for
U.S. Department of Energy
Used Fuel Disposition Program
Charles R. Bryan, David G. Enos, Larry Brush,
Andy Miller, and Kirsten Norman, SNL
Neil R. Brown, LLNL
October 27, 2011
FCRD-USED-2011-000407
SAND 2011-7896P

Appendix E
FCT Document Cover Sheet

Name/Title of Deliverable/Milestone	Engineered Materials Performance: Gap Analysis and Status of Existing Work
Work Package Title and Number	Engineered Materials Performance - FT-12SN080506
Work Package WBS Number	1.02.08.03 Milestone Number M3FT-12SN0805065

Responsible Work Package Manager

Charles R. Bryan / _Charles R. Bryan_   10/27/11

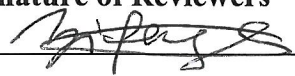(Name/Signature)   (Date Submitted)

Quality Rigor Level for Deliverable/Milestone	☒ QRL-3	☐ QRL-2	☐ QRL-1 ☐ Nuclear Data	☐ N/A*

This deliverable was prepared in accordance with   Sandia National Laboratories
_____
                                                  (Participant/National Laboratory Name)

QA program which meets the requirements of

☐ DOE Order 414.1   ☐ NQA-1-2000   ☒ Other: FCT QAPD

This Deliverable was subjected to:

☒ Technical Review   ☐ Peer Review

Technical Review (TR)	**Peer Review (PR)**
Review Documentation Provided	**Review Documentation Provided**
☐ Signed TR Report, or	☐ Signed PR Report, or
TR Report No.: _____	PR Report No.: _____
☐ Signed TR Concurrence Sheet (attached), or	☐ Signed PR Concurrence Sheet (attached), or
☒ Signature of TR Reviewer(s) below	☐ Signature of PR Reviewers below

Name and Signature of Reviewers

Yifeng Wang _[signature]_   10-27-2011

_____   _____

(Name/Signature)   (Date)

*Note: In some cases there may be a milestone where an item is being fabricated, maintenance is being performed on a facility, or a document is being issued through a formal document control process where it specifically calls out a formal review of the document. In these cases, documentation (e.g., inspection report, maintenance request, work planning package documentation, or the documented review of the issued document through the document control process) of the completion of the activity along with the Document Cover Sheet is sufficient to demonstrate achieving the milestone. QRL for such milestones may also be marked N/A in the work package provided the work package clearly specifies the requirement to use the Document Cover Sheet and provide supporting documentation.

FCRD-TIO-2011-000050, Rev. 0

SUMMARY

It is the task of the Engineered Materials Performance work package to evaluate the long-term performance of materials used to isolate high level waste and spent nuclear fuel for long-term interim storage or permanent disposal. This report provides a literature survey and gap analysis that identify research needs required to increase the state of knowledge of materials performance in repository and storage environments. Engineered materials in the repository and storage settings include the waste package and waste package internals, but also include other drift components, such as ground support and invert materials, backfill and buffer materials, overpacks, cement bunkers, and any other manmade components of, or within, the emplacement drifts or interim storage bunkers. Although all of these materials fall within the scope of the Engineered Materials Performance work package, the work package focuses on waste packages and interim storage canisters, and considers other components only in the ways that they impact the performance of the package. Other Used Fuel Disposition (UFD) program work packages (Engineered Barrier System, Storage, and Waste Form) are evaluating other aspects of the engineered systems.

Potential disposal options that are considered include mined repositories in granite, shale or clay, and salt, and deep borehole disposal in crystalline rock. For each of these disposal options, and for interim storage options, this report provides a summary of the general characteristics of the chemical and physical environment, a description of the current repository concepts that are being considered, and a description of the relevant corrosion work that has been carried out in those environments. Then it identifies additional research needs and ranks them by relative importance. Those which can be addressed by the Engineered Materials Performance work package, with the available resources, are identified. This gap analysis is used to develop a preliminary test plan for future work, which is provided in Appendix A of this report (a final test plan is an FY12 milestone, due January 31, 2012).

This analysis assumes that the physical/chemical conditions encountered and the waste package materials chosen will reflect current repository and storage concepts around the world, and it evaluates research needs in the context of those existing repository programs. For repositories in host rocks that constitute a robust natural barrier to radionuclide releases (e.g., clay and salt), it is assumed that waste packages will be made of a corrosion allowance material. Carbon steel is the consensus choice for clay-based repositories, and waste package lifetimes are only required to be on the order of 1,000-10,000 years. For repository programs in host rocks with a less robust natural barrier, which place a greater reliance on the waste package as a barrier (saturated and unsaturated crystalline rock repositories), the waste package is made of corrosion resistant materials. Copper is the consensus choice for saturated, reducing repositories, while Alloy 22 and Titanium Grade 7 were the choices for Yucca Mountain, a vadose-zone repository considered for spent nuclear fuel and high level waste. For interim storage, stainless steels are the container material of choice. The gap analysis limits its evaluation to additional data needs for understanding the behavior of these materials in the relevant environments.

The final part of the report provides the status of existing experimental work at Sandia. This work, originally started under the Yucca Mountain Project, consists of two sets of experiments. The first set evaluates corrosion of Alloy 22, a Ni-Cr-W-Mo alloy, under immersed conditions in three different brines. This set of experiments is a two-year effort which will be completed in FY12. A final report will be provided by June 30, 2012. The second set of experiments evaluates corrosion of several metals under atmospheric conditions, due deliquescence of salts on the metal surface. Many aspects of this work are relevant to interim storage, and the experimental work will continue in FY12, albeit with a greater focus on materials relevant to interim storage.

CONTENTS

FIGURES

TABLES

ACRONYMS

ACI	American Concrete Institute
AEC	Atomic Energy Commission
AISI	American Iron and Steel Institute
AMP	Aging Management Program
ANDRA	Agence nationale pour la gestion des déchets radioactifs (French agency for radioactive waste management)
ASI	American Standards Institute
ASM	American Society for Metals
ASTM	American Society for Testing and Materials
BRAGFLO	BRine And Gas FLOw
BSW	basic saturated water
BSS	borated stainless steel
BWIP	Basalt Waste Isolation Project
BWR	boiling water reactor
CCA	Compliance Certification Application
CNNC	China National Nuclear Corporation
COBECOMA	COrrosion BEhavior of COntainer Materials report
DBD	deep borehole disposal
DBE	German company for the construction and operation of waste repositories
DCSS	dry cask storage system
DHLW	defense high level waste
DOE	United States Department of Energy
DPC	dual purpose canister
E_{Corr}	open-circuit corrosion potential
$E_{Critical}$	critical potential
E_{NP}	pit nucleation potential
E_{PP}	protection potential
E_{rcrev}	repassivation potential
EBS	engineered barrier system
ECDF	empirical cumulative distribution functions
ENRESA	Empresa Nacional de Residuos Radiactivos, S.A. (Spanish agency for radioactive waste management)
EPA	Environmental Protection Agency

EPRI	Electric Power Research Institute
ERDA	Energy Research and Development Administration
ESCP	Extended Storage Collaboration Program
FCT	Fuel Cycle Technologies
FEP	feature, event or process
Fm.	formation
FZK	Forschungszentrum Karlsruhe (Research Center Karlsruhe)
GSF	Gesellschaft für Strahlen- und Umweltforschung mbh München (Corporation for Radiation and Environmental Research)
GWB	generic weep brine
HLW	high level waste
IfT	Institut für Tieflagerung (Institute for Underground Disposal)
ILW	intermediate level waste
INL	Idaho National Laboratory
ISFSI	independent spent fuel storage installation
ITS	important to safety
LC	localized corrosion
LLNL	Lawrence Livermore National Laboratory
LLW	low level waste
LRO	long range ordering
LTCTF	Long Term Corrosion Test Facility
LWA	Land Withdrawal Act
LWR	Light Water Reactor
MHM	Meuse/Haute-Marne
MHSH	magnesium hydroxide sulfate hydrate
MIC	microbiologically induced corrosion
MOx	mixed oxide
MPC	multi purpose canisters
NADP	National Atmospheric Deposition Program
NAGRA	Nationale Genossenschaft für die Lagerung Radioaktiver Abfälle (Swiss national cooperative for the disposal of radioactive waste)
NIREX	Nuclear Industry Radioactive Waste Executive (former British agency for radioactive waste management)
NNWSI	Nevada Nuclear Waste Storage Investigations
NRC	Nuclear Regulatory Commission

NDA   Nuclear Decommissioning Authority (British agency for radioactive waste management)

NUMO   Nuclear Waste Management Organization of Japan

NWPA   Nuclear Waste Policy Act

NWTRB   Nuclear Waste Technical Review Board

NWTS   National Waste Terminal Storage Program

ONDRAS/NIRAS   Belgian agency for management of radioactive waste and enriched fissile materials

ONWI   Office of Nuclear Waste Isolation

ORNL   Oak Ridge National Laboratory

PA   performance assessment

PBB   Permian Basin brine

PNNL   Pacific Northwest National Laboratory

PWR   pressurized water reactor

QA   quality assurance

R&D   research and development

RW   radioactive waste

SAW   simulated acidified water

SCC   stress corrosion cracking

SCW   simulated concentrated water

SDFR   slip-dissolution film-rupture model

SDP   Subseabed Disposal Program

SDW   simulated dilute water

SKB   Svensk Kärnbränslehantering AB (Swedish Nuclear Fuel and Waste Management Co.)

SNF   spent nuclear fuel

SNL   Sandia National Laboratory

SRP   Salt Repository Project

SSC   saturated silver chloride (electrode) *or* structures, systems, and components

TCP   tetrahedral close packed

TDS   total dissolved solids

TMI   Three Mile Island

TRU   transuranic waste

TTT   time, temperature, transition

UFD   Used Fuel Disposition [program]

UNF   used nuclear fuel

UNS   Unified Numbering System

URL   underground research laboratory

U.S.   United States

USGS   United States Geological Survey

WIPP   Waste Isolation Pilot Plant

WPP   Waste Package Program

XRD   X-ray diffraction

YMP   Yucca Mountain Project

REPOSITORY SCIENCE: ENGINEERED MATERIALS PERFORMANCE WORK PACKAGE: GAP ANALYSIS AND STATUS OF EXISTING WORK

1.   INTRODUCTION

It is the task of the Engineered Materials Performance work package to evaluate the long-term performance of materials used to isolate high level waste and spent nuclear fuel (SNF) for long-term interim storage or permanent disposal. Engineered materials waste packages, canisters, and internals; components of the emplacement drifts or interim storage bunkers, including cement and backfill materials; and other engineered materials including seals and casing. Although all of these materials fall within the scope of the Engineered Materials Performance work package, it focuses on waste packages and interim storage canisters, and considers other components only in the ways that they impact the performance of the package. Other Used Fuel Disposition (UFD) program work packages (Engineered Barrier System and Storage, Waste Form) are evaluating other aspects of the engineered systems. Potential disposal options that are considered include mined repositories in granite, shale or clay, and salt, and deep borehole disposal in crystalline rock.

This report provides the status of the work package, and consists of two parts. First, a literature survey and gap analysis are provided (Section 2), that identify potential future experimental and modeling work to increase the state of knowledge with respect materials performance in repository and storage environments. This gap analysis is used to develop a preliminary test plan for future experiments which is provided in Appendix A of this report. The second part of the report (Section 3) provides the status of existing experimental work at Sandia. This work, originally started under the Yucca Mountain Project, consists of two sets of experiments. The first set evaluates corrosion of Alloy 22, a Ni-Cr-W-Mo alloy, under immersed conditions in three different brines. This set of experiments is a two-year effort scheduled to be completed in FY12. A final report will be provided by June 30, 2012. The second set of experiments evaluates corrosion of several metals under atmospheric conditions, due deliquescence of salts on the metal surface. Many aspects of this work are relevant to interim storage, and the experimental work will continue in FY12, albeit with a greater focus on materials relevant to interim storage.

This report summarizes studies of engineered materials performance in repository settings. For each of the generic waste repository and storage concepts, the following information is provided:

- the countries that are considering or have considered that repository concept,

- the general characteristics (chemistry, redox, temperature range) of the environment,

- engineered materials in the current repository designs that are being considered,

- relevant experimental work that has been carried out (both inside and outside the repository science literature),

- additional research needs.

This reports draws heavily from compilations and assessments by other groups. These include the proceedings of two international workshops on long-term corrosion behavior in nuclear waste systems (Féron and Macdonald 2003; 2005) and an article summarizing the results of these meetings (Féron et al. 2008), the European Commission COBECOMA (State-of-the-art document on the COrrosion BEhavior of COntainer MAterials) report (Kursten et al. 2004a) and summary article (Kursten et al. 2004b); and additional summary articles, including King et al (2001; 2010), Smart et al. (2004), Bennett and Gens (2008), Feron et al. (2009), Kursten et al. (2011a; 2011b), and Kwong (2011). Additional resources include reports on deep borehole disposal by the Massachusetts Institute of Technology (Sapiie and

Driscoll 2009) and by Sandia National Laboratories (Brady et al. 2009). For interim storage conditions, the gap analysis carried out by the Storage R&D Opportunities group (Hanson et al. 2011) is relied upon.

2.   Literature Survey and Gap Analysis

This report evaluates the state of knowledge with respect to engineered materials performance in a series of environments, corresponding to potential disposal options for spent nuclear fuel (SNF) and high level radioactive waste (HLW). The environments span the conditions currently being considered by repository programs worldwide. They include mined repositories in crystalline rock, both in the vadose zone and in the deep subsurface; mined repositories in shale or clay, and salt; and deep borehole disposal in crystalline rock. In addition, environments related to long-term interim storage are considered. Vadose zone and interim storage environments are oxic, while the other environments are reducing. In this report, the existing state of knowledge with respect to corrosion in each environment is considered, and knowledge gaps are identified. Table 1 summarizes environments being considered, the international programs involved, and the candidate waste package materials being considered. Other countries that have operating or decommissioned nuclear reactors and stored used nuclear fuel include the Czech Republic, China, India, Korea, Lithuania, Russia, the Slovak Republic, and Slovenia. However, their repository programs are still in their infancy, and current repository concepts do not extend beyond general plans to dispose of SNF in anoxic environments in either clay or crystalline host rocks.

Engineered materials in the repository and storage settings include the waste package and waste package internals, but also include other drift components, such as ground support and invert materials, backfill and buffer materials, overpacks, cement bunkers, and any other manmade components of, or within, the emplacement drifts or interim storage bunkers. Although all of these materials fall within the scope of the Engineered Materials Performance work package, the work package focuses on waste packages and interim storage containers, and considers other components only in the ways that they impact the performance of the package. Other Used Fuel Disposition (UFD) program work packages (Engineered Barrier System and Storage, Waste Form) are evaluating other aspects of the engineered systems.

In general, repository programs have used two approaches with respect to waste package materials. The first is corrosion-resistant materials. These are metals which are highly resistant to corrosion in the environment in which they are intended for use. These metals and alloys form a passivating oxide surface layer and exhibit very slow rates of general corrosion. They are, however, generally susceptible to localized corrosion (pitting and crevice corrosion) under some conditions. Waste packages and interim storage containers made of corrosion-resistant materials are generally relatively thin—on the order of a few centimeters—and strength requirements may play as large a role as corrosion performance in determining the thickness. The second approach is to use a corrosion-allowance material. These metals do not form passive oxide layers, and undergo active corrosion under the anticipated conditions. They corrode more rapidly than corrosion-resistant materials but larger thicknesses are used, and their performance is sufficient to guarantee that penetration does not occur within the specified time interval. Although general corrosion rates are higher, corrosion allowance materials are not susceptible to localized attack, allowing better estimation of penetration times. Also, because of the mass of material present and the relatively high corrosion rates, corrosion allowance materials provide a redox buffer, promoting reducing conditions, under which many radionuclides have low solubilities. Corrosion resistant metals and corrosion allowance metals may be used exclusively, or may be used in combination, to restrict radionuclide releases from the waste package/storage container.

Table 1.   Summary of the different repository concepts being pursued by international repository science programs

Country	Responsible organization	Host rock[1]	Candidate Container Material	Container Thickness (mm)	Buffer Material	T_{max} at Waste Package Surface, °C
Belgium	NIRAS/ ONDRAF	Boom clay	carbon steel	30	Portland cement	<100
France	ANDRA	Callovo-Oxfordian clay (granite)	carbon steel	55	Bentonite (SNF); none (HLW)	<100
Switzerland	NAGRA	Opalinus clay (granite)	carbon steel	150 (SNF) 250 (HLW)	Bentonite	~140–160
Spain	ENRESA	clay (granite)	carbon steel	100	Bentonite	100
Canada	NWMO	granite sed. rocks	copper carbon steel	25 –	Bentonite Bentonite	100 –
China	CNNC	granite	–	–	–	–
Finland	Posiva	granite	cast iron (inner container) copper (outer container)	60 50	bentonite	<100
Japan	NUMO	granite	carbon steel (alternative: titanium)	300 -	Bentonite	100
Sweden	SKB	granite	cast iron (inner container) copper (outer container)	50 50	Bentonite	<100
Germany	DBE	salt (clay)	HLW: Cr-Ni steel SNF: carbon steel	4-5 430	Crushed salt	200
USA	U.S. DOE	tuff [2]	stainless steel (AISI 316 or 316L) (inner container) Ni- alloy (alloy C-22) (outer container) Ti-grade 7 (drip shield)	50 10 20	None	>200
UK	NDA	n.d.	stainless steel	n.d.	Cementitious material	100

Sources: (Kursten et al. 2004a; Féron et al. 2009).

[1] Lithologies in parentheses have also been evaluated

[2] The US repository program work at Yucca Mountain Nevada has been halted—the future of the program is uncertain.

2.1   Corrosion Processes of Important Metal Alloys

This section provides a basic discussion of the corrosion behavior under oxic and anoxic conditions, for four commonly considered metal and alloy groups; Fe-based, Ni-based, Cu-based, and Ti-based materials. This summary relies heavily on the COBECOMA report (Kursten et al. 2004a). More recent articles and summaries are cited for work after that publication.

2.1.1   Fe-based Materials

Under oxic conditions, which will be present immediately after closure of a repository, iron based materials, including carbon steel and stainless steel, will corrode by reaction of iron with oxygen, via two reactions:

$$4 \, Fe + 3O_2 \rightarrow 2Fe_2O_3 \tag{1}$$

$$2Fe + 2H_2O + O_2 \rightarrow 2Fe(OH)_2 \tag{2}$$

The second reaction is fast in carbon steel, but stainless steel forms a passive oxide layer (mostly Cr_2O_3), inhibiting further reaction. The ferrous hydroxide produced in the second reaction can be further oxidized in the presence of oxygen:

$$4Fe(OH)_2 + 2H_2O + O_2 \rightarrow 4Fe(OH)_3 \tag{3}$$
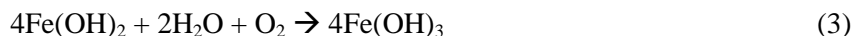
Because of metal corrosion, and because of biotic and abiotic reactions with organic material and sulfides, the repository eventually becomes anoxic. Under anoxic conditions, iron corrosion can still occur, by reaction with water:

$$Fe + 2H_2O \rightarrow Fe(OH)_2 + H_2 \tag{4}$$

$Fe(OH)_2$ is not the most thermodynamically stable phase, however, and will eventually react to form magnetite:

$$3Fe(OH)_2 + 4H_2O \rightarrow Fe_3O_4 + 2H_2O + H_2 \tag{5}$$
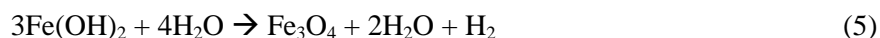
This reaction may be kinetically inhibited, though, especially at low temperatures. Moreover, substitution of ions into the $Fe(OH)_2$ (e.g., Mg), can stabilize the hydroxide, inhibiting the reaction to magnetite. In alkaline environments, a dense magnetite layer forms on iron, passivating the surface, and greatly slowing further corrosion (Smart et al. 2004).

As indicated above, the anoxic corrosion of steel produces H_2. If corrosion is sufficiently fast relative to movement of H_2 away from the metal surface, the H_2 may build up. However, it will not significantly inhibit corrosion, because the H_2 partial pressures necessary to suppress the corrosion reaction are high—many times the hydrostatic pressure at a typical repository depth. However as discussed later, the hydrogen could potentially build up and disrupt the buffer material, creating a fast pathway for flow and transport to and from the waste package surface.

Environmental factors, including concentrations of chemical species, temperature, pH, and radiation flux, affect iron and steel corrosion rates. General corrosion is generally faster under oxic conditions, as oxygen provides an additional electron acceptor. Oxic conditions also generally favor localized corrosion processes. Chloride and fluoride destabilize passive films in stainless steels, resulting in pitting if concentrations are sufficiently high, and increase general corrosion rates as well (Kursten et al. 2004a; Smart et al. 2004). Thiosulfate, an intermediate oxidation product of sulfide, stabilizes pits, lowering the pitting potential, and is especially detrimental if present with chloride, which can induce the pitting. Other anions (sulfate, hydroxide, nitrate, carbonate) generally inhibit corrosion, via either competitive sorption or the formation of more protective films. Temperature generally increases corrosion rate, because it is an activation-controlled reaction. However, in an oxic open system, corrosion slows with increasing temperature above 80ºC, as the solubility of oxygen decreases to the point that aqueous

concentrations are no longer sufficient to support further increases in the corrosion rate. Temperature can also change the corrosion products, affecting their ability to form a protective layer. At elevated pH (>10), iron materials form a passive film and corrode very slowly. However, as the pH drops the corrosion rate increases until passivity is lost; the actual value at which this occurs depends on other environmental parameters (e.g., chloride concentration, temperature, redox potential). Decreasing pH also moves the pitting potential in the active direction, eventually resulting in pitting. However, pit propagation is independent of pH, as corrosion in the pit generates its own environment.

2.1.2   Ni-based Materials

The corrosion behavior of nickel varies greatly with Eh and pH (Kursten et al. 2004a). In anoxic neutral to basic waters, nickel behaves as a noble metal and does not corrode. In oxic waters in the same pH range, it behaves as a passive metal, forming a protective layer of $Ni(OH)_2$, or, in aerated waters, Ni_3O_4. Under oxic conditions, Ni is very corrodible in acid or very alkaline solutions. Under acidic, anoxic conditions, the Pourbaix diagram indicates that Ni metal should corrode readily, but in practice, the reaction is kinetically inhibited. Chromium, molybdenum and tungsten are commonly used as alloying elements with nickel, and their presence generally increases its resistance to corrosion. In general, Ni and Ni-alloys are very resistant to corrosion in freshwater, nonoxidizing acids, and alkaline solutions. They are not resistant to corrosion in strongly oxidizing solutions, or to sulfur-bearing gases at high temperature. The localized corrosion (LC) susceptibility of Ni-Cr-Mo alloys and stainless steels improve with increasing Cr and Mo content and with additions of small amounts of nitrogen. The effects of other environmental factors on LC susceptibility of Ni-Cr-Mo alloys are similar to the effects on stainless steel. A more detailed discussion of the corrosion behavior of Ni-based alloys is provided in Section 2.5.

2.1.3   Cu-based Materials

2.1.3.1   Oxic conditions

Krusten et al. (2004a) provide a good general description of copper corrosion behavior under oxic and anoxic conditions. In the presence of oxygen, copper metal corrodes by the overall reaction:

$$4Cu + O_2 \rightarrow 2Cu_2O \tag{6}$$

which can be broken down into the anodic and cathodic half-reactions:

$$4Cu + 2H_2O \rightarrow 2Cu_2O + 4H^+ + 4e^- \quad (anode) \tag{7}$$

$$O_2 + 2H_2O + 4e^- \rightarrow 4(OH)^- \quad (cathode) \tag{8}$$
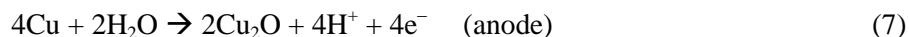
The Cu(I) species further oxidize to form Cu(II) species, via the following schematic reaction:

$$4Cu(I) + O_2 + 2H_2O \rightarrow 4Cu(II) + 4(OH)^- \tag{9}$$

Under oxic conditions, as will persist in a clay or granite repository for a period after closure, the copper metal surface is coated with duplex corrosion product layer of Cu_2O and Cu(II) salts, the actual composition of which depends upon the composition of the pore water. The Cu_2O layer is protective, but the Cu(II) salts are porous and discontinuous, allowing further oxidation of the Cu_2O layer to take place, and corrosion continues to occur. The rate of corrosion depends on the properties of the electrically-conducting Cu_2O layer.

In oxic conditions, chloride plays an important role in several copper corrosion reactions. It contributes to the anodic oxidation of copper via:

$$Cu + Cl^- \rightarrow CuCl_{(ads)} + e^- \tag{10}$$

$$CuCl_{(ads)} + Cl^- \rightarrow CuCl_2^-{}_{(ads)} \tag{11}$$

$$CuCl_2^-{}_{(ads)} \rightarrow CuCl_2^-{}_{(aq)} \tag{12}$$

However, chloride can also contribute to the formation of the protective Cu_2O layer via a variety of reactions.

- At higher pH, the following reactions become important:

$$CuCl_{(ads)} + OH^- \rightarrow Cu(OH)_{(ads)} + Cl^- \tag{13}$$

$$2Cu(OH)_{(ads)} \rightarrow Cu_2O + H_2O \tag{14}$$

  Whether reactions 10-12 or 13-14 dominate depends on the pH and on mass transport rates to and from the metal surface.

- $CuCl_2^-{}_{(aq)}$ produced by reaction 12, can further react to form Cu_2O:

$$2CuCl_2^- + H_2O \rightarrow Cu_2O + 2H^+ + 4\ Cl^- \tag{15}$$

- And precipitated CuCl can form Cu_2O by:

$$2CuCl + H_2O \rightarrow Cu_2O + 2H^+ + 2Cl^- \tag{16}$$

Chloride may also contribute to the destruction of the Cu_2O film. In chloride-containing oxic environments, the Cu_2O layer is commonly coated with a cupric chloride-hydroxide layer. Although the mechanism of formation of this layer is not clear, one possible reaction is:

$$2Cu_2O + O_2 + 2Cl^- + 4H_2O \rightarrow CuCl_2 \cdot 3Cu(OH)_2 + 2OH^- \tag{17}$$

At the cathode, chloride can also aid in reduction of cupric species:

$$Cu(II) + 2Cl^- + e^- \rightarrow CuCl_2^- \tag{18}$$

This helps preserve the protective layer. Finally, incorporation of chloride ions into the protective Cu_2O layer changes its conductive properties. At high chloride concentrations, the layer can become so defected that it ceases to protect the surface, and copper will corrode by pitting or even corrode actively.

2.1.3.2   Anoxic conditions

The general corrosion rate of copper in anoxic environments is anticipated to be extremely slow, because thermodynamic data indicate that copper does not corrode via reaction with water. The generally accepted corrosion reaction for copper by water is:

$$2Cu_{(s)} + H_2O \rightarrow Cu_2O + H_2 \tag{19}$$

However, a vanishingly small f_{H2} is required to suppress this reaction ($\sim 10^{-16}$ bars), so it is not anticipated to occur at a measurable rate.

However, corrosion in anoxic natural waters may be enhanced by the presence of complexing species, especially chloride and sulfide. Under conditions of high chloride content, high temperature, and low pH (<6), chloride can enhance Cu corrosion:

$$Cu + nCl^- + H^+ \rightarrow CuCl_n^{1-n} + \tfrac{1}{2}H_2 \tag{20}$$
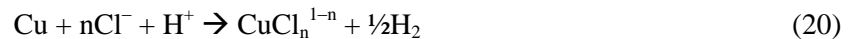
In the absence of another electron acceptor, this reaction is limited by transport of H^+ to the metal surface or transport of $CuCl_n^{1-n}$ away from the surface.

Sulfide is anticipated to be present in both clay pore waters and granitic pore waters. Sulfide causes corrosion of a copper waste package under anoxic conditions via formation of a copper sulfide corrosion product layer. Similar to the oxide layers that form, sulfides form a duplex corrosion product film, consisting of a thin inner layer of Cu_2S, and an outer layer of CuS. The Cu_2S forms by:

$$2Cu + HS^- + H_2O \rightarrow Cu_2S + H_2 + OH^- \tag{21}$$

"The Copper Controversy"

The discussion above is the classical view of how copper corrodes under anoxic conditions. However, the assumption that copper will not hydrolyze water recently has been questioned; a group of researchers has reported high measured rates of hydrogen generation in anoxic systems containing only copper and deionized water. These experimental results were first reported in 1986 (Hultquist 1986), but were dismissed at the time as being experimental artifacts (Simpson and Schenk 1987). However, more recent experimental work verified the elevated H_2 production (Szakalos et al. 2007; 2008; Hultquist et al. 2009; Hultquist et al. 2010; Hultquist et al. 2011), and indicated that the f_{H2} required to suppress copper corrosion by water is actually on the order of 10^{-3} bars. In a separate, long-running experiment reported in Hultquist et al. (2008), copper samples were aged for 15 years under nominally anoxic conditions in two different containers. One container was sealed with palladium (through which H_2 diffuses readily) and the other, with platinum (through which H_2 does not diffuse). The samples in the Pd-sealed container corroded heavily, while those in the Pt-sealed container did not (Figure 1). The authors suggested that H_2 diffusion in the Pd-sealed allowed the copper corrosion reaction with water to occur without suppression, while build-up of H_2 in the Pt-sealed container suppressed the reaction.

The research group hypothesized that the two sets of observations could be explained by formation of a hydroxide-bearing corrosion product (instead of copper oxide) as in the following schematic reaction:

$$Cu + yH_2O \rightarrow H_xCuO_y + (2y-x) H_{ads} \tag{22}$$

Moreover, a set of molecular dynamics simulations indicated that formation of stable hydroxide-containing surface complexes may be possible (Belonoshko and Rosengren 2010). If they exist, these surface complexes would lower the energy barrier for H_2O dissociation.

Source: Hultquist et al. (2008)

Figure 1. Copper samples immersed in water in a glass container for 15 years. In the container on the left, hydrogen is allowed to diffuse from the bottle through a palladium membrane. The container on the right is completely sealed with platinum

However, the experimental and modeling work, and the conclusions in the above papers, have been criticized (Johansson 2008; Werme and Korzhavyi 2010). The proposed mechanism for copper corrosion is inconsistent with a large body of experimental work and thermodynamic data. No such copper hydroxide corrosion product has been identified experimentally, and recent molecular dynamics modeling indicates that copper hydroxides or oxyhydroxide are not stable (Korzhavyi and Johansson 2010). In the long-term aging experiment, the observed corrosion could simply indicate leakage of oxygen into the Pd-sealed system.

Because of the reliance on the copper waste package in the Swedish and Finnish repository programs, this issue has received a great deal of attention. It has come to be known as "The Copper Controversy." In 2009, the Swedish repository organization SKB convened a workshop and an expert panel to discuss the issue. The final report of this workshop (Swedish National Council for Nuclear Waste 2009) concluded that further research was needed to:

- Evaluate the validity of the H_2 generation experiments–the H_2 data are widely regarded as being an experimental artifact.

- Identify/characterize the hydrogen-bearing corrosion product, if it exists.

- Evaluate corrosion under relevant repository environments, using relevant water compositions (Cl, bicarbonate, etc), and, potentially, adding a bentonite buffer to limit H_2 diffusion.

2.1.4   Ti-based Materials

In contrast to non-corrosive metals, titanium owes its excellent corrosion behavior not to being noble, but to being highly reactive (Kursten et al. 2004a). In contact with water or air, titanium instantly forms a protective layer of titanium oxides, generally TiO_2 (rutile at elevated temperatures, and anatase at lower temperatures). In addition, damage to the oxide film instantly heals if water or air is present. Because of the titanium oxide layer, Ti is highly resistant to corrosion under almost all conditions, except for exposure to hot, concentrated acids or bases. In the passive state, Ti corrodes very slowly, by oxidation and thickening of the TiO_2 film. Ti alloys, especially Ti Grade 7 (Ti99.8-Pd), are generally immune to pitting and stress corrosion cracking under potential repository conditions. A more detailed discussion of the corrosion behavior of Ti-based alloys is provided in Section 2.5.

2.2   Clay-hosted Repositories

Repository programs that have identified clay and shale units as repository host rocks include Belgium, France, Switzerland and Spain, while Germany, Japan, and some eastern European countries (Lithuania and the Slovak Republic) are also pursuing research in such sites. This section first presents a short description of each program and the site, and the current waste package design. Then, corrosion research supporting the clay repository concept is described. Finally potential areas of additional research— knowledge gaps—are identified.

2.2.1   The Natural System

In this section, a short description of the host rock mineralogy and general pore water composition is provided for several repository programs that have chosen clay and shale host rocks. The choice of waste package material is strongly dependent on the chosen host rock (e.g., granite, clay, salt) and the anticipated environment.

2.2.1.1   *Belgium*

Geologic setting

The planned Belgian repository is in the Oligocene (31 Ma; Lagrou et al. 2004) Boom Clay formation, a soft, poorly indurated marine clay with a high porosity of ~30-40% (Francois et al. 2009). The Belgian repository program has an underground research laboratory (URL) in the Boom Clay at Mol, at a depth of ~225 m. The Boom Clay exhibits significant layering and clay content varies from 30-70 wt% of the total; dominant clays are illite (~50%) and smectite/illite-smectite mixed layer clays (30%), with minor amounts of kaolinite, chlorite, degraded chlorite/chlorite-illite interlayer clays, and glauconite (Volckaert et al. 2004). Minor amounts of carbonate, pyrite, and organic materials (1-5%) are also present. The clay contains 1-5% organic materials, mostly kerogen of marine and to a lesser extent terrestrial origin (Maes et al. 2004). Ground water in the unit is sodium-bicarbonate type but contains 50-250 mg L^{-1} organic carbon (perhaps as much as 400 mg L^{-1}), dominantly as humic acids (Maes et al. 2004). Because of the organic matter and pyrite, conditions are quite reducing, and the redox conditions are well buffered.

Pore water geochemistry

As noted in ANDRA (2005c), characterization of pore water compositions in deep clay formations is quite difficult. Because of the very low permeability, water extraction is difficult and only small volumes of water can be sampled. Also, a significant amount of the water in the rock is not free but is rather bound to clay mineral surfaces and within the interlayers as waters of hydration (Bradbury and Baeyens 2002). In addition, electrostatic forces can result in anion exclusion and in a non-homogeneous spatial distribution of solutes within pores; water solute concentrations extracted from clays commonly vary with the squeezing pressure used to extract the sample. Thus, defining a characteristic pore water composition is difficult, and estimated compositions are generally derived from a combination of elemental analysis and thermodynamic modeling. The pore water compositions presented here must be considered within this framework.

Table 2 provides a typical Boom Clay pore water composition. Boom Clay waters are chemically simple; the waters are dilute, slightly basic, sodium bicarbonate-type waters, with only minor concentrations of other solutes. Also provided is a bentonitic pore water composition used by the Belgian program to represent backfill pore water compositions. The bentonitic water will be discussed later, in the context of corrosion experiments, but is presented here as a contrast to the formation water. When considering the waste package environment, it is important to note that backfill water compositions are commonly very different than the formation waters and will represent at least the short-term corrosion environment. In the long-term, backfill waters will approach formation waters in composition.

Table 2.   Boom Clay water composition

Constituent	Boom Clay pore water mg L^{-1}	Bentonite pore water mg L^{-1}
pH	8.2-9.7	n.d.
Ca^{2+}	4.0	583
Mg^{2+}	2.9	37.5
Na^+	408	183
K^+	11.0	8.4
Fe	0.9	<0.10
Al	0.08	0.45
Mn	n.d.	0.145
B	7.5	n.d.
Si	5.0	n.d.
Cl^-	27.0	68.0
F^-	3.6	1.56
Br^-	0.49	n.d.
SO_4^{2-}	0.2	1633.0
NO_3^-	—	<2.50
HCO_3^-	828.0	84.0
HPO_4^{2-}	3.8	<0.25
$S_2O_3^{2-}$	—	<2.50
TOC	41.3-144.0	106
TIC	—	6.82

Source: Kursten et al. (2004a), Table 2-5

n.d. – not determined   TOC – total organic carbon   TIC – total inorganic carbon

2.2.1.2   France

Geologic setting

The planned French repository is described in a preliminary safety case published by ANDRA in 2005, the "Dossier 2005 Argile" (ANDRA 2005a; 2005b; 2005c; 2005d). It is sited in the Callovo-Oxfordian Clay (Jurassic; approximately 150-160 Ma; Wenk et al. 2008), which is a claystone as opposed to a soft clay, with a lower porosity(~11.5-17%; Volckaert et al. 2004) relative to the Belgian clay. On average, the argillites contain 40 to 45 % clay minerals (illite, illite-smectite ordered and disordered mixed phases, and subordinate kaolinite and chlorite), 20-30 % carbonates (calcite±dolomite, ankerite), and 20-30 % silt-sized quartz and feldspars (Volckaert et al. 2004; Wenk et al. 2008). The French repository program has a URL in the Callovo-Oxfordian clay at Bure, the Meuse/Haute-Marne (MHM) URL, 420-550 m below the surface. At Bure, the unit is about 130 m thick and consists of three transgressive-regressive cycles, varying somewhat in mineralogy and separated by thin carbonate deposits. The lower sequence is siltier than average, the central one is clay-rich and the upper sequence has the largest carbonate contents. In the upper half of the section, the illite-smectite mixed layer clay is disordered and contains 50-70% illite; in the lower half, it is ordered and contains 20-40% smectite. Kaolinite is more abundant in the lower part. These differences are depositional, and not due to variations in degree of diagenesis (Wenk et

al. 2008). Organic matter is present in amounts of 0.5-1% (Claret et al. 2004; Hautevelle et al. 2007), and pyrite, in amounts of 2-3% (ANDRA 2005c).

Pore water geochemistry

Recognizing the difficulties in extracting and analyzing accurate pore water compositions from clays, the French program used a combined approach, in which a few important components that are not sorbed by clays (e.g. Cl) were measured by leaching, and then other major components are estimated by assuming equilibrium with mineral phases in the rock and using thermodynamic modeling calculations (ANDRA 2005b). This approach provides a probable concentration range for each component, and these ranges are given in Table 3. Because the Callovo-Oxfordian clay is mineralogically similar to the Opalinus clay, the estimated concentrations are more similar to pore waters from that unit (provided later in this section) than to waters from the Boom Clay.

Table 3.   Callovo-Oxfordian clay water compositions

Constituent	Range, mg L^{-1}
pH	6.9–7.6
Eh	-180–-150 mV
Ca^{2+}	401–601
Na^+	575–1012
Cl^-	425–1064
SO_4^{2-}	327–3266
HCO_3^-	45.8–207

Source: ANDRA (2005b), Table 3.3-1

2.2.1.3   Switzerland

Geologic setting

The planned Swiss repository is in the middle Jurassic Opalinus Clay (178-180 Ma; Pearson et al. 2003). The Swiss URL in the Opalinus clay at Mont Terri is located ~270 meters below the land surface, but it is only a research site and is not being considered for the final repository location. At a proposed site in the Zurich Weinland region near Benken, the Opalinus Clay is flat-lying at a depth of 550-650 m. Porosity in the unit varies from 5 to about 15% (Pearson et al. 2003), with values at the high end of that range at Mont Terri, where the maximum depth of burial was less (Volckaert et al. 2004). The Opalinus Clay is relatively homogeneous on the meter-scale, but contains silty, quartz-rich lenses and siderite concretions on the centimeter-scale (Wenk et al. 2008). Although slightly older than the Callovo-Oxfordian Clay, it is mineralogically similar (ANDRA 2005a). The clay contains 40-70 wt% clay minerals (averaging 54% at Benken and 66% at Mont Terri), which are mostly illite, illite-smectite interlayer clays, and kaolinite in about equal amount; minor amounts of chlorite and kaolinite are also present. The remainder of the claystone consists of 10-30% carbonates (calcite, with lesser amounts of siderite and ankerite) (averaging 26% at Benken); 10-30% quartz (averaging 20% at Benken); and small amounts of feldspars (1-2%), pyrite (up to 2%), and organic matter (~0.2-1%). The organics, pyrite and siderite indicate that conditions are reducing, and that the clay has a relatively high redox buffering capacity (Pearson et al. 2003; Volckaert et al. 2004; Wenk et al. 2008).

Pore water geochemistry

Waters from the carbonate-rich Opalinus argillite (Table 4) are near-neutral to slightly basic, and have a much higher ionic strength than the Boom Clay waters. They are similar to pore waters from the

mineralogically similar Callovo-Oxfordian Clay. Na^+ is the dominant cation, but divalent cations, including Ca^{2+} and Mg^{2+} are also abundant, and significant amounts of K^+ and Sr^{2+} are present. Although Cl^- is the dominant anion, sulfate and bicarbonate are also important.

Table 4.   Opalinus clay water compositions

Constituent	BWS-A1 $mg\ L^{-1}$	BWS-A2 $mg\ L^{-1}$	BWS-A3 $mg\ L^{-1}$
pH	8.06	8.26	7.6
Ca^{2+}	587	43.2	283
Mg^{2+}	398	311	151
Sr^{2+}	40.3	2.15	31.6
Na^+	5538	4315	2864
K^+	58.7	130	40.6
Fe*	0.2	0.4	0.25
Al	0.3	0.03	<0.006
Mn*	0.35	0.20	0.30
B	—	—	2.373
Si	0.638	0.99	3.45
Cl^-	10005	6067	4908.9
F^-	0.77	0.17	0.47
Br^-	36.3	23.9	15.2
SO_4^{2-}	1282	1903	1082.2
NO_3^-	<20	<20	<20
Alkalinity (as HCO_3^-)	57	620	311
HPO_4^{2-}	—	—	—
TOC	19.1	448	9.52
TIC	7.93	118	64.42

Source: Pearson et al. (2003, Table 5-14)

* Average of several analyses

2.2.1.4   *Other Repository Programs*

Canada

Canada has not selected a disposal site, so the specific geologic environment of the repository is unknown. Historically, the Canadian program has focused on disposal in the crystalline basement of the Canadian Shield. However, since 2004, repository placement in sedimentary rocks has also been considered, with interest centering on a Devonian sedimentary sequence in southern Ontario (Mazurek 2004). Proceeding from shallowest (100 m) to deepest (1500 m), the "layer cake" sedimentary sequence at this locality consists of: shale, limestone, limestone/dolomite, dolomite, evaporites, dolomites, shale, and limestone. Potential repository host rocks include both "hard" and "soft" sedimentary rock (limestone and shale, respectively) (Garisto et al. 2009; Maak et al. 2010). For areas and depths that have been characterized, the pore waters are dominated by Na-Ca-Cl compositions, and have very high TDS

values (140-325 g L^{-1}). These high values are most likely influenced by the relative abundance of evaporites in the basin and by nearby active limestone aquifers (Mazurek 2004).

Spain

The Spanish waste program is run by the Spanish national radioactive waste management company, Empresa Nacional de Residuos Radioactivos (ENRESA). Spain has not yet selected a final disposal site for SNF or HLW, nor even chosen a host rock, but research has focused on disposal in either salt, clay, or granite host rock.

2.2.1.5   *General Chemical and Physical Environment in Clay Repositories.*

Clay hosted repositories have similar general characteristics. In the long term, conditions are reducing; the clays contain significant proportions of organic material and small amounts of sulfides. The abundance of organic material means that the redox buffering capacity is large. Sulfide concentrations in the host rock pore water can be high, due to the activity of sulfate-reducing bacteria. The host rock is very low permeability, and transport rates to and from the repository are extremely slow. For a short period after closure, trapped oxygen in the buffer and host rock will result in oxic conditions. During this period, dissolved sulfide in pore water infiltrating the buffer can be partially oxidized, leading to relatively high concentrations of thiosulfate, a corrosive species. Because of biotic and abiotic reactions with organic material and sulfides, and because of metal corrosion, conditions rapidly evolve to anoxic. Host rock pore waters have greatly varying compositions depending on the host rock, from dilute sodium bicarbonate waters (Boom Clay) to moderately saline Ca-Na-Cl-SO$_4$ waters (Callovo-Oxfordian and Opalinus waters). The water contacting the waste package, however, is strongly influenced by interactions with backfill materials (generally bentonite clay), which can have very high surface area and ion exchange capacities, and varying exchangeable cation compositions. Waste package surface temperatures will not exceed 100ºC by design (150º-160ºC in the Swiss concept), to avoid potentially damaging the swelling and sealing properties of the backfill and host-rock clays. Planned repository depths are 225 m in Belgium and 500-600 m in France and Switzerland.

2.2.2   Current Clay Repository Concepts

This section provides the current repository concepts for repository programs considering clay as a host rock. In each case, the current waste package design, emplacement plan, and the composition of the chosen backfill material are provided. The backfill material is generally a bentonitic material. After resaturation, it has a very low permeability, and a high sorption/ion exchange capacity. It provides protection to the waste package by limiting movement of reactive species to and from the waste package surface, and by providing a buffered environment conducive to the lifetime of the waste package. After breach, the backfill limits releases of the radionuclides from the waste package. Because of the high ion exchange capacity and specific surface area of the clay, it has a large impact on the composition of the water contacting the waste package—bentonitic water compositions are generally very different than the host rock pore water compositions.

2.2.2.1   *Belgium*

In the Belgian repository concept, the selected waste canister design is known as "Belgian supercontainer" (Figure 2). The supercontainer is a composite package with several components. The waste, vitrified HLW or spent fuel, is encased in a 30 mm thick and 50 cm diameter carbon steel overpack. Each overpack contains two HLW canisters, four UO$_2$ fuel assemblies, or one MOx assembly (Van Humbeeck et al. 2008). The overpack is in turn is embedded in a 70 cm thick Portland cement buffer. The cement buffer is encased in a thin stainless steel liner. The outside radius of the supercontainer is about 1.9 m, and the total length is 4.2 m for HLW, or 6 m for spent fuel (Craeye et al. 2009). The anticipated performance of the Belgian repository relies largely on the natural barrier represented by the Boom clay, so the main function of the supercontainer is to contain the waste during the thermal period (Poyet 2006), which will last a few hundred years for HLW and a few thousand years

for spent fuel. The cement buffer provides a favorable geochemical environment (high pH), in which corrosion of the carbon steel overpack will be limited. It also provides radiation shielding, for workers during handling and transport of the container. The supercontainers will be pre-assembled and sealed at the surface prior to transport underground and emplacement (Poyet 2006). Following emplacement, the space between the supercontainer and the drift walls will be filled with cementitious material. There is no clay backfill or buffer in the Belgian supercontainer concept; however, prior to developing the supercontainer, Belgium carried out extensive corrosion research using test waters extracted from PRACLAY, a candidate backfill material consisting of a mixture of 60% Fo-Ca bentonite clay, 35% sand, and 5% graphite (for thermal conductivity). The composition of that "bentonite pore water" was provided in a previous section (Table 2).
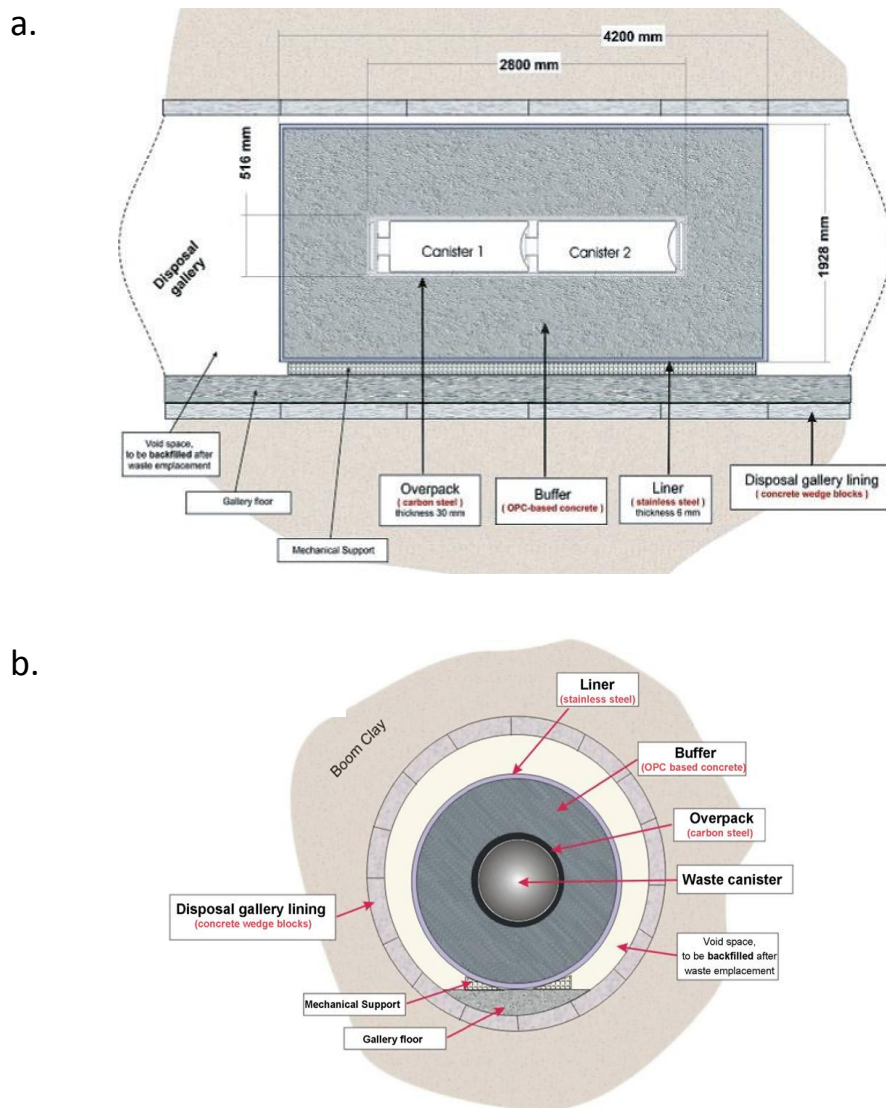
Sources: a) Poyet (2006); b) Craeye et al. (2009)

Figure 2.   The Belgian supercontainer: a) side view; b) end view

2.2.2.2   France

The proposed French waste package for SNF is shown in Figure 3 (ANDRA 2005b). The outer wall of the waste package consists of non-alloy (carbon) steel (P235) body with 110 mm thick walls. It contains a cast iron "insert", with four emplacements for fuel assemblies, each lined with 5 mm stainless steel. The cast iron insert serves two major purposes—to provide mechanical stability to the package during gradual loading under repository conditions, and to mitigate criticality risk by separating the assemblies (ANDRA 2005b). Although referred to as an insert, it is actually poured in place to minimize gaps between it and the carbon steel body. The stainless steel liners for the waste emplacements are put into position prior to pouring—they simply provide a mold for the waste emplacements. The waste emplacements may be either round or square, depending upon whether the individual assemblies are clad or bare, respectively. Once filled, the package is sealed using electron beam welding to minimize the extent of the thermally affected zone (ANDRA 2005b). The bottom and lid of the container are 130 and 149 mm thick, respectively, to allow them to be used as a root face for electron beam welding. The package diameter is 1.25 m and the total length is 4.5 to 5.4 meters, depending upon the length of the assemblies; the weight is 35 to 43 metric tons. A modification of this basic design (steel outer shell and cast iron insert) is used for MOx assemblies—it contains only a single fuel assembly, and has steel walls 120 mm thick. Four-assembly SNF waste packages are emplaced in disposal cells, circular horizontal tunnels with a steel liner (thickness, 3 cm), and a 0.8 m thick swelling clay buffer (Figure 3). The liner is perforated to allow water flow and swelling of the buffer material. A steel sleeve (thickness, 4 cm) extends through the core of the buffer, and it is within this sleeve that the waste packages are emplaced, using a cradle equipped with air cushions, which can be deflated to allow the cradle to be removed after emplacement. The single MOx assembly is emplaced similarly, but in a smaller tunnel.

Packaging for HLW vitrified waste differs from the SNF container. The glass waste is contained in thin stainless steel primary waste canisters, which are placed directly within a carbon steel overpack with 55 mm thick walls (Figure 4). The HLW containers are emplaced in smaller tunnels, directly within the steel liner (thickness 2.5 cm), with no clay buffer (ANDRA 2005b).

The limitation of either four PWR UO_2 assemblies, one MOx assembly, or one/two HLW canisters per container is required to meet repository thermal design bases (ANDRA 2005b). As per design specifications, the temperature within a waste package must remain below 100ºC, and the maximum temperature in contact with the rock or buffer must remain below 90ºC (ANDRA 2005a).

In the long term, waters contacting the waste package and other engineered barrier components will resemble the host formation waters. However, for an extended period after closure, the bentonite backfill will have a major effect on water chemistry because of its high surface area and cation exchange capacity. For repository feasibility studies, ANDRA used MX-80, a smectite-rich clay from Wyoming (USA) (ANDRA 2005c). Mineralogically, MX-80 consists of approximately 80 % sodium-calcium montmorillonite. The remaining 20 % consists of silica minerals (quartz and cristobalite), feldspars (plagioclase and potassium feldspar), biotite – phlogopite, carbonates (calcite and ankerite), sodic-calcic phosphate, pyrite, hematite, and trace quantities of anhydrite, barite, and celestite. The cationic exchange capacity, determined for a purified clay fraction, is 87.5 meq per 100 g.

As with clay host rocks, extraction of representative pore water from compacted bentonite is difficult, and is further complicated because the pore water composition varies with the degree of compaction, which determines the water-rock ratio. In a manner similar to the ANDRA approach for the Callovo-Oxfordian clay discussed above, Bradbury and Baeyens (2002) calculated porewater compositions for MX-80 as a function of bentonite compaction (Table 5). These calculations include the effects of the amphoteric surface sites and interlayer cation exchange, and assume that the pore waters are saturated with respect to calcite, gypsum, celestite, fluorite, and quartz. Neither pH nor PCO_2 are held constant; the cited values are derived from the assumptions above and from the assumed porewater chloride concentrations, which are, in turn, based on the measured dry rock chloride content and the degree of compaction.

a

b
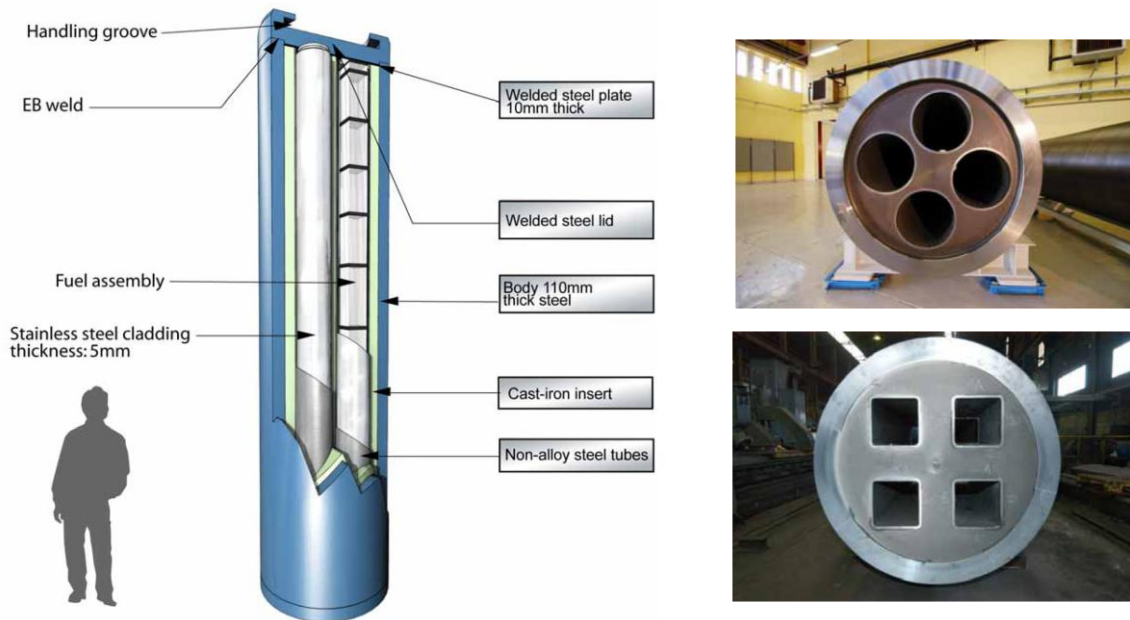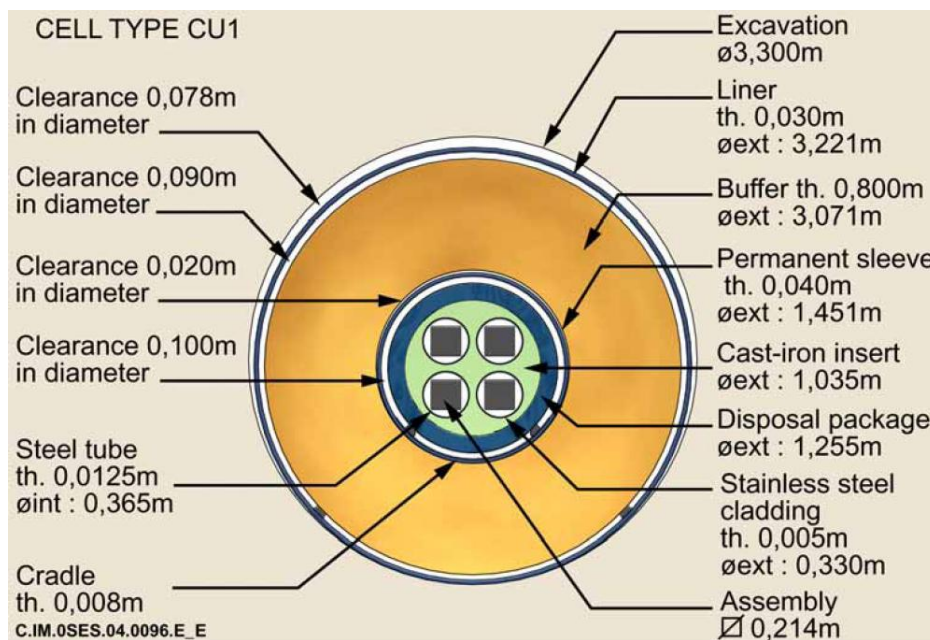
Sources: a) ANDRA (2005b), Figures 4.3.1 and 4.3.10; b) ANDRA (2005b), Figure 5.3.11

Figure 3.   The ANDRA waste package concept for SNF: a) general waste package configuration; b) cross-sectional view of emplaced configuration

a

b
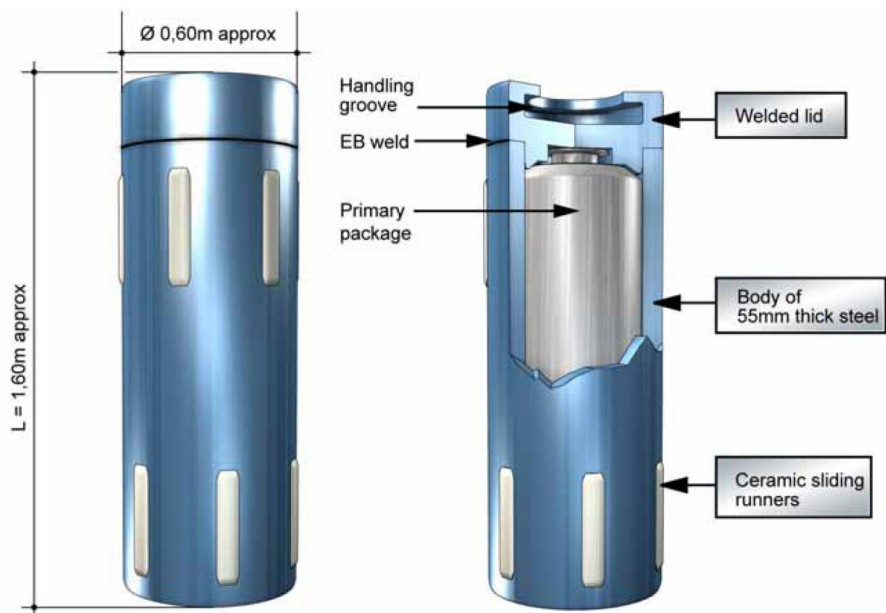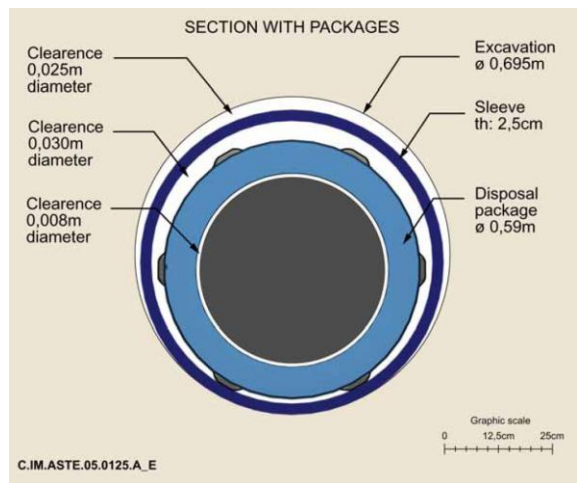
Sources: a) ANDRA (2005b), Figures 4.2.2; b) ANDRA (2005b), Figure 5.2.9

Figure 4.   The ANDRA waste package concept for HLW vitrified glass: a) side view; b) cross-sectional view of emplaced configuration

Table 5.   Compacted MX-80 porewater compositions calculated for a closed system as a function of the initial dry compacted density

Dry density (kg m^{-3}) :	1200	1300	1400	1500	1600
log P_{CO2} (bar)	-3.38	-3.39	-3.41	-3.43	-3.48
Ionic strength (M)	0.295	0.3	0.306	0.314	0.327
pH	8	8	8	8	8
	Concentration, mg L^{-1}				
Ca^{2+}	361	364	369	380	405
Mg^{2+}	149	155	162	172	187
Na^+	5060	5200	5360	5590	6000
K^+	44.2	45.0	46.5	48.1	51.6
Si	5.14	5.14	5.14	5.14	5.14
Cl^-	957	1230	1680	2390	3830
F^-	4.31	4.29	4.26	4.16	3.95
SO_4^{2-}	10800	10700	10500	9990	9080
HCO_3^-	58.9	58.2	56.4	53.7	47.5
TIC	11.6	11.5	11.1	10.6	9.36

Modified from Bradbury and Baeyens (2002)

2.2.2.3   Switzerland

Waste package

The NAGRA reference design for SNF and vitrified HLW waste packages are shown in Figure 5. The SNF package consists of a cast steel body, about 5 m long and 1 m in diameter, with a machined central square channel fitted with steel crossplates to permit emplacement of either 4 PWR or 9 BWR fuel assemblies (NAGRA 2002a). The minimum wall thickness is 15 cm. The HLW container is a steel canister containing one stainless steel flask of HLW glass. The container has a wall thickness of 25 cm, a length of about 2 m and a diameter of about 1 m. The containers will be emplaced horizontally in 2.5 m diameter cylindrical tunnels. They will be placed on pallets composed of compacted bentonite bricks, and following emplacement, the free space around the waste packages will be filled with pelletized bentonite pellets (Figure 6).

Bentonite buffer

As with the French program, NAGRA has used the Wyoming bentonite MX-80 to represent the eventual backfill material (NAGRA 2002a). Hence, the mineralogy is the same as was discussed in the past section. As was done for the French program, bentonite porewater compositions were estimated based on thermodynamic modeling that included protonation/deprotonation of surface sites, ion exchange, and mineral equilibrium (Curti and Wersin 2002). However, the NAGRA approach assumed equilibration with Opalinus clay pore water from Mont Terri, and calculated the pore water after several pore volumes had been flushed through the bentonite. Moreover NAGRA fixed the P_{CO2} in the simulations, using the estimated Opalinus porewater value of $10^{-2.2}$ bars. Because of the importance of this parameter, bounding P_{CO2} values of $10^{-1.5}$ and $10^{-3.5}$ bars were also considered. The three potential water compositions are shown in Table 6.
.

SNF package
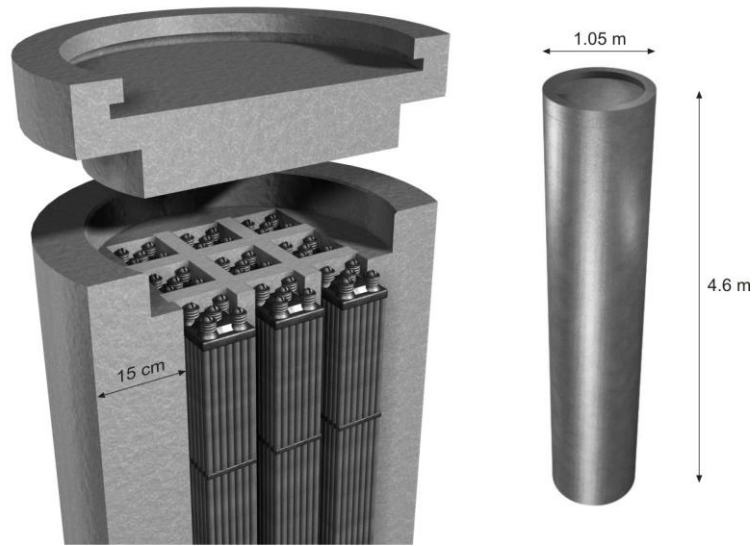
HLW package
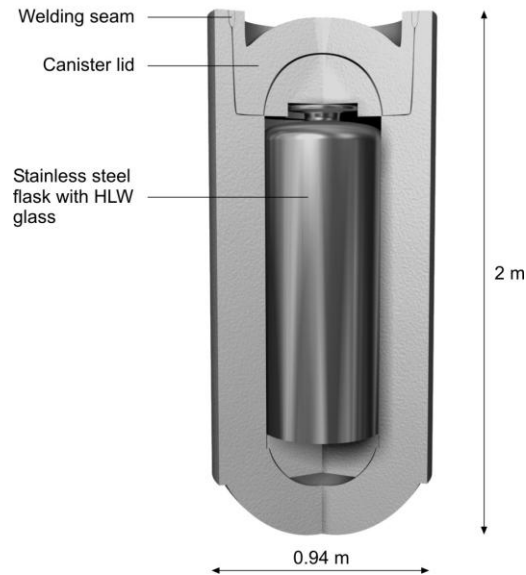
Source: NAGRA (2002b), Figures 4.5-4 and 4.5-5.

Figure 5.   The Swiss concepts for SNF and HLW vitrified waste packages
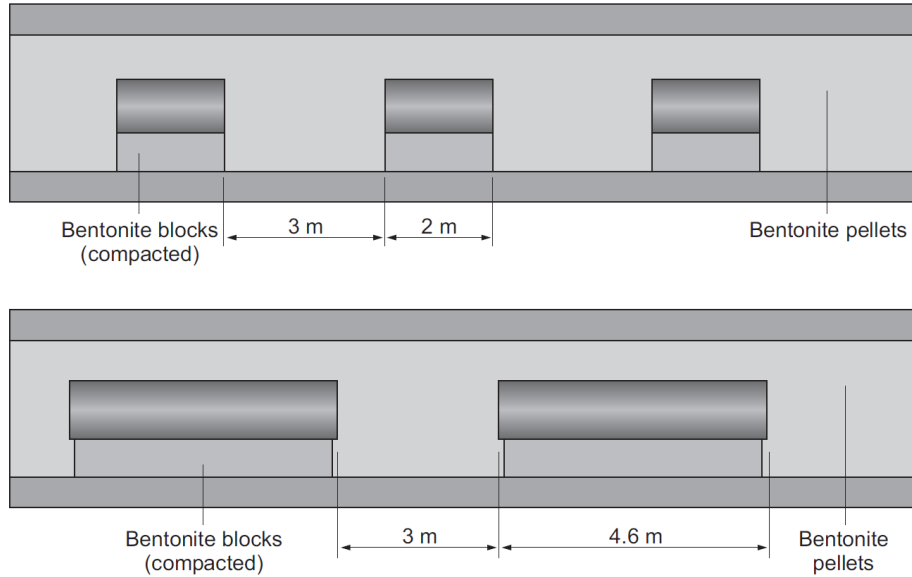
Source: NAGRA (2002b), Figure 4.5-7.

Figure 6.   The Swiss emplacement concepts for vitrified HLW (upper) and SNF (lower) waste packages

Table 6.   Reference bentonite pore water and alternative porewater compositions ("high pH" and "low pH") obtained by fixing P_{CO2} at the bounding values

Component	Low pH	D-RBPW	High pH
log P_{CO2} (bar)	-1.5	-2.2	-3.5
pH	6.9	7.25	7.89
pε	-2.22	-3.27	-4.78
Ionic strength (M)	0.356	0.323	0.263
	Conc. (mg L^{-1})		
K^+	65.3	60.6	54.0
Na^+	6690	6300	5720
Ca^{2+}	533	529	537
Sr	3.22	1.66	0.256
Mg^{2+}	217	186	149
Mn	2.01	1.29	0.264
Fe	4.32	2.42	0.447
Al	4.13E-04	5.18E-04	2.04E-03
Si	5.06	5.06	5.17
SO_4^{2-}	6140	5920	5370
HCO_3^-	427	173	35.8
Br^-	24.0	19.2	9.59
F^-	2.83	3.17	3.02
Cl^-	7300	5890	3050

Source: NAGRA (2002b)

2.2.2.4   Other Repository Programs

Canada

As noted in Section 2.2.1.4, Canada has historically focused on crystalline rock repositories, and has developed repository concepts for that setting. Concepts for disposal in sedimentary rocks have not been developed, but will likely include a carbon steel waste package and will be based on the Belgian, French, or Swiss designs (King 2010).

Spain

Spain has not yet selected a disposal site or host lithology for SNF or HLW. Preliminary repository concepts for clay and granite are provided in Kursten et al. (2004a) and are similar; in both, the waste package is carbon steel, 0.9 m in diameter and 4.5 m in length, with 10 cm thick walls, emplaced in a clay barrier of compacted bentonite bricks. The reference bentonite is sourced from the Almeria province. The mineralogical composition of the bentonite backfill is shown in Table 7. It is slightly higher in smectite content than the MX-80 reference material used by many other international organizations, but the accessory mineral assemblage is similar to those found in other potential backfill materials. Although no site has yet been chosen, the Spanish nuclear waste program has vigorously pursued research into metals corrosion in potential granite, clay, and salt environments. For representative conditions in clay, the Spanish program used two versions of Boom clay pore water, corresponding to oxic water and interstitial (anaerobic) pore water.

Table 7.   Mineralogical composition of the bentonitic backfill material being considered by the Spanish repository research program

Species	Content (%)
Major Minerals	
Smectite	92 ± 3
Plagioclase	2 ± 1
Quartz	2 ± 1
Cristobalite	2 ± 1
Tridymite	traces
Calcite	traces
Feldspars-K	Traces
Minor Minerals	
Carbonates (calcite, dolomite)	0.60 ± 0.13
Organic matter (expressed as CO_2)	0.35 ± 0.05
Sulfates (soluble, gypsum)	0.14 ± 0.01
Sulfates (low solubility, barite, celestite)	0.12 ± 0.05
Sulfides (pyrite)	0.02 ± 0.01
Chlorides (halite)	0.13 ± 0.02

Source: Kursten et al. (2004a), Table 2-9

2.2.2.5   Summary of Current Waste Package Concepts for Clay Repositories

To summarize, all current clay repository programs have chosen to use carbon steel waste packages. In the French and Swiss designs, the buffer is bentonite, and pH values will be near-neutral. The carbon steel acts as a corrosion allowance material and will corrode actively under both oxic and anoxic conditions; thick waste package walls (11 cm and 25 cm, respectively) are required to maintain waste package integrity for a period of 1,000–10,000 years. In the Belgian design, the waste package is enveloped in a cementitious buffer material; carbon steel behaves as a passive metal in the high pH environment. A thinner waste package (5 cm) is required to survive for the desired time interval, which corresponds to the thermal period (Kursten et al. 2011b). In all three cases, the waste packages are only intended to provide waste isolation for a relatively limited time; beyond that, the natural barrier is relied upon. Carbon steel was chosen for these environments because of the relatively short requirement for the waste package lifetime because although it may corrode rapidly, it does so at a very predictable rate; localized attack is not anticipated to occur. Although the corrosion rate may be locally elevated for a period of time, leading to a pitting-like attack, these regions are eliminated/consumed as the corrosion front advances.

2.2.3   Corrosion Studies Relevant to Clay Repositories

This section summarizes corrosion research that has been carried out by major repository science programs that is relevant to clay-hosted repositories. For experimental data produced prior to 2004, this summary relies heavily on the COBECOMA report (Kursten et al. 2004a), which provides an excellent summary of European research up to that date. More recent articles and summaries are cited for work after that publication. Corrosion research in environments relevant to clay repositories has largely been carried out by two programs, Belgium and the United Kingdom.

2.2.3.1   Belgium

Experiments carried out by the Belgian repository science program prior to development of the supercontainer concept in 2004 evaluated many different types of metals at conditions anticipated in a repository with a bentonite backfill, as opposed to a cementitious materials backfill. The work is summarized in Kursten et al. (2004b; 2004a) and in Kursten and Druyts (2006), and the discussion below is based on those works.

The Belgian Nuclear Research Centre carried out a large suite of *in situ* corrosion experiments in the Boom Clay at the Meuse/Haute-Marne (MHM) URL. They also carried out laboratory-based corrosion experiments in media representing expected environments in a Boom-Clay-hosted repository as it evolves over time. Testing in the *in situ* experiments was carried out by placing samples in contact with the following 3 media:

- a "humid clay atmosphere" (unsaturated clay)

- a "concrete-saturated humid clay atmosphere"

- undisturbed, saturated Boom clay

The first two represent potential conditions in the repository prior to complete rewetting of the backfill, and the last, the lost-term condition. The metal samples were placed in or on a steel support tube with a heater inside and inserted into the medium of interest, and then brought to the desired temperature (16ºC, 90ºC, or 170ºC) (Figure 7). After aging for up to several years, the tubes were withdrawn, and the samples analyzed.

Source: Kursten et al. (2004a), Figure 4-29

Figure 7.   Corrosion testing tube, being prepared for insertion into a test borehole in the Boom Clay formation

The laboratory-based experiments consisted of two types of electrochemical tests: (1) cyclic potentiodynamic polarization measurements; and (2) monitoring of the free corrosion potential (E_{CORR}) as a function of time. A limited number of immersion tests were also run. The test media were chosen to represent the repository environment as it evolved over time, and included synthetic oxidized Boom Clay water, synthetic interstitial Boom Clay water, synthetic bentonite water, real interstitial Boom Clay water, and slurries based on Boom Clay and on PRACLAY, a bentonite-sand mixture (Section 2.2.2.1).

A large suite of materials was used (Table 8), including carbon steel, stainless steels, and nickel and titanium alloys; many of these were also used in the *in situ* experiments. As most of these are anticipated to behave passively in repository environments, the experiments were largely directed at evaluating pitting and other localized corrosion processes. The experiments were designed to investigate the influence of important environmental parameters on the pitting behavior of the metal, including:

- Chemical composition of the medium. As noted above, several compositionally distinct bulk solution compositions were used, and individual species (chloride, sulfate, and thiosulfate) were varied over even larger ranges. The pH was not varied systematically, however, and all the test solutions fell within the relatively narrow range of pH 6.0 to 6.5.

- Temperature. Experiments were carried out at 16ºC, 90ºC, and 140ºC.

- Redox condition. Experiments were carried out under both oxic and strictly anoxic conditions.

- Radiolytic products. In one set of experiments, the H_2O_2 content was varied to simulate the effects of gamma radiation flux on solution composition at the waste package surface.

Results for in situ experiments

Following exposure for time periods varying from 1.7 to 7 years, the samples were analyzed. Maximum pit depth was determined by optical microscopy, and average general corrosion rate was determined by weight loss upon cleaning.

Carbon steel

The experimental results are shown in Table 9, and can be summarized as follows:

- Uniform corrosion rate increased with increasing temperature.

Table 8. Materials used in the Belgian corrosion testing program

Component:	Fe	Cr	Ni	Mn	Mo	Ti	Si	Cu	Pd	C	S	P	N	Others
In Situ Corrosion Programme														
EEG USINOR (C-steel)	bal	0.02	0.04	0.04	<0.01	<0.01	0.27	0.015	-	0.11	<0.01	0.02	-	Al: 0.04; Sn< 0.01
AISI 430 (f S.S.2)	bal	16.5	-	-	-	-	0.37	-	-	0.045	-	-	0.026	-
1803 MoT (f S.S.2)	bal	18.07	0.28	0.28	2.07	0.36	0.27	-	-	-	-	-	0.009	-
AISI 309 (a S.S.3)	bal	23	13	2	-	-	1	-	-	0.2	-	-	-	-
AISI 316 (a S.S.3)	bal	17.8	10.8	1.63	2.13	-	0.56	-	-	0.03	-	-	0.032	-
AISI 316Ti (a S.S.3)	bal	16-18	10-14	<2.0	3-Feb	>5×%C	<1.0	-	-	<0.08	-	-	-	-
UHB 904L (h.-a. S.S.4)	bal	18.65	26.34	1.12	4.49	-	0.44	0.12	-	0.014	-	-	0.0497	-
Hastelloy C-4 (Ni-alloy)	0.5	15.6	68	0.22	15.4	0.11	0.03	-	-	-	-	-	-	Co< 0.1
Inconel 625 (Ni-alloy)	3.57	12.2	bal	0.1	8.85	<0.02	0.2	0.02	-	0.0207	-	-	0.023	Nb: 2.7; Ca: 0.005; Mg: 0.02; Al: 0.01; Co< 0.05
IMI 115 (com. pure Ti)	-	-	-	-	-	bal	-	-	-	-	-	-	-	-
Ti 99.8-Pd (Ti-alloy)	0.06	-	-	-	-	bal	-	-	0.16	0.01	-	-	-	V< 0.03; Al: 0.008; Sn: 0.07
Laboratory Corrosion Programme														
TStE 355 (C-steel)	bal	0.03	0.03	1.12	-	0.003	0.344	-	-	0.18	0.002	0.01	0.005	Nb: 0.017
AISI 309S (a. S.S.3)	bal	22.58	13.51	1.7	-	-	0.33	-	-	0.063	0.002	0.021	-	-
AISI 316L (a. S.S.3)	bal	16.9	11	1.54	2.08	-	0.54	-	-	0.017	0.001	0.032	-	-
AISI 316L hMo (a. S.S.3)	bal	17.67	12.53	1.16	2.84	-	0.61	-	-	0.015	0.001	0.03	-	-
AISI 316Ti (a. S.S.3)	bal	16.8	10.7	1.08	2.05	0.3	0.4	-	-	0.044	0.009	0.028	-	-
UHB 904L (h.-a. S.S.4)	bal	19.7	25	1.48	4.47	-	0.19	1.51	-	0.019	0.001	0.019	0.08	-
Cronifer 1925hMo (h.-a. S.S.4)	45.45	20.6	24.85	0.92	6.4	-	0.3	0.86	-	0.005	0.002	18	0.198	-
Hastelloy C-4 (Ni-alloy)	0.98	15.75	67	0.04	15.85	<0.01	0.02	-	-	0.003	0.003	0.004	-	Co: 0.01
Ti 99.8-Pd (Ti-alloy)	0.04	-	-	-	-	bal	-	-	0.16	0.01	-	-	<0.01	O2: 0.13; H2: 0.001

Source: Kursten et al. (2004a), Table 4-29

Table 9.   Measured corrosion rates and maximum depths of penetration for carbon steel

Corrosion Medium	T (ºC)	Exposure period (yr)	γ dose rate (Gy h^{-1})	v$_{CORR}$ (μm yr^{-1})	d$_{MAX}$ (μm)
Direct contact with Boom Clay	170	4.7	0	8.59	n.d.
	90	1.7	0	7.68	240 (parent mat.)
	90	7	0	4.65	90 (parent mat.)
					130 (weld region)
	16	4.7	0	1.81	100-120 (parent mat.)
	16	3	0	8.57 (as)	260 (as)
				5.47 (p)	45 (p)
	80	5	400	3.8	150 (parent mat.)
				20.3	2,170 (weld region)
Contact with humid clay atmosphere	90	2	0	9.03 (as)	180 (as)
				3.24 (p)	30 (p)
				8.09 (cc)	245/105 (cc)
	16	2.5	0	5.13 (as)	195 (as)
				0.40 (p)	75 (p)
				5.18 (cc)	245/65 (cc)
Contact with concrete saturated clay atmosphere	90	2	0	0.73 (as)	60 (as)
	16	2.5	0	9.48 (as)	235 (as)
				1.31 (p)	50 (p)

Source: Kursten et al. (2004a), Table 4-32

v$_{CORR}$: average uniform corrosion rate

d$_{MAX}$:   maximum pit depth

as :   samples tested in the 'as received' condition (no surface treatment was applied)

p :   samples tested in the 'polished' condition

cc :   samples with an artificial crevice (max. pit depth edge of crevice / max. pit depth inside crevice)

- The uniform corrosion rate decreased over time.

- Pitting corrosion occurred, and maximum pit depths were many times the uniform corrosion depth.

- Both the uniform corrosion rate and the maximum pit depths were greater for "as received" samples than for polished samples.

- Maximum pit depths were slightly greater in weld and thermally affected regions relative to the parent metal; also, although data are sparse, pit depths in the weld region increased greatly in a high gamma flux environment.

- Corrosion rates were similar in the unsaturated, humid atmospheres and in the saturated clay environment.

The mechanism of corrosion was hemispherical pitting. Corrosion products varied little with temperature, and consisted largely of magnetite, hematite, and an iron oxy-hydroxide (goethite and/or lepidocrocite). The iron oxyhydroxide and hematite probably formed immediately after emplacement, while conditions in the emplacement boreholes were still oxic. Once anoxic conditions were re-established, iron corroded by reaction with water to form $Fe(OH)_2$ (see Reaction 4). The $Fe(OH)_2$ further oxidized to form magnetite (see Reaction 5).

Stainless steels and Ni- and Ti-based alloys

Several stainless steels, nickel alloys, and titanium alloys were included in the materials tested (Table 8). All of these alloys had very slow uniform corrosion rates in the test systems. Maximum corrosion rates were: stainless steel, 0.15 μm yr^{-1}; Ni-alloys, 0.018 μm yr^{-1}; and Ti-alloys, 0.06 μm yr^{-1}. For each of these metals, many tests yielded negative corrosion rates, indicating that these rates are largely at or near the detection limit for the weight loss procedure. In all cases, weld material was no more susceptible than the parent material, and a gamma radiation field had no measurable effect. Pitting was not observed on any of these materials.

Results for laboratory experiments

Cyclic potentiodynamic polarization measurements were used to evaluate the pit nucleation potential (E_{NP}) and the protection potential (E_{PP}) for each of the materials as a function of the environmental variables discussed previously. The results are as follows:

- Carbon steel—carbon steel corroded actively (uniform corrosion) in all media

- Stainless steels—the ranking of the of the materials tested from lowest to highest E_{NP}, is:

  AISI 309S < AISI 316L, AISI 316L hMo, AISI 316Ti < UHB 904L < CHRONIFER 1925hMo

  Both E_{NP} and E_{PP} shifted lower with temperature, indicating that pitting occurs more readily. Under both oxic and anoxic conditions, increasing chloride content decreased the resistance to pitting. Sulfate had an inhibiting effect with respect to pitting, slightly increasing the E_{NP} with increasing concentration, but having no appreciable effect on E_{PP}. Varying thiosulfate concentrations had no significant effect on E_{NP} or E_{PP} in cyclic polarization experiments, but elevated thiosulfate did increase the number of pits that formed in pit propagation experiments. All four stainless steels tested performed adequately under oxic conditions, such as would prevail in a Boom Clay repository for a time after closure. The pitting resistance increased dramatically under anoxic conditions, which would prevail in the repository over the long term. Although increasing temperature results in a large drop in the chloride concentration above which pitting occurs, at the expected maximum repository temperature of 140ºC, $[Cl^-]_{MAX}$ is still above the maximum value anticipated to contact the waste package (216 mg L^{-1}).

- Ni-alloys—Under oxic conditions, Hastelloy C-4 and C-22 did not pit in any test media at temperatures of 90ºC or lower, including those with elevated concentrations of chloride (up to 50,000 mg L^{-1}); however, the alloys did undergo crevice corrosion at 140ºC in solutions containing 20,000-50,000 mg L^{-1} chloride. Under anoxic conditions, no pitting was observed in any test media.

- Ti99.8Pd—Grade 7 titanium was resistant to pitting in all test solutions, at all temperatures.

Following development of the supercontainer concept in 2004, experimental work by the Belgian program focused on evaluation of localized corrosion processes for carbon steel, the chosen waste overpack material. In alkaline conditions (pH >10), carbon steel forms a passive oxide film which limits general corrosion rates to very low values. Under oxic conditions, the passive layer on carbon steel is hematite; under anaerobic conditions, it is magnetite (Kursten et al. 2011b). Should the pH drop below 10, the layer is destabilized, and carbon steel will corrode actively by reaction with water.

As carbon steel behaves passively in the high alkalinity environment of a cementitious buffer material, the type and extent of localized corrosion processes that might occur represent the greatest uncertainty in the performance of the waste package.

> *Proving the validity of the 'exclusion principle'. It is generally recognized that carbon steel exposed to concrete can undergo depassivation due to, for example, ingress of aggressive species. This can result in subsequent localised corrosion attack, such as pitting corrosion, crevice corrosion and stress corrosion cracking, which can lead to very rapid penetration of the overpack. The stochastic nature of localised corrosion makes it very difficult to predict the lifetime of the overpack. Therefore, we will have to present well reasoned arguments to prove that the carbon steel overpack will not be susceptible to localised corrosion phenomena under the high pH conditions prevailing within the Supercontainer.* (Kursten et al. 2011b)

This experimental work has been summarized in several recent publications (Macdonald et al. 2011; Winsley et al. 2011; Kursten et al. 2011b). In these experiments, carbon steel wafers were exposed to cement buffer pore waters under varying conditions of chloride content (0-100 mg L^{-1}), temperature (25ºC and 80ºC), and gamma radiation flux (0 Gy hr^{-1} and 25 Gy hr^{-1}). In other tests, the effects of sulfide and thiosulfate were evaluated. Corrosion behavior was monitored by measuring hydrogen generation rate over time in the experiment, by monitoring the passive current density, and by weight loss upon cleaning at the end of the experiment. Each method gave consistent results. The results for the hydrogen generation experiments are shown in Figure 8. Over the range of environmental conditions considered, corrosion rates were initially very high, but rapidly dropped to a very low level. The overall corrosion rate for the duration of the experiments, measured by integrating the hydrogen production results, was 2.1µm yr^{-1}, and agreed with the rate determined by weight loss measurements of 1.9 µm yr^{-1}. However, instantaneous corrosion rates, measured by hydrogen gas generation, dropped to 0.1–0.2 µm yr^{-1} by the end of the testing period (~18,000 hours). These results are consistent with the premise that localized corrosion will not adversely affect carbon steel overpack lifetimes in the Belgian Supercontainer design.

It should be noted however, at higher concentrations of aggressive aqueous species (chloride, sulfide, and thiosulfate), the passivity of carbon steel is reduced, eventually to the point that localized corrosion can occur. Concentrations of aggressive species in the Boom Clay pore waters are much greater than the range examined in these experiments. The conclusion that localized corrosion will not affect overpack lifetimes is based on concentrations predicted by modeling of the transport of these species through the cement buffer to the waste package surface.

2.2.3.2   United Kingdom

Prior to the development of the Belgian supercontainer, disposal of SNF or HLW in a cementitious backfill was not generally considered. However, the United Kingdom did evaluate such a concept for disposal for low and intermediate-level waste, and performed corrosion experiments with carbon steel (BS4360 grade 43A) and with stainless steels (AISI 316L and AISI 304L) in cementitious environments under both aerobic and anaerobic conditions. As noted previously, Fe-based materials behave as passive metals in highly alkaline environments. The experimental work carried out in the United Kingdom is summarized in Smart et al. (2004) and Kursten et al. (2004a).
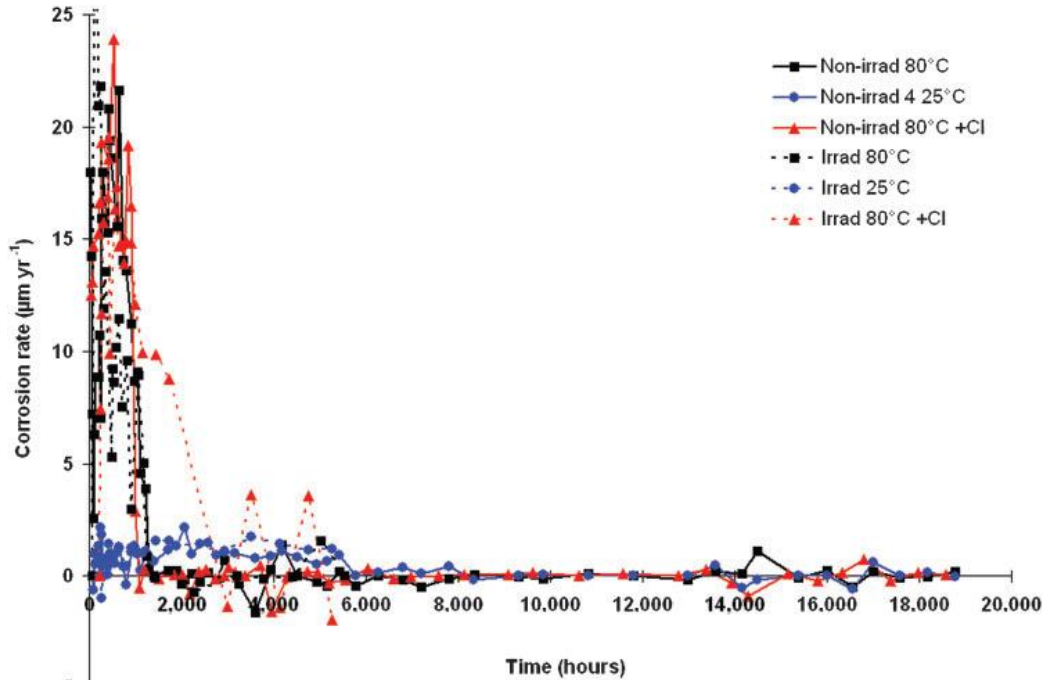
Source: Winsley et al. (2011), Figure 2

Figure 8.   Anaerobic corrosion rate for carbon steel in concrete pore solution, under non-irradiated and irradiated conditions (25 Gy hr^{-1}), as a function of temperature and chloride concentration (100 mg L^{-1})

Carbon steel

Under aerobic conditions, uniform corrosion rates for carbon steel were 0.08 µm yr^{-1} at 30ºC, and 1.6 µm yr^{-1} at 80ºC. Measured anaerobic corrosion rates varied widely with the method of measurement. Electrochemical corrosion measurements and weight loss measurements yielded much larger corrosion rates than volumetric gas measurement and gas chromatography, techniques which are based on hydrogen generation rate. At the very low corrosion rates typical of anaerobic corrosion of steel, the measurements based on hydrogen generation are considered more accurate. Corrosion occurred in three stages (Smart et al. 2004):

- a period of high corrosion rates, varying linearly with time; this initial rate increased with increasing temperature, following an Arrhenius relationship, but decreased more quickly with time at higher temperatures,

- a period during which the corrosion rate fell by up the three orders of magnitude, with the rate decreasing in proportion with the logarithm of time,

- a third stage in which a very slow decrease in corrosion rates was observed, with rates falling below 0.1 µm yr^{-1} in all environments tested.

Measured corrosion rates were initially as high as ~29.6 µm yr^{-1} (at 80ºC in 0.1 M NaOH), but rapidly dropped to much lower values. The decrease in corrosion rate coincided with the development of an oxide layer, which was identified as ferrous hydroxide at 30ºC and as magnetite at 50ºC and 80ºC (Smart et al. 2004). The two hydrogen generation methods gave consistent estimates of the long-term anaerobic corrosion rate of carbon steel of <0.1 µm yr^{-1} at 30ºC and <1.0 µm yr^{-1} at 80ºC (Kursten et al. 2004a).

Localized corrosion of carbon steel embedded in cement can occur if chloride concentrations are sufficiently high. The British evaluated the effect of chloride content on pitting as a function of temperature, and found that chloride concentrations of 6,000 to 28,000 mg L^{-1} were sufficient to cause

pitting at ambient temperatures; however, the threshold dropped to 4,000 mg L^{-1} at 50ºC and to less than 300 mg^{-L} at 80ºC. Pitting occurred quite rapidly, and maximum depths of penetration, after test durations of a few years, were up to several mm (Table 10). At this rate of penetration, carbon steel would not be an effective waste package material. However, Kursten et al. (2004a) conclude that rates may not be sustainable under repository conditions because oxygen diffusion through the saturated backfill will be insufficient to support pitting more than a few years after closure. Hence pitting penetration of more than a few mm is unlikely.

Table 10.   Measured maximum penetration depths for carbon steel plates, fully embedded in cementitious material, and immersed in Ca(OH)$_2$ solutions containing 10,000 mg L^{-1} chloride

T (°C)	Test duration (yrs)	Observed P_{MAX} (mm)
Ambient	1.55	3.94
Ambient	2.55	2.08
50	1.55	2.36
50	2.53	2.21
80	1.53	3.99
80	2.49	1.12

Source: Kursten et al.(2004a), Table 4-52

Stainless steel

Under oxic, alkaline conditions, uniform corrosion rates for stainless steels are low. Measured data for 316L stainless steel, in alkaline environments with no added chloride, varied from <0.1 μm yr^{-1} at 30ºC to 0.2-0.8 μm yr^{-1} at 80ºC. Under anoxic conditions, estimated corrosion rates are much lower, ranging from 0.1 μm yr^{-1} to 0.001 μm yr^{-1} over the same temperature range. However, the higher rates were measured in electrochemical polarization experiments designed to be favorable for corrosion. Based on the British experimental program, the best estimates of the long-term general corrosion rate for stainless steel under anaerobic conditions is <0.01 μm yr^{-1} (Kursten et al. 2004a).

The British program also investigated localized corrosion of stainless steel. No pitting of 316L was observed under any experimental conditions, in alkaline solutions containing up to 100 g L^{-1} chloride at ambient temperatures, or 50 g L^{-1} chloride at 45ºC and 70ºC. Pitting of 304L stainless was only observed at 60ºC is systems with >50 g L^{-1} chloride. Pitting and repassivation potentials for 304L and 316L as a function of pH, at 50ºC and with 20 g L^{-1} added chloride, were also measured. Except for 304L at the lowest pH conditions (<pH 4.0), the corrosion potentials were significantly below the pitting potentials, indicating that stainless steels are not susceptible to pitting under the range of conditions tested. Crevice corrosion of 304L stainless steel was also evaluated at 40ºC and 80ºC and varying chloride contents. Crevice corrosion can generally initiate at less aggressive conditions than pitting corrosion. No crevice corrosion was observed at 40ºC in chloride concentrations up to 20 g L^{-1}; at 80ºC, the crevice corrosion was only observed at chloride concentrations of 20 g L^{-1} or higher (Kursten et al. 2004a).

Stress corrosion cracking (SCC) of stainless steel is not anticipated to occur in repository settings. However, it was observed incidentally in an unstressed sample of 304L stainless steel that had been aged in cementitious material containing 100 g L^{-1} chloride for 2 years, occurring in areas on the sample with residual stresses. Additional testing in alkaline solutions containing elevated chloride and thiosulfate (potentially present through sulfide oxidation, at least early in the post-closure history) showed that

thiosulfate greatly enhances the occurrence of SCC, but only at chloride and/or thiosulfate concentrations in excess of what would be expected in a repository setting (Kursten et al. 2004a).

2.2.4   Additional Research Needs for Engineered Materials Performance in Clay Repositories

Evaluation of engineered materials performance in environments represented by clay repositories is a mature field of research, as clay units have been selected as repository host rock by several members of the European Community and are under consideration by several other nations with repository programs. Several recent summaries of that corrosion work identify research needs (Féron and Macdonald 2003; Kursten et al. 2004b; Kursten et al. 2004a; Bennett and Gens 2008; Féron et al. 2008; 2009; Kursten et al. 2011a; Kursten et al. 2011b). Although carbon steel is the consensus choice for waste package material in clay-hosted repositories, many of the issues that have been identified have a general application to corrosion allowance materials as a group.

In clay repositories, a great reliance is placed on the natural barrier as the long-term barrier to radionuclide releases. The clay host rocks have no fracture porosity and very low matrix permeabilities, and radionuclide transport is slowed further by sorption and ion exchange. The waste package is important for waste isolation only for a relatively short period after closure, when the thermal pulse perturbs the natural system. During this period, use of the observed natural system as an analog for post-closure processes is less certain. The thermal period lasts 1000-10,000 years, and that is the requirement for the lifetime of the waste package in clay repositories. The most important characteristic of the waste package material is not that the corrosion rate be low, but rather that the corrosion process be well understood and the penetration rate well constrained. The approach used to achieve this in the French and Swiss repository programs is to use carbon steel, a corrosion allowance material. Corrosion allowance materials corrode actively not only during the short oxic period immediately after repository closure, but also during the long-term anoxic period (water itself will corrode iron). Although the corrosion rate of carbon steel is not low, the penetration rate for a given thickness is well constrained, because the effects of localized corrosion are minimal. Localized corrosion (e.g., pitting) generally contributes uncertainty to the penetration rate, but for active materials, the advancing general corrosion front rapidly consumes any pits that form, and localized corrosion has little effect on the overall lifetime of the thick waste package (11 and 15 cm for the French and Swiss waste package designs).

In the Belgian supercontainer concept, a carbon steel waste overpack is also used. However, it is embedded in a cementitious buffer, and in alkaline environments, carbon steel is a passive metal and behaves as a corrosion resistant material. General corrosion rates are very low and the 3 cm thick waste package is estimated to have a lifetime of >1000 years.

Therefore, although many materials have been tested in the relevant environments, knowledge gaps for clay repositories largely address confirmation of the expected behavior of carbon steel in the clay environment. The following topics have been identified as potentially requiring further research:

- Carbon steel interactions with buffer/backfill materials.

  Several aspects of carbon steel interaction with the buffer materials require further research. Additional research is necessary to understand diffusion of corrosion-active species (e.g. chloride or sulfide) through buffer material, and the potential effects on long-term corrosion rate. In addition, potential feedbacks between H_2 production and transport, water saturation and corrosion are poorly understood (Bennett and Gens 2008). If H_2 is generated at a more rapid rate than it can diffuse from the metal surface, it can inhibit further corrosion, or, in extreme cases, it could build up, form a gas bubble, and disrupt the buffer material. This could result in formation of preferred-flow pathways and potentially rapid radionuclide release. Also, if a high H_2 overpressure can occur, then use of steels that are not susceptible to hydrogen embrittlement must be considered (Féron et al. 2009). Finally, interactions between aqueous Fe species and smectite clays in the backfill are of concern.

Aqueous Fe can destabilize smectites, causing dissolution of smectite and precipitation of Fe-rich serpentine minerals and carbonates (Bildstein et al. 2006; Wilson et al. 2006a; Wilson et al. 2006b; Schlegel et al. 2008; Gaudin et al. 2009; Mosser-Ruck et al. 2010; Savage et al. 2010). This results in loss of cation exchange and swelling capacities and changes in porosity, and potentially limits radionuclide sorption and the effectiveness of the backfill as a barrier to releases. Even in the absence of recrystallization, exchange of Fe species into smectite will reduce the degree of swelling and modify ion exchange properties relative to, for example, a Na-smectite (Manjanna et al. 2009).

- Use of archaeological analogs.

  Archaeological analogs provide information for long-term carbon steel corrosion rates in natural environments (Dillmann et al. 2007). However, corrosion product mineralogy and structure could provide insights into long-term corrosion processes and are rarely well characterized. Also, better methods of characterizing the thickness of the corrosion layer, used to estimate the corrosion rate, are needed (Kursten et al. 2004a; Féron et al. 2008; 2009).

- Verification of the localized corrosion behavior of carbon steel in alkaline environments.

  The Belgian supercontainer is a relatively new concept, first proposed in 2004. In the alkaline environment of the cementitious buffer, the metal behaves passively and general corrosion rates will be very low. This strategy assumes that localized corrosion processes cannot take place in the alkaline environment, an assumption which has been identified as requiring further confirmation in assessments of the Belgian concept. However, the Belgian repository program has been actively addressing this, and recent studies summarized in Kursten et al. (2011b) have shown that LC processes are unlikely to have a significant impact on container lifetime. This topic may not require additional research.

There are several other general research needs that have been identified (Kursten et al. 2004b; Kursten et al. 2004a; Féron et al. 2008; 2009). These apply not only to clay repositories, but to all types of repositories, and in some cases, to interim storage as well. These include:

- Aspects of container fabrication and design that may affect corrosion—e.g., effects of thermal treatments and welding and effects and mitigation of residual stresses.

- Long-term metallurgical modifications due to long term radiation flux or thermal aging. These include dealloying, segregation, creep, and growth of grains.

- Influence of radiation effects on the environment for corrosion. In anoxic repository settings in particular, radicals produced by radiolysis could contribute significantly to container corrosion rates.

- Determining the evolutionary path of the near-field environment through time and its impact on corrosion. The repository environment evolves through time, and impacts on corrosion rates and mechanisms are poorly understood. Early in the repository history, conditions will be oxic, until the available oxygen is consumed. The waste package temperature changes over time, and redox conditions may evolve further as hydrogen is produced by corrosion and builds up or diffuses away from the waste package surface. The evolving radiation field will affect the chemical environment (e.g. concentration of H_2 and oxidizing radicals) around the package. Interactions between products of corrosion (e.g. Fe^{2+}) and the clay buffer may lead to irreversible changes in the clay and its ability to buffer the local environment.

- Modeling. Most approaches for modeling the penetration rates of passive corrosion resistant materials and localized corrosion effects on corrosion allowance materials are empirical or semi-empirical. More mechanistically-based models would provide greater confidence in predicted long-term penetration rates and waste package lifetimes.

2.3   Granite-hosted Repositories

Several international repository programs have chosen to pursue repositories in crystalline rock, commonly referred to as "granite" repositories. Programs considering granite-hosted sites include Sweden, Finland, Canada, Japan, and Korea, although only Sweden and Finland have identified repository sites. The structure of this section will follow that of the clay repository discussion; each repository site and potential waste package concept is described, followed by a discussion of relevant corrosion research, and an identification of additional research needs.

2.3.1   The Natural System

In this section, a short description of the host rock mineralogy and general pore water compositions is provided for the repository programs that have chosen granite host rocks.

2.3.1.1   Sweden

Geologic setting

Sweden will dispose of SNF and HLW in a permanent geologic repository in crystalline rock. It has considered two major sites, Forsmark and Laxemar, and submitted a preliminary safety analysis for both in 2006 (SKB 2006b). In 2011, Svensk Karnbranslehantering AB (SKB), the Swedish Nuclear Fuel and Waste Management Company, submitted a license application and a finalized safety analysis for the Forsmark site (SKB 2011). Both sites are located in crystalline rock. At Forsmark, the planned host rock is crystalline Precambrian (1,860 to 1,890 Ma; Selnert et al. 2008) meta-igneous rocks of granitic to granodioritic composition, with lesser amounts of tonalite. The normative mineralogy of the rocks (Sandström and Tullborg 2006), is 21.6–39.0 wt% quartz; 14.2–29.0 wt% K-feldspar; 27.0–41.0 wt% plagioclase (An_{10-30}); 3.4–11.6 wt% biotite; and minor muscovite, epidote, and titanite. Trace amounts of calcite, magnetite, apatite, and rarely, pyrite, are also present. Open fractures are present throughout the rock and persist to the repository depths of ~500 m. At depth, fracture minerals include quartz, calcite, hematite, pyrite, albite, and chlorite/corrensite (Arcos et al. 2006).

Similarly, Laxemar is dominated by igneous rocks formed during the end of the Svecokarelian orogeny (1,810-1,760 Ma). The dominant rocks include granites, syenites, diorites, and gabbros, as well as related volcanic rocks. Eight different rock domains were found and defined (SKB 2006a), including areas dominated by the Avro granite, fine grained diorite, quartz monzodiorite, and mixtures of these. Smaller bodies of more mafic composition (diorite to gabbro) are common in the Avro granite and diorite domains, and low grade ductile shear zones cut through all the domains.

Fracture filling minerals are quite diverse, and include clays, zeolites, oxides, carbonates, and others. The general frequency of occurrence is:

> calcite and chlorite >> epidote, quartz, and clay minerals > pyrite >
> hematite, adularia and prehnite >> zeolites.

Other minerals are less common, but can locally dominate the fracture mineralogy. These minerals include gypsum, muscovite, amphibole, talc, and goethite (Drake and Tullborg 2009).

Pore water chemistry

Pore water compositions in the Forsmark area are a mixture of waters from several different sources, and vary with depth. Meteoric water dominates the first several hundred meters and this water is typically quite fresh with <200 mg L^{-1} Cl. As depth increases (~250-900 m) the Cl concentration increases to 200-10,000 mg L^{-1}, and the waters are a mixture of two brackish waters, including a non-marine groundwater that was present before the last deglaciation and water introduced since the last deglaciation. Within the 600-900m depth range, groundwater flow rates are slow and the age of the water increases considerably. Below 900 m the groundwater composition changes from brackish non-marine to saline groundwater.

The saline groundwater is on the order of 10^5 years old. Below 1200 m there is a transition to very highly saline waters (>20,000 mg L^{-1} Cl).

Pore waters extracted from drill cores have similar concentrations to the fracture water. At shallower depths (<~620 m) the water is a dilute Na-HCO$_3$ type. Below this level the pore water makes an abrupt transition to Na-Ca-SO$_4$. It is surmised that the reason for the transition is due to the reduced presence of transmissive fractures and a change in lithology from Avro granite to quartz monzodiorite. The Na-Ca-SO$_4$ type pore waters have a locally unique geochemical evolution and a restricted vertical distribution. Below this water, there is another layer of dilute Na-HCO$_3$ type water. At the deepest extent of the drill cores (~820-930 m), the water is dominated by Na-Ca-Cl type waters. At the same depth, the frequency of water-conducting fractures also decreases (Laaksoharju et al. 2009). In modeling studies, five different end-member pore water compositions have been defined: Deep Saline, Glacial, Littorina, Old Meteoric, and Altered Meteoric. Each of these waters was calculated to be in equilibrium with a different set of minerals and fracture fills based on their origins (Salas et al. 2010). In performance assessment calculations, it is recognized that several processes could affect the degree of mixing that occurs at the repository level, including changes in rainfall, glaciation, and sea level changes.

Three of the end-member compositions are shown in Table 11. The first is a relatively saline water from Forsmark, which is suspected to originate as Littorina sea water. The Littorina sea existed prior to 8,000 years ago, and was more saline that modern sea water. Also shown is a dilute water composition representing typical glacial melt water (Arcos et al. 2006). Finally, a representative concentration for the deep saline water from the Forsmark area is shown. These end-member compositions bound the range of likely water compositions at the Forsmark and Laxemar sites.

Table 11.   Chemical composition of groundwaters at the Forsmark and Laxemar sites

Component	Forsmark	Grimsel Ice-melting	Laxemar Saline
pH	7.2	9.6	7.9
pe	-2.42	-3.38	-5.08
HCO$_3^-$	134.2	27.46	6.10
Ca	933.9	5.61	18,597
Cl	5424	5.67	45,379
Fe$_{tot}$	1.85	1.68×10^{-4}	1.68×10^{-4}
K	34.21	0.20	27.37
Mg	712.1	0.02	2.43
Na	2041	15.86	8023
SO$_4^{2-}$	653.2	5.86	864.5
Si	5.20	5.76	2.25

Source: Arcos et al. (2006)

Note: pH and pe in standard units, all others in mg L^{-1}.

2.3.1.2   Finland

Geologic setting

The lithology at the Olkiluoto site consists of high-grade metamorphic and igneous rocks of the Svecofennian domain. The metamorphic rocks include magmatic gneisses and homogenous, banded or weakly migmatized gneisses such as mica gneisses, quartz gneisses, mafic gneisses, or tonalitic-

granodioritic-granitic genisses. The gneiss variants are gradationally present, with no distinct boundaries between these end-members. The igneous rocks include pegmatitic granites and sporadic diabase dykes. The rocks vary from >1900 Ma to about 1600 Ma (diabase dikes) in age (Andersson et al. 2007). All rock types are present within the volume comprising the planned repository emplacement drifts, at a depth of ~420 m (Pastina and Hellä 2006). Major minerals in these rock types include: mica, quartz, feldspars, cordierite, hornblende, chlorite, amphibole, pyroxene, olivine, and albite. Three different periods of alteration have been identified: a retrograde metamorphic phase (~1900-1800 Ma ago), a hydrothermal phase (~1580-1570 Ma and 1270-1250 Ma) associated with late-state igneous intrusions, and surface weathering (~10 Ma-present). The first of these is regional in extent and has little effect on construction and long-term safety of the site. The hydrothermal alteration is present as both fracture-related and pervasive alteration, and led to significant fracture fillings of Fe-sulfides, clay minerals (illite, smectite, and kaolinite), and calcite. The surface weathering is spatially related to the hydrothermal alteration and is caused by the interaction with meteoric waters and atmospheric oxygen (Andersson et al. 2007).

Pore water geochemistry

The hydrogeochemical history and setting of the Olkiluoto site is similar to that of the two Swedish sites. The groundwaters are marine in origin, and have high TDS with depth, where waters correspond to older, more saline Littorina Sea waters (~8000 years ago). Brackish water (TDS<10 g L^{-1}) is found between 30 and 400 m, representing mixing of modern recharge (rain water and seawater), glacial melt water from the last glacial melt (~10,000 years ago) with original Littorina marine waters. Within this interval, the dominant anion is chloride, but carbonate is significant at shallow depths, and there are high sulfate waters from 100-300 m, indicating a marine origin. Sodium and calcium are the dominant cations, although magnesium is present in the high sulfate waters. The pH range is from 7.5-8.2. Deeper waters become more saline (up to 83 g L^{-1}); the original saline end-member is attributed to brines that intruded long ago during hydrothermal activity (possibly early Phanerozoic, or even preCambrian), and that have since been diluted with meteoric water (Andersson et al. 2007). Below 400 m, the waters are mostly chloride-rich; there is little or no sulfate. This complex hydrochemical mixing is illustrated in Figure 9.

Oxygen is consumed via oxidation of organics in the upper few tens of meters, and sulphidic redox reactions (SO_4^{2-}/HS^-) appear to control redox to values of -170 to -280 mV at depths of 100-300 m. Below that, methanogenesis (the CO_2/CH_4 redox pair) controls the redox to values of -330 to -270 mV. The boundary between the two zones occurs at about 300 m; at this depth, SO_4-rich, marine-derived groundwater mixes with methane-rich saline waters, and microbial activity results in locally high levels of dissolved sulphide (up to 12 mg L^{-1}) and carbonate, which may precipitate as pyrite and calcite. Isotopic and dissolved gas studies indicate that below 300 m depth the groundwater system has not been affected by glacial transients. These same studies show no connection to oxidizing glacial melt, or to present-day marine waters (Andersson et al. 2007).

The salinity in the repository horizon (~400 m) is 10-20 g L^{-1} TDS, and the waters are slightly alkaline. They are below the mixing zone between the sulfate-rich upper waters and the methane-rich saline waters, and have low alkalinity and low dissolved sulfide concentrations. However, the Finnish safety case considers not only these waters, but possible downward infiltration of oxic waters or sulfide-rich waters, or upwelling of the deep, concentrated, Cl-rich brines, and the results of mixing of those waters. Thus, a range of water compositions must be considered as potentially relevant to the repository environment. Individual water compositions are not provided here, but are generally similar to those given in Table 11 for the Swedish sites.
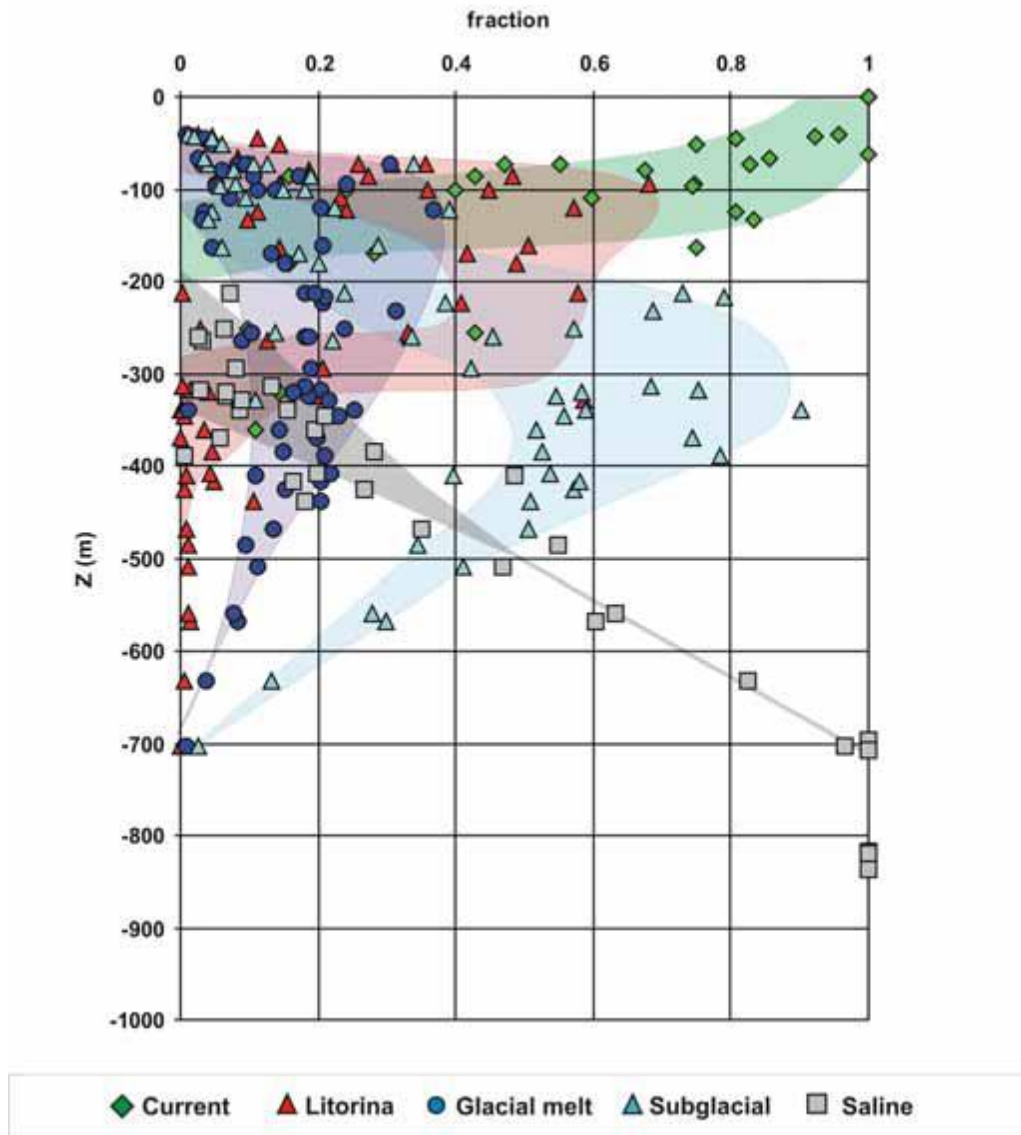
Source: Pastina and Hellä (2006), Figure 2-16

Figure 9.   Based on chemical and isotopic studies, Olkiluoto fracture waters represent a mixture of several sources

2.3.1.3   Other Repository Programs

France

In addition to repository research in clay ("Dossier 2005 Argile"; ANDRA 2005a; 2005b; 2005c; 2005d), the French program has evaluated nuclear waste disposal in granite. Since a French URL does not exist in granite, the French effort consisted of participation in experiments conducted in other granite-based URLs, including Sweden (Äspö), Switzerland (Grimsel), Canada (Lac du Bonnet) and Finland (Olkiluoto). A preliminary generic safety analysis based on this work is presented in the "Dossier 2005 Granite" (ANDRA 2005e; 2005f; 2005g; 2005h). As no potential granite site has been identified, the safety analysis did not produce specific conclusions regarding the performance of a granite repository. Instead, it assessed the potential of the granite medium, proposed generic concepts for meeting the long-term safety objectives, and verified that none of the problem areas examined ruled out feasibility. As this

work was generic in nature and took place at locations (environments) discussed elsewhere in this report, it is not discussed further here. The reader is referred to the "Dossier 2005 Granite" for additional information on the French granite program.

Canada

As noted previously, site selection has not yet occurred in Canada, but the Canadian program has largely focused on disposal in the crystalline basement of the Canadian Shield. The Canadians have a URL in the Lac du Bonnet batholith, which was emplaced during the end of the Kenoran event (2760-2670 Ma). The pluton consists primarily of biotite granite, but xenoliths and tonalites and amphibolites, with some granitoids are also present. Dikes, consisting of irregular pegmatite masses, porphyroblastic schlieren, and quartz veins also occur throughout the area (Everitt and Lajtai 2004).

Ambient groundwater chemistry in the crystalline basement rock has been determined from 86 individual fractures identified in 53 boreholes near the URL (Gascoyne 2004). The boreholes cover a depth regime up to 1000 m. Also, the shallow hydrogeochemistry was characterized through 28 ground water wells extending into the clay-rich overburden at the site. Overburden pore water is dominated by Ca-Mg-HCO_3-SO_4. In the shallow fractured environment, the water is dilute (TDS < 0.3 g L^{-1}) and is dominated by Ca-Na-HCO_3. These waters do not appear to be actively mixing with the overburden waters. However, down to depths of ~200 m, the water appears to be relatively well connected to meteoric cycles with a ground water age on the order of tens to hundreds of years. With increasing depth (200-400 m) the water becomes more saline (5-20 g L^{-1}), more alkaline, and is dominated by Na-Ca-HCO_3-Cl-SO_4 while ages increase to 10^3-10^5 years. At great depths (>500 m), the fracture waters are increasingly saline (up to 50 g L^{-1} at 1000 m) and are increasingly dominated by Na-Ca-Cl. Isotopic data suggests the deeper saline waters are greater than 10^6 years old, and may be much older, possibly even originating as evaporated brine from marine incursions in the early Devonian (400 Ma) (Bottomley et al. 1994; Gascoyne 2004), although high fracture water salinity has been attributed to water-rock interactions in other parts of the Canadian shield (Gascoyne and Manineni 1994).

Pore waters collected at ~400 m in the Lac du Bonnet URL vary compositionally from the fracture waters at the same depth. They are Ca-Cl waters, and isotopic data indicate they are older than the fracture waters and have experienced a greater degree of water-rock interaction (Gascoyne 2004).   The salinity varies with the collection method; seepage into sealed boreholes is more saline (up to 90 g L^{-1}) than water collected from core samples by ultracentrifugation or porewater compositions determined by leaching cores (10-39 g L^{-1}). It is possible that the borehole waters were concentrated by evaporation; alternatively, the samples extracted from core fragments may have been diluted by drilling fluids (Russell et al. 2007).

Spain

As noted previously, Spain has not yet selected a final disposal site for SNF or HLW, nor even chosen a host rock. However, Spain has conducted extensive corrosion research in environments characteristic of salt, clay, and granite host rock.

2.3.1.4   General Chemical and Physical Environment in Granite Repositories

Granite-hosted repositories are reducing in the long term, but the host rock is organic poor and generally contains only minor (and sometimes very local) sulfides. The redox buffering capacity is low. As with the clay repositories, the engineered barrier system will initially be oxic but will eventually become anoxic, because of biotic and abiotic reactions with organic material and sulfides in the buffer and in the host rock and because of metal corrosion. While the host rock matrix permeability is very low, there is significant fracture permeability. At planned repository depths, fracture and pore waters represent mixtures of water from many different sources, and the end-members vary widely in composition and salinity. Surface infiltration and glacial meltwaters are highly dilute, modern and ancient seawater are moderately saline, and deep, very old waters are highly saline. As with the clay repositories, the

composition of water contacting the waste package will be strongly influenced by interactions with the bentonitic backfill material. Although the host rock is not as temperature sensitive as clay, maximum waste package surface temperatures are limited to 100ºC, to protect the swelling properties of the buffer. Planned repository depths are 400-600 m in Sweden and Finland and 500-1000 m in Canada (site not chosen).

2.3.2   Current Granite Repository Concepts

This section provides the current repository concepts for repository programs considering granite as a host rock. As with the clay repositories, all repository concepts for granite include a bentonitic backfill.

2.3.2.1   *Sweden*

Waste package

The Swedish waste package concept is known as the KBS-3 (Figure 10). The waste package has an outer corrosion barrier of high purity copper, with a wall thickness of 49 mm and end plate thicknesses of 50 mm. The package has an insert of nodular cast iron, with either four channels for PWR fuel assemblies, or twelve channels for the smaller BWR fuel assemblies. The channel tubes are made of steel and are welded to form a cassette which is placed in the mould during casting. Once fuel assemblies are placed in the channels, the insert is sealed with a gasketed steel lid. Then, the end plate is welded onto the copper outer shell by friction stir welding. The waste package length is 4.84 m, width, 1.05 m. Empty, the heavier PWR package weighs 23.9 metric tons (SKB 2010b). The waste packages will be emplaced vertically, in short boreholes in the floor of the underground adits (Figure 11). A horizontal emplacement strategy has also been considered and is included in the license application as an option. However, it is not as developed as the vertical option; additional technology development and research are required before it could be implemented (SKB 2011).

The primary function of the copper outer shell is to provide corrosion protection, while the insert provides strength and pressure-bearing capacity to withstand bentonite swelling and hydrostatic pressures in the repository setting. Copper metal is generally considered to be the thermodynamically stable phase under reducing conditions (although recent studies have disputed this; Section 2.1.3.2), and the lifetime of the copper outer barrier is anticipated to be >1,000,000 years (Kursten et al. 2004a; King et al. 2010; King et al. 2011; Kwong 2011).

Bentonite backfill

The major functions of the backfill are to limit the transport of copper corroding agents to the canister and the transport of radionuclides away from the canister. The basic criteria to fulfill both of these requirements are that the hydraulic conductivity is $<10^{-12}$ m s^{-1} and that the swelling pressure is >1 MPa. It is further preferred that the swelling pressure be >2 MPa to limit microbial activity. The two reference bentonite materials for the Swedish repository are MX-80 (USA origin) and IBECO RWC (Greek origin). Table 12 shows the average mineral compositions and Table 13 shows the average chemical compositions of the two reference materials. The averages represent analyses from different samples of the clay source. The swelling capability is linked to the montmorillonite content, and the value in both clays is fairly consistent. The presence of more soluble minerals can affect long term backfill performance. For example, large amounts of gypsum can potentially be dissolved and removed as time proceeds, which can lead to a decrease in backfill density and swelling pressure. Ancillary materials and minerals are limited by the following criteria: total sulfide content <0.5% of total dry mass, total sulfur <1% and total organic carbon <1%. Few other hard criteria exist.
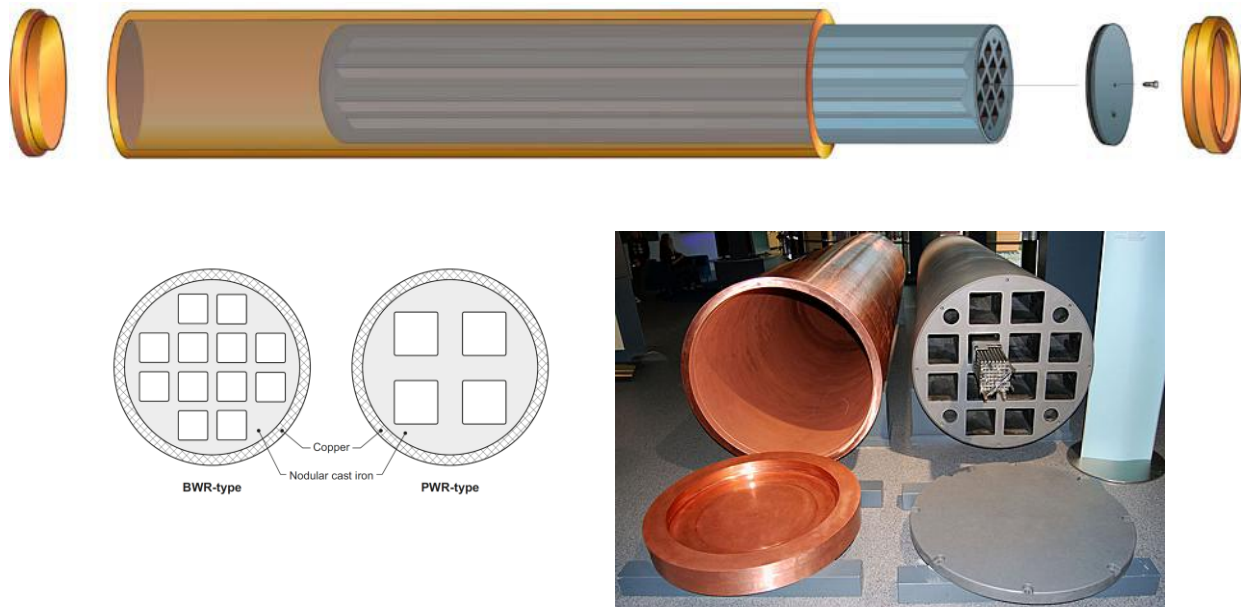
Source: SKB (2010b), Figures 3.2 and 3.3

Figure 10.   The Swedish KBS-3 waste package concept
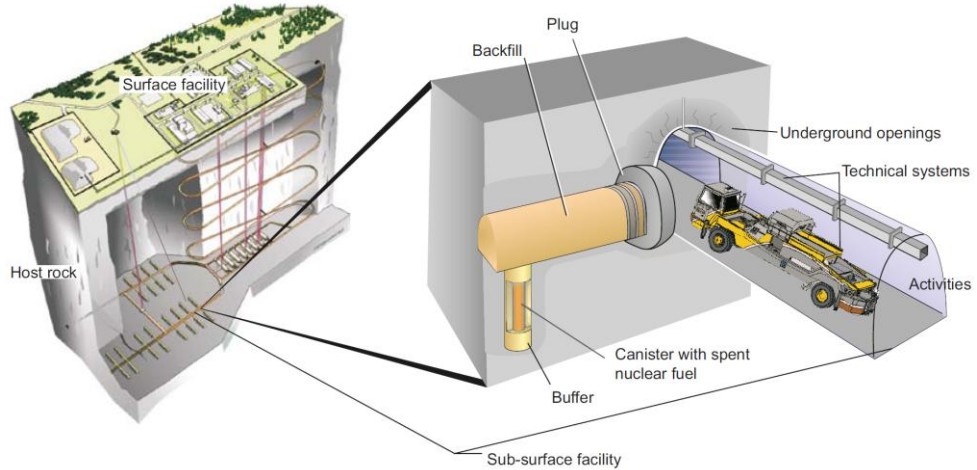
Source: SKB (2010b), Figure 1.1

Figure 11.   The Swedish KBS-3 repository and emplacement design

Table 12.   Average and standard deviation of mineralogical composition of the two reference bentonites as determined by XRD (values in wt%)

Mineral	MX-80		IBECO RWC	
	Average	Std. Dev.	Average	Std. Dev.
Montmorillonite	81.4	1.7	81.4	1.4
Illite	0.8	0.1	4.6	0.4
Calcite	0.2	0.5	5.3	1.0
Dolomite			1.3	0.1
Cristobalite	0.9	0.8		
Gypsum	0.9	0.2		
Muscovite	3.4	1.0	1.4	0.5
Plagioclase	3.5	1.0		
Goethite			1.5	0.1
Pyrite	0.7	0.2	1.1	0.1
Quartz	3.0	0.4		
Tridymite	3.8	1.2		

Source: Adapted from Karnland (2010)

Table 13.   Chemical composition of the two reference clays considered as possible backfill in the Swedish program (values in wt%)

Component	MX-80	IBECO RWC
SiO_2	67.4	60.89
Al_2O_3	21.2	19.77
Fe_2O_3	4.14	5.75
MgO	2.61	3.68
CaO	1.46	6.77
Na_2O	2.25	0.82
K_2O	0.55	0.98
TiO_2	0.17	0.88
P_2O_5	0.05	0.15
C	0.36	1.27
S	0.34	0.85
LOI	9.90	20.00

Source: Adapted from Karnland (2010)

2.3.2.2   Finland

Waste package

The Finnish repository program has worked closely with the Swedish program, and the waste package materials are identical to the Swedish BSK-3 design, consisting of a copper shell, nominally 48 mm thick, with a cast iron insert for strength. The diameter of the packages is 1.05 m. Three different lengths (3.6 m, 4.8 m, and 5.25 m) will be used, corresponding to three different fuel configurations used in Finland (Pastina and Hellä 2006).

Bentonite backfill

The bentonite backfill compositions under consideration are also identical to that of the Swedish program. One is the Wyoming based MX-80, the other is the Greek based IBECO RWC (also referred to as Deponit CA-N) (Andersson et al. 2007).

2.3.2.3   Other Repository Programs

Canada

The Canadian program has historically focused on disposal in a crystalline rock repository on the Canadian Shield and has fully-developed repository concepts similar to the Swedish BSK-3 design for disposal in that environment. The canister consists of an outer sleeve made of oxygen-free, phosphorus-doped copper, and an inner carbon steel load-bearing inner vessel (Garisto et al. 2009; Kwong 2011). One major distinction is that the internal fuel basket is a cylindrical metal cast holding 108 fuel bundles compared to 4 or 12 individual fuel bundle channels used by the Swedes and Finns. This difference mostly relates to the nature of the fuel; most Canadian reactors are of the CANDU type, which has different isotopic characteristics than light water reactor (LWR) type fuels (Husain and Choi 2003).

In an evaluation of container placement methods, Maak et al. (2010) considered use of carbon steel containers, and even a Belgian-style supercontainer, in a granite-based repository. However, the authors noted that research is necessary to show that a steel container would be appropriate in a crystalline rock repository environment.

In the event that a crystalline rock repository is chosen, the Canadian program will use bentonite-based backfill (Garisto et al. 2009), although a specific material has not been identified. Given the similarities with the Scandinavian repositories, it is likely that the Canadian backfill choice will be similar compositionally and mineralogically to that chosen by the Scandinavian programs.

Spain

Spain has not yet selected a disposal site or host lithology for SNF or HLW. Preliminary repository concepts for clay and granite are provided in Kursten et al. (2004a) and are similar; in both, the waste package is carbon steel, 0.9 m in diameter and 4.5 m in length, with 10 cm thick walls, and is emplaced in a clay barrier of compacted bentonite bricks. The reference bentonite is sourced from the Almeria province. The mineralogical composition of the bentonite backfill is shown in Table 6. It is slightly higher in smectite content than the MX-80 reference material used by many other international organizations, but the accessory mineral assemblage is similar to those found in other potential backfill materials. Although no site has yet been chosen, the Spanish nuclear waste program has vigorously pursued research into metals corrosion in potential granite, clay, and salt environments. The Spanish have defined a bentonite-buffered granite pore water and used it extensively in corrosion studies. The composition of this pore water is given in Table 14.

Table 14.   Composition of the bentonite-buffered granitic pore water used in ENRESA corrosion experiments

Constituent	Composition (mg L^{-1})
pH (25°C)	7.3
Ca^{2+}	135 +/- 10
Mg^{2+}	600 +/- 30
Na^+	3,750 +/- 100
K^+	20 +/- 1
SiO_2	8.3 +/- 0.5
Cl^-	6,550 +/- 250
Br^-	15 +/- 1
SO_4^{2-}	1,500 +/- 30
NO_3^-	110 +/- 10
HCO_3^-	27 +/- 5

Source: Kursten et al. (2004a), Table 2-15

2.3.2.4   *Summary of Current Waste Package Concepts for Granite Repositories*

All granite repository programs have chosen copper waste packages, with cast iron inserts to provide structural support. By the accepted understanding of copper corrosion processes, copper metal will not hydrolyze water (recent studies have disputed this; Section 2.1.3) and hence corrosion under anoxic conditions is limited by the rate of delivery of aggressive species (sulfide and chloride) to the waste package surface. This rate is very low for a waste package embedded in an intact clay buffer. As a corrosion resistant material, thin waste package walls are sufficient to maintain waste package integrity for very long time periods. Several repository science programs have estimated copper waste package lifetimes of >1,000,000 years (Kursten et al. 2004a; King et al. 2010; King et al. 2011; Kwong 2011); largely based on transport limitations through the bentonite backfill. It is important to note that even in the case of a corrosion-resistant material under anoxic conditions, the bentonite backfill plays an important role in limiting corrosion.

2.3.3   Corrosion Studies Relevant to Granite Repositories

This section summarizes, for each major repository program, the corrosion research that has been carried out that is relevant to granite-hosted repositories. This summary relies heavily on the COBECOMA report (Kursten et al. 2004a) for work prior to 2004, and cites additional articles and summaries for more recent work. The two major programs that have performed experimental work on materials performance in granitic repository settings are the Spanish program and the Swedish and Finnish Programs. With respect to waste package performance, Canadian work has largely been modeling efforts, as opposed to experimental work.

2.3.3.1   *Spain*

Although Spain has not selected a host lithology for its eventual repository, it has carried out a suite of corrosion experiments under conditions relevant to a granitic repository. Unlike the Swedish-Finnish work, which has always concentrated on copper, Spain evaluated several different alloys, including carbon and stainless steels, Hastelloy C-22, and Cu alloys (Table 15). Two different media were used, a

Table 15.   Materials used in Spanish corrosion testing program

Materials	Fe	Ni	Cu	Cr	Mo	Mn	Si	Al	C	P	S	N	Others
Carbon steels													
AE-355D (DIN 1.0570)	bal.	-	-	-	-	1.4	0.4	0.04	0.17	0.02	0.012	0.006	-
TStE 355 DIN 1.5066)	bal.	-	-	-	-	1.5	0.41	0.036	0.16	0.017	0.002	0.006	-
TStE 460 (DIN 1.8915)	bal.	-	-	-	-	1.4	0.35	0.027	0.14	0.01	0.001	0.56	V: 0.17
15 MnNi 6.3 (DIN 1.6210)	bal.	0.82	-	-	-	1.5	0.23	0.027	0.18	0.012	0.003	-	-
Ni-Cr steels													
AISI 316L (ASTM A-240)	bal.	11.5	-	17.4	2.2	1.3	0.31	-	0.021	0.029	0.002	-	-
Ni-base alloys													
Hastelloy C-22 (UNS N06022)	2.8	bal.	0.03	21.8	13.3	0.22	-	0.22	0.014	0.01	<0.005	-	W: 3.0 ; Co: 0.38 ; V: 0.16
Cu-base alloys													
Cu-OF (UNS C10200)	<0.005	-	bal.	-	-	-	-	-	-	<0.01	0.0015	-	Pb: <0.01 ; Bi: <0.01; Zn: <0.005
Cu10Ni (UNS C70600)	1.0-1.8	9-11	bal.	-	-	<1.0	-	-	-	-	-	-	Pb: <0.05 ; Zn: <1.0
Cu30Ni (UNS C71500)	0.7	31.2	bal.	-	-	1	<0.01	-	0.011	<0.01	0.005	-	Pb: <0.01 ; Zn: <0.01

Source: Kursten et al.(2004a), Table 4-46

OF – oxygen-free

synthetic bentonite-buffered granitic groundwater (Table 14), and bentonite (Table 7) saturated with deionized water. In both media, general corrosion rates were measured in immersion experiments, by weight loss upon cleaning to remove the oxide layer. Potential for SCC was measured by slow strain rate testing, at different temperatures and strain rates. For the 316 stainless steel, crevice corrosion was also evaluated, using an artificial crevice assemblage wrapped with Teflon tape.

Carbon steels

The behavior of carbon steels in the two test media is illustrated by results for TStE 355 in Figure 12 and Figure 13. In the granitic-bentonite water, general corrosion rates, determined by weight loss, declined asymptotically with time at both 90º and 120ºC, reaching approximately constant values of about 6 μm yr^{-1} at 90ºC and 14 μm yr^{-1} at 120ºC. No localized attack was observed on the non-welded samples in the granitic-bentonite water; however, welded samples were found to be pitted in welded and heat-affected regions at the higher test temperature. The corrosion layer was analyzed and found to be hematite—however, it was suspected that this formed by reaction with air after the test and prior to analysis (Kursten et al. 2004a).

The samples in the saturated bentonite were run at 50ºC, 75ºC, and 100ºC. The corrosion rates also asymptotically decreased over time, reaching a value after 18 months of about 10 μm yr^{-1}, regardless of temperature. In the saturated bentonite tests, pitting was observed on the copper surface; this was attributed to the formation of potential cells due to inhomogeneity in the hydrated and compacted bentonite (Kursten et al. 2004a). Results for saturated bentonite tests are summarized in Table 16.

Slow strain rate testing of carbon steel was only carried out in the granitic-bentonite water, and no evidence of SCC was observed

Stainless steel

No appreciable general corrosion (<0.1 μm yr–1) and no localized corrosion were observed in tests using 316L stainless steel in either medium. No SCC was observed in slow strain rates tests carried out in granitic-bentonite pore water at 90ºC (Kursten et al. 2004a).

Cu-based alloys

Two copper alloys, Cu-OF (oxygen-free copper) and Cu30Ni, were tested in the Spanish program. Both corroded at a slow rate (uniform corrosion rates measured by weight loss of <1 μm yr^{-1}) when exposed to saturated bentonite for 18 months. However, Cu-OF showed no signs of localized corrosion, while corrosion of Cu30Ni changed from uniform corrosion at 50ºC, to uniform corrosion and pitting at 75ºC, to pitting at 100ºC, with maximum penetration depths of 25μm. X-ray diffraction analysis showed that the corrosion product layer on the Cu30Ni included Ni-oxides and (Cu, Ni) oxides, as well as Cu_2O (Kursten et al. 2004a).

Slow strain rate tests were carried out in granitic bentonite water at 90ºC with both Cu alloys. Cu-OF did not show damage by SCC, even in additional tests with greatly elevated chloride (50,000 mg L^{-1}). It is not clear why increased chloride was used, however, as this generally has the effect of suppressing SCC by promoting general corrosion, or, at very high concentrations, active corrosion (King et al. 2011). Unlike Cu-OF, Cu30Ni showed a high susceptibility to SCC, developing many cracks in the strained area, as much as 230 μm deep (Kursten et al. 2004a).

2.3.3.2   *Sweden and Finland*

As noted previously, SKB and Posiva have worked jointly to evaluate the efficacy of copper as a waste package material in granitic rock. The following discussion is based on several recent summaries of copper corrosion processes in repository environments, including King et al. (2001) and Kursten et al. (2004a), King et al.(2010), Kwong (2011), and Litke and Ikeda (2011).
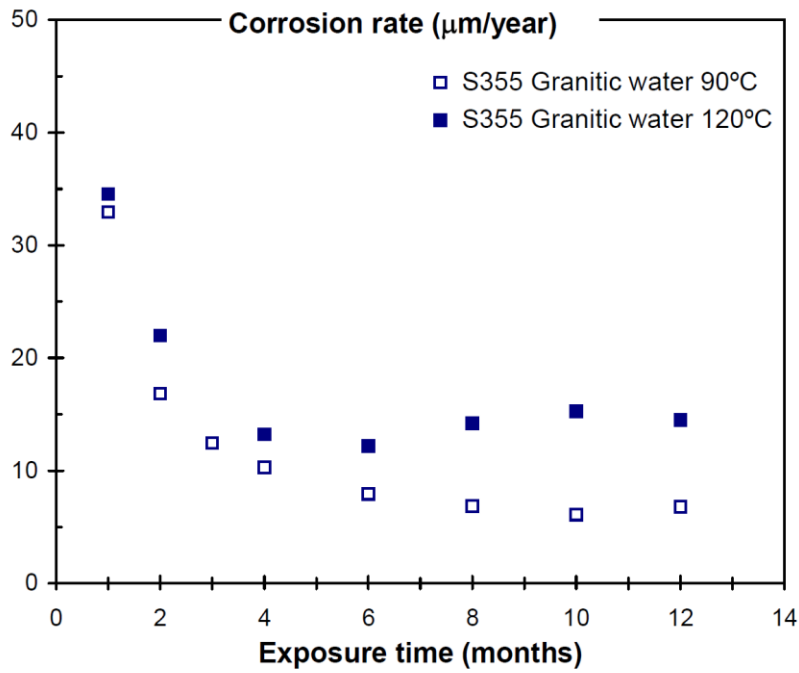
Source: Kursten et al. (2004a), Figure 4-54

Figure 12.   General corrosion rates as a function of time, for carbon steel TStE 355 in granitic-bentonite water at 90ºC and 120ºC
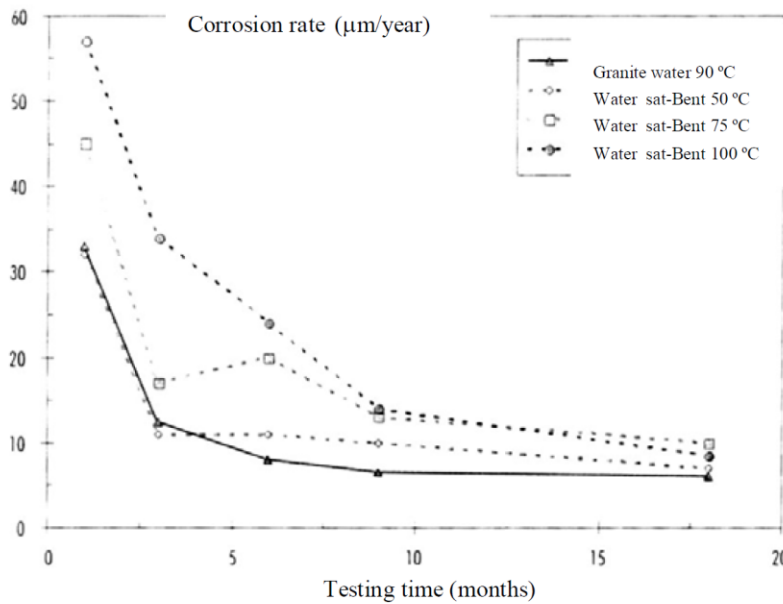
Source: Kursten et al. (2004a), Figure 4-55

Figure 13.   General corrosion rates as a function of time, for carbon steel TStE 355 in granitic-bentonite water at 90ºC and 120ºC

Table 16.   Measured general corrosion rates and pitting depths for carbon steel TStE 355 exposed to saturated bentonite at various temperatures

T (°C)	Exposure period (months)	General corrosion v_{CORR} ($\mu m \, yr^{-1}$)	Localized corrosion d_{MAX} (μm)	D_{AVG} (μm)	Pitting Factor
50	1	32	-	-	-
	3	11	15	2.8	5.4
	6	11	20	5.5	3.6
	9	10	43	7.5	5.7
	18	6.7	56	10.5	5.9
75	1	45	-	-	-
	3	17	30	4.3	7
	6	20	44	10	4.4
	9	13	53	9.8	5.4
	18	10	98	15	6.5
100	1	57	30	4.75	6.3
	3	34	40	8.5	4.7
	6	24	58	12	4.8
	9	14	60	10.5	5.7
	18	6.3	50	6.3	7.9

Source: Kursten et al.(2004a), Table 4-48

v_{CORR} – average uniform corrosion rate

d_{MAX} – maximum depth of pitting attack

d_{AVG} – average depth of pitting attack

Pitting factor – ratio of d_{MAX} to d_{AVG}

General corrosion of copper

Over the lifetime of a granite-hosted repository, a copper waste package will be exposed to three very different environments. First, the waste package will be exposed to oxic, dry conditions during storage and after emplacement but before saturation of the backfill. If it is assumed that the relative humidity is sufficiently high to allow corrosion, the copper will corrode by general corrosion under these conditions. Storage prior to disposal is anticipated to last only weeks, but in extreme cases, could last as long as 2 years. Even after 2 years, corrosion is anticipated to be less that 1 μm, with the dominant corrosion product being Cu_2O (King et al. 2001). Following emplacement, corrosion will be limited by the rate of mass transport through the buffer material, and by the rates of oxygen consumption by reaction with accessory minerals in the buffer material and by microbial activity within the buffer. Ignoring all secondary processes, a mass balance calculation assuming all the oxygen initially present in the buffer reacts with the copper yields maximum corrosion depth of 300 μm of corrosion if spread evenly over the canister surface. Realistically, limitations on transport through the bentonite, reaction kinetics within the bentonite, and the formation of an oxide layer on the metal surface will greatly reduce corrosion and penetration rates relative to this maximum value (King et al. 2001; Kursten et al. 2004a).

As the bentonite backfill around the waste package begins to absorb water, saturation will increase and the buffer material will swell. It is anticipated that water absorption and swelling will be inhomogeneous (King et al. 2001). Electrochemical reduction of oxygen should be faster in areas where there is a good

supply of oxygen and where an electrolyte is present, and in areas in close proximity to a site where electrochemical corrosion of copper can occur. This corresponds to areas near a copper/moist bentonite/air boundary; therefore, sites where the buffer first contacts the waste package could become latent sites for corrosion pits. However, this period is transient, and areas in contact with the wet clay are constantly evolving. Also, the total mass of residual oxygen still limits the total attack to 300 μm, when averaged over the waste package surface. The amount of corrosion during the rewetting period is anticipated to be negligible (King et al. 2001).

Following complete saturation of the buffer material, the environment will evolve from warm and oxic to cool and anoxic. During the oxic period, general corrosion is expected to occur by reaction with dissolved oxygen. However, as oxygen is consumed by canister corrosion, microbial activity, and oxidation of trace impurities in the clay (e.g., sulfide, organics), conditions become anoxic, and will remain that way. If water will not corrode copper, as is generally accepted, then further corrosion will occur only by reaction with sulfide, and will be limited by mass transport of sulfide to the container surface.

Kursten et al. (2004a) discusses the general corrosion of copper following saturation. During the oxic period, both the corrosion potential (E_{CORR}) and corrosion current (I_{CORR}) are influenced by the changing concentrations of several species at the metal surface. Chloride concentrations increase over time as chloride diffuses into the clay, and increasing chloride serves to both lower E_{CORR} and to raise I_{CORR} because of the various reactions discussed in Section 2.1.3. As O_2 is depleted by cathodic reduction at the metal surface, it must be replenished by diffusion through the clay. Both E_{CORR} and I_{CORR} vary directly with O_2 concentration. At the cathode, transport of $CuCl_2^-$ away from the metal surface, or Cl^- to the metal surface, can also limit reaction rates. Therefore, corrosion of the waste package is largely limited by mass transport of reactants through the buffer material. King et al.(1995) modeled transport through the buffer and suggested that O_2 diffusion is the rate limiting process, but neglected to consider reaction of Cu(I) with oxygen to form Cu(II); in a more recent study, King et al. (2011) included that reaction and concluded that during the oxic period, reduction of Cu(II) was the dominant reaction at the cathode. Experimental studies using compacted bentonitic buffer materials have indicated that diffusion of Cu away from the surface is the rate-limiting step (Kursten et al. 2004a). Regardless of the rate of reaction, the overall oxic corrosion of copper is still limited by mass balance considerations to the amount of residual oxygen trapped in the backfill and host rock upon closure. As noted previously, if distributed evenly across the waste package, this would result in a penetration depth of 300 μm.

Once anoxic conditions are established, copper corrosion is anticipated to be extremely slow. As noted in Section 2.1.3.2, corrosion of copper by water is not generally accepted to occur. Copper corrosion under anoxic conditions will occur by reaction with sulfide (Reaction 21), in which sulfide films form at the anode and water is hydrolyzed to produce H_2 at the cathode. As water is abundant and H_2 gas cannot build up sufficiently to inhibit the reaction at repository hydrostatic pressures, this reaction will be limited by sulfide transport through the buffer. An additional mechanism that may be significant in concentrated chloride solutions is copper oxidation by reduction of H^+ (Reaction 20), although this will also be tranposrot-limited.

Other environmental factors that have been evaluated with respect to copper corrosion include pressure and methane concentration (Kursten et al. 2004a). Pressure will increase in the repository due to the development of a hydrostatic head and will have a minor effect on corrosion rate, mostly because dissolved O_2 concentrations increase with increasing O_2 partial pressure. However, the overall amount of O_2 and maximum extent of corrosion will not change. Methane concentrations can be elevated in natural waters at depth, but experimental studies have not shown that methane has any direct effect on corrosion of copper.

Estimates of copper waste package lifetime, for wall thickness of 2.5-5 cm, are >1,000,000 years (Kursten et al. 2004a; King et al. 2010; King et al. 2011; Kwong 2011). King et al. (2011) estimates the total

penetration of the package, over a 10^6 year assessment period, to be less than 1 mm, with the majority of this occurring under anaerobic conditions by formation of Cu_2S. Kwong (2011) estimates 1.27 mm penetration over that time period.

Localized corrosion of copper

The form of localized corrosion considered most likely in granite repository settings is pitting corrosion during the initial oxic period. Considerable effort, both in terms of modeling and experimental work, has been done to evaluate this in repository settings. In general, there are three phases in the life of a pit: initiation, propagation, and death. Pit initiation is strongly linked to damage of the CuO_2 layer by precipitation of CuCl in or under the Cu_2O layer on the copper surface (Section 2.1.3); hence, the pitting potential (E_{NP}) is a function of chloride concentration and elevated chloride concentrations, which occur in deep granitic pore waters, promote pitting. However, bicarbonate competes with chloride with respect to Cu complexation and formation of sorbed surface species, and inhibits pitting. Once a pit is formed, O_2 is required for pit growth, and due to mass transport limitations in O_2 movement through the buffer to the corrosion site and limitations in total O_2, the pits will rapidly die. A number of experiments have evaluated copper corrosion in contact with oxic, saturated buffer material and have found no evidence for pitting (Kursten et al. 2004a).

Crevice corrosion is not anticipated to affect copper canisters because complexation of Cu(I) with chloride limits hydrolysis and prevents acidification of the crevice. Moreover, formation of Cu(II) species, which could hydrolyze, will be inhibited by the restricted access of O_2 to the occluded region (Kursten et al. 2004a).

Stress corrosion cracking is of concern for copper canisters because copper, especially copper containing phosphorous, has been found to be highly susceptible to SCC. Moreover, tensile stresses, either residual manufacturing stresses or stresses due to loading (a combination of hydrostatic pressure and clay swelling pressure), are likely to occur. Finally, ammonia and acetate, two species known to promote SCC, are present in significant quantities in Fenno-Scandian ground waters. However, elevated chloride concentrations promote general corrosion and can inhibit SCC. King et al.(2011) and Kwong (2011) summarize the current understanding of copper SCC and the effects of environmental factors, including ammonia, acetate, and nitrate concentrations. Both Posiva and SKB have evaluated the potential occurrence of SCC in synthetic repository groundwaters at elevated temperatures (Kursten et al. 2004a). The Posiva slow strain rate tests covered an especially wide range of conditions. The effects of ammonia were evaluated at 80ºC, at ammonia concentrations of 0.5 to 100 mg L^{-1} and chloride concentrations of 3,700 or 17,000 mg L^{-1} (Kursten et al. 2004a). The effects of acetate were evaluated at 100ºC, at acetate concentrations of 1.0 to 100 mg L^{-1} (TOC in Olkiluoto groundwater is generally 4-14 mg L^{-1}) and chloride concentrations of 8,000 or 53,800 mg L^{-1} (Kinnunen 2006). Stress corrosion cracking was not observed under any of the test conditions, in which the range of aggressive species concentrations greatly exceeds that expected in granite repository settings. The Canadian repository program evaluated nitrite-induced and ammonia-induced copper SCC in aggressive solutions, containing up to 1.0 M nitrite or ammonia (Litke and Ikeda 2011). The experiments were run at room temperature (copper is less susceptible to SCC with increasing temperature). They found that SCC could not initiate at nitrate concentrations less than 0.01 M or ammonia concentrations less than 0.1 M; these thresholds are far above levels anticipated to occur in repository settings. Sulfite has also been shown to promote SCC if present in high concentrations (Taniguchi and Kawasaki 2008). However, anticipated concentrations at the container surface are low and are limited by diffusion through the buffer material, leading King et al. (2010) to conclude that sulfide induced SCC will not occur under repository conditions. For these reasons, failure of copper waste packages by SCC is not considered credible (Kwong 2011).

Microbiologically induced corrosion (MIC) is not anticipated to have a large effect on copper waste package lifetimes. The dominant effect of microbial activity is to generate metabolic by-products (acetate, ammonia, and sulfide) that react with copper. However transport of microbial byproducts

through the bentonite to the waste package surface is limited. Moreover, microbial activity in the bentonite is suppressed at swelling pressures of >2MPa, or at high compaction pressures, which raise the ionic strength of pore waters in the clay. For these reasons, microbial activity has an insignificant effect on waste package lifetimes (Kwong 2011).

Radiation has little effect on the corrosion rate of copper prior to saturation as conditions are already quite oxic. Under saturated conditions, a gamma radiation field has been shown to actually reduce copper corrosion, possibly by stabilizing the protective oxide layer (Kursten et al. 2004a).

2.3.4   Additional Research Needs for Engineered Materials Performance in Granite Repositories

In granite-based repositories, the natural barrier is less robust than in clay or salt. Although matrix permeabilities are low, fracture systems allow advective water movement, and excavation-induced damage zones do not heal. Moreover, the complex water chemistries found in subsurface granite URL sites indicates that at depths being considered for waste disposal, fracture waters are generally mixtures of waters from many sources, suggesting complex and variable hydrology. In such an environment, the waste package itself must form the primary barrier to radionuclide release, not only during the thermal period, but throughout time. For this type of environment, a corrosion-resistant metal is appropriate, and pure copper is the consensus choice. Therefore, knowledge gaps for granite repositories largely address confirmation of the expected behavior copper in the granite environment.

Perhaps the greatest research need is to resolve "The Copper Controversy." As discussed in Section 2.1.3, the experimental data by Hultquist and others are largely believed to be experimental artifacts. However, although additional work has been initiated by SKB and Posiva, no convincing explanation has yet been offered for the experimental data:

> "…neither the mechanism proposed by Hultquist and co-workers for the generation of H_2 involving a CuOH species nor alternative explanations proposed by others seem able to explain the reported observations of H_2." (King et al., December 2010)

Hence, experimental work to better understand the processes that occurred in the Hultquist and Szakalos experiments, as well as to verify the expected behavior of copper in anoxic environments, is a high-priority research need. Additional efforts to understand the effects of the buffer in potentially limiting H_2 diffusion are also required.

One additional research need is evaluation of the LC/SCC behavior of copper in the granite-repository environment (Bennett and Gens 2008). Cu is not considered susceptible to LC or SCC in repository conditions, but the potential effects of environmental variables (e.g., chloride, sulfide) are not fully understood. Given the reliance on the waste package to limit releases in a granite-hosted repository, even small breaches may affect estimates of radionuclide release.

2.4   Salt Repositories

2.4.1   Background

The Federal Republic of Germany is considering, and the United States considered, disposal of SNF or HLW in salt formations. Germany is considering disposal of spent fuel or HLW in salt domes; the U.S. considered mainly bedded salt for disposal of spent fuel or HLW. In addition, the U.S. Department of Energy (DOE) opened the Waste Isolation Pilot Plant (WIPP) in March 1999 for disposal of defense-related transuranic (TRU) waste in a bedded salt formation and has been emplacing TRU waste in the WIPP since then.

2.4.1.1   *Recommendation of Salt for Disposal of Radioactive Wastes*

The Earth Sciences Division of the National Research Council organized a meeting of geologists and engineers in September 1955 to discuss possible deep geologic disposal of radioactive wastes (Boegly et al. 1966). Those present concluded that salt is the most promising geologic medium for the disposal of solid or liquid radioactive wastes. The advantages of salt relative to other geologic media were, according to Boegly et al. (1966), that

1.   Salt formations are widely distributed throughout the U.S.

2.   The thermal conductivity of salt is higher than that of most other rocks and would allow larger quantities of heat to be dissipated.

3.   Salt has a high compressive strength (similar to that of concrete) but, unlike most other rocks, it would flow plastically and remove the stress produced by mining and heating.

4.   There are salt formations in the U.S. that are located in areas with low seismicity.

5.   Salt is essentially impermeable because of its plastic behavior under pressure. Therefore, any cracks that might develop would be self-healing.

6.   The cost of miming salt is less than that of most other rocks.

2.4.1.2   *Disposal of Radioactive Wastes in Domal Salt Formations in Germany*

In 1963, the Second German Atomic Program also recommended salt for disposal of radioactive wastes, including SNF and HLW. A report by the Federal Institute for Soil Research, now the Federal Institute for Geosciences and Natural Resources (the German Geologic Survey) agreed with these recommendations.

As a result, the German government purchased the abandoned Asse salt mine in 1964 for research and development (R&D) related to radioactive waste disposal. The Asse mine, located in the state of Lower Saxony in one of the more than 200 salt domes in northern Germany, had produced potash and rock salt from 1909 to 1964. Research and development began at Asse in 1965; disposal of low-level waste (LLW) began there in 1967; and disposal of intermediate-level waste (ILW) began in 1972 (DBE 2011). During the 1970s, a series of high-temperature in situ experiments were carried out to study the thermal and thermomechanical behavior of domal salt (Rothfuchs et al. 1988). In the 1980s, a new drift was excavated for brine-migration tests; data on room closure were collected during construction of this drift. The brine-migration tests simulated borehole disposal of HLW. In the 1990s, the Thermal Simulation of Drift Emplacement experiment simulated HLW disposal in drifts.

The German government also began a survey in 1974 to determine a suitable location for an integrated nuclear waste management center. Preliminary site-characterization studies were started at three locations in Lower Saxony, but were terminated in 1976 after protests at all three sites and opposition from the government of Lower Saxony. The government of Lower Saxony appointed its own task force to select suitable locations for the integrated nuclear waste management center in 1976 and nominated the Gorleben salt dome as a possible repository for LLW, ILW, and HLW in 1977. Surface exploration

(geologic mapping, geophysical surveys, hydrogeologic studies, etc.), started at Gorleben in 1979, and was essentially completed in 1985. The first shaft was excavated from 1986 to 1997, and a second shaft was excavated from 1989 through 1995. Excavation of drifts and development of underground infrastructure began in 1995.

A coalition of the Social Democrats and the Alliance '90/The Greens took control of the Bundestag after winning the 1998 German federal election held that year. In 2000, this collation government decided to: (1) phase out the use of nuclear power in Germany, (2) stop reprocessing spent fuel after June 30, 2005, (3) halt most work on the Gorleben site for a period of three to ten years, and (4) consider the disposal of heat-generating radioactive waste in argillaceous rock (shale) and crystalline rocks (granite or related igneous or metamorphic rocks), two rock types that have been studied extensively in other European countries (Anonymous 2005). In Germany, all radioactive waste is classified as "waste with negligible heat generation," (LLW and some ILW) or "heat-generating waste" (spent fuel, HLW, and some ILW) (Stenhouse et al. 2010).

Comparisons of the disposal of heat-generating radioactive waste in clay, granite, and salt resulted in renewed interest in salt; the moratorium on characterization of Gorleben ended in 2010. However, clay and granite are still under consideration in Germany (Stenhouse et al. 2010).

Furthermore, concerns about carbon-dioxide emissions and global warming led many to reconsider Germany's decision to phase-out nuclear power. However, reaction to the recent Fukushima Daiichi accident in Japan has reinvigorated public pressure to phase-out the use of nuclear power in Germany.

In addition to Asse and Gorleben, Germany has conducted studies at Morsleben, an abandoned salt mine in the East German state of Saxony-Anhalt, and Konrad a former iron mine in Lower Saxony. Both of these mines were used for disposal of LLW and/or ILW.

2.4.1.3   *Disposal of Radioactive Wastes in Bedded Salt Formations in the U.S.A.*

Meanwhile, back in the U.S.A., Oak Ridge National Laboratory (ORNL) carried out Project Salt Vault for the Atomic Energy Commission (AEC) from 1965 to 1967 to evaluate disposal of HLW in salt. ORNL conducted this project in a mine in a bedded salt formation near Lyons, Kansas. The results initially appeared to be favorable and did not identify any processes that ruled out bedded salt for disposal of HLW. Therefore, the AEC tentatively selected Lyons as a potential site for a repository in 1970 and the National Academy of Science tentatively endorsed this selection (NRC Committee on Radioactive Waste Management 1970).

The Hutchinson Member of the Permian Wellington Formation (Fm.), which was tentatively selected to host the repository, is about 300 ft thick at the Lyons site and extends from a depth of 780 to 1080 ft subsurface. It consists of about 60% halite (NaCl) interbedded with shale and anhydrite ($CaSO_4$) (NRC Committee on Radioactive Waste Management 1970).

The Nuclear Regulatory Commission (NRC) (1970) recommended that the AEC carry out several studies to resolve "several site problems … before radioactive materials are committed to the salt beds." One of these issues was that

> *Location of previous oil and gas wells and inspection of records, where available, should determine if these former wells have been adequately plugged to avoid an entrance of water to the salt.*

> *Recommendation: A survey should be made of neighboring wells in order to avoid threats to the integrity of the proposed bedded salt disposal site.*

The AEC completed a conceptual design for a repository for HLW and TRU waste in 1971 (Mora 1999). However, two serious problems with the Lyons site arose in 1971: (1) numerous exploratory boreholes for oil and gas were discovered near the site, and many of them had not been identified or recorded during

site characterization; (2) solution mining about three miles from the proposed site often resulted in large, unexplained losses of water, which was considered to be an unfavorable characteristic of the site. Consequently, the AEC abandoned the Lyons site in 1972 (Mora 1999).

ORNL and the U.S. Geological Survey (USGS) restarted site-selection activities for the AEC in the Permian Basin in 1972. The AEC designated the Los Medaños ("The Dunes") area as its "prime study area in 1973; this area included the current WIPP site. The U.S. Congress passed the Energy Reorganization Act in 1974. This legislation split the AEC into the Energy Research and Development Administration (ERDA) and the Nuclear Regulatory Commission in 1975. Also that year, the ERDA chose Sandia National Laboratories (SNL) as the scientific advisor for the new bedded-salt project. SNL and the USGS identified a "prime exploration zone" within the Los Medaños area in early 1976, and identified the current site within this zone by the end of 1976. The ERDA also designated the project as the WIPP Project in 1976. These site-selection activities all focused on the Salado Fm., a thick, Permian bedded-salt formation, as the host formation for the WIPP.

Congress combined the ERDA and the Federal Energy Administration into the U.S DOE, America's 12th cabinet-level department, in 1977. During the mid-to-late 1970s, the ERDA and the DOE considered the possibility of using the WIPP for disposal of commercial spent fuel and HLW and/or defense HLW in addition to TRU waste. Some ERDA and DOE officials envisioned a two-level repository with TRU waste in the upper level of the repository and spent fuel and HLW 500 m below it. However, the WIPP Authorization Act, passed by Congress in 1979, restricted the WIPP to defense-related TRU waste.

Nevertheless, the DOE used an experimental area in the northern part of the WIPP underground workings to carry out studies relevant to the behavior of spent fuel or HLW in bedded salt during the 1980s and early 1990s (Section 2.4.4.2). The DOE also funded laboratory studies of waste-package materials for spent fuel or HLW (Section 2.4.4.2). The objective of these studies was to provide information applicable to a potential salt repository for spent fuel or HLW at sites other than the WIPP site. Furthermore, the DOE's characterization and licensing of the WIPP for TRU waste provided invaluable information that can be applied to the disposal of spent fuel or HLW in salt, especially bedded salt. Therefore, results obtained from studies of the WIPP site are included in many of the following discussions.

The DOE developed the WIPP site as a repository for defense-related, TRU waste from 1981 through 1988. This included: (1) excavation of four shafts, access drifts, design-validation, and experimental rooms; (2) construction of surface waste-handling facilities and support buildings; (3) excavation of Panel 1, the first of the ten panels required for disposal of the WIPP contact-and remote-handled TRU waste inventory. Congress passed the WIPP Land Withdrawal Act (LWA) in 1992. The LWA transferred the WIPP site to the DOE and designated the U.S. Environmental Protection Agency as the main WIPP regulator. The DOE submitted its Compliance Certification Application (CCA) to the Environmental Protection Agency (EPA) in 1996 (DOE 1996). The EPA reviewed the CCA and certified that the WIPP complied with its regulations for TRU waste in 1998 (EPA 1998). The WIPP opened in 1999. Because the LWA also specifies that the DOE must submit a compliance recertification application to the EPA every five years after the 1999 opening of the WIPP, the DOE submitted these applications in 2004 and 2009 (DOE 2004; 2009); and the EPA recertified the WIPP in 2006 and 2010 (EPA 2006; 2010a).

The DOE's Salt Repository Project (SRP) also investigated the possible disposal of (mainly) commercial spent fuel and defense HLW in bedded salt. The SRP was one of three major projects that partially characterized sites for possible use as repositories for spent fuel and HLW under the Nuclear Waste Policy Act (NWPA) of 1982 (DOE 1986). The other two were the Basalt Waste Isolation Project (BWIP), which investigated basalts of the Columbia River Group near Hanford, Washington; and the Nevada Nuclear Waste Storage Investigations (NNWSI) Project, which later became the Yucca Mountain Project (YMP). Congress terminated the SRP (and the BWIP) when it amended the NWPA in 1987 to designate Yucca Mountain as the only potential site for spent fuel or HLW to be characterized, and renamed the NNWSI Project the YMP.

The SRP selected a site in Deaf Smith County, TX, as the site to be characterized for a possible salt repository for spent fuel and HLW. As in the case of the WIPP Project, the SRP selected the Salado Fm. as the host formation. At the Deaf Smith Co. site, the Salado is also a bedded-salt formation. However, the salt section, which also includes evaporite deposits above and below the Salado, is thinner at the Deaf Smith Co. site than at the WIPP site.

In addition to these three major site-characterization projects, the DOE also carried out preliminary site-screening activities that included other bedded-salt formations and salt domes along the Gulf Coast. These activities included an *in situ* brine-migration experiment in the preexisting Avery Island salt mine, Avery Island, LA (Krause 1983). This test is described in Section 2.4.2.1.

2.4.2   Geological and Geochemical Environment—Expected Conditions

The conditions expected in salt formations depend in part on whether one considers bedded or domal salt for disposal of spent fuel or HLW. However, there are several general features common to both types of formations:

1. Salt deforms viscoplastically (creeps) in response to the lithostatic pressure imposed by overlying formations. Therefore, creep closure of the drifts or boreholes used to dispose of radioactive waste eventually results in encapsulation of the waste by the host formation. The rate of creep closure increases with the thickness of the overburden (i.e., the lithostatic pressure at the depth of the repository) and the temperature of the waste.

2. The water (brine) content of domal salt is on the order of thousandths, hundredths, or tenths of a wt. %; that of bedded salt is on the order of tenths to a few wt% (Roedder and Belkin 1979; Jockwer 1981; Knauth and Kumar 1981; Roedder and Bassett 1981; Rothfuchs 1986; De Las Cuevas and Pueyo 1995). These brines are present within individual salt crystals (i.e., intragranular brine or fluid inclusions), along the boundaries between salt crystals (intergranular brine), and as structural water in hydrous minerals such as clay minerals and the evaporite minerals gypsum ($CaSO_4 \cdot 2H_2O$), and polyhalite ($K_2MgCa_2(SO_4)_4 \cdot 2H_2O$).

3. The ionic strength of brines in salt is very high relative to the fluids in most other geologic media.

4. The permeability of salt is very low relative to most other media.

5. Redox conditions in salt are usually poorly poised (i.e., neither oxidizing nor reducing agents are present in sufficient quantities to affect the oxidation states of elements that can speciate in more than one oxidation state). Because of this feature and the very low permeability of salt, the processes that occur in a salt repository for radioactive waste will determine the Eh or f_{O2}. These include, but are not necessarily limited to reduction of the water in brine by steels or other Fe-base materials in waste packages (see below), microbial consumption of organic constituents of ILW or TRU waste, and radiolysis.

6. The thermal conductivity of salt is very high relative to other media.

7. The thermal stability of the minerals in bedded and domal salt formations is high.

2.4.2.1   *Possible Brine Migration in a Salt Repository*

Roedder (1984) stated that

> *The fluids in salt consist of two very different types that might be termed "external" and "internal." "External" fluids consist of incursions of outside waters, as have taken place in numerous salt mines in the past. An artificial cavity far below the water table is basically unstable; those in salt are especially subject to flooding as the flow of water through any leak dissolves salt and opens the passage to more flow. The recent flooding of the salt mine at Jefferson Island salt dome, Louisiana (Groat 1981) apparently started*

> *from a drilling accident, but many other miens have filled, some catastrophically, generally after starting with natural leaks of unknown source. ...*

> *The "internal" fluids are those that are essentially inherent to the salt, although they may have originally come from external sources. They include the various types of fluid inclusions, and since radioactive waste will cause heating and decomposition of at least some hydrous minerals, they also include water in hydrous minerals in the beds.*

Clearly, the possibility that fluids from external sources might enter a repository must be evaluated as part of the safety case for disposal of spent fuel or HLW in salt. However, these fluids will not be considered further in this report; instead, the reader is referred to sources such as Groat (1981), Kumar and Martinez (1981), Knauth et al. (1980), Knauth and Kumar (1983), and Kumar (1983).

Numerous investigators carried out laboratory and/or modeling studies of the possible migration of fluid inclusions in thermal gradients imposed on NaCl, other alkali halides, or other soluble solids (e.g., Whitman 1926; Young et al. 1959; Hoekstra et al. 1965; Bradshaw and Sanchez 1969; Wilcox 1969; Anthony and Cline 1971; 1972; Cline and Anthony 1972; Anthony and Cline 1973; Cline and Anthony 1977; Hohlfelder and Hadley 1979; Lambert 1979; Roedder and Belkin 1980; Hadley 1981; Hadley and Faris 1981; Jenks and Claiborne 1981; Jockwer 1981; Olander 1982; Olander et al. 1982; Pigford 1982; Carter and Hansen 1983; Yagnik 1983; Olander 1984; Muller 1985; Schlich and Jockwer 1985; Yih 1986; Hwang et al. 1990). Nevertheless, this process remains controversial. Some investigators who have worked on disposal of spent fuel or HLW in salt, but not necessarily on brine migration, have concluded that this is a "showstopper," others have concluded that is an "urban legend." (No references have been identified yet for either one of these strong but often-stated opinions.)

A review of these laboratory and modeling studies of brine migration in response to thermal gradients from spent fuel or HLW in salt is beyond the scope of this report. However, some conclusions that might be relevant to the behavior of waste-package materials, and their potential effect on repository conditions, are that:

1. All-liquid (brine-filled) fluid inclusions may move up the thermal gradient toward the heart source. Clearly, this process would bring intragranular and (perhaps) intergranular brine (see below) into contact with the waste packages if it were to occur in a repository for spent fuel or HLW. However, this remains controversial because, while some investigators concluded that fluid inclusions cannot cross grain boundaries, others reported that they did cross grain boundaries, or at least moved along these boundaries with a component of motion in the direction of the heat source.

2. Gas-liquid fluid inclusions may move down the thermal gradient if the gas bubble in the inclusion is large enough. Based on all of the references identified to date, Wilcox (1969), paraphrasing the discussion of Young et al. (1959), offered the best explanation for this phenomenon:

> *The experimental evidence shows that gravity is not required for the solution to return from the cool to the hot side of the bubble. It is proposed that surface tension supplies the driving force for this circulation. Due to the evaporation-condensation process, the salt concentration is higher on the hot side of the bubble. Since surface tension increases with salt concentration, a surface tension gradient is produced. The gradient in surface tension then causes circulation from the low- to the high-surface tension region and also causes a net force on the bubble directed toward the low-surface tension region (Young et al. 1959). Thus, for example, heating the crystal from above causes the bubble to move down the inclusion and produces dissolution at the bottom.*

The above mechanism must also be responsible for bubbles moving away from the heat source in liquid inclusions of natural crystals.

Movement of gas-liquid fluid inclusions down the thermal gradient has been identified as a process that could transport radioelements away from breached waste packages, albeit for short distances. However, this process could just as likely be beneficial for the performance of a salt repository for spent fuel or HLW, inasmuch as it could also transport brine away from the waste packages before it could corrode waste-package materials.

3. Brine migration up (or down) a thermal gradient is more likely to be significant in a bedded-salt repository than in a domal-salt repository, because the brine content of the former typically exceeds that of the latter by a factor of 50 to 100 (see above).

There have been at least four in situ studies of brine migration in response to thermal gradients in bedded or domal salt formations. These included: (1) the cavity-migration test included in Project Salt Vault (Bradshaw and McClain 1971), (2) the Avery Island, LA, brine-migration test (Krause 1983); (3) the WIPP brine-migration study (Nowak 1986; Nowak and McTigue 1987), and (4) the German-American brine-migration test in the Asse salt mine in Lower Saxony, Germany (Rothfuchs et al. 1988).

Project Salt Vault cavity-migration test

ORNL carried out Project Salt Vault in a mine near Lyons, KS, from 1965 to 1967 for the AEC. ORNL conducted several in situ tests with electrical heaters and spent-fuel assemblies to simulate the response of a bedded-salt repository to spent fuel or HLW (Bradshaw and McClain 1971). In one of these tests, ORNL quantified the amount of brine that migrated into three boreholes, each with a 1.5 kW heater, in separate rooms (designated rooms 1, 4, and 5) in new workings excavated for the project. Each of these boreholes contained an "off-gas condensate collection system" to quantify the amount of brine collected during the ~12-to-19-month tests. ORNL turned on the electrical heaters in rooms 1 and 4 on November 15, 1965; and began the test in room 5 on June 6, 1966. ORNL intended to maintain a maximum temperature of 200 °C in the salt adjacent to the midplanes of the boreholes. However, various problems resulted in variable maxima of 150–200 °C in rooms 1 and 4, and a maximum of 142 °C in room 5, despite increases to the power applied to the heaters (eventually up to 2.1 kW) and modifications to prevent loss of heat from the salt through the floors of the rooms. ORNL turned off all three heaters on June 5, 1967 (Bradshaw and McClain 1971).

The total amounts of water collected (and the rates at which they were collected) during the heater tests were ~1.7 L (0.43 mL day^{-1}) in room 1; 0.8 L (0.22 mL day^{-1}) in room 4; and 3.1 L (10–93 mL day^{-1}) in room 5 (Bradshaw and McClain (1971) described the uncertainties responsible for the range of rates reported for room 5).

ORNL conducted pretest modeling and laboratory studies to predict the amount of brine migration that would occur during the in situ tests (Bradshaw and McClain 1971). Bradshaw and McClain (1971) used (1) the equations for theoretical predictions of the temperature-dependent solubility and diffusion of H_2O from the high- to low-temperature ends of fluid inclusions in ice (Hoekstra et al. 1965), corrected for the different densities of and thermal gradients in seawater inclusions and the surrounding ice (Seidensticker 1966); (2) the assumption that the salt in the Lyons mine contains 0.5 vol % brine; and (3) confirmatory laboratory experiments with fluid inclusions in single crystals of halite. They concluded that

> *[O]ne might expect a total inflow per waste [package] disposal hole of perhaps 2 to 10 liters, taking place over a period of 20 to 30 years after burial. The peak inflow rate would occur at around one year after burial and be somewhere in the range of 200 ml to 1 liter per year per hole. This corresponds to about ½ to 3 ml per day per hole, a range similar to that estimated in the demonstration waste container holes. This water inflow rate would be expected to taper off and approach zero after 20 to 30 years. Other considerations indicate that such volumes and inflow rates will be tolerable in a waste disposal facility.*

Therefore, the predicted and observed values were in good agreement.

Avery Island brine-migration test

RESPEC Inc. carried out brine-migration tests in domal salt in the Avery Island salt mine, near New Iberia, LA, from 1979 to 1981 as part of the DOE's National Waste Terminal Storage Program (NWTS). RESPEC used three boreholes, spaced 15 m apart in the same room, to quantify: (1) migration of the naturally occurring brine in the salt under ambient (unheated) conditions (Site AB), (2) migration of naturally occurring brine under heated conditions (Site NB), and (3) migration of naturally occurring and synthetic, isotopically (D2O-) labeled brine under heated conditions (Site SB) (Krause 1983). Each of the three central boreholes at Sites AB, NB, and SB each contained a water-collection system; the central boreholes at Sites NB and SB also contained ~1.0 kW electrical heaters. RESPEC turned on these heaters on October 4, 1979. According to Krause (1983, p. 2) the heater at NB operated at or near its nominal power for ~350 days, after which the power was reduced by ~30 watts per day for 30 days; the heater at Site 3B operated at nominal power for ~325 days, after which it was reduced by 20% per day for 5 days. Krause (1983, Table 3), however, stated that both heaters operated for 315 days. After steady-state conditions had been attained, the maximum temperature in the salt adjacent to the midplanes of the boreholes was 51 °C. Krause (1983) did not explain why the maximum temperature was so low during these tests. (Most *in situ*, laboratory, and modeling studies carried out under the NWTS around this time assumed a maximum near-field temperature of 200 °C or higher.)

Krause (1983) reported that the masses of water collected from the heated salt at Sites NB and SB and the steady-state rates at which it was collected were approximately twice those observed under ambient conditions (Site AB). He subtracted the mass of water collected at Site AB and the steady-state rate at which it was collected from the measured masses and rates at Sites NB and SB. The total masses collected at Sites NB and SB that were attributed to heating were 8.27 and 5.10 g, respectively; the steady-state rates attributed to heating were 0.0175 and 0.0107 g day^{-1}. Note that the duration of water collection, 205 days at Site NB and 235 days at Site SB, was less in both cases than the duration of heating (see above).

Krause (1983) used the model of Anthony and Cline (1971) to predict the masses of brine to be collected at Site NB and SB.   This model included (1) the equations for the temperature-dependent solubility and diffusion (both Fickian and Soret) of KCl from the high- to low-temperature ends of fluid inclusions in single crystals of sylvite (KCl) (Anthony and Cline 1971); and (2) temperature-dependent material properties for saturated NaCl solutions and halite from various sources. For example, Martinez et al. (1980) reported that the brine content of the brine content of intact Avery Island salt varies from 0.02-0.10 wt%; but Krause (1983) concluded that the brine content of the salt adjacent to the heated boreholes contained 0.054 wt%. Krause (1983) computed that the maximum thermal gradient in the salt was 1.44 °C cm^{-1}, and the maximum depth in the salt from which brine was removed during the heater tests was about 5 mm. Most important, Krause (1983) calculated that, for a period equivalent to that of the operation of the heaters at Sites NB and SB, the total brine migration would be 5.44 g with a steady state rate of 0.0173 g day^{-1}. Therefore, the predicted and observed values agreed well. Krause (1983) did not predict the total amount of brine that would migrate during the thermal period expected for spent fuel or HLW in domal salt.

WIPP brine-migration study

SNL performed brine-migration tests in the northern (experimental) part of the WIPP underground workings in the mid-to-late 1980s (Nowak 1986; Nowak and McTigue 1987). SNL used four boreholes in two rooms (boreholes A1041 and A1042 in room A1; and boreholes B041 and B042 in room B). Boreholes A1041 and A1042 each contained a 470 W electrical heater to simulate a defense HLW (DHLW) canister. Boreholes B041 and B042 contained 1.5 kW electrical heaters to establish near-field overtest conditions. All four boreholes contained water-collection systems. During the 7.1 days prior to heating in room A1, SNL collected a total of 230 g of water from borehole A1041 (32 g day^{-1}) and 90 g

from borehole A1042 (13 g day^{-1}). In the 4.2 days prior to heating in room B, SNL collected a total of 22.4 g of water from borehole B041 (5.33 g day^{-1}) and 19.3 g of water from borehole B042 (4.60 g day^{-1}).

SNL turned on the heaters in room B on April 23, 1985, and in room A1 on October 2, 1985 (Nowak 1986). The maximum temperatures in the salt adjacent to the midplanes of the boreholes increased exponentially throughout the 441- and 600-day periods described by Nowak and McTigue (1987), eventually rising to 55 °C in boreholes A1041 and A1042 at 441 days, and to 120 °C in borehole B041 and 130 °C in borehole B042 by 600 days. After the heaters were turned on, the water-collection rates rose to a peak, decreased, and then remained nearly constant for 441 days (boreholes A1041 and A1042) or 600 days (boreholes B041 and B042). The total masses of water collected in the boreholes in room A1 were both 4.3 kg at 441 days. Neglecting a couple of outliers, the collection rates in these boreholes peaked at about 17 g day^{-1} in borehole A1041 and 14-15 g day^{-1} in borehole A1042 then decreased to about 8 g day^{-1} in both boreholes by 441 days. The total masses collected in room B and were 36 and 38 kg in boreholes B014 and B042, respectively, at 600 days. The maximum rates could not be determined in these boreholes because they exceeded 30 g day^{-1}, the most that could be measured by these systems. The rates decreased to about 20 and 50 g day^{-1} at 600 days.

Nowak and McTigue (1987) used a Darcy flow model to predict the brine-migration rate prior to heating. Their model used one-dimensional radial flow to a circular tunnel caused by the pore-pressure gradient established by mining the rooms used for their study. Their results were relatively insensitive to whether the upper end of the pore-pressure gradient was hydrostatic or lithostatic, and obtained water mass-flow rates of 10 g day^{-1} with permeabilities in the range of 10^{-20} to 10^{-18} m^2 (10^{-8} to 10^{-6} darcy), which they considered to be representative of the permeabilities measured in the Salado by that time. However, their attempt to predict the effect of heating on the brine-migration rate by incorporation of temperature-dependent viscosity was unsuccessful; they predicted increases that were significantly less than those observed. Nowak and McTigue (1987) did not attempt to include brine migration in response to the thermal gradients caused by heating in their model and concluded that vapor-phase migration of water was insignificant in their experiments.

Asse brine-migration test

The German-American brine-migration test was carried out in the Ass salt mine in Lower Saxony, Germany, during the early-to-mid 1980s. The Institut für Tieflagerung (IfT), or Institute for Underground Disposal, in Braunschweig, Lower Saxony; part of the Gesellschaft für Strahlen- und Umweltforschung mbh München (GSF), or Corporation for Radiation and Environmental Research, participated on behalf of Germany. The Office of Nuclear Waste Isolation (ONWI), in Columbus, OH, managed by the Battelle Memorial Institute for the DOE's Civilian Radioactive Waste management Program, participated on behalf of the U.S. Westinghouse – Advanced Energy Systems, a subcontractor to ONWI, designed the test facility and fabricated most of the test equipment and instrumentation, except for the radiation source handling system, which was designed and fabricated by GANUL mbh under a subcontract with the GSF-IfT. Rothfuchs et al. (1988) provided the final report for this test.

The Asse brine-migration test was conducted in a test room mined from December 1981 through March 1982 at the 800 m level of the mine. The boreholes for the test, including the pretest core samples, were drilled from June through December 1982. The test equipment and instrumentation were installed from March through May 1983. The test comprised four test sites spaced 15 m apart. Each test site contained a central borehole for an electrical heater and, in the case of test sites 3 and 4, two 9430 Ci ^{60}Co sources (t½ = 5.3 years) with an initial power of 145W. In addition to the central heater and (at test sites 3 and 4) the ^{60}Co sources, there were eight "guard heaters" (peripheral heaters) in an octagonal array of boreholes 1.5 m from the centerline of the central borehole.

All four test sites were deployed in the Main Halite, which contains more water than most of the other units in the Asse (see below). Test sites 2 and 4 collected water continuously from their central

boreholes, at tests sites 1 and 3, the pressure was allowed to build-up and the water content was determined at the end of the test.

Power was applied to the heaters at tests sites 1 and 2 on May 25, 1983. To obtain a maximum temperature of ~210 °C in the salt adjacent to the midplanes of the central boreholes the power on the central heater was set to 2530W and the total power on the guard heaters was set to 7220W. However, this power was inadequate to establish a maximum temperature of 210 C, so the power on the central heater was increased to 3000W on September 12, 1983. The ^{60}Co sources were installed at test sites 3 and 4 on December 13 and 14, 1983, and the power was turned on at these test sites on December 15 (central heater power = 2710W; guard heater power = 7220W). The guard heater power at test site 4 was increased to 7600 W on March 14, 1984; the central heater power at that site was increased to 2810 W on June 5, 1984, and to 2850W on June 12 of that year. These adjustments maintained the maximum temperatures in the salt close to 210°C. On October 4, 1985, power reductions began on the central and guard heaters at all four test sites after 863 days of heating at test sites 1 and 2 and 659 days of heating (and 660 and 661 days of irradiation, respectively) at test sites 3 and 4. The power on all the heaters was turned off completely on October 28.

Rothfuchs et al. (1988) reported that the total volumes of brine that flowed into the central boreholes were 125, 125, 100, and 137 mL at test sites 1, 2, 3, and 4, respectively. The average collection rates, obtained by dividing these volumes by 863 or 659 days of heating, were 0.145, 0.145, 0.152, and 0.208 mL day^{-1}.

Pretest modeling of the Asse brine-migration test was conducted using: (1) a model that assumed that transport would occur by migration of fluid inclusions up the thermal gradient, and (2) a vapor-phase transport model. The brine content of the salt was assumed to be 0.05 wt% for both of these models. The fluid-inclusion model predicted that about 400 mL of brine would flow into the central borehole after about 2 years; the vapor-phase transport model predicted about 2 L (assuming a permeability of 0.1 µdarcy) and 4 or 5.L (1 µdarcy). Rothfuchs et al.(1988) concluded that despite the fact that the brine volume predicted by the fluid-inclusion model was "in the same range as the measured values" (100–137 mL), "this agreement is of no significance" because the quantity of fluid inclusions assumed to be present for this calculation (0.05 wt%) was much higher than that present in the Main Halite at test sites 1, 2, 3, and 4 (see below). They also concluded that, although the shape of the water volume versus time curve predicted using the vapor-phase transport model was similar to the measured curves, the predicted volumes were much higher than the measured values.

The average, pretest, total water content of the Main Halite at test sites 1, 2, 3, and 4 was 0.213 wt% (Rothfuchs et al. 1988, Table 7-1). However, most of this water was present as structurally bound water in the mineral polyhalite ($K_2MgCa_2(SO_4)_4 \cdot 2H_2O$), which varied from 1.88 to 6.68 wt% of the samples of the Main Halite obtained for pretest analysis. (The other minerals present at significant concentrations were halite, which varied from 92.00 to 96.58 wt%; and anhydrite, which varied from 0.47 to 5.48 wt%.) Rothfuchs et al.(1988) subtracted the water content of the polyhalite from the total water content and reported the difference as "adsorbed water." The average, pretest adsorbed water content of the Main Halite was 0.030 wt%. However, they did not specify how much, if any, of the adsorbed water was present as fluid inclusions, intergranular brine, or in other forms. The average, posttest, total water content of the Main Halite at test sites 1, 2, 3, and 4 was 0.123 wt% and the average, posttest, adsorbed water content was 0.023 wt% (Rothfuchs et al. 1988, Table 7-2). The difference between the average, pretest and the average, posttest, total water contents (0.213 wt% − 0.123 wt% = 0.090 wt%) probably does not represent the amount of brine that migrated to the central boreholes during the test, because most of the total water content of the Main Halite is contained in polyhalite, which does not start to dehydrate until the temperature exceeds 235 °C. Instead, the difference in the average, pretest and the average, posttest, total water contents — and the average, pretest and the average, posttest, adsorbed water contents — probably represents the small-scale, heterogeneous distribution of polyhalite and adsorbed water in the Main Halite at test sites 1, 2, 3, and 4 (Rothfuchs et al. 1988).

Table 17 compares the experimental parameters and results of the four in situ studies of brine migration described above. The amounts of brine collected under heated conditions and the rates at which brine was collected in these studies decreased in the order WIPP > Project Salt Vault > Asse > Avery Island. This is consistent with the observation that bedded salt contains significantly more brine than domal salt, because both the volumes collected and the rates at which they were collected were higher in the WIPP and Project Salt Vault than in the Asse and Avery Island. In the case of the domal salts, it is also consistent with the maximum temperatures attained in these tests, because the volumes and rates in the Asse were higher than those at Avery Island. The only inconsistency is that more brine was collected in the WIPP than in Project Salt Vault, despite the fact that the maximum temperatures in Project Salt Vault were higher than those in the WIPP. It is unclear why so much more brine was collected in the WIPP than in Project Salt Vault.

The uncertainties described in this brief summary of the brine-migration literature clearly identify this process as one that would require additional investigation, if a salt site were considered for disposal of spent fuel or HLW. This is especially true for bedded salt, which contains more brine that domal salt (see above). This knowledge gap is described in Section 2.4.5.1.

Table 17.   Comparisons of Four *In Situ* Studies of Brine Migration.

Characteristic or Parameter	Project Salt Vault[A]	Avery Island[B]	WIPP[C]	Asse[D]
Type of salt	Bedded	Domal	Bedded	Domal
Brine content	0.5 vol %	0.054 wt%	0.1-1 or 2 wt%	0.02-0.03 wt%[E]
Duration of test	~12–19 months	325 & 350 days	441 & 600 days	659 & 863 days
Heater power	1.5-2.1 kW	1.0 kW	470 W & 1.5 kW	9.75-10.74 kW
Maximum temperature	150–200 & 142°C	51 °C	55, 120, & 130°C	~210°C
Brine collected, prior to heating or unheated	NA	NA	230, 90, 22.4, & 19.3 g	NA
Average rate, prior to heating or unheated	NA	NA	32, 13, 5.33, & 4.60 g day^{-1}	NA
Brine collected, heated	1.7, 0.8, & 3.1 L	8.27 & 5.10 g	4.3, 4.3, 36, & 38 kg	100, 137, 125, & 125 mL
Avg. or steady-state rate, heated	0.43, 0.22, & 10-93 mL day^{-1}	0.0175 & 0.0107 g day^{-1}	8, 8, 20, & 50 g day^{-1}	0.152, 0.208, 0.145, & 0.145 mL day^{-1}

Sources:

A. Bradshaw and McClain (1971)

B. Krause (1983)

C. Nowak (1986), Nowak and McTigue (1987)

D. Rothfuchs et al. (1988)

2.4.2.2   Possible Effects of Brine-Steel Interactions on Chemical Conditions

Perhaps the most important consequence of possible brine migration towards the waste packages in a salt repository for spent fuel or HLW is that water could react with steel, other Fe-base materials, or other metallic components of the waste packages and produce hydrogen (H_2) gas via anoxic corrosion. Anoxic corrosion is the corrosion of steel, other Fe-base materials, or other metals such as Al and Al-base alloys by the oxygen in H_2O instead of by the free molecular O2 in dissolved in the aqueous or gaseous phase (Westerman et al. 1986; Haberman and Frydrych 1988; Westerman et al. 1988; Simpson and Schenk 1989; Brush et al. 1990; Grauer et al. 1991; Telander and Westerman 1993; 1997; Smart et al. 2002a; 2002b).

Telander and Westerman (1993; 1997) carried out a laboratory study of anoxic corrosion as part of a series of studies of gas generation by TRU waste in the WIPP (Brush 1990; Brush et al. 1990; Davies et al. 1991; Mendenhall et al. 1991; Brush et al. 1991a; 1991b; 1993; 1994; Brush 1995; Freeze et al. 1995a; 1995b; Wall and Enos 2006b; Roselle 2009; 2010; 2011a; 2011b). Although conducted for the WIPP, these studies of anoxic corrosion and the hydrologic and mechanical responses of bedded salt to gas generation have provided insights applicable to a salt repository for spent fuel or HLW.

Telander and Westerman (1993; 1997) concluded that, absent microbial production of CO_2 and H_2S — which might occur in the WIPP (Francis and Gillow 1994; 1997; Gillow and Francis 2003) but would not be expected in a repository for spent fuel or HLW, anoxic corrosion occurs in WIPP brines at 30 ºC via the reaction:

$$Fe + (x + 2)H_2O \rightarrow Fe(OH)_2 \cdot xH_2O + H_2 \tag{23}$$
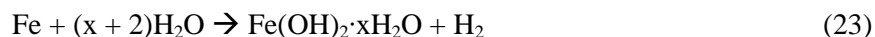
In this reaction, Fe represents metallic iron in the mild-steel waste containers being emplaced in the WIPP and the Fe-base materials in TRU waste; H_2O is the water in WIPP brines; $Fe(OH)_2 \cdot xH_2O$ is a solid, Fe(II)-bearing, corrosion product similar in composition to the mineral amakinite, but with a distinct and unidentified X-ray diffraction (XRD) pattern; and H_2 is the gaseous corrosion product released by the reduction of the water in brines.

Westerman et al. (1986; 1988) observed anoxic corrosion similar reactions in three synthetic Permian Basin brines at 90, 150, and 250 ºC in a laboratory studies carried out for the SRP (Section 2.4.4.2). The corrosion product in their experiments depended on the Mg concentration of these brines. Anoxic corrosion of mild steel representative of the candidate waste package material for a commercial salt repository for spent fuel or HLW produced magnetite (Fe_3O_4) or magnesioferrite ($MgFe_2O_4$) in the two brines with low Mg concentrations (134 and 122 mg L^{-1}, respectively). The simplified, Mg-free reaction is:

$$3Fe + 4H_2O \rightarrow Fe_3O_4 + 4H_2 \tag{24}$$
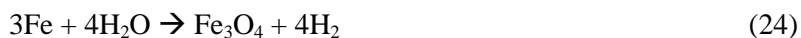
In this reaction, Fe_3O_4 is a solid, Fe(II,III)-bearing corrosion product in which one third of the Fe is present as Fe(II)O and the other two thirds are present as Fe(III)$_2$O$_3$. (In magnesioferrite, the Mg is present as Mg(II)O and the Fe occurs as Fe(III)$_2$O$_3$.) However, anoxic corrosion produced Mg-bearing amakinite ((Fe,Mg)(OH)$_2 \cdot$xH$_2$O) in a high-Mg brine (60,000 mg L^{-1}).

Simpson and Schenk (1989) calculated that the equilibrium H_2 fugacities (similar to the partial pressure) for reactions 23 and 24 are approximately 100 and 500 atm, respectively. In other words, reactions 23 and 24 will proceed, as long as both reactants (metallic Fe and H_2O) are present, until the fugacity of H_2 reaches ~100 or ~500 atm. At these fugacities, metallic Fe and H_2O are in equilibrium with $Fe(OH)_2 \cdot xH_2O$ or Fe_3O_4 and H_2, and these reactions stop. Brush (1990) calculated that the equilibrium values of f_{H2} for these reactions are ~60 and ~400 atm. Wall and Enos (2006b), however, used recently obtained thermodynamic data from Chivot (2004) and obtained values of ~600 and ~500 atm.

The calculations by Wall and Enos (2006b) imply that both of these reactions would produce H_2 partial pressures well in excess of lithostatic pressure prior to reaching equilibrium in repositories at depths of several hundred meters. (Lithostatic pressure at 655 m, the depth of the WIPP repository horizon, is about 150 atm.) Therefore, fracturing of the host geologic formation at pressures at or near lithostatic pressure would probably prevent the build-up of H_2 partial pressures to those required to stop reactions 23 and 24.

However, Telander and Westerman (1993; 1997) found this reaction is self-limiting: it proceeds if brine is present but stops once all of the brine has been consumed, because the relative humidity of water vapor in the WIPP (~73-75%) is too low for anoxic corrosion to occur, at least at 30 °C.

The WIPP performance-assessment (PA) code Brine and Gas Flow (BRAGFLO) (DOE 2009, Appendix PA-2009) predicts that, for various combinations of the parameters sampled by PA, the quantities of brine that will enter the repository after it is filled and the panel seals are emplaced are only sufficient to react with about 40 to 50% of the steel waste containers and Fe-base materials in the waste. Therefore, anoxic corrosion in the WIPP will probably be brine-limited. Furthermore, most of the PA personnel familiar with these calculations think that the quantities of brine predicted to enter the repository are probably highly conservative (i.e., greatly overestimated), mainly because of the highly conservative assumptions and parameter values that were "grandfathered" into the PA baseline when the EPA certified the WIPP in 1998.

WIPP PA also predicts (DOE 2009, Appendix PA-2009) that: (1) the gas generated by TRU waste could increase the pressure to lithostatic pressure (~150 atm at 655 m) under some combinations of the parameters sampled for PA calculations; (2) any additional gas generation and pressure increases will enlarge preexisting fractures in the anhydritic ($CaSO_4$-rich) marker beds in the Salado Fm., or initiate new fractures in these units; (3) storage of gas in these fractures will preclude pressures in excess of lithostatic in the repository; (4) gas will migrate outward into fractures above the waste and brine will migrate outward into fractures below the waste, thereby preventing additional anoxic corrosion and H_2 production even before all of the brine in the near field has been consumed; (5) fracturing is limited in extent relative to the regulatory boundaries of the WIPP site and hence will not deleteriously affect the performance of the WIPP. The fifth conclusion is especially significant, given that the quantities of brine predicted to enter the repository are probably highly conservative.

On the other hand, anoxic corrosion of the steel waste containers and Fe-base materials in the waste will create strongly reducing conditions in the WIPP, or in a salt repository for spent fuel or HLW. These conditions will be so strongly reducing that they would plot below the lower stability limit of water on an Eh-pH diagram. This is because the lower stability limit of water on such a diagram is typically calculated for a total pressure of 1 atm but, according to Wall and Enos (2006b), the equilibrium H_2 partial pressure at equilibrium between metallic Fe and its corrosion products is ~500 to ~600 atm, well below the stability field of water. Consequently, the conditions created by anoxic corrosion would reductively immobilize radioelements such as Se, Tc, U, Np, Pu, and Am, if the waste packages were breached and they were released to the near field. Furthermore, laboratory and field studies too numerous to cite here have shown that metallic Fe, and Fe(II)- and Fe(II,III)-bearing corrosion products such as amakinite and magnetite effectively reduce Se, Tc, U, Np, Pu, and Am from their higher to their lower oxidation states. In the case of the WIPP, the beneficial effects on the long-term performance of the repository of the lower solubilities and higher K_ds of U(IV), Np(IV), and especially Pu(III,IV), predicted for these strongly reducing conditions far outweigh any concerns about highly localized fracturing from pressurization caused by H_2 production. Moreover, it is possible that the same beneficial effects on performance could be demonstrated for a salt repository for spent fuel or HLW in thick, corrosion-allowance, Fe-base waste packages.

2.4.3   Current Salt Repository Concepts

German disposal concepts have focused on two main waste package designs: POLLUX and BSK-3. POLLUX canisters, made of carbon steel, were the first to be considered. The large POLLUX canisters can be used for storage as well as disposal, eliminating the need for repackaging prior to emplacement. Because they are intended for storage as well as disposal, the POLLUX casks are self-shielding, and thus do not require an exterior shielding cask during emplacement. This simplifies and limits the waste handling steps prior to final disposition. However, because they must be self-shielding, they are quite large. The largest POLLUX cask weighs ~60,000 kg and has the capacity to dispose of fuel rods from up to 10 PWR assemblies or 30 BWR assemblies (Gmal et al. 2003). The dimensions of the canister are:

- Wall thickness (shielding cask)   27 cm

- Wall thickness (fuel container)   16 cm

- Outer diameter   1.56 m

- Length   5.52 m

The casks will be emplaced horizontally in mined drifts within the salt, and the area around the cask will be backfilled with crushed salt Figure 14.

The BSK-3 design is a lighter, slimmer canister capable of being placed vertically in boreholes extending down from mined drifts in the salt (Peiffer and Weber 2010). Borehole dimensions are 60 cm in diameter and up to 300 m deep (Figure 14). The BSK-3 emplacement concept is based on the German disposal plan for HLW waste, so the same equipment can be used for emplacement. Each canister can hold 3 to 9 fuel assemblies, with a loaded weight of 5,000kg (Figure 15). The thin-walled canister is not self-shielding. The handling of BSK-3 canisters will need to be done remotely, and delivery vehicles require a shielding sleeve around the canister (Bollingerfehr et al. 2009). The dimensions of the canister are:

- Outer diameter   43 cm

- Outer diameter at the collar   44 cm

- Wall thickness (without collar)   4 cm

- Height (including grab attachment)   4.98 m

- Weight approx.   5.2 tonnes

The boreholes are unlined during emplacement and are backfilled with crushed salt during filling, with a crushed salt layer between canisters.

A decision has not been made whether the POLLUX or BSK-3 canisters, or both, will be used for SNF disposal. The advantages of the POLLUX design are (1) it is the same cask as used for storage, so repackaging is not necessary; (2) it has a larger capacity, requiring fewer be fabricated; and (3) it is self-shielding. The main disadvantage is that the high heat load generated by the large mass of fuel requires interim storage to meet the mandated maximum waste package surface temperature of 200ºC after emplacement. Advantages of the BSK-3 design are (1) the lower heat load—they can be emplaced 3-7 years after removal from the reactor; and (2) it is identical to the HLW disposal scheme, so that the same emplacement equipment could be used. Disadvantages are (1) the waste must be repackaged after storage; (2) the canister is not self-shielding; and (3) the retrievability is questionable—the German program requires retrievability for 500 years, and the BSK-3 waste package may fail before that time (Peiffer and Weber 2010).
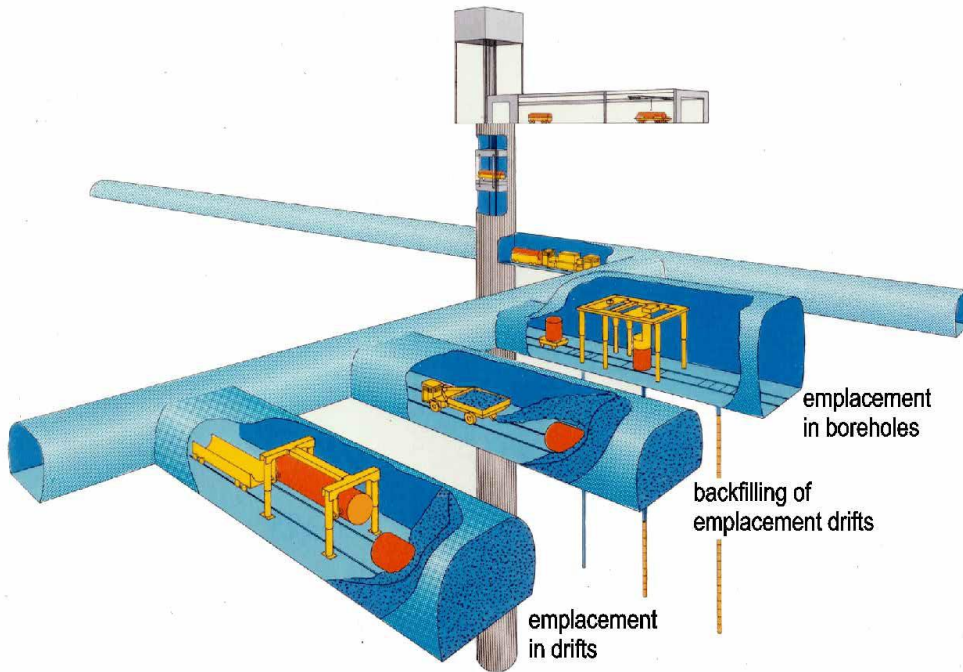
Source: Bollingerfehr et al. (2008), Figure 1.

Figure 14.   Basic disposal conceptual model for the POLLUX and BSK-3 in a mined salt repository
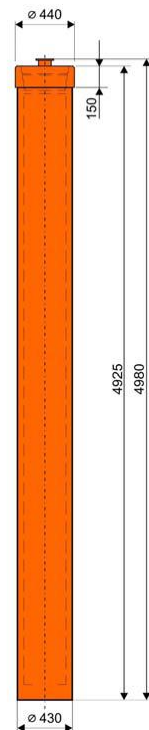
Source: Bollingerfehr et al. (2009), Figure 2.

Figure 15.   Picture and schematic of a dummy BSK-3 waste container (dimensions in mm)

2.4.4   Current State of Knowledge of Waste-Package Materials in a Salt Repository for Spent Fuel or HLW

2.4.4.1   Germany

The German government and the European Commission funded laboratory and in situ studies of waste-package materials for spent fuel or HLW in salt at the Forschungszentrum Karlsruhe (FZK), or Research Center Karlsruhe; the Gesellschaft zur Förderung der Natur-wissenschaftlichtechnischen Forschung, or Corporation for the Promotion of Scientific Research, in Berlin-Adlershof e.V./Institut für Umwelttechnologien GmbH, or Institute for Environmental Technology; and ENRESA, the Spanish national radioactive waste management company.

The Germans have carried out extensive studies of several corrosion-allowance and corrosion-resistant alloys during the 1980s, 1990s, and 2000s (Schwarzkopf et al. 1989; Smailos et al. 1990; Schwarzkopf et al. 1992; Smailos et al. 1992a; Smailos et al. 1992b; Smailos 1993; Smailos et al. 1993; 1994a; Smailos et al. 1994b; Grambow et al. 1998; Janberg and Spilker 1998; Smailos et al. 1998b; Smailos et al. 1998a; Smailos et al. 1999; Smailos 2002; Smailos et al. 2002). Kursten et al. (2004a) reviewed these results and other results from the German program, and the results of other European countries' studies of waste-package materials for spent fuel or HLW in other geologic media.

Based on this work, the Germans have identified carbon steels, especially the mild steel TStE 355, as "the most promising materials" for corrosion-allowance waste packages; and the Ni-base alloy Hastelloy C-4 and the Ti-base alloy Ti 99.8-Pd as the most promising for corrosion-resistant waste packages (Kursten et al. 2004a). Table 18 provides the chemical compositions of these materials.

The Germans conducted a screening study that included both corrosion-allowance and corrosion-resistant alloys (Smailos et al. 1990; Kursten et al. 2004a). These studies included (1) two mild steels (the fine-grained steel TStE 355 and the cast steel GS 16Mn5), (2) two low-alloyed steels (TStE 460 and 15 MnNi 6.3, (3) a nodular cast iron (GGG 40.3) and a Si-cast iron, (4) two Ni-resists (D2 and D4), (5) two Cr-Ni steels (AISI 304L and AISI 309S stainless), (6) three Ni-base alloys (Inconel 625, Inconel 825, and Hastelloy C-4), and (7) a Ti-base alloy (Ti 99.8-Pd) (Kursten et al. 2004a). Smailos et al. (1990, Table 1) and Kursten et al. (2004a) provided the compositions of all of these alloys.

The screening study used two brines, both with high concentrations of $MgCl_2$ — brine 1, also referred to as "Q brine," with 26.8 wt% $MgCl_2$; and another brine with 45 wt% $MgCl_2$ — at 170 °C for periods of up to 400 days. The Germans typically use three standard brines: brine 1; brine 2, with 33.03 wt% $MgCl_2$; and brine 3, which is essentially an NaCl-saturated brine with much lower concentrations of $MgSO_4$, K_2SO_4, and $CaSO_4$. Table 19 provides the chemical compositions of these brines. Therefore, the screening study used a brine with an $MgCl_2$ concentration significantly higher than those of brines 1 and 2.

None of the publications or reports on the German waste-package work obtained to date explains why the standard brines 1, 2, and 3 were chosen. However, the choice of these brines appears to be analogous the SRP's choice of its intrusion brine, Permian Basin Brine 1 (PBB1) and its inclusion brine (PBB3), respectively (Section 2.4.4.2).

According to Kursten et al. (2004a), "The criteri[a] for the selection of the materials as candidate packaging materials was their resistance to local[ized] corrosion, selective corrosion, and stress corrosion cracking (SCC)." Therefore, the screening study used coupons, two coupons clamped together (for crevice corrosion), and U-bend specimens (for SCC). Metallography and surface profilometry were used for post-test analysis (Kursten et al. 2004a).

Table 18.   Chemical compositions (wt%) of TStE 355, Hastelloy C-4, and Ti 99.8-Pd "the most promising materials" for waste-packages for spent fuel or HLW in a German salt repository

Element	TStE 355	Hastelloy C-4	Ti 99.8-Pd
H_2			0.001
C	0.17	0.006	0.01
O_2			0.04
Si	0.44	0.05	-
Ti		0.33	Balance
Cr		15.4-16.8	
Mn	1.49	0.09	
Fe	Balance	0.05	0.05
Ni		Balance	
Mo		15.2-15.9	
Pd		-	0.18

Source: Kursten et al.(2004a), Table 4-1

Table 19.   Chemical compositions of standard brines used for German studies of waste-package materials for spent fuel or HLW in a salt repository. The compositions of these brines are representative of those expected in the Gorleben salt dome

Dissolved Concentration (wt%) or Property	Brine 1 (Q Brine)	Brine 2	Brine 3
NaCl	1.4	0.31	25.9
$MgCl_2$	26.8	33.03	-
$MgSO_4$	1.4	-	0.16
K_2SO_4	-	-	0.23
KCl	4.7	0.11	-
$CaSO_4$	-	0.005	0.21
$CaCl_2$	-	2.25	-
H_2O	65.7	64.3	73.5
Dissolved O_2 (mg L^{-1})	0.8-2.8	0.6-1.5	1.2-4.9
pH (scale unspecified)	4.3-4.6	4.1	6.5-6.9

Source: Kursten et al.(2004a), Table 4-3

The screening study demonstrated that: (1) the two Ni-resists (D2 and D4) and the nodular cast iron (GGG 40.3) exhibited "heavy intergranular corrosion;" (2) the two Cr-Ni steels (304L and 309S stainless) and two of the Ni-base alloys (Inconel 625 and 825) displayed "severe pitting/crevice corrosion" and, in the case of the stainless steels, SCC; (3) the unalloyed steels (TStE 355 and GS 16Mn5), the low-alloyed steels (TStE 460 and 15 MnNi 6.3), the third Ni-base alloy (Hastelloy C-4), and Ti 99.8-Pd were all resistant to crevice corrosion, pitting, and SCC. Therefore, the Germans selected TStE 355, GS 16Mn5), TStE 460, 15 MnNi 6.3, Hastelloy C-4, and Ti 99.8-Pd as the best candidate materials for further study (Kursten et al. 2004a).

The follow-on studies of these materials (Kursten et al. 2004a) included the effects of several factors:

1. Brine composition. Brines 1, 2, and 3 were used for these and other waste-package corrosion studies (see Table 3 above). It is unclear whether brines 1 and 2 were chosen to simulate inclusion brines, analogous to PBB3 (used for the SRP's corrosion studies described in Section 2.4.4.2); or whether brine 3 was selected to simulate an intrusion brine, analogous to the SRP's PBB1 and PBB2.

2. pH. The pH of brine 1 was varied from 3 to 7, and that of brine 3 from 1 to 10, by addition of HCl or NaOH.

3. Other brine constituents. The concentrations of $B(OH)_4^-$, a constituent of domal (and bedded) salt; dissolved Fe(III) species, possible waste-package corrosion products that could form from radiolysis or intrusion of O2 into the repository; and H_2O_2 and ClO_4^-, both produced by γ radiolysis of brines; were varied from 10^{-3} to ~10^{-1} M. Another study determined the effects of H_2S, a thermally released salt impurity, on TStE 355. For this study, H_2S as $Na_2S \cdot 9H_2O$ was added to brine 1 at concentrations of 25, 100, and 200 mg L^{-1} to simulate the amounts of H_2S that could be released from 10-, 20-, 40-cm-thick annular volumes, respectively, around HLW boreholes.

4. Temperature. The Germans used temperatures of 90, 150, 170, and 200°C for their long-term, brine-inundated experiments. The maximum temperature on the surface of a waste package depends, of course, on parameters such as the length of the interim-storage period of the waste, the waste-package loading, and the distance between the POLLUX casks containing spent fuel, or HLW boreholes. Because these design parameters have not been specified yet for a German repository, temperatures of 150, 170, and 200°C were used to simulate the maximum waste-package temperature. A temperature of 90°C was used to simulate that which would be established after about 500-1000 years, depending on these design parameters. Furthermore, temperatures of 90 and 170°C were also the reference temperatures used in the early European cooperative near-field research programs.

5. Radiation dose rate. The effects of γ radiation on corrosion were simulated using doses of 10^0 to 10^3 Gy hr^{-1} (10^2 to 10^5 rad hr^{-1}). A γ dose rate of 101 Gy hr^{-1} corresponds to that expected at the surface of a roughly 15 cm-thick, corrosion-allowance waste package; a rate of 103 Gy hr^{-1} simulates a roughly 5 mm-thick corrosion-resistant waste package.

6. Welding. Welded specimens were added to the specimens fabricated of the parent materials to simulate the effects of electron-beam welding, metal-active gas welding, submerged-arc welding, and tungsten-inert gas welding for sealing container lids. Submerged-arc welding has also been considered for surface-welding a 3-to-4 mm-thick layer of corrosion-resistant Hastelloy C-4 to a mechanically strong container made of carbon steel.

None of the papers or reports obtained to date explains why the Germans chose TStE 355 as "the most promising [corrosion-allowance] material" instead of GS 16Mn5, TStE 460, or 15 MnNi 6.3. Kursten et al.(2004a), however, explained that Ti 99.8-Pd is "the most promising [corrosion-resistant] material" because Hastelloy C-4 exhibited crevice corrosion in brine 1 at 90, 170, and 200 °C in 3 year experiments, and pitting in brine 1 at 200 C in a 3-year test.

The following text briefly summarizes the review in Kursten et al.(2004a) of the results of studies of the mild steel TStE 355 and the Ti-base alloy Ti 99.8-Pd.

Both the brine composition and the temperature affected the corrosion rate of TStE 355. The rates measured after immersion in brine 1 at 90, 170, and 200 °C for 4 years were 69.7 ± 1.8, 199.4 ± 15.0, and 462.8 ± 33.6 µm yr^{-1}, respectively. The corresponding rates for brine 2 were 37.6 ± 15.0, 307.9 ± 45.3, and 651.2 ± 155.2 µm yr^{-1}. Those for brine 3 were 5.1 ± 2.2, 46.0 ± 7.3, and 18.3 ± 3.6 µm yr^{-1} (Kursten et al. 2004a, Table 4-5). These investigators concluded that the uniform corrosion rate increased with temperature in all three brines because TStE 355 corroded by "a thermally activated process" and because the pH of all three brines decreased as the temperature increased. They concluded that the higher corrosion rates observed in brines 1 and 2, especially at higher temperatures, were caused by the higher Mg^{2+} concentrations of these brines, which affected the identity of the corrosion products (see below), and the higher Cl^- concentrations of these brines.

Post-test XRD analysis showed that the corrosion products at 90 °C were hematite (α-Fe_2O_3) and magnetite (Fe_3O_4) in brine 1, akaganeite (β-FeOOH) in brine 2, and magnetite and akaganeite in brine 3. At 170 °C, they were amakinite ($(Fe,Mg)(OH)_2$) in brines 1 and 2, and magnetite in brine 3. Kursten et al.(2004a) did not provide results for 200 °C. Apparently, the high concentration of Mg in brines 1 and 2 prevented the formation of magnetite in these brines, and — because magnetite inhibits the corrosion of mild steels but amakinite does not — the corrosion rates were higher in brines 1 and 2 than in brine 3. Section 2.4.4.2 describes in more detail the mechanisms by which high Mg concentrations affect the high-temperature corrosion of mild steels.

Metallographic examination and surface profiling of TStE 355 after these experiments did not reveal any crevice corrosion or pitting. However, some nonuniform corrosion occurred due to inhomogeneities in the steel; the maximum depth of this nonuniform attack corresponded to the average reduction in thickness of the specimens.

The effect of pH on the corrosion rate of TStE 355 was determined after immersion in brines 1 and 3 at 170 °C for up to 1 year. The pH of brine 1 was set at 3 to 7 and that of brine 3 at 1 to 10 by adding HCl or NaOH. The rates measured in brine 1 were 207, 209, 186, and 177 µm yr^{-1} at a pH of 3, 4, 5, and 7, respectively. In brine 3, the rates were 50, 42, 46, 28, and 26 µm yr^{-1} at a pH of 1, 2, 5, 6, and 10 (Kursten et al. 2004a, Figures 4-8 and 4-9). Although the differences among the rates measured in brine 1 at all four pH values and those in brine 3 at a pH of 1, 2, and 5 were insignificant statistically, those measured in brine 3 at a pH of 6 and 10 were significantly less than those measured in this brine at pH = 1, 2, and 5 (Kursten et al. 2004a). This difference was tentatively attributed to the thick layer of corrosion products that formed on the specimens in this brine at pH = 6 and 10.

After these experiments were terminated, the pH of both brines migrated to nearly identical values, 4.5 to 4.8 in brine 1 and 5.4 to 5.7 in brine 3, regardless of their initial pH, possibly due to buffering by reactions among dissolved solids and the corrosion products.

Posttest analysis of TStE 355 did not reveal any crevice corrosion or pitting. However, some non-uniform corrosion occurred.

The effects of the $B(OH)_4^-$, Fe(III) species, and H_2O_2 and ClO_4^- on the corrosion rate of TStE 355 were relatively modest in most cases. Immersion in brine 1 at 90 °C for up to 1 year yielded rates of 70 µm/year for brine 1 with no added species and rates of 93 µm/year for brine 1 with 1.4×10^{-1} M $B(OH)_4^-$ to 123 µm/year for this brine with 1×10^{-3} or 1×10^{-2} M H_2O_2. (Kursten et al. 2004a, did not specify which these concentrations of H2O2 was actually used in these experiments.) The corresponding tests in brine 1 at 170 °C gave rates of 224 µm yr^{-1} for brine 1 with no added species and rates of 115 µm yr^{-1} for brine 1 with 1.4×10^{-1} M $B(OH)_4^-$ to 254 µm yr^{-1} for brine 1 with all four species present simultaneously (1.4×10^{-1} M $B(OH)_4^-$, 3.5×10^{-2} M Fe(III), 1×10^{-3} or 1×10^{-2} M H_2O_2, and 1×10^{-3} M ClO^-). The results for brine 3 at 170 °C were similar: the rate with no added constituents was 46 µm yr^{-1} and the

rates with each or all of these species varied from 30 μm yr^{-1} with 1×10^{-3} or 1×10^{-2} M H$_2$O$_2$ to 73 μm/year with all four species. In the case of brine 3 at 70 °C, however, addition of these species significantly increased the corrosion rate of TStE 355: the base rate (no added species) was 5 μm yr^{-1}, but additions of these species increased the rate to 26 μm yr^{-1} with 1×10^{-3} or 1×10^{-2} M H$_2$O$_2$ and up to 236 μm yr^{-1} with all four constituents present simultaneously (1.4×10^{-1} M B(OH)$_4^-$, 3.5×10^{-2} M Fe(III), 1×10^{-3} or 1×10^{-2} M H$_2$O$_2$, and 1×10^{-3} M ClO$^-$).

B(OH)$_4^-$, Fe(III) species, and H$_2$O$_2$ and/or ClO$_4^-$ resulted in more nonuniform corrosion of TStE 355 in brine 1 at 170 °C. In the pure brine, the maximum depth of nonuniform attack was about 200 μm. However, pitting occurred when these species were added − individually or simultaneously — with a maximum depth of 500 μm. Pitting was not observed in brine 1 with these species at 90 °C for up to 1 year. In brine 3, nonuniform corrosion occurred in only one experiment: the 170 °C test with all four species present simultaneously. The maximum depth of nonuniform corrosion in this test was 130 μm.

The presence of H$_2$S (added as Na$_2$S·9H$_2$O) at concentrations of 25, 100, and 200 mg L^{-1} did not affect the rate of uniform corrosion or the extent of nonuniform corrosion of TStE 355 in brine 1 at 170 °C for 325 days, or in brine 3 at 150 °C for slightly more than 1 year. Post-test XRD analysis did not detect any sulfides among the corrosion products.

The Germans determined the effects of γ radiation on the corrosion of TStE 355 at 90 °C in brine 1 and at 150 °C in brines 1, 2, and 3 (Kursten et al. 2004a). At 90 °C, γ dose rates of 10^0 to 10^2 Gy hr^{-1} (10^2 to 10^4 rad hr^{-1}), which correspond to those expected at the surfaces of thick, corrosion-allowance waste packages, did not affect the corrosion rate or the type of corrosion of TStE 355. However, at 90 °C and a dose rate of 103 Gy hr^{-1}, which corresponds to that expected at the surface of a 5 mm-thick, corrosion resistant waste package, the corrosion rate of TStE 355 was 464.2 μm yr^{-1} after experiments of up to 244 days, about 10 to 20 times greater than the rates measured at 90 °C after comparable periods in the absence of γ radiation. Furthermore, pitting occurred, but the maximum depth of pitting was only slightly greater than the average uniform corrosion rate. These differences were attributed to the presence of H$_2$O$_2$ and ClO$_3^-$, both of which are strong oxidizing agents, from γ radiolysis of the brine.

The corrosion rates of TStE 355 in both unirradiated and irradiated (10^1 Gy hr^{-1}) brines 1, 2, and 3 at 150 °C were relatively rapid for about the first 100 days, then decreased to scattered values that were fitted with straight lines representing relatively constant rates from 100 to about 500–600 days. For brine 1, the long-term rates were 47.1 μm yr^{-1} (unirradiated) and 72.6 μm yr^{-1} (10^1 Gy hr^{-1}); for brine 2 they were 119.6 μm yr^{-1} (unirradiated) and 162.4 μm yr^{-1} (10^1 Gy hr^{-1}); and in brine 3 they were 15.3 (unirradiated) and 13.5 μm yr^{-1} (10^1 Gy hr^{-1}). TStE 355 was resistant to pitting corrosion in both the unirradiated and irradiated brines. Kursten et al.(2004a) did not describe any experiments at higher dose rates.

Experiments on the effects of welding on the uniform and nonuniform corrosion of TStE 355 showed that, for conditions under which adverse effects were observed, heat treatment consisting of stress-relief thermal treatment for 2 hours at 600 °C prior to testing eliminated these adverse effects. For more details on this and a review of the German experiments on stress corrosion cracking, the reader is referred to Kursten et al.(2004a, pp. 88-90 and 91–95, respectively).

The corrosion rates of the corrosion-resistant, Ti-base alloy Ti 99.8-Pd in brine 1 were very low initially and generally decreased with time. The rates measured after immersion in this brine 1 at 90 °C for 559 and 1280 days were 0.17 ± 0.03 and 0.06 ± 0.02 μm yr^{-1}, respectively. The corresponding rates for 170 °C after 180, 529, and 1280 days were 0.16 ± 0.02, 0.07 ± 0.03, and 0.04 ± 0.02 μm yr^{-1}. Those for 200 °C after 540 and 1280 days were 0.14 ± 0.03 and 0.15 ± 0.02 μm yr^{-1}. Ti 99.8-Pd was resistant to crevice corrosion, pitting, and stress corrosion cracking.

The corrosion rate of Ti 99.8-Pd in brine 1 at 90 °C and a γ dose rate of 10^3 Gy hr^{-1} was 0.7 μm yr^{-1} after 609 days; the corresponding rate calculated for unirradiated conditions was 0.17 μm yr^{-1}. No evidence of nonuniform corrosion was observed under these irradiated conditions. The corrosion rates of Ti 99.8-Pd

in brine 1 at 150 °C and a dose rate of 10^1 Gy hr^{-1} after 63, 174, 244, and 356 days were 0.06, 0.14, 0.62, and 0.21 μm yr^{-1}; the corresponding rates absent radiation after 63, 125, 191, and 268 days were 0.09, 0.02, 0.73, and 0.02 μm yr^{-1}. Therefore, Kursten et al.(2004a, p. 100) concluded that "The imposition of a 10 Gy hr^{-1} γ irradiation field [on brine 1 at 150 °C] did not increase the corrosion rate of Ti 99.8-Pd."

2.4.4.2   USA

The DOE funded laboratory and in situ studies of waste-package materials for spent fuel or HLW at SNL as part of its research and development activities for the WIPP. The DOE also funded similar studies at Pacific Northwest National Laboratory (PNNL) as part of the SRP.

WIPP Project

SNL studied the Ti-base alloy American Society for Testing and Materials (ASTM) Grade-12 Ti, usually referred to as TiCode-12, for possible use as a corrosion-resistant waste-package material in a salt repository for commercial or defense HLW (Braithwaite et al. 1979; Braithwaite and Molecke 1980; Molecke et al. 1981; Matalucci et al. 1982; Molecke et al. 1982; Molecke 1983; Molecke et al. 1983; Molecke 1984; Moody et al. 1985; Sorensen and Ruppen 1985; Molecke 1986; Moody and Robinson 1986; Molecke and Avyle 1988; Molecke et al. 1988; Schutz and Hall 1988; Tyler et al. 1988; Molecke et al. 1993). Because the 1979 WIPP Authorization Act restricted the WIPP to defense-related TRU waste (Section 2.4.1.3), the objective of these studies was to provide information applicable to disposal of spent fuel or HLW in salt at potential sites other than the WIPP site. Table 20 provides the composition of TiCode-12 specified by the ASTM.

SNL selected TiCode-12 based the results of a screening study that included 20 corrosion-allowance and corrosion-resistant alloys (Braithwaite and Molecke 1980, Table 2). This study compared the rates of general corrosion of all 20 of these alloys in three deoxygenated (30 ppb O2) solutions (Brine A, Brine B, and seawater) at 250 °C and 5 MPa after 28 days (Braithwaite and Molecke 1980, Table 3). It also compared the corrosion rates of 7 of these alloys in two oxygenated solutions (Brine A with 600 ppm O_2 and seawater with 1750 ppm O_2) at 250 °C and 7 MPa after 14 days (Braithwaite and Molecke 1980, Table 6).

Table 20.   Chemical Composition of TiCode-12

Element	Concentration (wt%)
H (max.)	0.015
C (max.)	0.08
N (max.)	0.03
O (max.)	0.25
Fe (max.)	0.30
Ni (range)	0.6–0.9
Mo (range)	0.2–0.4
Other (total)	0.30
Ti	Balance

Source: Molecke et al. (1983), Table 1

Brine A and Brine B were WIPP standard brines established by Molecke (1976) and Dosch (1976) for use in WIPP-related laboratory experiments; Molecke (1983) provided additional documentation of these brines. Braithwaite and Molecke (1980) used seawater in addition to the two WIPP brines because the U.S. Subseabed Disposal Program (SDP) cofunded SNL's initial screening study and subsequent studies of TiCode-12. Subsequent to these studies of TiCode-12, Brush (1990) replaced Brine B with ERDA-6 and Snider (2003) replaced Brine A with Generic Weep Brine (GWB), a synthetic brine representative of intergranular Salado Fm. brines at or near the stratigraphic horizon of the WIPP (Krumhansl et al. 1991). Table 21 provides the chemical compositions of Brine A, Brine B, and seawater.

Table 21.   Chemical compositions of the two standard brines and seawater used for studies of TiCode-12 by the WIPP Project

Total Dissolved Concentration (ppm) or Property	Brine A	Brine B	Seawater
pH (25 °C)	6.5	6.5	8.1
Ca^{2+}	600	900	400
Mg^{2+}	35,000	10	1,272
Sr^{2+}	5	15	13
Na^+	42,000	115,000	10,651
K^+	30,000	15	380
Cl^-	190,00	175,000	18,980
Br^-	400	400	65
I^-	10	10	0.05
SO_4^{2-}	3,500	3,500	884
B	1,200	10	NA
TIC (as HCO_3^-)	700	10	146

Source: Molecke et al. (1983), Table 3

Braithwaite and Molecke (1980, Table 3) reported that the corrosion rates of Corten A steel (a low-C steel), Type 1018 mild steel, and TiCode-12 in deoxygenated Brine A at 250 °C and 5 MPa after 28 days were 0.9, 1.7, and 0.003 mm yr^{-1}, respectively. Therefore, the two corrosion-allowance Fe-base materials corroded 300 and 567 times faster than the corrosion-resistant alloy TiCode-12.

The SNL studies reviewed by Molecke et al. (1983) showed that the uniform corrosion rate of TiCode-12 in deoxygenated Brine A increased with temperature, from 7×10^{-5} mm yr^{-1} at 70 °C to 9×10^{-4} mm yr^{-1} at 150 °C and 3.2×10^{-3} mm yr^{-1} at 250 °C. The corrosion rate in Brine A at 250 C decreased with dissolved O_2 concentration, from 3.2×10^{-3} mm yr^{-1} at 30 ppb O_2 to 1.8×10^{-3} mm yr^{-1} at 450 ppm O_2. Gamma irradiation at 107 rad hr^{-1} increased the corrosion rate in Brine A at 70 °C to 2×10^{-3} mm yr^{-1} in a 49-day experiment, and to 2×10^{-2} mm yr^{-1} in an 87-day run. Molecke et al.(1983) pointed out that rates $< 1 \times 10^{-4}$ mm yr^{-1} were based on very small weight gains, and should regarded as semiquantitative.

Furthermore, the SNL studies did not reveal any evidence of localized corrosion of TiCode-12 (i.e., crevice corrosion or pitting) in experiments in brine at temperatures up to 250 °C for 30 days (1983). However, Ahn and Soo (1982a; 1982b; 1982c) observed crevice corrosion of TiCode-12 in Brine A at 150 and 200 °C in experiments as short as 21 days, and Westerman et al. (1988) reported crevice corrosion of TiCode-12 in irradiated, hydriding experiments with PBB3, a high-Mg SRP brine (Section 2.4.4.2). The observation of crevice corrosion in some, but not all, of these studies clearly identifies crevice corrosion as a process that would require additional investigation if TiCode-12 were considered as a waste package material for spent fuel or HLW in a salt repository. This knowledge gap is described in Section 2.4.5.2.

The DOE expected that calcined, commercial or defense-related HLW would be vitrified using an in-canister melting process in a stainless steel 304L canister to produce a borosilicate glass (the reference waste form). The DOE also considered alternative waste forms such as synroc, but concluded that synroc and other alternatives were too expensive and that the enhanced performance of these alternatives was insufficient to justify their additional cost. Furthermore, the DOE expected that the barrier properties of the geologic medium chosen for disposal would be robust enough so that the overall performance of the repository would be insensitive to the performance of the waste packages, as long as they isolated the waste form from the environment for the duration of the thermal period (a few hundred to a thousand years).

Molecke et al. (1983) proposed that, instead of using TiCode-12 as an overpack material for a 61 cm-diameter-by-3.0 m-long 304L stainless-steel canister and a surrounding 0.5 cm-thick steel overpack, a multipurpose 61 cm-diameter-by-3.0 m-long TiCode-12 canisters be used for: (1) a waste-glass-melting canisters/receptacles for the continuous melting process, (2) temporary storage canisters (if required), (3) a transportation canisters within a reusable shipping casks, and (4) the waste packages emplaced in boreholes in the repository. None of the publications or reports on the SNL waste-package work obtained to date describes how this proposal was received prior to Congressional amendment of the NWPA in 1987, which designated Yucca Mountain as the only potential site for spent fuel or HLW to be characterized.

SRP

PNNL studied the cast mild steel alloy ASTM A216, Grade WCA, for use as a corrosion-allowance waste-package material for spent fuel or HLW as part of the SRP's Waste Package Program (WPP) (Westerman 1980; Westerman et al. 1982; 1984; 1986; 1988). Table 22 provides the chemical compositions of the two lots of A216 used for the PNNL studies (Westerman et al. 1988). PNNL also studied ASTM Grade-12 Ti (TiCode-12) (Ti-0.8 wt% Ni-0.3 wt% Mo) as an alternative, corrosion-resistant material (Westerman et al. 1988). Table 20 provides more detailed information on the composition of TiCode-12.

PNNL carried out an initial screening study that considered metallic, ceramic and polymeric materials for possible use as waste-package materials (Westerman 1980). Later, PNNL conducted a follow-on screening study to determine the susceptibility of six Fe-base alloys to uniform corrosion, nonuniform corrosion, and SCC (Westerman et al. 1986). These alloys included (1) high-purity Fe (0.018 wt% C), (2) American Iron and Steel Institute (AISI) 1025 wrought steel sheet (0.07 wt% C), (3) two mild steels (ASTM A27, Grade 60-30; and ASTM A216, Grade WCA), (4) a ductile cast Fe (ASTM A536-77, Grade 60-40-18), and (5) an alloyed cast steel with 2.46 wt% Cr and 1.02 wt% Mo (Westerman et al. 1986). Finally, PNNL briefly considered TiCode-12 as an alternative to A216l (Westerman et al. 1988). None of the papers or reports on the SRP or WPP obtained to date explains why A216 was chosen as the reference corrosion-allowance waste-package material, or why TiCode-12 was selected as the reference corrosion-resistant material.

Table 22.   Chemical composition of two lots of ASTM A216, Grade WCA

Element	Lot 1 (wt%)	Lot 2 (wt%)
C	0.23	0.16
Si	0.45	0.58
P	0.018	0.014
S	0.018	0.014
Cr	0.41	0.13
Mn	0.71	0.60
Ni	0.23	0.08
Cu	0.14	0.08
Fe	Balance	Balance

Source: Westerman et al. (1988), Table 4.1

As PNNL's work on the WPP progressed, the SRP specified various standard brines and solids for use in their laboratory studies: Westerman et al. (1984) used PBB1 and PBB2; Westerman et al.(1986) used PBB1, PBB2, and PBB3; and reagent-grade NaCl; Westerman et al. (1988) used the same three brines, but used PBB1 solids (the solids dissolved in PBB1) and a standard salt referred to as "surrogate salt." It should also be noted that the reported compositions of these "standard" brines changed with time, especially that of PBB3(and Westerman et al. 1986, Table 4.3; compare Westerman et al. 1988, Table 2). Table 23 provides the chemical compositions of these brines and solids from Westerman et al. (1988, Table 4.3).

Table 23.   Chemical compositions of standard brines and solids used by PNNL for the SRP's WPP

Total Dissolved Elemental Concentrations	PBB1 Brine (mg L^{-1}) and PBB1 Solids (mg)	PBB2 Brine (mg L^{-1})	PBB3 Brine (mg L^{-1})	Surrogate Salt (ppm)
Ca^{2+}	1,560	1,110	18,700	11,200
Mg^{2+}	134	122	60,000	258
Sr^{2+}	35	35	NA	78
Na^{+}	123,000	123,000	23,000	377,000
K^{+}	39	39	11,000	78
Cl^{-}	191,000	191,000	240,000	583,000
Br^{-}	32	24	3,400	NA
SO_4^{2-}	3,200	1,910	250	26,900
HCO_3^{-}	30	23	NA	246

Source: Westerman et al. (1988), Table 4.3

The SRP established these standard brines based on its conclusion that there were two scenarios under which brines could form, migrate, and contact the waste packages in a bedded-salt repository for spent fuel or HLW (Westerman et al. 1988):

1. In the dissolution-brine scenario, low-ionic-strength groundwater was assumed to enter the repository horizon from some external source and dissolve rock salt, thereby attaining a composition a saturation similar to the overall composition of the formation (i.e., essentially an NaCl-saturated brine). This brine, referred to as "PBB1," was established by dissolving samples of rock salt obtained from a subsurface depth of 743.77 to 785.01 m in the G. Friemel Hole No. 1; a depth corresponding to the halite horizon the San Andres Cycle 4 at the SRP's study site in Deaf Smith County (Westerman et al. 1988).

    PBB2, obtained by maintaining PBB1 in a pressurized autoclave at 150 °C for several days and then analyzing the supernatant solution, represents the composition of PBB1 after approaching or contacting the waste packages, heating, and precipitation of solids with retrograde solubilities (solubilities inversely proportional to temperature). Westerman et al. (1988, p. 4.7) concluded that these solids comprised mostly carbonates, but comparison of the compositions of PBB1 and PBB2 in Table 23 shows that anhydrite and/or gypsum also precipitated. Use of PBB2 also solved the problem of precipitation of these solids from PBB1 in the inlet lines of the flow-through autoclaves used for many of PNNL's experiments.

2. In the inclusion-brine scenario, which the SRP considered more likely than the dissolution-brine scenario, fluid inclusions in the formation were assumed to migrate up the thermal gradient or down the pressure gradient towards the waste packages. The SRP expected that these inclusion brines would have higher $MgCl_2$ and $CaCl_2$ concentrations than the dissolution brines, based on analyses of fluid inclusions from the halite horizon in the San Andres Cycle 4 at the site (Westerman et al. 1988). (This report did not provide the actual results of these analyses, but did give the composition of PBB3 derived from them.)

PBB1 salt consisted of the solids used to synthesize PBB1 brine, but without the addition of water. The "surrogate site-specific salt," generally referred to as the "surrogate salt," was established by dissolving samples obtained from a subsurface depth of 816.04 to 826.22 m in the Detten Hole No. 1, about 22.5 km southeast of the SRP's study site (Westerman et al. 1988).

Westerman et al. (1986; 1988) conducted corrosion experiments in Hastelloy C-276 or Inconel 625 autoclaves (volume unspecified). They used these autoclaves for one-phase (brine only) tests under recirculated, refreshed, or static conditions, or for two-phase tests (brine plus salt) tests under static conditions. They used a flow rate of ~35 mL hr^{-1} for their recirculated tests. This was the lowest flow rate that they could easily maintain with their high-pressure pumps. Westerman et al. (1986; 1988) placed these autoclaves in a 60Co irradiation facility for tests under recirculated, refreshed, or static conditions, and used them to test bolt-loaded fracture specimens under two-phase, static conditions.

Westerman et al. (1986; 1988) also performed "excess-salt tests" in welded Inconel 600 or Inconel 625 cans with inside diameters or 64 or 100 mm. They did not explain the differences, if any, between the two-phase autoclave tests and then excess salt tests in these welded cans.

Westerman et al. (1986) determined the effects of anoxic (~50 ppb O_2) and oxic (~1.5 ppm O_2) conditions on the corrosion rates of the six steels used for their follow-on screening study (see above) in the inclusion brine PBB2 (Table 7) in a series of one-phase, recirculated (~35 mL hr^{-1}) experiments. However, they concluded that — given the low flow rate used for these tests — the O_2 dissolved in this brine was insufficient to form the quantities of magnetite (the only corrosion product identified by XRD analysis) inferred from posttest weight-loss determinations of the corrosion rates. Therefore, most of the corrosion observed under these "oxic" conditions was likely anoxic corrosion that proceeded via the reduction of water (Equations 23 and 24). The average corrosion rate of as-cast specimens of A216

mild steel in anoxic PBB2 at 150 °C after ~8 months was 14 μm yr^{-1} (Westerman et al. 1986, Appendix A.1). The corresponding rate under oxic conditions was 25 μm yr^{-1} (Westerman et al. 1986, Appendix A.2). Therefore, the O_2 present in the oxic tests increased the average corrosion rate of these specimens significantly, even if it was insufficient to form the quantities of magnetite that formed during these tests. Subsequently, however, Westerman et al. (1988) used only anoxic conditions.

Westerman et al. (1986) reported that the corrosion of the steels in these experiments was "reasonably uniform, with little evidence of pitting;" and that nonuniform corrosion had not penetrated more than about a tenth of a millimeter below the surface of the specimens.

PNNL performed a series of static autoclave experiments on as-cast, normalized, and weldment specimens of A216 in PBB3 at 90, 150, and 200°C. The 90 and 150°C tests lasted for 1, 3, and 6 months; and the 200°C tests for 1 month. The average corrosion rates of as-cast specimens of lot 1 after 1 month at 90, 150, and 200°C were 0.056, 1.14, and 5.56 mm yr^{-1}, respectively. The average corrosion rate of as-cast lot 2 from the same 200°C test was 4.28 mm yr^{-1}. A duplicate 200°C test for 1 month yielded average rates of 6.52 mm yr^{-1} for as-cast lot 1 and 3.56 mm yr^{-1} for as-cast lot 2 (Westerman et al. 1988, Appendix A).

The average corrosion rates for as-cast, normalized, and weldment specimens of lot 1 in PBB3 at 90 ºC after 1 month were 0.056, 0.060, and 0.045 mm yr^{-1}; the corresponding rates for 150 °C were 1.14, 1.52, and 0.87 mm yr^{-1}; and those for 200 °C were 5.56, 6.44, and 3.24 mm yr^{-1}. The average corrosion rates for as-cast, normalized, and welded specimens of lot 1 from the duplicate 200 ºC test after 1 month were 6.52, 6.14, and 2.39 mm yr^{-1}. Heat treatment did not affect the corrosion of lot 2 significantly. The average rates for as-cast and normalized specimens at 200 °C after 1 month were 4.28 and 4.19. The corresponding rates for lot 2 from the duplicate test were 3.56 and 3.34 mm yr^{-1} (Westerman et al. 1988, Appendix A).

At 90 °C, the corrosion rates of A216 were essentially constant as the duration of the tests (1, 3, and 6 months) increased. The corresponding rates at 150 °C decreased somewhat (Westerman et al. 1988, Figure 6.2).

PNNL determined the effects of the dissolved Mg concentration of "PBB3-like brine" with 1,000, 5,000, and 10,000 ppm Mg on the corrosion of as-cast and normalized specimens of lots 1 and 2 of A216 at 150 C for 1 and 6 months. The results show a large data gap between the results for 10,000 ppm Mg and those for 48,000 ppm Mg (nominal PPB3), which were provided above. Westerman et al. (1988, p. 7.1) concluded that the corrosion product changed from magnetite to amakinite at an undefined Mg concentration between 18,000 and 48,000 ppm.

Clearly, the dissolved Mg concentration of brines has a significant effect on the corrosion of A216 mild steel and other Fe-base materials, especially at high temperatures. PNNL measured significantly higher corrosion rates for A216 in PBB3 than in PBB1 or PBB2 at any given temperature. Similarly, The Germans observed higher corrosion rates for TStE 355 in the high-Mg brines 1 and 2 than in brine 3 (Section 2.4.4.1), and as described above, SNL reported higher rates for Fe-base materials in Brine A than in Brine B during their initial screening study. There are at least two reasons for this behavior:

First, the pH of high-Mg brines decrease significantly as the temperature increases and acidification increases the corrosion rates of mild steels such as A216 and TStE 355 (Section 2.4.4.1). This phenomenon has been studied extensively, both in terms of the reactions that cause acidification and the implications of this process for disposal of spent fuel and HLW (Baes and Mesmer 1976; Bischoff and Seyfried 1978; Janecky and Seyfried 1983; Molecke et al. 1983; Thornton and Seyfried 1985; Krumhansl 1989). One of the reactions that causes acidification of both Mg-rich brines and seawater is hydrolysis of Mg^{2+} (Baes and Mesmer 1976; Westerman et al. 1988):

$$Mg^{2+} + H_2O \rightleftharpoons Mg(OH)^+ + H^+ \qquad\qquad (25)$$

This reaction produces more acid as the temperature increases because the stability constant for the complex species $Mg(OH)^+$ increases with temperature.

Another reaction that causes acidification of seawater and could cause acidification of Mg-rich brines is the formation of magnesium hydroxide sulfate hydrate (MHSH), which precipitates as the temperature increases (Bischoff and Seyfried 1978; Janecky and Seyfried 1983; Thornton and Seyfried 1985; Krumhansl 1989). According to Krumhansl (1989), this reaction can be written as

$$(n + 1)\, Mg^{2+} + SO_4^{2-} + H_2O \rightleftharpoons 2nH^+ + n(Mg(OH_2)\cdot MgSO_4 \cdot (1 - 2n)H_2O) \tag{26}$$
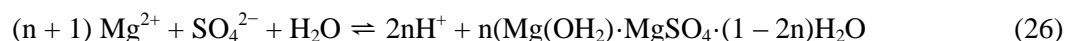
Based on his review of the literature, Krumhansl (1989) concluded that precipitation of MHSH becomes important in seawater at $T \geq 250\ °C$. Therefore, this reaction would probably not be important in salt repositories for spent fuel and HLW unless it occurs at lower temperatures in Mg-rich brines than in seawater.

Yet another reaction that results in acidification of seawater and could acidify Mg-rich brines is the formation of Mg-rich smectites in clay minerals. Molecke et al. (1983), Thornton and Seyfried (1985) and Krumhansl (1989) wrote this reaction as

$$3Mg^{2+} + 4SiO_{2(aq)} + 4H_2O \rightleftharpoons Mg_3Si_4O_{10}(OH)_2 + 6H^+ \tag{27}$$
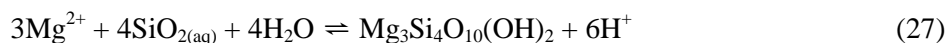
Molecke et al. (1983) hypothesized that reaction 27 could proceed with $SiO_{2(aq)}$ from the dissolution of clay minerals or quartz (SiO_2) that could be present as accessory minerals in evaporite formations, or from the dissolution of a borosilicate glass waste form. Thornton and Seyfried concluded that, although a reaction similar to reaction 26 (see above) was the most important cause of acidification during the first few hours of their experiments on the interactions of seawater and deep-sea sediments at 200° and 300ºC and 500 bars, reaction 27 rapidly superseded reaction 26 as the more important cause. They reported that dissolution of amorphous silica and quartz (both SiO_2) were the source of the $SiO_{2(aq)}$ in their experiments, and that talc ($Mg_3Si_4O_{10}(OH)_2$) formed either as a distinct smectite phase with most of its octahedral sites occupied by Mg, or as talc-like layers in existing clay minerals. Krumhansl (1989) reported, based on posttest analysis of the run products from his hydrothermal experiments with analytical transmission electron microscopy, that $Mg_3Si_4O_{10}(OH)_2$ was present as smectite.

The other major reason that the dissolved Mg concentration of brines has a significant effect on the corrosion of A216 mild steel and other Fe-base materials is that Mg either promotes the formation of an Mg-rich form of amakinite or prevents the formation of magnetite (Westerman et al. 1988; Kursten et al. 2004a). Westerman et al. (1988) and Telander and Westerman (1993; 1997) typically reported that amakinite was nonadherent in their experiments and thus provided no protection for the corroding A216 surfaces. The only exception to this behavior occurred in some of the longer-term (12-month), excess-salt tests with PBB3 (see below), in which the salt in the welded cans held the amakinite in place next to the corroding surfaces. This caused the corrosion rate of the A216 specimens to decrease with time, but not enough to approach the significantly lower rates observed in the excess-salt tests with PBB1 and PBB2. On the other hand, the magnetite that formed in tests with PBB1 and PBB2 developed an "onion-skin" structure that provided some protection from corrosion by these brines, even though the outer layers tended to slough off after the formation of a rind that was a few layers thick (Westerman et al. 1988).

PNNL carried out several series of two-phase experiments in Hastelloy C-276 or Inconel 625 autoclaves and excess-salt experiments in welded Inconel 600 or 625 cans. Each of these test series included various combinations of specimens of A216, standard brines and salts, amounts of brines added to the salts, and test durations. For the results of these tests, the reader is referred to Westerman et al. (1988, pp. 6.7 to 6.21 and Appendices B through G; and pp. 6.29 to 6.51 and Appendices H trough L, respectively).

PNNL also studied the effects of H_2 and Ar overpressures on the corrosion of A216 in PBB3 with short-term (2- or 4-week) autoclave experiments at 150 °C. See Westerman et al. (1988) for the results of these tests.

Westerman et al. (1986) determined the effects of γ radiation on the corrosion of the six steels used for their follow-on screening study (see above) in anoxic PBB2 at 150 °C in a recirculated autoclave in a 60Co irradiation facility. The dose rates were 2×10^3 and 1×10^5 rad hr^{-1} (2×10^1 and 1×10^3 Gy hr^{-1}). Both of these dose rates were greater than the maxima expected for DHLW in borosilicate glass in a stainless-steel canister with an 8.63 cm-thick steel overpack (3.3×10^2 rad hr^{-1}), commercial HLW in a stainless-steel canister with an 8.92 cm-thick steel overpack (1.6×10^3 rad hr^{-1}), and spent fuel (12 PWR assemblies) with a 10 cm-thick steel overpack (1.9×10^2 rad hr^{-1}) (Westerman et al. 1984, Table III). A dose rate of 2×10^3 rad hr^{-1} had essentially no effect on the corrosion of A216. The average corrosion rates of as-cast specimens of A216 after 1, 4, 6, and 9 months were 22, 14, 11, and 14 μm yr^{-1}, respectively. The corresponding rates for unirradiated, anoxic PBB2 at 150 °C after 1, 4, and 8 months were 20, 14, and 14 μm yr^{-1}. However, a dose rate of 1×10^5 rad hr^{-1} significantly increased the average corrosion rates of as-cast specimens of A216. The irradiated rates after 1, 4, and 5 months were 140, 120, and 100 μm yr^{-1}. The corresponding unirradiated rates after 1, 4, and 8 months were 20, 14, and 14 μm yr^{-1}. Posttest analysis of these specimens showed that the corrosion product was magnetite in all cases, and did not reveal any crevice corrosion or significant pitting. A specimen of A216 in which several holes had been predrilled was exposed to anoxic PBB2 at 150 °C and irradiated at 1×10^5 rad hr^{-1} for 4 months. After this test, the specimen was ground to half of its original thickness and the corrosion products were removed from the predrilled "pits;" no nonuniform corrosion was observed.

PNNL also examined the effects of γ radiation on the corrosion of as-cast or weldment specimens of A216 in two-phase, static autoclave experiments at 150 °C for 1 to 6 months. For these experiments, PNNL used surrogate salt filled to the top with PBB1 or PBB3, and dose rates of 1.1×10^1 to 1.1×10^3 rad hr^{-1} (seeWesterman et al. 1988, pp. 6.52 through 6.56 and Appendices M through O).

Westerman et al. (1988, pp. 7.1 to 7.3) concluded that, based on three years of studies, no crevice corrosion or pitting of A216 mild steel occurred in unirradiated experiments at temperatures up to 200 °C, or in γ-irradiation experiments at 150 °C at dose rates up to 2×10^3 rad hr^{-1}. No stress corrosion cracking was observed in U-bend tests of as-cast and welded specimens of A216 in surrogate salt filled with PBB3 at 90, 150, or 200 °C. Furthermore, no stress corrosion crack extension was observed in bolt-loaded fracture specimens of what treatments of A216 in surrogate salt with PBB3 at 150 °C for 6 months. Elongation and areal reduction during slow-strain-rate tests of A216 was lower in PBB3 than in air, and these processes were not affected by irradiation or the presence of salt.

However, PNNL observed significant crevice corrosion of TiCode-12 in PBB3 at 150 °C during γ irradiation at a dose rate of 2×10^4 rad hr^{-1} after about 6 to 10 months.

2.4.5   Identification of Additional Data Requirements and Possible Studies to Address Them

2.4.5.1   Brine Migration

Based on the information reported in the previous sections, it is clear that the issue of possible brine migration in a salt repository would require additional investigation, if salt were considered for disposal of spent fuel or HLW. This is especially true for corrosion-allowance or corrosion-resistant waste packages in bedded salt. This is because both the corrosion-allowance and the corrosion-resistant concepts require reliable predictions of how much brine will migrate up the thermal gradient and contact the waste packages during the thermal period, and because bedded salt contains much more brine than domal salt (Section 2.4.2.1). The four in situ studies of brine migration described in Subsection 2.1 and summarized in Table 1 showed that the amounts of brine collected under heated conditions and the rates at which brine was collected were greater during the tests in bedded salt than in domal salt, consistent with the observation that bedded salt contains significantly more brine than domal salt.

Both the corrosion-allowance and the corrosion-resistant concepts also require reliable predictions of the composition(s) of the brine(s) that will contact the waste packages. This is because the Mg concentration of brines affects the corrosion rates of the mild steels identified as candidate waste-package materials, especially at high temperatures (Section 2.4.4). The Mg concentration could also affect the corrosion rates of the corrosion-resistant alloys identified as promising. None of the publications or reports on the laboratory or in situ brine-migration studies obtained to date has determined the compositions of these brines.

Although brine migration up the thermal gradient could be an important process for corrosion-allowance and corrosion-resistant waste packages in bedded salt, intrusion of brine(s) could also be important. The quantities and compositions of such brine(s) will also have to be included in the design of both corrosion-allowance and corrosion-resistant waste packages if bedded salt were considered for disposal of spent fuel or HLW.

Brine migration up the thermal gradient will probably be less of an issue for both corrosion-allowance and corrosion-resistant waste packages in domal salt. Intrusion of brine could be a more important issue than brine migration up the thermal gradient in domal salt.

Additional site-specific studies of brine migration will be required, because the brine content of both bedded and domal salt formations can vary significantly. Furthermore, it might be necessary to carry out full-scale, in situ tests that include the effects of high-temperature creep closure on the mechanical properties of grain boundaries to determine the extent to which both intragranular and intergranular brines migrate along and across these boundaries towards the heat source. It is also important that the brines be collected and analyzed from the vicinity of the heaters. Such tests may be included in the field-scale heater test that would be included in the Salt Disposal Investigations proposed for a new experimental area that would be excavated in the northeast part of the WIPP underground workings if the proposal for this work were funded (DOE 2011).

2.4.5.2   Waste Package Materials

The Germans have identified carbon steels, especially the mild steel TStE 355, as "the most promising materials" for corrosion-allowance waste packages for spent fuel or HLW in a repository in domal salt; and the Ni-base alloy Hastelloy C-4 and Ti-base alloy Ti 99.8-Pd as the most promising for corrosion-resistant waste packages (Kursten et al. 2004a). Hastelloy C-4, however, exhibited crevice corrosion in high-Mg brine at 90, 170, and 200 °C in 3 year experiments, and pitting in this brine at 200 °C in a 3 year test (Kursten et al. 2004a). TStE 355 and Ti 99.8-Pd appear to be adequate for use as corrosion-allowance or corrosion-resistant materials in a repository in domal salt. This conclusion is based on the premise that the quantities and compositions of brine that will contact the waste packages can be predicted as a function of the time and temperature after emplacement, thus enabling the design and

fabrication of waste packages thick enough to isolate the waste during the thermal period (~300 to 1000 years). None of the publications or reports obtained to date described what additional data, if any, are still required for the use of TStE 355 or Ti 99.8-Pd in Germany. Further consideration of Hastelloy C-4, however, would require additional data to determine the conditions under which this material can be used absent crevice corrosion or (perhaps) other types of localized attack.

It seems likely that TStE 355 and Ti 99.8-Pd would also be suitable for use in a repository for spent fuel or HLW in bedded salt, although additional studies of the corrosion of these materials in site-specific brines and evaporite minerals would probably be required. However, thicker waste packages might be required because bedded salt typically has higher brine contents than domal salt (Section 2.4.2.1).

The mild steel ASTM A216, Grade WCA, also appears to be suitable for use in corrosion-allowance waste packages for a repository for spent fuel or HLW in bedded salt (Section 2.4.4.1).

Further consideration of TiCode-12, which the SNL/WIPP/SDP identified as the most promising material for disposal of spent fuel or HLW in bedded salt or seabed sediments (Section 2.4.4.2), would require additional work to determine the conditions under which it can be used without crevice corrosion.

An additional research need concerns the BSK-3 disposal concept. In order for borehole disposal of SNF in the thin-walled (5 cm) steel BDK-3 waste packages to be considered, waste package lifetimes must exceed 500 years, the mandated German retrievability period for SNF. Testing is required to evaluate the corrosion performance of the BSK-3 alloy in salt (Peiffer and Weber 2010).

2.5   Repositories in Unsaturated Crystalline Rock

This section considers possible Waste Package and Engineered Barrier System (EBS) materials, their degradation mechanisms, and needed research to support their possible use in an unsaturated crystalline rock repository. In this context, unsaturated describes a repository that may see water influx but is not completely denuded with water. Possible crystalline rocks include granite, basalt, and welded tuff. The U.S. Yucca Mountain repository concept is one example of such a repository, which was to be located in welded tuff. Other countries (Canada, Finland, Spain, Sweden, and Switzerland) are proposing granite repositories, but they are located within saturated rock. Most of these repository concepts include bentonite backfill which will not be saturated for a period of up to a hundred years, so some of their corrosion testing and water chemistries are relevant. This document takes advantage of the many reviews that have been performed over the years (BSC 2004; Kursten et al. 2004a; BSC 2006; SNL 2007b; 2007a; 2009; Wall and Brown 2009; Jove-Colon 2011; NRC 2011c).

This section discusses the following issues associated with degradation of engineered barrier materials within an unsaturated crystalline rock repository: possible environments (Section 2.5.1); possible EBS materials (Section 2.5.2); Features, Events or Processes (FEPs) that could lead to degradation of the EBS materials (Section 2.5.3); discussion of applicable FEPs and associated recommended research activities (Section 2.5.4).

2.5.1   Description of the Environment

As an unsaturated environment, the environment would be relatively dry with water flowing onto the package, but not encasing it in water. In terms of corrosion, however, it is expected that there would be sufficient liquid to effectively coat the waste package in a film of water that is routinely replenished. Also the environment would be relatively oxidizing, which tends to enhance corrosion behavior. The water composition would be in equilibrium with the host rock, and backfill if present. Due to the relatively low humidity within such a repository and potentially elevated temperatures, the ionic constituents are likely to be concentrated due to evaporation.

2.5.1.1   *Yucca Mountain Unsaturated Tuff Environment*

The predicted Yucca Mountain corrosion environment may be of relevance to a generic US unsaturated crystalline rock repository. Early in the YMP, several solutions were postulated and used for corrosion testing. These solutions were later compared to solutions predicted by the performance assessment and found to be appropriate(SNL 2010). The U.S. NRC staff reviewed the solutions and found them to be more aggressive than predicted by modeling (NRC 2011c). These solutions were SAW – simulated acidified water, SCW – simulated concentrated water, SDW– simulated dilute water, and BSW – Basic Saturated Water (SNL 2010). SAW represents dilute water that was adjusted to a pH of around 3.3 for corrosion testing purposes. SCW represents pore water that has been concentrated by a factor of approximately 2000X to account for possible evaporation concentrations during the dryout phase. BSW represents saturated water that has been modified to a high pH. These compositions are shown in Table 24. Table 25 shows the minimum and maximum ionic concentrations used for corrosion studies on the YMP. Finally, Table 26 shows the predicted minimum and maximum concentrations for periods from initial emplacement up to one million years and for the timeframe after 10,000 years. The timeframe beyond 10,000 years may be of particular relevance for a repository with lower initial temperatures than was predicted for Yucca Mountain.

Table 24.   Average ionic concentrations for YMP corrosion study solutions (molal)

Ion	SCW Average	SCW SD	SDW Average	SDW SD	SAW Average	SAW SD	BSW-11 Average	BSW-11 SD
Ca	1.9	0.6	12.9	20.2	67.3	20.3	0.7	0.0
Mg	0.1	0.1	6.6	11.3	53.1	3.0	0.0	0.0
Si	43.9	28.8	6.5	8.1	45.2	21.1	615.7	281.1
Na	39,890.0	3,541.4	410.4	47.7	42,227.5	2,056.6	97,510.0	4,228.5
K	3,476.8	1,047.7	36.9	1.4	3,505.2	302.0	60,400.0	2,121.3
F	1,259.0	151.7	9.4	12.1	268.3	439.4	3,825.0	35.4
Cl	6,468.6	818.5	112.3	28.0	22,499.3	511.0	115,550.0	3,535.5
NO_3	6,773.6	508.8	223.5	297.8	24,702.3	854.7	130,550.0	3,959.8
SO_4	15,209.1	2,791.9	232.3	58.5	60,042.1	14,382.3	12,225.0	742.5
HCO_3	29,464.1	10,097.5	208.5	244.0	0.3	0.4	387.1	149.0
pH	10.4	0.3	9.5	0.6	3.3	0.6	11.1	0.1

Source: SNL (2010), Table 1

Table 25.   Minimum and maximum ionic concentrations used in corrosion testing for Yucca Mountain (molal)

Ion	SCW Minimum	SCW Maximum	SDW Minimum	SDW Maximum	SAW Minimum	SAW Maximum	BSW-11 Minimum	BSW-11 Maximum
Ca	1.1	2.7	0.0	45.1	49.5	96.5	0.6	0.7
Mg	0.0	0.2	0.0	27.5	49.9	57.2	0.0	0.0
Si	16.0	107.2	0.0	22.1	26.0	67.7	416.9	814.4
Na	33,570.0	43,620.0	329.8	468.1	39,170.0	43,590.0	94,520.0	100,500.0
K	1,348.8	4,963.5	35.8	39.4	3,251.5	3,855.0	58,900.0	61,900.0
F	1,034.9	1,480.0	0.0	30.2	0.0	775.4	3,800.0	3,850.0
Cl	5,417.0	7,560.0	58.3	136.0	22,137.9	27,670.0	113,050.0	118,050.0
NO_3	6,043.6	7,445.0	40.4	753.5	23,724.2	25,305.0	127,750.0	133,350.0
SO_4	12,135.0	19,161.5	155.0	295.6	43,490.0	69,489.7	11,700.0	12,750.0
HCO_3	11,777.8	42,805.3	11.0	539.3	0.0	1.0	281.8	492.5
pH	10.1	10.8	8.4	10.2	2.8	3.9	11.0	11.2

Source: SNL (2010), Table 2

Table 26.   Minimum and maximum ionic concentrations predicted by performance assessment modeling at Yucca Mountain (molal)

Species or Parameter	Closure to 10^6 Years After Closure		10,000 Years to 10^6 Years After Closure	
	Minimum Value	Maximum Value	Minimum Value	Maximum Value
pH	3.7590	11.507	5.1588	10.241
Cl (molal)	3.9822×10^{-6}	26.689	3.9822×10^{-6}	2.8739
NO_3 (molal)	5.5747×10^{-7}	51.774	5.5747×10^{-7}	0.83549
NO_3/Cl (molal/molal)	0.015593	9.2835	0.015593	1.2772
F (molal)	1.4390×10^{-7}	0.53165	1.4390×10^{-7}	0.27730
Total C (molal)	7.9128×10^{-6}	3.0720	3.8108×10^{-5}	1.4373
Total S (molal)	1.6656×10^{-6}	2.0370	1.6656×10^{-6}	0.79663
Ca (molal)	6.7633×10^{-7}	13.295	6.7633×10^{-7}	0.12914
Mg (molal)	7.2017×10^{-8}	3.0709	7.2017×10^{-8}	0.22173
Ionic Strength	4.1605×10^{-5}	25.850	4.1605×10^{-5}	5.2403
pCO_2	1.0909×10^{-4}	0.02077	1.9802×10^{-4}	0.0042933

Source: SNL (2010), Table 8

As can be seen from Table 26, for times beyond 10,000 years, the water chemistry becomes more benign and less concentrated. This is due to the reduced temperatures resulting in less pore water evaporation. Figure 16 shows the temperature profile for the waste package and drift walls as a function of time. Considering that corrosion tends to be more aggressive (following an Arrhenius-type relationship) as temperatures increase and the solution chemistry is more benign for lower temperatures, from a corrosion standpoint limiting the repository temperature would be significantly advantageous.
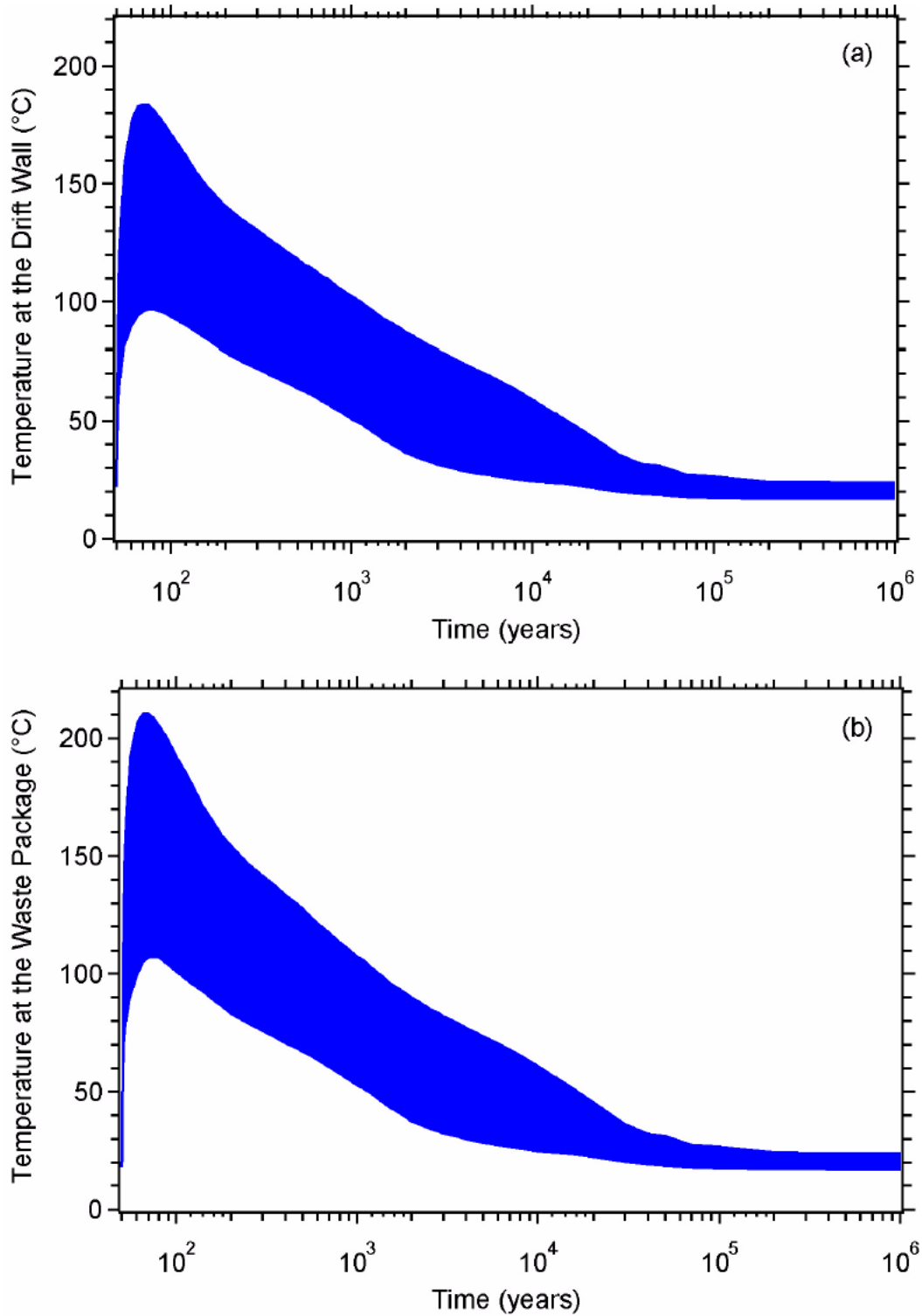
Figure 16.   Range of time-temperature histories predicted for the Yucca Mountain repository: a) at the drift wall; b) at the waste package surface

2.5.1.2   Other Crystalline Rock Unsaturated Environments

As stated earlier, several other countries are considering crystalline rock repositories, but these are all below the water table, and will eventually be fully saturated. However, those concepts use bentonite backfill, and an unsaturated environment exists after emplacement of the waste and prior to complete saturation of the bentonite. From a corrosion standpoint, these environments may be overly benign for an unsaturated crystalline rock repository as they do not account for ionic concentration due to evaporation. Also, the water compositions are strongly buffered by the bentonite backfill, and it is unlikely that such a backfill would be use in an unsaturated repository. The anticipated composition of waters in the bentonite backfills for the Swedish and Finnish repository programs are provided in King et al. (2001). Because it is unlikely that these water compositions are relevant, they are not presented here.

2.5.1.3   Corrosion Environment to be used for Future Unsaturated Crystalline Rock Repository Research and Development

From a corrosion standpoint, until the repository conditions are better defined, it is appropriate to continue to use the Yucca Mountain SDW water composition. This effectively bound the ions that promote corrosion, yet are not overly aggressive for a repository with lower thermal profiles than was planned at Yucca Mountain. This is demonstrated by comparison of Tables 1 and 2 to the post 10,000 year column of Table 3. The use of SCW, BSW and SAW can be of benefit, but should be used with some caution so as to not be overly aggressive and potentially dismiss candidate alloys that would be appropriate for less aggressive environments that may be encountered in a lower initial temperature repository.

2.5.2   Possible EBS Materials for an Unsaturated Crystalline Rock Repository

Two general concepts have been proposed for the waste package. The first uses a corrosion resistant material for delaying the eventual breach of the waste package. The corrosion resistant material offers low corrosion rates, mainly due to the extremely corrosion resistant adherent oxide layer that forms on the metal surface as corrosion initiates. This approach offers the advantages of low corrosion rates, thinner waste package walls, and corrosion resistance over a wide variety of environments. However, these materials tend to be more expensive than corrosion allowance materials. The second approach is to use corrosion allowance materials. These materials actively corrode at a well predicted rate as they do not possess highly adherent oxide films. This predictability results in lower modeling uncertainty, however, these rates can be very dependent upon the environment. Corrosion allowance materials tend to be less expensive than corrosion resistant materials. In regions of low permeability, they also offer the advantage of producing reducing environments as they corrode, which result in lower actinide solubilities and the corrosion products can act as sorbing sites for certain radionuclides. Of course, there are variants to these approaches, in one of which the outer layer of a waste package is the corrosion allowance material and the inner layer is a corrosion resistant material. This can be reversed with the outer layer being corrosion resistant and the inner corrosion allowance. At the Yucca Mountain Project, the waste package consisted of an outer shell of Alloy 22, a nickel based corrosion resistant material, and the inner vessel of 304 stainless steel, a corrosion allowance material; however, in the Yucca Mountain case, the inner vessel contributed to container lifetime primarily through providing structural support.

Without better knowledge of the waste package environment, the overall repository design, philosophy of what is expected of the waste package, etc. it is not possible to select neither a waste package design nor the materials that may be used. Therefore, this section will describe possible materials and whether they should be considered for inclusion in future research and development activities.

2.5.2.1   Corrosion Resistant Materials

Nickel based alloys

Nickel based alloys are under consideration by Germany (C-4) and the waste package outer barrier for the YMP (Alloy C22, also referred to as Alloy 22). There are numerous Nickel based alloys, some of which are presented in Table 27.

Based upon extensive previous efforts, it is apparent that if a nickel based alloy were to be chosen for an unsaturated crystalline rock repository, C-4 or Alloy 22 (C22) are the most appropriate. This is due to their high resistance to localized corrosion owing to additions of molybdenum (C-4) and molybdenum and tungsten (in the case of Alloy 22). These alloying elements also serve to make the two alloys corrosion resistant over a wide pH range. Alloys 825, C276 and G3 may be of use from a surrogate standpoint as they contain lower quantities of alloying elements, and thus are less corrosion resistant which may be of benefit where obtaining some corrosion signal in a shorter timeframe may be of benefit.

Table 27.   Chemical compositions of nickel based alloys

ASI	UNS	Fe	Cr	Ni	Mn	Mo	Nb	Ti	W	Other
C-4	N06455	<3.2	11.0-18.0	Balance	<1.0	14.0-17.0				
C22	N06022	2.0-6.0	20.0-22.5	Balance	0.5	12.5-14.5			2.5-3.5	
C276	N10276	4.0-7.0	14.5-16.5	Balance	<1.0	15.0-17.0				
G3	N06985	20	22	48		7				
600	N06600	6.0-10.0	14.0-17.0	Balance	1.0					
617	N06617	3.0	20.0-24.0	Balance	0.5	8.0-10.0		0.6		
625	N06625	5.0	20.0-23.0	Balance	0.5		3.15-4.15	0.4		
718	N07718	Balance	17.0-21.0	50.0-55.0	0.35		4.75-5.5	0.3		
825	N08825	Balance	19.5-23.5	38.0-46.0	<1.0	3.0		0.6-1.2		1.5-3.0

Note: ASI – American Standards Institute; UNS – Unified Numbering System

Titanium based alloys

Titanium based alloys are very corrosion resistant owing to their adherent oxide film. Relevant grades of titanium are shown in Table 28. Titanium is alloyed with aluminum and vanadium for strength and with palladium or ruthenium for increased corrosion resistance and localized corrosion resistance in particular. As can be seen from Figure 17, small additions of palladium or ruthenium dramatically increase the corrosion resistance, especially at extremely low pH (SNL 2007a).

Canada, Germany (Ti-Grade 7), and Japan are currently considering titanium as a layer of their waste package designs (Kursten et al. 2004a). The YMP was considering a titanium drip shield comprised of Titanium Grade 7 plates, with a structural frame of Titanium Grade 29 ribs. The two alloys were to be welded with Titanium Grade 28 as the weld filler material to reduce the risk of hydrogen migration from the Titanium Grade 7 to the Grade 29.

Table 28.   Compositions of titanium alloys

ASTM Grade	UNS	N	C	H	O	Fe	Al	V	Pd	Ru	Residual (each)	Residual (total)
12	R53400	0.03	0.08	0.015	0.25	0.30	—	—	—	—	0.2 to 0.4 Molybdenum	0.6 to 0.9 Nickel
2	R50400	0.03	0.08	0.015	0.25	0.30	—	—	—	—	0.1	0.4
7	R52400	0.03	0.10	0.015	0.25	0.30	—	—	0.12 to 0.25	—	0.1	0.4
16	R52402	0.03	0.08	0.015	0.25	0.30	—	—	0.04 to 0.08	—	0.1	0.4
5	R56400	0.05	0.08	0.015	0.20	0.40	5.5 to 6.75	3.5 to 4.5	—	—	0.1	0.4
23	R56407	0.03	0.08	0.0125	0.13	0.25	5.5 to 6.5	3.5 to 4.5	—	—	0.1	0.4
24	R56405	0.05	0.08	0.015	0.20	0.40	5.5 to 6.75	3.5 to 4.5	0.04 to 0.08	—	0.1	0.4
9	R56320	0.03	0.08	0.015	0.15	0.25	2.5 to 3.5	2.0 to 3.0	—	—	0.1	0.4
28	R56323	0.03	0.08	0.015	0.15	0.25	2.5 to 3.5	2.0 to 3.0	—	0.08 to 0.14	0.1	0.4
29	R56404	0.03	0.08	0.015	0.13	0.25	5.5 to 6.5	3.5 to 4.5	—	0.08 to 0.14	0.1	0.4

Source: SNL (2007a), Table 3
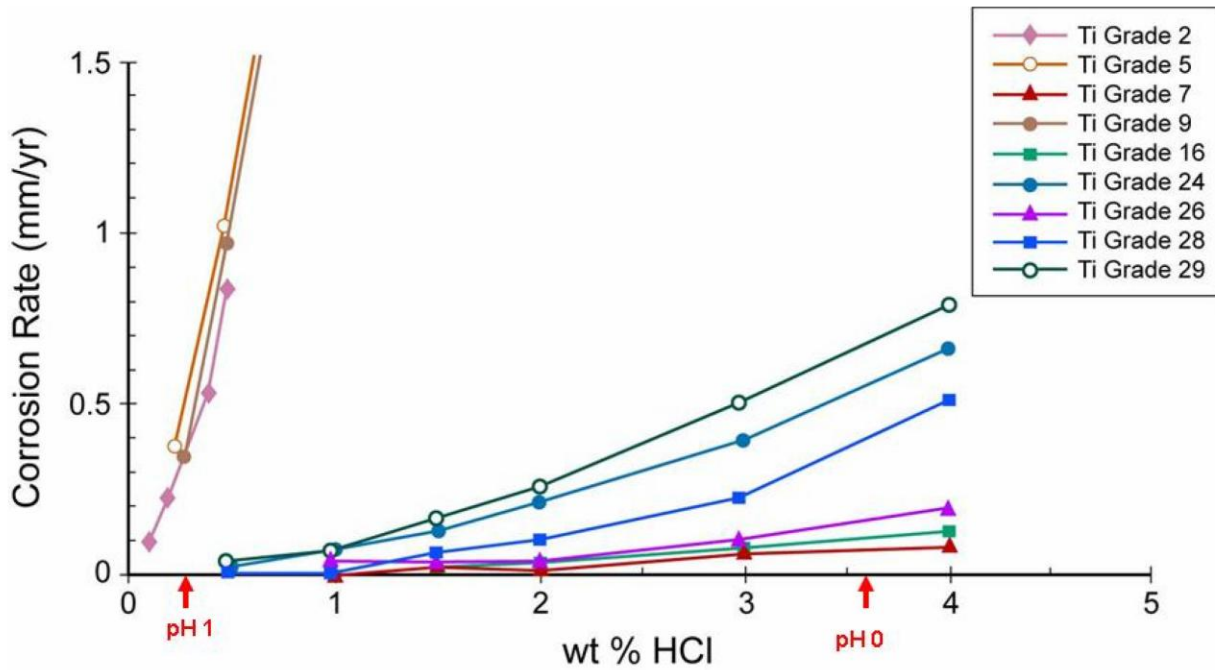
Source: SNL (2007a), Figure 6-22[a]

Figure 17.   Corrosion rate comparison of titanium alloys in boiling hydrochloric acid

The mean corrosion rate of Ti-7 exposed to SCW at 90C is ~46 nm yr^{-1} and only 5 nm yr^{-1} for SAW and SDW, while the corrosion rate for Ti-29 is less than twice that of Ti-7 for these environments. Considering the low general corrosion rates and excellent resistance to localized corrosion, titanium alloys are a viable option for an unsaturated crystalline rock repository.

Copper alloys

The chemical compositions of several copper-based candidate alloys are shown in Table 29. While copper based alloys are under consideration in Canada, Finland, and Sweden, they are not good candidates for use in an unsaturated crystalline rock repository. These materials are of interest only in saturated repositories with very limited oxygen, where the corrosion rates are quite low. This is due to the fact that in the presence of oxygen, copper tends to corrode rather quickly (tests on copper in unsaturated bentonite showed a corrosion rate of ~3-50 μm yr^{-1}) (Kursten et al. 2004a). Even in the relatively benign environment of lake water at low temperatures corrosion the corrosion rates for CDA102, CDA613, and CDA715 were all ~5 μm yr^{-1}, which would result in container lifetimes of less than 25,000 years for a 25 mm thick waste package (Farmer et al. 1988). Furthermore, these rates are similar to or greater than that for stainless steel type 316 (BSC 2006) which is significantly less expensive.

Table 29.   Chemical composition of Cu-based candidate alloys

Alloy	Cu	Ni	Al	Mn	Sn	Fe	Zn	Other
CDA102	99.95	-	-	-	-	-	<0.001	Pb<0.001, Cd<0.001, S<0.0018, Hg<0.0001, P<0.003
CDA613	90.82	0.05	6.75	0.16	0.20	2.46	0.01	Pb<0.01, Co<0.01
CDA715	69.18	29.60	-	0.51	-	0.53	0.07	Pb 0.01, P 0.002, C 0.04, S 0.01

Source: Farmer et al. (1988), Table 1

2.5.2.2   *Corrosion Allowance Materials*

Austinitic alloys may be used as a corrosion allowance material either by themselves, or above or below a layer of corrosion resistant materials. Alloy 825 can be considered either a corrosion allowance material or a corrosion resistant material as has one of the highest corrosion rates for a corrosion resistant material). In almost any case, stainless steels will need to be used in the design to act as structural supports for the used fuel and/or other waste forms. Corrosion allowance materials become more corrosion resistant as the quantity of nickel and chromium is increased, due to the formation of adherent oxide films (Farmer et al. 1988). Candidate material compositions are shown in Table 30. The YMP waste package design used an inner vessel comprised of 304 stainless steel.

Table 30.   Chemical composition of austenitic candidate alloys

Element	304L	316L	Alloy 825
C	0.03 max	0.03 max	0.05 max
Mn	2.00 max	2.00 max	1.0 max
Si	1.00 max	1.00 max	0.5 max
Cr	18.0 - 20.0	16.0 - 18.0	19.5 - 23.5
Ni	8.0 - 12.0	10.0 - 14.0	38.0 – 46.0
P	0.045 max	0.045 max	-
S	0.03 max	0.03 max	0.03 max
Cu	-	-	1.5 – 3.0
Ti	-	-	0.6 – 1.2
N	0.10	0.10	-
Mo	-	2.0 – 3.0	3.0
Fe	Bal.	Bal.	Bal.

Source: Farmer et al. (1988), Table 4

2.5.2.3   Neutron Poison Materials

If a waste package were to contain a critical mass of fissile material (such as the 21 PWR and 44 BWR YMP packages) then it is likely that a neutron poison material will be required in the waste package design. Furthermore, this material will have to have properties (corrosion resistance, fate of the neutron poison component during corrosion) to support a features, events, and processes (FEPs) exclusion argument. Under the existing US Regulations, this requires that a criticality event have less than a 10^{-8} chance of occurrence per year for at least 10,000 years. Possible materials include borated stainless steel, borated aluminum alloys, and a nickel/gadolinium alloy.

Borated stainless steel

Borated stainless steel plate is specified within ASTM A 887. Eight alloy types based upon 304 stainless steel with a boron addition are specified from 304B (0.2-0.29% B) to 304B7 (1.75-2.25% B). The ASTM A 887 specification does not explicitly state the manufacturing methods bus is based upon mechanical property minimums. To meet the requirements of the Grade A specifications the alloys have been manufactured by a powder metallurgy process and the Grade B materials are based on ingot metallurgy. Previous testing has shown that only the Grade A materials have sufficient corrosion resistance for disposal applications. Also as the B content increases the corrosion rates increase rapidly and resistance to localized corrosion is reduced (Fix et al. 2004; Lister et al. 2007; He 2008; Lister et al. 2008). For these reasons, for the YMP Grade A 304B4 (1.1-1.2 wt% B) was specified (DOE 2008) and is most appropriate for repository use.

Extensive corrosion testing for long durations has not been performed, and it is assumed that the boron becomes water soluble after corrosion. Because of the lack of long term corrosion testing extremely conservative assumptions regarding corrosion rates are necessary. Furthermore, since the fate of the released boron is unknown, it must be assumed that the boron is not available as a neutron poison after corrosion. These areas are well worth further study, for both disposal and long term storage applications.

Borated aluminum

Borated aluminum is specified within ASTM C1617-07. Aluminum and borated aluminum are susceptible to pitting in the presence of minor chloride concentrations (Emmerich et al. 2004) and thus are not appropriate for disposal purposes.

Nickel gadolinium

The US Department of Energy, (DOE) has developed a nickel alloy with gadolinium as a neutron absorber (Table 31), UNS N06464, which is specified within ASTM B932-04. Gadolinium is a more effective thermal neutron absorber than boron, and nickel alloys tend to be more corrosion resistant than stainless steels. Testing of N06464 has had mixed results with evidence that the material is somewhat susceptible to localized corrosion. This may be due in part to corrosion of the gadolinide particles contained within, while the nickel matrix remains passive (Lister et al. 2005; Mizia et al. 2005). However, the corrosion rates are fairly high (~30-500 nm yr^{-1}). One advantage that Ni-Gd has over borated stainless steels is that the dissolved Gd will form GdF_3 and remain within the waste package to absorb thermal neutrons.

This alloy remains an interesting possibility for disposal, particularly for DOE Fuels with high enrichments. Research work for this alloy should include long term corrosion testing and determining the corrosion rates of the Ni matrix (C-4 UNS N06455) by itself to determine if the initial corrosion rates can be expected to drop as the gadolinium particles are consumed.

Table 31.   Chemical composition of UNS N06464 nickel-gadolinium alloy

Composition Limits (wt%)	
Element	Alloy N06464
Molybdenum	13.1 to 16.0
Chromium	14.5 to 17.1
Iron	1.0 max
Cobalt, max	2.0
Carbon, max	0.010
Silicon, max	0.08
Manganese, max	0.5
Phosphorus, max	0.005
Sulfur, max	0.005
Nickel	Remainder[a]
Oxygen	0.005
Nitrogen, max	0.010
Gadolinium	1.9 to 2.1
a. Shall be determined arithmetically by difference.	

Source: Mizia et al. (2005), Table 1

2.5.2.4   Summary

Based upon the above discussions and reviews of the literature, Table 32 lists materials that should be considered for further research for use in an unsaturated crystalline rock repository.

Table 32.   Materials recommended for further study

	UNS Number	Possible Application	Comments	Section
Nickel Alloys				
C22	N06022	Corrosion Resistant Material	Considered for Yucca Mountain Project. Significant quantity of repository relevant data available.	2.5.4.1
C-4	N06455	Corrosion Resistant Material	Considered for use by Germany, Similar to C22 without Tungsten	2.5.4.2
C276	N10276	Corrosion Resistant Material Surrogate.	Contains less alloying elements than C-4 or C22, so could be used as a surrogate for testing to achieve faster corrosion rates for analysis.	2.5.4.3
G3	N06985	Corrosion Resistant Material Surrogate.	Contains less alloying elements than C-4 or C22, so could be used as a surrogate for testing to achieve faster corrosion rates for analysis.	2.5.4.3
825	N08825	Corrosion Resistant Material Surrogate.	Contains less alloying elements than C-4 or C22, so could be used as a surrogate for testing to achieve faster corrosion rates for analysis.	2.5.4.3
Titanium Alloys				
Grade 7	R53400	Corrosion Resistant Material	Considered for use by Germany and the Yucca Mountain Project. Contains Pd for enhanced corrosion resistance. Poor mechanical properties.	2.5.4.4
Grade 29	R56404	Corrosion Resistant Material	Considered for use by Yucca Mountain Project. Contains alloying elements for strength and Ru for corrosion resistance. Not as corrosion resistant as Grade 7.	2.5.4.5
Grade 28	R56323	Corrosion Resistant Material	Considered for use by Yucca Mountain Project as weld filler material to minimize concentration gradients and thus reduce possibility of hydrogen migration from Grade 29 to Grade 7.	2.5.4.6
Corrosion Allowance Materials				
304 L	S30400/ S30403	Corrosion Allowance Material	304L was considered for Yucca Mountain Project for inner vessel, transportation and disposal canister, and structural support structures.	2.5.4.7
316L	S31600/ S31603	Corrosion Allowance Material	316 L is more corrosion resistant than 304L, but more expensive.	2.5.4.7
Alloy 825	N08825	Corrosion Allowance/Resistant Material	Alloy 825 is the most corrosion resistant of the corrosion allowance materials.	2.5.4.8
Neutron Absorber Materials				
304B4	ASTM A 887	Borated Stainless Steel, powder metallurgy	Contains 1.1-1.2 wt% B, considered by Yucca Mountain Project	2.5.4.9
304B5	ASTM A 887	Borated Stainless Steel, powder metallurgy	Contains 1.2-1.4 wt% B. May have higher corrosion rates than B4, but could be used as a surrogate.	2.5.4.9
Ni-Gd	N06464	Nickel Gadolinium alloy	Matrix is similar to C-4 with large gadolinide intermetallics. Some work has been done to increase corrosion resistance of matrix through addition of extra chromium.	2.5.4.10

2.5.3 Features, Events, and Processes Relevant to an Unsaturated Crystalline Rock Repository

The *Used Fuel Disposition Campaign, Features, Events, and Processes (FEPs): FY10 Progress Report* (Freeze et al. 2010, Table A-1) contains a list of FEPs for a generic repository. This list was reviewed for corrosion mechanisms relevant to an unsaturated crystalline rock repository (Table 33). No additional FEPs were identified as a result of this review.

Table 33.   Features events and processes relevant to corrosion within an unsaturated crystalline rock repository

UFD FEP Number	Description	Associated Processes Related to Corrosion	Related YMP FEPs
1.1.08.01	Deviations from Design and Inadequate Quality Control (see also Early Failure of Waste Packages in 2.1.03.01)	• Error In waste emplacement (waste forms, waste packages, waste package support materials) These errors were incorporated into Early Waste of Waste Packages. See 2.1.03.01 These errors could include improper welding, improper weld material, improper heat treatment, etc. These errors could result in accelerated corrosion, including stress corrosion cracking. For the Yucca Mountain Project, the likelihood of these errors were estimated based upon human failure analyses and included in the early failure scenario. No attempt was made to estimate how much these errors would have on corrosion, but rather it was assumed that stress corrosion cracking resulted from the failure and the consequences considered. This treatment seems reasonable; it would be extremely difficult to model accelerated corrosion without knowing the exact failure. If the failure were known, then it could be fixed. Therefore, no further research into this FEP is recommended.	1.1.03.01.0A 1.1.03.10.0B 1.1.04.01.0A 1.1.07.00.0A 1.1.08.00.0A 1.1.09.00.0A
1.2.04.01	Igneous Activity Impacts EBS and/or EBS Components	• Mechanical damage to EBS (from igneous intrusion) • Chemical interaction with magmatic volatiles For the Yucca Mountain Project, the waste packages subjected to magma were assumed to completely fail. Based upon estimated temperatures and pressures, this was determined to be a reasonable approach. It is unlikely that additional research would change this conclusion. Therefore no further research into this FEP is recommended.	1.2.04.02.0A 1.2.10.02.0A
2.1.03.01	Early Failure of Waste Packages (See also Deviations from Design in 1.1.08.01)	• Manufacturing Defects • Improper sealing These errors could include improper welding, improper weld material, improper heat treatment, etc. These errors could result in accelerated corrosion, including stress corrosion cracking. For the Yucca Mountain Project, the likelihood of these errors were estimated based upon human failure analyses	2.1.03.08.0A

UFD FEP Number	Description	Associated Processes Related to Corrosion	Related YMP FEPs
		and included in the early failure scenario. No attempt was made to estimate how much these errors would have on corrosion, but rather it was assumed that stress corrosion cracking resulted from the failure and the consequences considered. This treatment seems reasonable as it would be extremely difficult to model accelerated corrosion without knowing the exact failure. If the failure were known, then it could be fixed. Therefore, no further research into this FEP is recommended.	
2.1.03.02	General Corrosion of Waste Packages	- Dry-air oxidation - Humid-air corrosion - Aqueous phase corrosion - Passive film formation and stability This FEP is discussed for each of the candidate waste package materials in Section 2.5.4.	2.1.03.01.0A
2.1.03.03	Stress Corrosion Cracking (SCC) of waste packages	- Crack initiation, growth and propagation - Stress distribution around cracks This FEP is discussed for each of the candidate waste package materials in Section 2.5.4.	2.1.03.02.0A
2.1.03.04	Localized Corrosion of Waste Packages	- Pitting - Crevice Corrosion - Salt deliquescence See also 2.1.09.06 Chemical Interaction with Backfill This FEP is discussed for each of the candidate waste package materials in Section 2.5.4.	2.1.03.03.0A 2.1.09.28.0A
2.1.03.05	Hydride Cracking of Waste Packages	- Hydrogen diffusion through metal matrix - Crack Initiation and growth in metal hydride phases Hydride cracking is only an issue for titanium based alloys and is therefore only discussed for titanium alloys. This FEP is discussed for each of the candidate waste package materials in Section 2.5.4.	
2.1.03.06	Microbially Influenced Corrosion (MIC) of Waste Packages	Under certain conditions, a biofilm can form that could result in localized patches of aggressive environments that could lead to enhanced corrosion. For an unsaturated repository, it is highly unlikely that these conditions could exist and thus no further research is recommended in this area.	2.1.03.05.0A
2.1.03.07	Internal Corrosion of Waste Packages Prior to Breach	Air oxidation could lead to some corrosion prior to waste package breach. Considering that the corrosion rates for all of the candidate materials in aqueous environments are orders of magnitude higher than for air oxidation at repository temperatures, no further research is recommended for this FEP.	2.1.03.06.0A
2.1.03.08	Evolution of Flow Pathways in Waste Packages (Also see 2.1.08.02)	- Evolution of physical form of waste package - Plugging of cracks in waste packages This FEP is related to corrosion in the sense that if a crack due to SCC were to form, the nature of the crack and how/and if water were to migrate through the crack needs to be determined and modeled. See Section 5, where this FEP is combined with FEP 2.1.03.04.	2.1.03.10.0A 2.1.03.11.0A

UFD FEP Number	Description	Associated Processes Related to Corrosion	Related YMP FEPs
2.1.07.05	Mechanical Impact on Waste Packages (See also Thermal-Mechanical Effects 2.1.11.06)	• Rockfall/Drift collapse • Waste package movement • Hydrostatic pressure • Internal gas pressure • Swelling corrosion products This FEP is more related to waste package design than material properties. Without a waste package design, no further research is recommended for this FEP.	2.1.03.07.0A 2.1.07.04.0A 2.1.09.03.0B
2.1.08.02	Flow in and through Waste Packages (Also see 2.1.03.08)	• Saturated/Unsaturated flow • Movement as thin films or droplets This FEP is related to corrosion in the sense that if a crack due to SCC were to form, the nature of the crack and how/and if water were to migrate through the crack needs to be determined and modeled. See Section 5 where this FEP is combined with FEP 2.1.03.04.	2.1.03.10.0A 2.1.03.11.0A
2.1.09.02	Chemical Characterization of Water in Waste Packages	• Water composition (radionuclides, dissolved species, …) • Initial void chemistry (air/gas) • Water Chemistry (pH, ionic strength…) • Reduction-oxidation potential • Reaction kinetics • Influent chemistry (from tunnels and/or backfill) • Evolution of water chemistry / interaction with waste packages This FEP relates to expected in package water composition, which will affect future corrosion testing. Other tasks need to supply this information to the corrosion testing group to arrive at reasonable but bounding corrosion testing solutions for in package materials such as neutron absorbers.	2.1.09.01.0B 2.1.02.09.0A 2.2.08.12.0B 2.1.09.06.0A 2.1.09.07.0A
2.1.09.03	Chemical Characteristics of Water in Backfill	• Water composition (radionuclides, dissolved species, …) • Initial void chemistry (air/gas) • Water Chemistry (pH, ionic strength…) • Reduction-oxidation potential • Reaction kinetics • Influent chemistry (from tunnels and/or backfill) This FEP relates to expected in tunnel water composition, which will affect future corrosion testing. Other tasks need to supply this information to the corrosion testing group to arrive at reasonable but bounding corrosion testing solutions for waste package materials.	2.1.04.02.0A 2.1.09.01.0A 2.1.09.06.0B 2.1.09.07.0B
2.1.09.04	Chemical Characteristics of Water in Tunnels	• Water composition (radionuclides, dissolved species, …) • Initial void chemistry (air/gas) • Water Chemistry (pH, ionic strength…) • Reduction-oxidation potential • Reaction kinetics • Influent chemistry (from tunnels and/or backfill) This FEP relates to expected in tunnel water composition, which will affect future corrosion testing. Other tasks need to supply this information to the corrosion testing group to arrive at reasonable but bounding corrosion testing solutions for waste package materials.	2.1.09.01.0A 2.1.09.06.0B 2.1.09.07.0B

UFD FEP Number	Description	Associated Processes Related to Corrosion	Related YMP FEPs
2.1.09.05	Chemical Interaction of Water with corrosion products • In Waste Packages • In Backfill • In Tunnels	• Corrosion product formation and composition (waste form, waste package internals, waste package) • Evolution of water chemistry in waste packages, in backfill, and in tunnels This FEP relates to expected in package water composition, which will affect future corrosion testing. Other tasks need to supply this information to the corrosion testing group to arrive at reasonable but bounding corrosion testing solutions for in package materials such as neutron absorbers	2.1.09.02.0A
2.1.09.06	Chemical Interaction of Water with Backfill • On waste packages • In backfill • In Tunnels	• Backfill composition and evolution (bentonite, crushed rock, …) • Evolution of water chemistry in backfill, and in tunnels • Enhanced degradation of waste packages (crevice formation) This FEP relates to expected in tunnel water composition, which will affect future corrosion testing. Other tasks need to supply this information to the corrosion testing group to arrive at reasonable but bounding corrosion testing solutions for waste package materials.	2.1.04.02.0A
2.1.10.01	Microbial Activity in EBS • Natural • Anthropogenic (See also Microbially Influenced Corrosion in 2.1.03.06)	• Effects on Corrosion • Formulation of complexants • Formation of microbial colloids • Formation of biofilms • Biodegradation • Biomass production • Bioaccumulation For an unsaturated repository, it is highly unlikely that these conditions could exist and thus no further research is recommended in this area.	2.1.10.01.0A
2.1.11.07	Thermal-Mechanical Effects on Waste Packages	• Thermal sensitization / phase changes • Cracking • Thermal expansion / stress/ creep This FEP is discussed for each of the candidate waste package materials in Section 2.5.4.	2.1.07.05.0A 2.1.11.06.0A 2.1.11.07.0A
2.1.13.02	Radiation Damage to EBS Components • Waste form • Waste Package • Backfill • Other EBS Components	• Enhanced waste form degradation • Enhanced waste package degradation • Enhanced backfill degradation • Enhanced degradation of other EBS components Materials of interest for waste package formulation have been demonstrated to be radiation tolerant under much more severe conditions (e.g. in reactor service, and dry cask storage of relatively young used fuels) and thus no research is recommended in this area at this time.	2.1.13.02.0A
2.1.14.01	Criticality In-Package	• Formation of critical configuration This FEP is discussed for each of the candidate waste package materials in Section 2.5.4.	2.1.14.15.0A 2.1.14.16.0A 2.1.14.21.0A 2.1.14.22.0A

2.5.4   Research Needs for Recommended Materials for an Unsaturated Crystalline Rock Repository

Based upon the discussions in Section 2.5.2, the FEPs contained in Table 34 will be discussed for each of the recommended materials, along with associated research needs for that particular material. In 2009, a report was written documenting the long-term testing needs in support of the Yucca Mountain Licensing defense (Wall and Brown 2009). The *Long-Term Corrosion Testing Plan* recommended an extensive corrosion testing program with expenditures on the order of 3-4M\$ per year for a ten year period. Unlike the *Long-Term Corrosion Testing Plan*, this document aims to identify gaps that could be closed on a much smaller scale while decisions are made concerning repository design, the host material, etc.

Table 34.   Relevant FEPs to waste package corrosion research for an unsaturated crystalline rock repository

Description	Associated Processes Related to Corrosion	UFD FEP Number
General Corrosion of Waste Packages	- Dry-air oxidation - Humid-air corrosion - Aqueous phase corrosion - Passive film formation and stability	2.1.03.02
Stress Corrosion Cracking (SCC) of waste packages	- Crack initiation, growth and propagation - Stress distribution around cracks - Flow through SCC cracks (2.1.03.08 and 2.1.08.02)	2.1.03.03
Localized Corrosion of Waste Packages	- Pitting - Crevice Corrosion - Salt deliquescence	2.1.03.04
Hydride Cracking of Waste Packages	- Hydrogen diffusion through metal matrix - Crack Initiation and growth in metal hydride phases	2.1.03.05
Thermal-Mechanical Effects on Waste Packages	- Thermal sensitization / phase changes - Cracking - Thermal expansion / stress/ creep	2.1.11.07
Criticality In-Package	Formation of critical configuration This FEP is only discussed with regards to neutron absorber materials.	2.1.14.01

2.5.4.1   Alloy 22 (C22)

As discussed earlier, Alloy 22 was the waste package outer barrier for the YMP. As such, it was the primary barrier to water influx and was researched in great detail (SNL 2009) and subject to many reviews (Farmer et al. 1988; NRC 2011c, etc.).

General corrosion of Alloy 22

Alloy 22 general corrosion is a uniform thinning of the material due to electrochemical processes. This thinning occurs at extremely low rates due to the formation and slow dissolution of a protective, passive oxide film on the metal surface. The passive film is self-forming and self-healing when the metal is

exposed to air and moisture as would be expected in an unsaturated crystalline rock repository. As long as the passive film remains stable (instability would result in localized corrosion) the general corrosion rates will remain extremely low. These passive films have been characterized with a wide variety of advanced techniques (Orme 2005; Dixit et al. 2006) and found to be between 2 and 7 nm thick. The outer layer was porous and consisted mostly of nickel oxide and oxides of other alloying elements. The inner layer was dense and rich in CR_2O_3 and $NiCr_2O_4$ oxides. Under the point defect film growth model, the dense inner layer will maintain a fairly uniform thickness, as the porous outer layer dissolves and the inner layer is repaired.

The NRC staff reviewed the data and models used to support the argument that the passive films would remain stable under repository conditions and determined that they would (NRC 2011c). The NRC staff noted that the SAW, SCW, SDW and BSW brines were more aggressive than expected within repository conditions and that many researchers (Lloyd et al. 2003; Montemor et al. 2003; Lloyd et al. 2004; Mintz and Devine 2004; Dunn et al. 2005; Gray et al. 2006; Hur and Park 2006), have reported similar descriptions for passive film for Alloy 22 and analogous nickel-based alloys (e.g., Alloy C-4, C276, 600, 625 and 690). The NRC staff reviewed the thermodynamic modeling and the point defect film growth model and reached similar conclusions to DOE (Pensado et al. 2002; Miserque et al. 2006; Jung et al. 2008).

One possible mechanism that could adversely affect passive film stability is anodic sulfur segregation (Marcus 2001). However, researches have noted that the molybdenum and chromium prevent passive film breakdown by anodic sulfur segregation in materials similar to Alloy 22 (Marcus and Moscatelli 1989; Marcus and Grimal 1990; Elbiache and Marcus 1992; Costa and Marcus 1993). Scratch repassivation tests of Alloy 22 in sulfide-containing solutions showed that even if passive-film breakdown occurred, the material repassivated within a few seconds (Jung, et al. 2008). The NRC staff reviewed this information and concluded that anodic sulfur segregation was not a mechanism that could affect passive film stability (NRC 2011c).

A second proposed mechanism for breakdown of the Alloy 22 passive film was based upon dripping tests that showed higher corrosion rates than for immersion tests (Ashida et al. 2008). However, the observed pitting was not stable and was due in part to thermal aging of the specimen. Similar experiments (Dunn et al. 2006) did not observe this effect, and thus was concluded to not be an issue.

Finally, some of the experiments contained silica deposits on the Alloy 22 surface which could have acted as a corrosion barrier. However, experiments without any silica did not show enhanced corrosion (Andresen and Kim 2007) and was concluded to not be an issue.

Because of the adherent passive film Alloy 22 corrosion rates are quite low. As shown in Figure 18 and Figure 19 (SNL 2009), the general corrosion rates for Alloy 22 under a range of conditions, including the aggressive SCW waters discussed earlier, corrosion rates for samples exposed at 60°C -90°C for 5 years exhibit corrosion rates of less than 14 nm yr^{-1}, a mean rate of 4.6 nm yr^{-1} and a 90th percentile rate of ~8 nm yr^{-1}. Even at twice the highest measured rate, it would take almost a million years to corrode through a 25 mm thick plate.

The general corrosion rate has been shown to drop as a function of time due to refinement of the passive film and for a given quantity of measurement uncertainty (noise) the signal to noise ratio improves with longer experimental durations. To date the data is insufficient to truly model a time-dependent corrosion rate. Therefore, as in the simple analysis above, modeling has assumed that the corrosion rates for a given temperature are constant. Considering that the Alloy 22 corrosion rates are so low, and general corrosion would not play a significant role in waste package degradation, research to defend a time-dependent general corrosion rate does not seem worthwhile. This statement may not be true for alloys with higher corrosion rates, where arguing a time-dependent corrosion rate could extend the life of the waste package. However, demonstrating that the oxide film would remain adherent could be difficult.
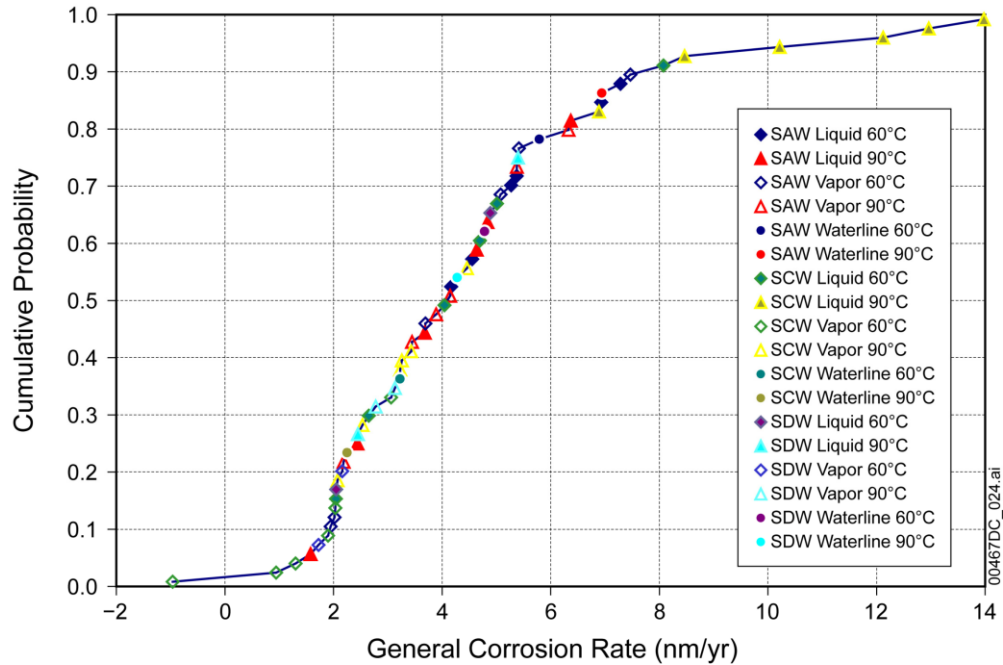
Source: SNL (SNL 2009), Figure 6-12[a]

Figure 18.   5-year general corrosion rates for Alloy 22 under a range of conditions
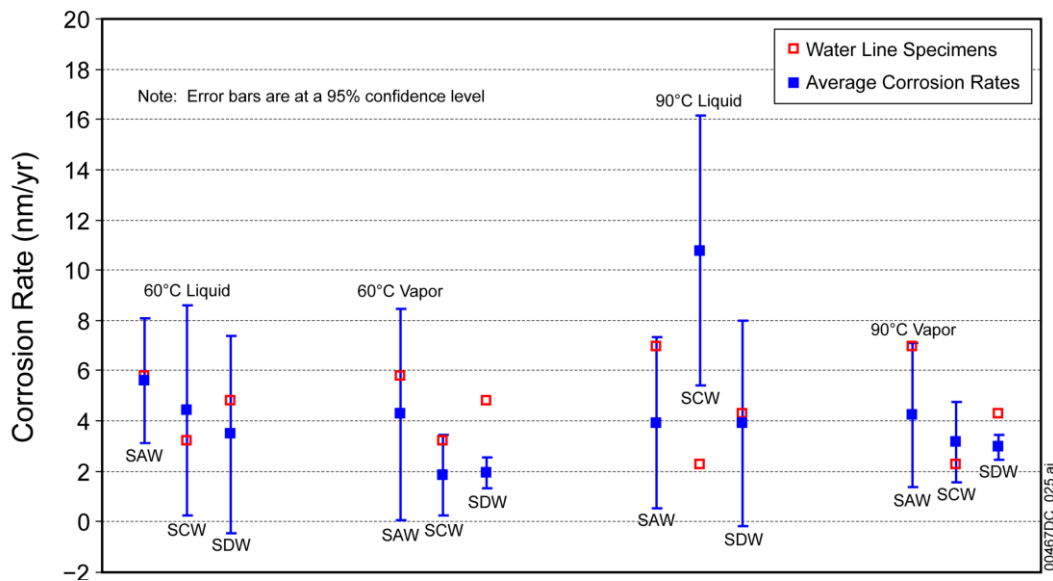
Source: SNL (SNL 2009), Figure 6-13[a]

Figure 19.   5-year Alloy 22 general corrosion rates grouped by environment

As can be seen from Figure 19, this data set does not readily demonstrate temperature dependence. While the Yucca Mountain model used a temperature dependant corrosion rate, a better data set would be helpful, particularly to estimate corrosion rates below 60°C.

One of the issues concerning general corrosion is that often metals are found to have much higher corrosion rates near welds. This is due to compositional changes and heat sensitization. However, as shown in Figure 20, Alloy 22 does not exhibit significantly higher corrosion rates for welded regions.
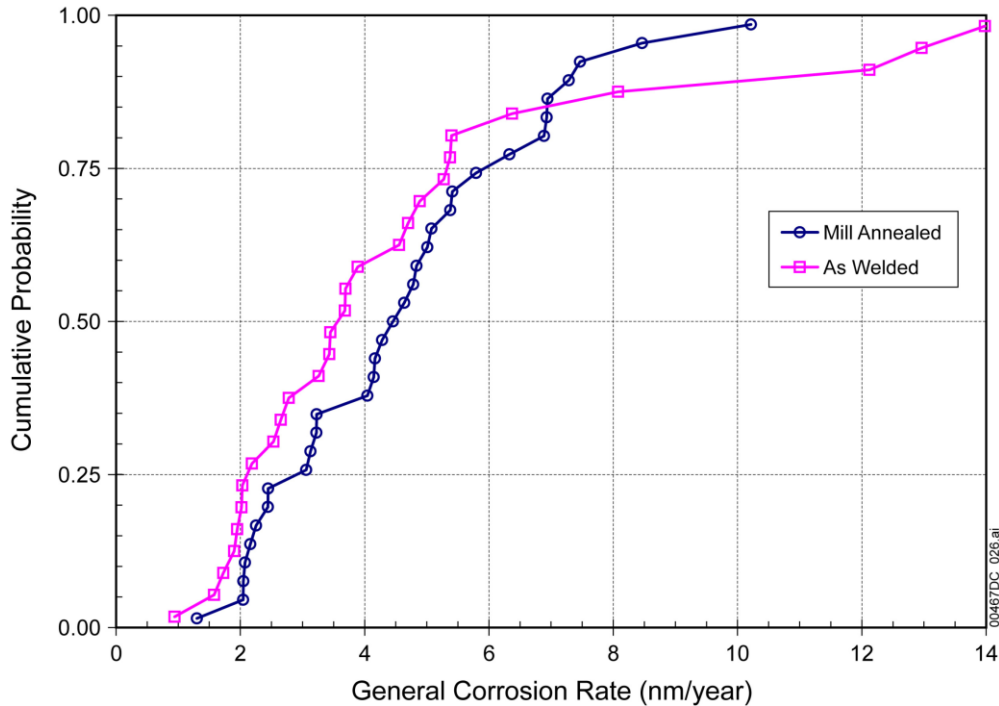
Source: SNL (SNL 2009), Figure 6-14[a]

Figure 20.   Welded and non-welded Alloy 22 5-year general corrosion rates

The discussion and figures of Alloy 22 general corrosion above are based upon the 5-year general corrosion rates obtained from samples from the Long-Term Test Facility (LTCTF). During cleaning of the 9.5-year samples, several issues were identified with the LTCTF experiments. It is important to remember that at the time the LTCTF experiments were started, the requirements for the waste package life-time were approximately 2,000 years. Thus the LTCTF experiments were more designed around comparing alloys and demonstrating that they would be sufficient for 2,000 years as compared to the current regulations that carry out performance assessment timeframes to one million years. These artifacts included a) not thoroughly cleaning the samples prior to testing – which leads to exaggerated weight loss; b) organic deposits from stir motors – leading to questions about corrosion rates, which were found to be similar for uncontaminated and contaminated specimens; and c) non-uniform oxide thicknesses near the sample holders (Wall and Brown 2009). Each of these conditions was resolved (SNL 2009), and the NRC staff found the resolutions to be reasonable (NRC 2011c), but leave some uncertainty for defending the data set. It was determined that the best way to defend the general corrosion rates for Alloy 22 would be a set of focused testing (Wall and Brown 2009). That work was initiated in 2009.

In these tests, Alloy 22 samples were prepared and then placed in solutions including 0.6M NaCl, SAW, and SCW. Care was taken to insure each sample had a nominally identical near mirror polish surface finish, and had been chemically cleaned/passivated in the same manner.

Specimens were removed after 3 and 9 months of exposure, and are presently being analyzed to determine the general corrosion rate in each environment. Specimens will be removed later in the

FY2011 at the 18 month mark. Data obtained to date is very self-consistent/reproducible, with much less variability than the LTCTF data, strongly suggesting that the physical/chemical factors which caused concern with the initial dataset have indeed been eliminated. This data set is not yet available.

Considering the breadth and depth of Alloy 22 research, other than finishing the ongoing general corrosion testing, no further Alloy 22 general corrosion testing is recommended at this time.

Stress corrosion cracking of Alloy 22

SCC is the process by which cracks initiate in a material under stress in the presence of a corrosive environment. In order for SCC to occur, three simultaneous conditions must be present: a susceptible material, critical environment, and sustained tensile stress. Sustained tensile test could be present in a repository environment due to residual stresses from welding, handling, seismic motion, or rockfall. Modeling of stress corrosion cracking involves two components initiation and crack growth.

SCC crack initiation

For the YMP, the crack initiation model was based upon a threshold stress (SNL 2007c) similar to that used elsewhere (ASM International 1987). Alloy 22 is highly resistant to SCC as shown in Figure 21 (Andresen and Kim 2010). Even at 105°C, with samples held at stresses up to 2.1 times the yield strength for as-received material and 2.0 times the yield strength of welded material, failures were not observed for well over 38,000 hours or 4.33 years, at which time the experiment was terminated. Note that this set of experiments was ongoing at the time of the Yucca Mountain License Application submittal and at that time the specimens had been on test for 3.2 years. To account for data uncertainty and the timescales being modeled the YMP established a crack initiation stress threshold with a safety factor of 2 compared to the long term data, or 90-105% of the Alloy 22 at-temperature yield stress (SNL 2007c) based upon applicable standards including ASTM G 30-94. The NRC staff considered this approach reasonable (NRC 2011c). The initiation stress threshold did not include an environmental component.
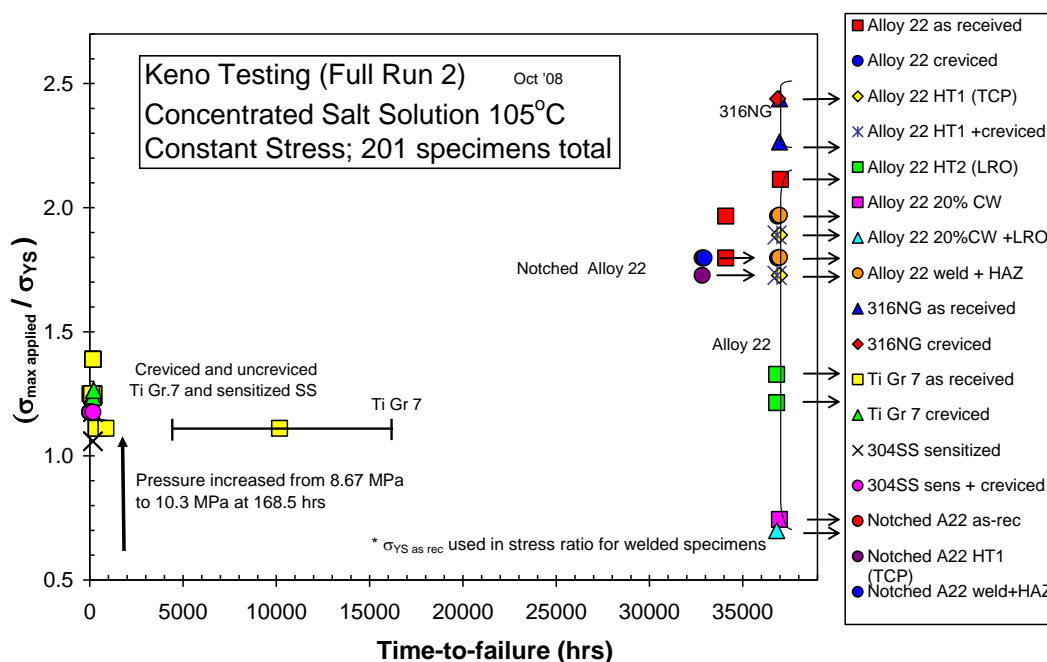
Source: Andreson and Kim (2010), Figure 25

Figure 21. Time to failure (or time on test) versus applied stress ratio in Basic Saturated Water solution at 105°C (note: LRO – long range ordering, TCP – tetrahedral close packed)

Threshold stress intensity factor

For existing cracks, such as may be present due to a weld flaw, a threshold stress intensity factor is necessary to determine whether cracks will grow. A threshold stress intensity factor with a mean of 6.62 MPa-m$^{0.5}$ and lower and upper bounds of 1.96 MPa-m$^{0.5}$ and 15.38 MPa-m$^{0.5}$ respectively has been used (SNL 2007c) and (Jones 1992). The NRC staff reviewed this approach and considered it reasonable (NRC 2011c).

SCC crack growth rates

Crack growth rates were modeled at YMP using the slip-dissolution film-rupture model (SDFR). In the SDFR model, crack growth is related to the rupture and subsequent reformation of the passive metal oxide at the crack tip (Andresen 1991; Andresen and Ford 1994; Ford and Andresen 1998) which has been shown to adequately model crack growth rates compared to experimental data (Figure 22). Other crack growth rate models include the coupled environmental fracture model which is based upon conservation of electrons (Macdonald and Urquidi-Macdonald 1991; MacDonald et al. 1994; Ford and Andresen 1998). The coupled environmental fracture model results in lower crack growth rates than the SDFR model (Ford and Andresen 1998). The NRC staff reviewed this approach and found it reasonable (NRC 2011c).
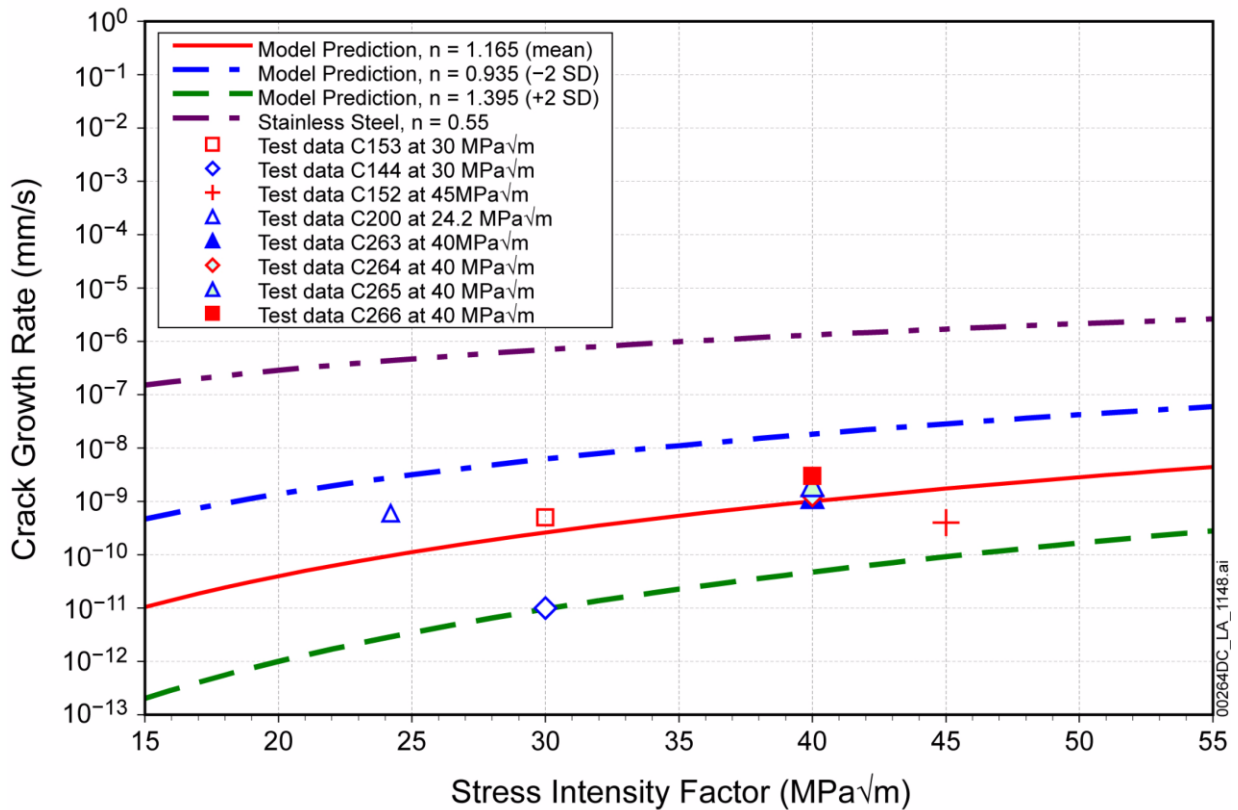
Source: SNL (2007c), Figure 6-9

Figure 22.   Comparison of crack growth rates predicted for stress corrosion cracking of Alloy 22 in Basic Saturated Water at 110ºC to experimental data

Engineering and operational aspects

As mentioned earlier, SCC can only occur if sustained tensile stresses are present. These stresses can result from welding, and drops during handling. The need for solution annealing Alloy 22 after welding to mitigate aging and phase stability issues is discussed later in this section. Solution annealing and quenching also relieves welding stresses on all but the final closure weld. Low plasticity burnishing has been shown to be effective at relieving welding stresses (SNL 2007c; BSC 2008) to a depth of several mm, which for Alloy 22 would prevent SCC for over a hundred thousand years. No further research in this area is warranted at this time.

Besides welding, mishandling of the waste package could result in dents with sufficient tensile stresses around the outer annulus of the dent as to allow for SCC. Without detailed handling analysis, waste package design, etc. it is not possible to plan for such dents. Therefore, it is not recommended that this topic be pursued at this time.

Localized corrosion of Alloy 22

Localized corrosion due to aqueous exposure

LC is a phenomenon in which corrosion progresses at discrete sites or in a non-uniform manner and includes pitting and crevice corrosion. At least upon initiation, the propagation rate of localized corrosion is faster than general corrosion. In a passive metal such as Alloy 22, for localized corrosion to occur the passive film must first be compromised to allow an aggressive environment to contact the bare metal surface. Pitting corrosion requires much harsher conditions for initiation than crevice corrosion (Cragnolino et al. 1999; Dunn et al. 2000; Rebak 2005). Therefore, localized corrosion models treat all localized corrosion as crevice corrosion, even in the absence of crevices. Localized corrosion initiation requires that the open-circuit corrosion potential (E_{corr}) exceed or equal a critical potential ($E_{critical}$). E_{corr} is the open-circuit corrosion potential attained by a metal immersed in a solution with no applied driving force. $E_{critical}$ is the potential below which the passive film is stable and above which localized corrosion can occur. $E_{critical}$ can be defined several different ways.   The most easy to measure and the most conservative (Shan and Payer 2007; He et al. 2009) is the repassivation potential (E_{rcrev}) which is the potential at which an actively corroding material repassivates, as shown in Figure 23. Figure 24 shows a schematic of cyclic polarization data for stainless steel, Alloy 22, and titanium.

Thus when E_{rcrev} is used to obtain $E_{critical}$, the initiation model is actually stating that when $E_{corr} > E_{rcrev}$ localized corrosion may occur, when in fact it is the potential at which localized corrosion would stop. Thus this approach is conservative and answers the question, 'what would occur if you waited a little longer?' with the answer being that at the E_{rcrev} potential nothing would occur because localized corrosion were occurring and it stopped.
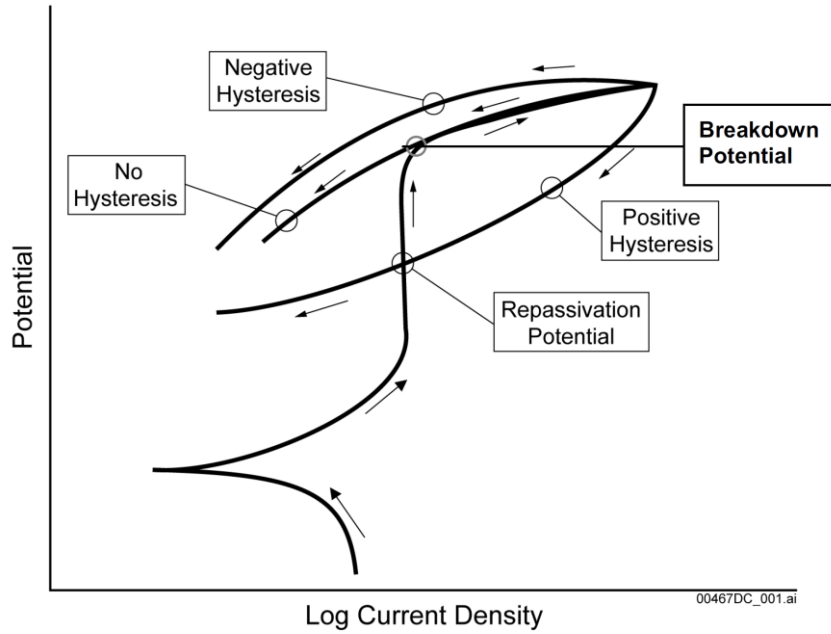
Source: SNL (2009), Figure 6-29

Figure 23.   Schematic potentiodynamic polarization curve showing likely behaviors of the curves during scanning of an alloy with high resistance to localized corrosion
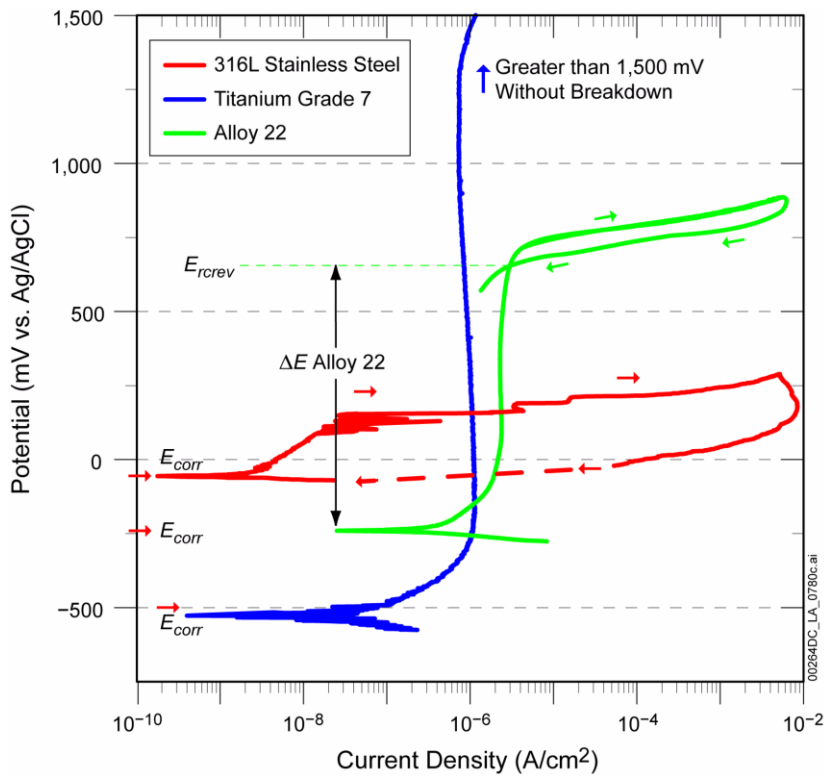
Figure 24.   Schematic cyclic potentiodynamic polarization curves for stainless steel type 316L, Alloy 22, and titanium in high chloride solutions

The localized corrosion data obtained for YMP included over a two-hundred data points over a wide range of conditions including: dilute solutions, multi-ionic solutions (e.g. SCW), and highly aggressive solutions containing concentrated salt solutions, all over a wide range of pH and temperatures (SNL 2009). The data indicates that both the long term corrosion potential (E_{corr}) and the repassivation (E_{rcrev}) potential are a function of temperature (more LC at high T), pH (more LC at low pH), NO_3^-/Cl^- ratio (more LC at low ratios), and Cl^- concentration (more LC at high concentrations). No localized corrosion was observed on any long term sample that did not have potential applied to it. However, the localized corrosion model did predict LC for some of the environments. The over-prediction of localized corrosion is due to two issues. First, there is large variation in the data sets. Figure 25 and Figure 26 show the model predictions compared to the data. As can be seen, the large data spreads (shown as circles on a vertical line) result in a wide uncertainty band for both E_{corr} and E_{rcrev}. Figure 27 shows that for a fairly benign environment (6 molal chloride, pH of 7 and 1.8 molar nitrate) that localized corrosion would be predicted to be possible at temperatures as low as 90°C. Secondly, the data sets tend to have been developed for very high solute concentrations, which as discussed in Section 2.5.2, is more aggressive than would be expected in repository conditions.

Therefore, it is recommended that additional data be systematically obtained in more relevant repository conditions. This data would be useful for any unsaturated crystalline rock repository, particularly if temperatures would be lower than modeled for YMP. In particular, data should be obtained across the full range of NO_3^-/Cl^- ratios. While a plot is not presented herein, the model treats this term as near linear, when it appears that an S function may be more applicable with E_{rcrev} increasing dramatically at intermediate ratios.
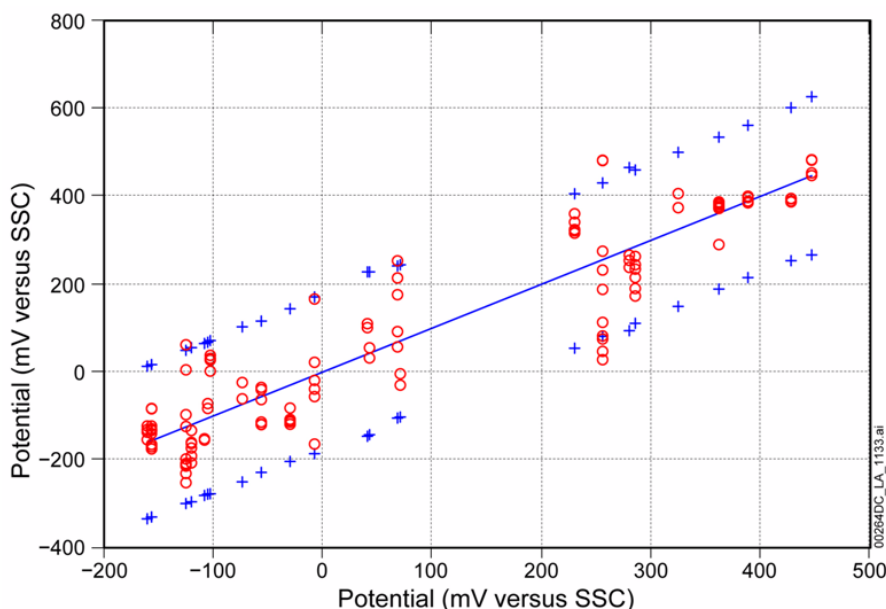
Source: SNL (2009), Figure 6-41

Note: The horizontal axis is the long-term corrosion potential predicted by the model while the vertical axis is either the measured potential (circles), the mean model prediction (solid line), or the ±2 standard deviation intervals (plus signs). SSC = saturated silver chloride electrode.

Figure 25.   Model prediction and experimental data for Alloy 22 long-term corrosion potential (E_{corr})
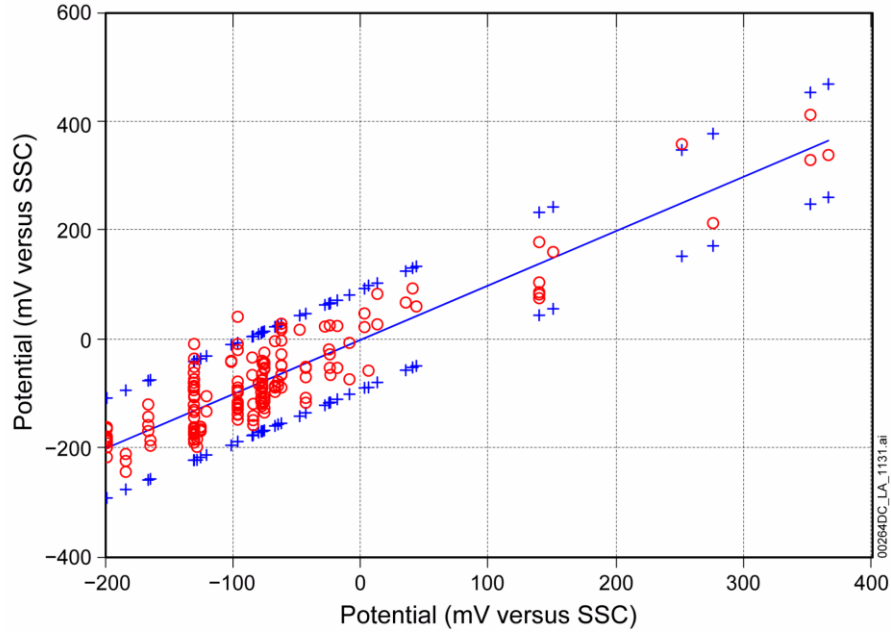
Source: SNL (2009), Figure 6-34

Note: The horizontal axis is the repassivation potential predicted by the model while the vertical axis is either the measured potential (circles), the mean model prediction (solid line), or the ±2 standard deviation intervals (plus signs). SSC = saturated silver chloride electrode.

Figure 26.   Model prediction and experimental data for Alloy 22 repassivation potential (E_{rcrev})
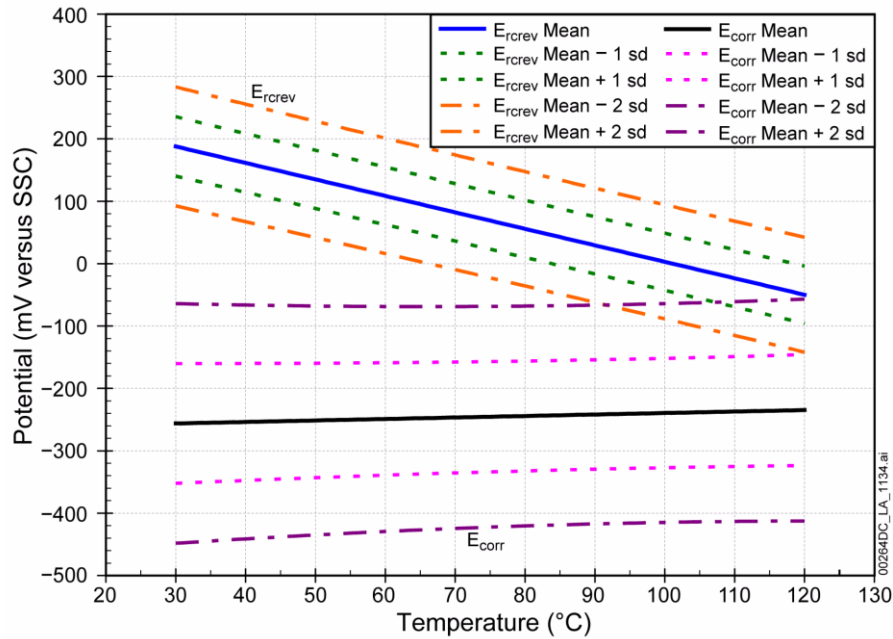
Source: SNL (2009), Figure 6-42

Note: Figure shows E_{rcrev} and E_{corr} versus temperature for a 6M chloride solution, with a pH of 7 and 1.8M nitrate.

Figure 27.   Alloy 22 localized corrosion initiation model results as a function of temperature at a pH of 7

Once localized corrosion initiates, the rate of attack tends to decrease fairly rapidly (Hunkeler and Boehni 1983; EPRI 2002b; He and Dunn 2006). The use of a time-dependent growth law model can be developed using a combination of electrochemical and corrosion exposure measurements. However, considering how resistant Alloy 22 is to localized corrosion, the use of a constant rate is appropriate and not overly conservative. The NRC staff reviewed this approach and found it reasonable (NRC 2011c). However, for less corrosion resistant materials, the use of a time dependent growth law may be necessary to avoid dramatic over conservatisms.

Localized corrosion due to dust deliquescence

Any waste package which is exposed to the atmosphere (as would be expected in an unsaturated crystalline rock repository) will have particulates (i.e., dust) carried by the atmosphere deposited on its surface. Extended periods of repository ventilation can result in large quantities of dust. A portion of most atmospheric dusts consists of various soluble salts. It has been suggested by several researchers that these salts may combine to form deliquescent brines on the surface of a waste package at temperatures well above the boiling point of water, and further, that these brines might be corrosive depending on the material used to construct the package.

Other researchers (BSC 2005) have suggested that for highly corrosion resistant/passive materials, several factors will prevent extensive localized corrosion due to deliquescence, including electrochemical limitations (e.g., insufficient cathode reaction area) and physical (e.g., limited brine quantities, coupled with consumption or sequestration of aggressive species in the corrosion product). The NRC staff have reviewed this approach and found it reasonable (NRC 2011c).

In an effort to determine if there is indeed a potential for deliquescent brines to result in localized corrosion, a series of experiments have been (and continue to be) performed. Materials of interest have been decorated with thin layers of salt in the presence of an occluded geometry in an effort to establish if localized corrosion (i.e., crevice corrosion) could initiate and propagate under such conditions. In these experiments, no inert species were added, and as such physical sequestration of the brine by the dust layer due to capillary forces have been eliminated, allowing all of the material deposited on the metal surface to participate in the corrosion reaction.

The chemical composition of the brines which can form are a function of temperature, as well as the available constituent materials. At very high temperatures, brines must be very nitrate rich, whereas at lower temperatures, the composition can be dominated by other species, such as chloride. In terms of the corrosiveness of the brine, both the chemistry (e.g., concentration of aggressive species) and the exposure temperature have a strong impact on corrosion processes.

Experiments have been performed in a multi-salt assemblage consisting of $NaCl$, $NaNO_3$, KNO_3, and $Ca(NO_3)_2$ with an overall nitrate to chloride ratio of 18. Samples of Alloy 22, Inconel 625, Hastelloy C276, and an 80:20 Ni:Cr alloy were evaluated. Each sample was polished to a mirror finish, loaded with salt to over 350 µg cm^{-2} on top of which a multi-crevice assembly was placed. Samples were then exposed to an environment at 180°C with a dewpoint of 94.5°C (tests were performed in Albuquerque, NM, and as such the boiling point of water is approximately 94.5°C and the environment was pure steam). After 30 days exposure, the samples were removed, the crevice formers taken off, and the extent of any crevice corrosion measured. In all cases, localized corrosion did not initiate on any of the materials. The experiment was then repeated at the same temperature with a slightly lower dewpoint (92°C) to determine if atmospheric oxygen was required for corrosion initiation. The test was run for 30 days, and again, no crevice corrosion initiation was observed on any of the materials.

At lower temperatures, closer to 100°C, it is possible to form a concentrated brine containing only chloride species. Mixtures of KCl and NaCl are capable of forming a brine at temperatures as high as 105°C. Experiments were performed in the same manner as those described above at a dewpoint of 94.5°C, only with a brine consisting only of KCl and NaCl at a temperature of 101°C for 100 days. In

addition to the materials used in the 4 component, nitrate-chloride brine, 303SS was added to the test matrix. This is a free-machining stainless steel which is extremely susceptible to localized corrosion, and was selected to demonstrate that the test procedure could support localized corrosion for a sufficiently susceptible material. The test was run for a total of 100 days, and for the nickel based alloys, no discernable crevice corrosion was observed. The 303SS, however, did initiate localized corrosion for many of the multi crevice assembly teeth.

Now that a system has been identified where localized corrosion can be readily initiated in a deliquescence formed brine, additional work is in progress to determine if the extent of attack is a function of the quantity of brine present on the metal surface. 303SS and 304SS samples have been loaded with the NaCl:KCl salt mixture at 50, 100, and 200 $\mu g\ cm^{-2}$ and placed again in an environment with a dewpoint of 94.5°C and a system temperature of 101°C. Upon completion of the exposure period (100 days), samples will be evaluated and it will be determined if the degree of attack is indeed a function of the quantity of reactant present at the onset of the experiment.

Engineering and operational aspects

As mentioned previously, Alloy 22 must be solution annealed and quenched to minimize stress corrosion cracking and aging and phase stability issues. The solution anneal and quench was successfully demonstrated on a full size used fuel waste package prototype. However, annealing leaves a black non-adherent oxide surface film. Localized corrosion testing was performed on the black annealed Alloy 22 and found to significantly increase the data variability compared to cleaned Alloy 22. On this basis the YMP project added a postclosure parameter requirement that the black anneal be removed prior to waste package usage (BSC 2008). Since the Alloy 22 performs fine after removal of the black annealing film, there is little reason to believe that this effect is real and it would cost significant amounts of money to have to remove the annealing film. Therefore it is recommended that research be performed to demonstrate that the annealing film does not increase the likelihood of localized corrosion.

Hydride cracking of Alloy 22

Nickel based alloys are essentially immune (particularly for repository relevant conditions) to hydride cracking and thus no research is needed in this area.

Thermal mechanical effects of Alloy 22

As a multi-component alloy with numerous possible phases, Alloy 22 could be subject to aging and phase stability issues. Long-term thermal aging is the process by which certain secondary phases may precipitate from the metal matrix. Thermal aging is caused by holding material at intermediate temperatures (below the solution annealing temperature) but at temperatures high enough that kinetics will allow solute atoms to move, forming thermodynamically favorable phases. The precipitation of key elements that provide corrosion resistant properties may reduce the corrosion resistance of the bulk material. This precipitation could also adversely impact mechanical properties such as making the material more brittle.

A significant amount of modeling and data have been gathered on Alloy 22 and phase stability. It has been demonstrated that for repository relevant temperatures that Alloy 22 will not undergo any adverse aging effects (Turchi 2001; BSC 2004). Some of the data and models are presented in Figure 28 and Figure 29. As can be seen, as temperatures fall, the rate of changes drops significantly and is not observable below 300°C even after 11 years.

Figure 30 shows the calculated quantity of transformation as a function of time for various temperatures. As can be seen, for temperatures below 250°C, no transformation is predicted to occur for over 100,000 years and below 200°C none is expected for over a million years.

As shown in Figure 31, calculated results predict more transformation than is observed from experiments, indicating that the overall effects of aging and phase stability are less than predicted by models.

In addition, Awaruite is a naturally occurring ordered nickel-iron metallic mineral with an approximate stoichiometry of Ni_3Fe. Josephinite, a 150 million year old rock, contains large quantities of awaruite and some taenite (a high-temperature, disordered nickel-iron matrix metallic phase). These phases formed in the temperature range of 400°C - 460°C and have not changed since that temperature. This natural analogue provides confidence that Alloy 22 will not undergo phase changes at moderate temperatures even for very long timeframes.

The NRC staff (NRC 2011c) reviewed the aging and phase stability data, model and natural analogue comparison and concluded that it is reasonable to assume that aging and phase stability would be of low consequence.
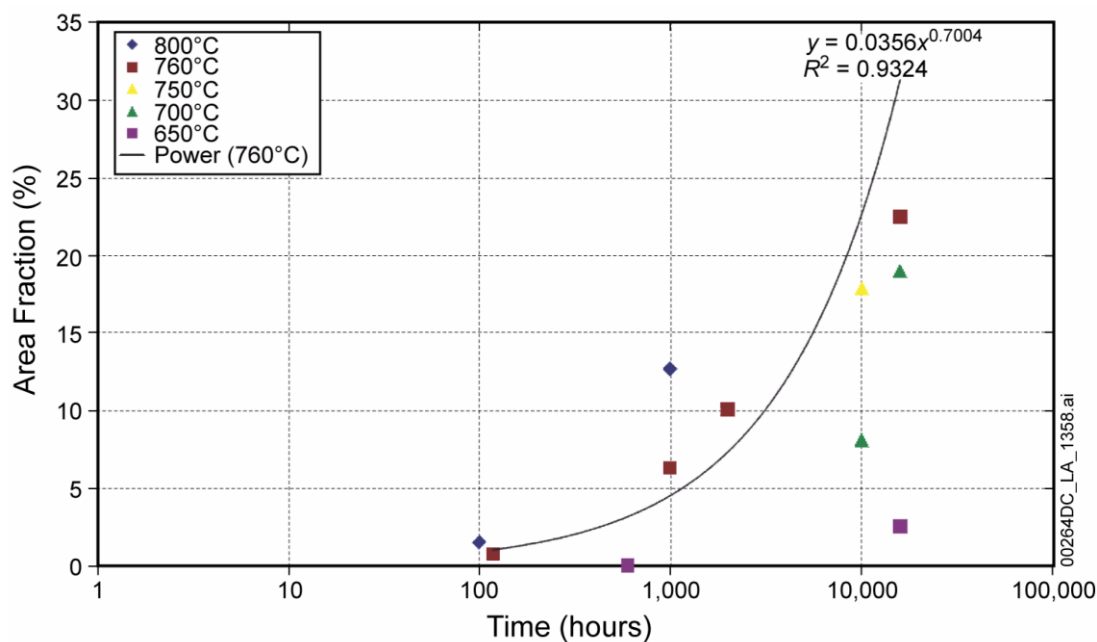
Source: BSC (2004), Figure 107

Figure 28.   Precipitation of tetrahedrally close-packed phases in Alloy 22 as a function of time and temperature
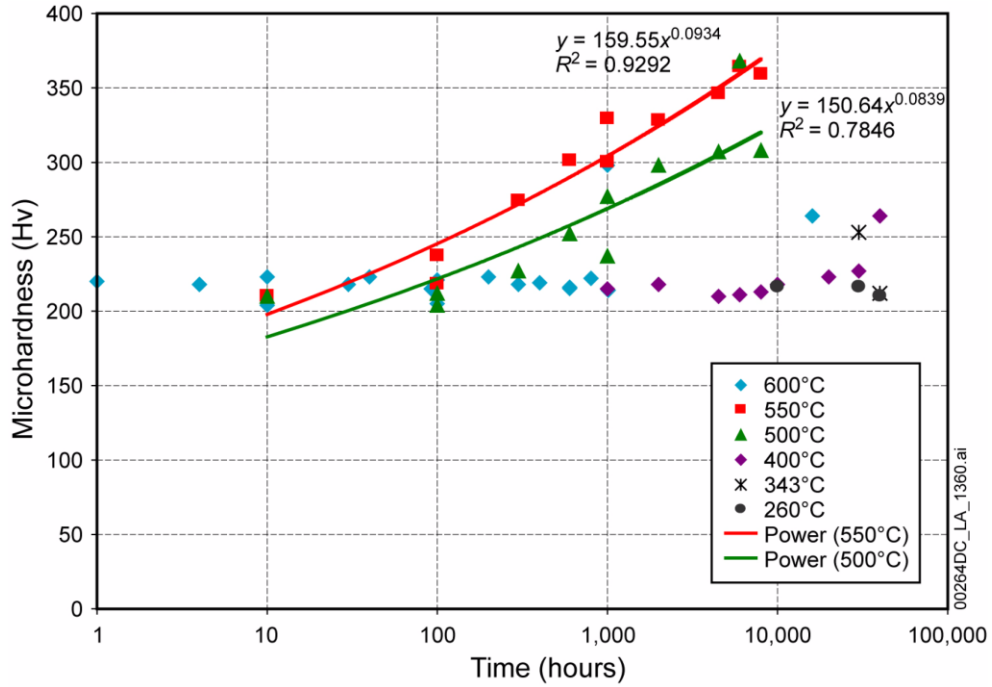
Figure 29.   Microhardness measurements on aged Alloy 22 shown as a function of time and temperature
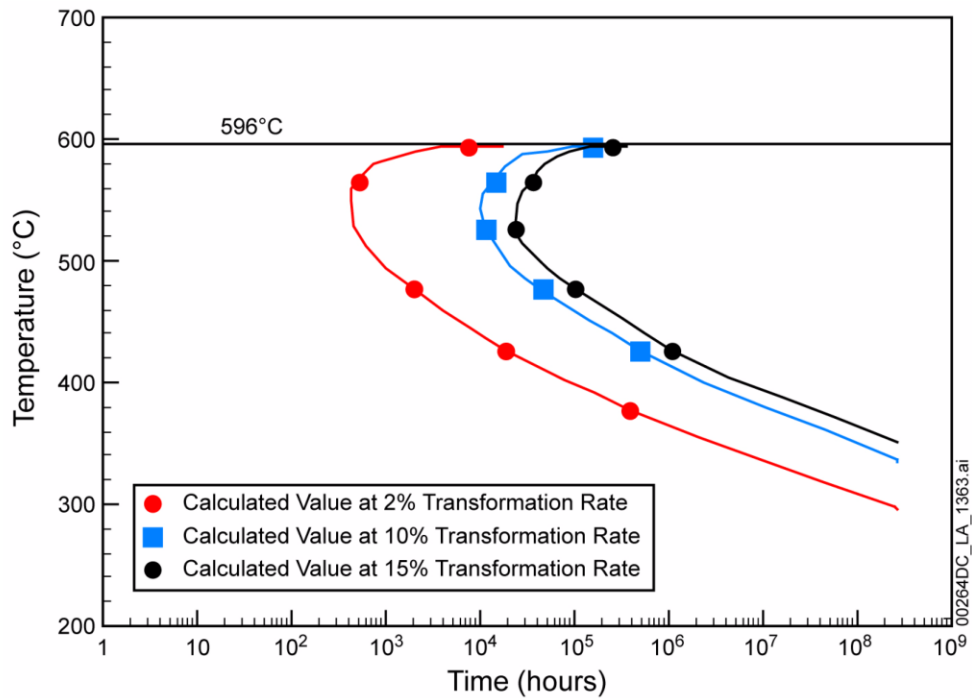
Figure 30.   Calculated isothermal time-temperature-transformation for a face-centered cubic matrix of a ternary Ni-21.1 Cr-13.5Mo (wt%) alloy (modeling surrogate of Alloy 22) transforming into the oP6-ordered phase
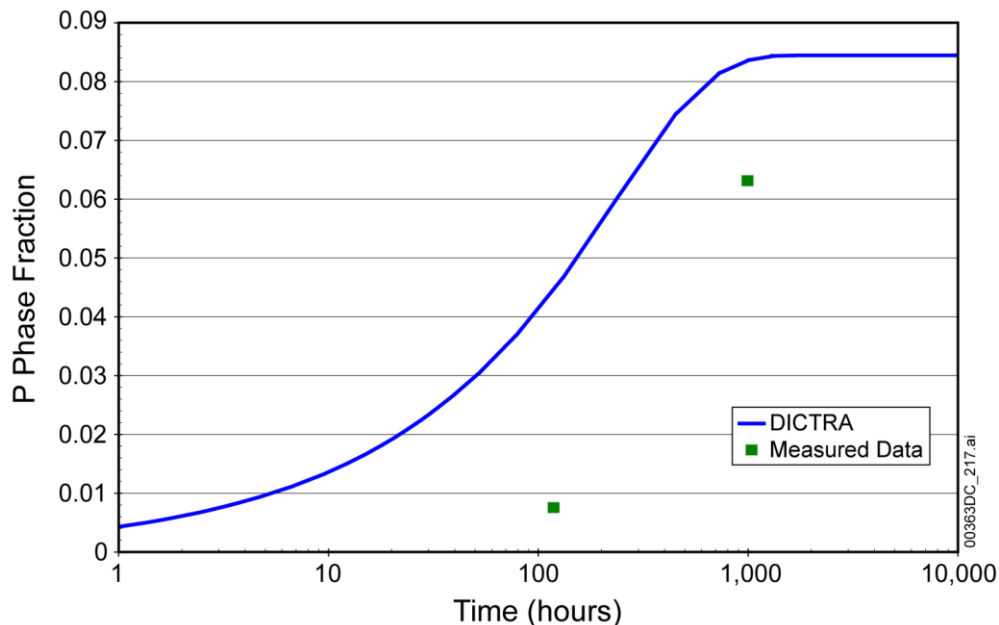
Source: BSC (2004), Figure 108

Note: The solid line represents modeling results using the computer code "DICTRA".

Figure 31.   Comparison of phase formation at 750°C for computational results (P phase) and measured data (TCP phase) on Alloy 22 base metal

Engineering and operational aspects

The aging and phase stability data available for Alloy 22 does not cover the full range of Alloy 22 compositions. There is some evidence and phenomenon based arguments to suggest that as an alloy becomes more enriched that it may be more susceptible to aging and phase stability issues. Therefore, YMP adopted a composition range for Alloy 22 (BSC 2008):

- Cr = 20.0 to 21.4 wt%
- Mo = 12.5 to 13.5 wt%
- Fe = 2.0 to 4.5 wt%
- W = 2.5 to 3.0 wt%

This is range is included within, but more restrictive than the UNS N06022 composition range:

- Cr = 20.0 to 22.5 wt%
- Mo = 12.5 to 14.5 wt%
- Fe = 2.0 to 6.0 wt%
- W = 2.5 to 3.5 wt%

If Alloy 22 were used for disposal purposes, the costs associated with this tighter specification and additional quality assurance needs would be significant. Therefore, it is recommended that some of the more alloy rich samples that have already been aged be examined for aging and phase stability issues.

These are identified in the *Long-Term Corrosion Testing Plan* (Wall and Brown 2009). This analysis would have the potential to expand the range to:

- Cr = 20.0 to 22.0 wt%

- Mo = 12.5 to 14.0 wt%

- Fe = 2.0 to 4.5 wt%

- W = 2.5 to 3.0 wt%

In addition to saving costs and reducing QA requirements, increasing the allowable Cr and Mo contents could allow for greater corrosion resistance.

2.5.4.2   Alloy C-4

The German repository program is considering Alloy C-4. It is chemically similar to Alloy 22 with less chromium, slightly more molybdenum, and no tungsten.

General corrosion of Alloy C-4

With a chemical composition similar to Alloy 22, Alloy C-4 should have similar general corrosion rates as Alloy 22 for the relatively benign repository relevant conditions. Indeed for welded Alloy C-4 samples tested at 150°C for 18 months, in sodium chloride brines samples corroded at a rate of ~ 60 nm yr^{-1}, which is similar to Alloy 22 corrosion rates under similar conditions (Smailos et al. 1993). At this time no further research is recommended. However, if the material were considered for an unsaturated crystalline rock repository, samples tested for 9.5 years are available for examination (Wall and Brown 2009).

Stress corrosion cracking of Alloy C-4

Little data is available for SCC of Alloy C-4 in repository relevant environments, but considering its composition, it should behave similarly to Alloy 22.

Localized corrosion of Alloy C-4

Little data is available for localized corrosion of Alloy C-4 in repository relevant environments, but considering its composition, it should behave similarly to Alloy 22. The lack of tungsten in Alloy C-4 may increase the susceptibility to pitting under certain environments, but these are not repository relevant.

Hydride cracking of Alloy C-4

Nickel based alloys are essentially immune (particularly for repository relevant conditions) to hydride cracking and thus no research is needed in this area.

Thermal mechanical effects of Alloy C-4

The aging and phase stability of Alloy C-4 should be similar to that of Alloy 22. In fact, the modeling done for Alloy 22 at YMP used a ternary alloy of Ni -21.1% Cr – 13.5%Mo, which is similar to Alloy C-4 except it is a little high in Cr and low in Mo. Alloy C-4 Aging and phase stability samples are available for analysis, which may be of benefit as it could help explain the role of tungsten (present in Alloy 22, but not Alloy C-4) (Wall and Brown 2009).

2.5.4.3   Other Ni-based alloys

Alloy C276

Alloy C276 is compositionally similar to Alloy C-4, but contains more iron, and less chromium. Its overall corrosion behavior would be expected to be less corrosion resistant than Alloy C-4 as a result. This may be of benefit for achieving higher signal to noise ratios in repository environments where studying small corrosion rates can be difficult.

Alloy G3

Alloy G3 is compositionally similar to Alloy C-4, but contains more iron and less molybdenum, which would tend to reduce its corrosion resistance. However, it contains more chromium, similar to Alloy 22. Its overall corrosion behavior would be expected to be less corrosion resistant than Alloy C-4 as a result. This may be of benefit for achieving higher signal to noise ratios in repository environments where studying small corrosion rates can be difficult. Samples of Alloy G3 that have been exposed to repository environments are available for testing (Wall and Brown 2009).

Alloy 825

Alloy 825 bridges the gap between the corrosion allowance materials and corrosion resistant materials. The discussion of Alloy 825 is Section 2.5.4.8.

2.5.4.4   Titanium Grade 7

As discussed earlier, Titanium Grade 7 was the drip shield proposed plate material for the YMP. As such, it played a large part in protecting the waste package from aggressive seepage environments and was researched in great detail (SNL 2007a) and subject to many reviews (Farmer et al. 1988; NRC 2011c).

General corrosion of Titanium Grade 7

Titanium Grade 7 general corrosion is a uniform thinning of the material due to electrochemical processes. This thinning occurs at extremely low rates due to the formation and slow dissolution of a protective, passive oxide film on the metal surface. The passive film is self-forming and self-healing when the metal is exposed to air and moisture as would be expected in an unsaturated crystalline rock repository. As long as the passive film remains stable (instability would result in localized corrosion) the general corrosion rates will remain extremely low. Unlike the nickel based alloys discussed above, Titanium Grade 7 is a single phase with only palladium additions to provide additional protection in extremely aggressive environments (Hua and Gordon 2004; Schutz 2005), and as shown in Figure 7. The passive film is stable continuous, highly adherent and protective. It is primarily TiO_2. The passive films on titanium and its alloys are stable over a wide range of potentials and pH values (Pourbaix 1974). Also due to its extremely high affinity for oxygen, a damaged oxide can reheal itself instantaneously, even when just traces of oxygen are present (Schutz and Thomas 1987). In the presence of fluoride brines, passive film instability has been observed for specimens exposed to fluoride shortly after the passive film was manually removed by polishing (Brossia and Cragnolino 2000; Brossia et al. 2001). However, when specimens were in an oxidizing environment for as little as four days prior to fluoride exposure the specimens exhibited resistance to fluoride attack (Lorenzo de Mele and Cortizo 1999). Also, samples subjected to fluoride containing brines (SCW, SAW and SDW) did not exhibit localized corrosion (SNL 2007a). Thus in an unsaturated crystalline rock repository, fluoride attack will not lead to localized corrosion. The NRC staff have reviewed the passive film stability arguments, models and data and found them to be reasonable (NRC 2011c).

The mean corrosion rate of Ti-7 exposed to SCW at 90°C is ~46 nm yr^{-1} and only 5 nm yr^{-1} for SAW and SDW while the corrosion rate for Ti-29 is less than twice that of Ti-7 for these environments (SNL 2007a). Figure 32 shows the cumulative distribution function for Ti-7 2.5 year corrosion rates, exposed to SAW, SDW and SCW at 60°C and 90°C. Figure 33 shows the corrosion rates for Ti-7 as a function of water chemistry. Note that corrosion rates are much lower than for SCW 90°C exposures. Under a wide range of conditions, including seawater up to 260°C, corrosion rates of titanium alloys are negligible (Schutz 2005). Considering the low general corrosion rates and excellent resistance to localized corrosion, titanium alloys are a viable option for an unsaturated crystalline rock repository.
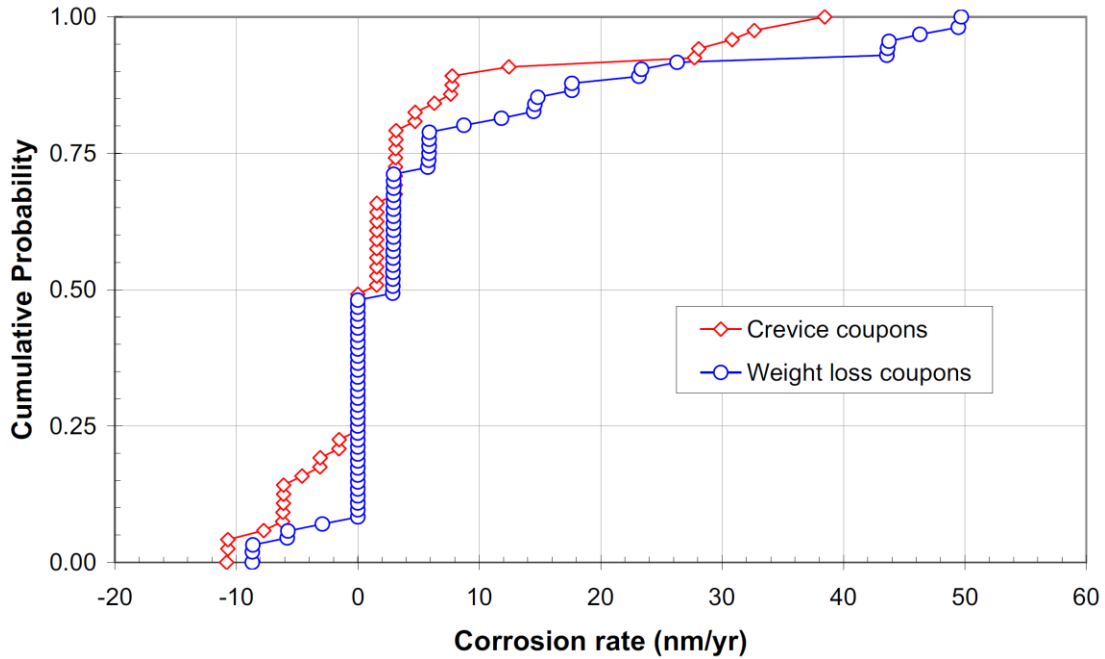
Source: SNL (2007a), Figure 6-4[a]

Figure 32.   Cumulative distribution functions for titanium Grade 7 weight loss and crevice samples after 2.5 year exposure
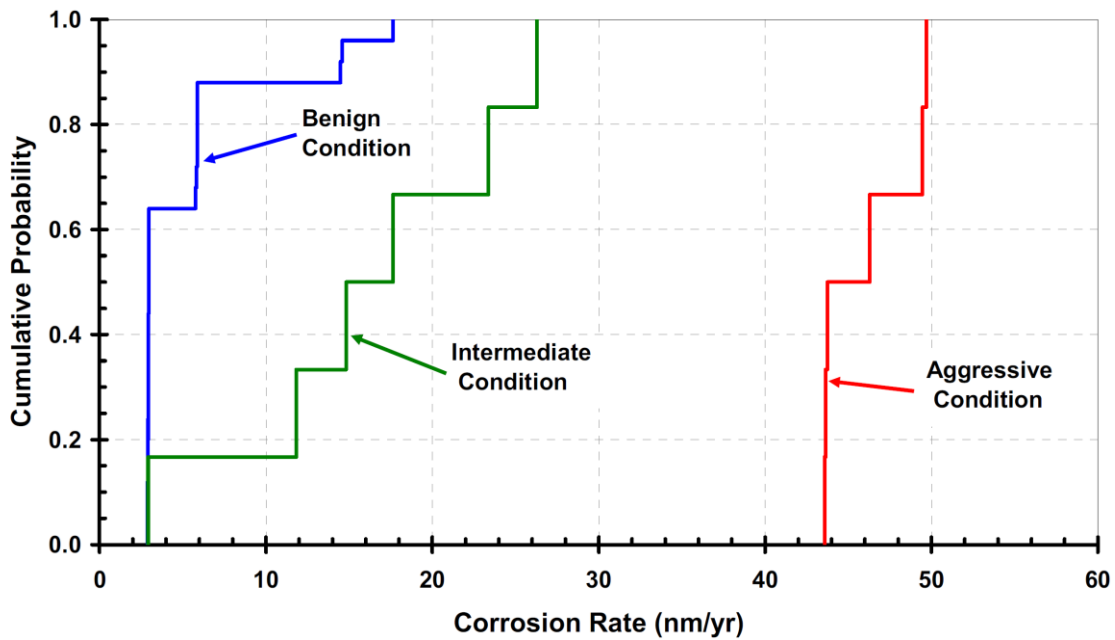
Source: SNL (2007a), Figure 6-8[a]

Note: Benign Conditions include SAW and SDW, Intermediate Conditions are SCW at 60°C, and Aggressive Conditions are SCW at 90°C).

Figure 33.   Cumulative distribution functions for titanium Grade 7 for different exposure conditions

The Titanium Grade 7 corrosion data did not indicate temperature dependence, so none was developed. The NRC staff reviewed this approach and found it reasonable (NRC 2011c).

The discussion and figures of Titanium Grade 7 general corrosion above are based upon the 2.5-year general corrosion rates obtained from samples from the Long-Term Test Facility. These samples were introduced after the Alloy 22 samples, but may be subjected to the same issues as were the Alloy 22 samples discussed in Section 2.5.4.1. Analysis of the oxide films were performed and estimated that the titanium general corrosion rates may have been underestimated by up to a factor of 2. Thus if Titanium Grade 7 were considered for use in an unsaturated crystalline rock repository, it would be appropriate to conduct a set of focused testing similar to that ongoing for Alloy 22 to confirm and bolster the suitability of the LTCTF data.

Stress corrosion cracking of Titanium Grade 7

The mechanism for SCC of titanium is the same as that presented for Alloy 22. As shown in Figure 6, Titanium Grade 7 samples failed after relatively short durations at 1.1 times the yield strength in constant load tests in immersion conditions. However, subsequent control tests in air at the same temperature exhibited failure times similar to those specimens tested in the brine environment, indicating that the failures were creep rupture rather than SCC.   U-bend specimens with surface stresses of 83% of yield strength and constant load tests did not exhibit stress corrosion cracking initiation (SNL 2007a).

Localized corrosion of Titanium Grade 7

The mechanism for localized corrosion of Titanium Grade 7 is the same as for Alloy 22, with localized corrosion initiation occurring when the open circuit potential (E_{corr}) exceeds the repassivation potential ($E_{critical}$). Due to the very protective adherent TiO_2 oxide film, titanium has excellent localized corrosion resistance as discussed in Section 2.5.2.1. As shown in Figure 34, even under applied potential for repository relevant brines, localized corrosion does not occur.

No localized corrosion attack was observed in long-term corrosion tests for up to 5 years of exposure in SAW, SWC, SDW and BSW (SNL 2007a). In addition, cyclic potentiodynamic polarization tests run in four different solutions: (1) *3.6 m $CaCl_2$ + 5.8 m KCL + 1.8 m KNO_3 + 2 m $NaNO_3$; (2) 7 m KCl + 1.8 m $NaNO_3$ + 1.2 m NaCl + 2.4 m Na_2SO_4; (3) 7.2 m KCl + 0.3 m KNO_3 + 3.3 m $NaNO_3$ + 2.1 m Na_2SO_4 + 0.2 m NaF; and (4) 5 m KCl + 2.8 m KNO_3 + 6.6 m $NaNO_3$ + 6.8 m Na_2SO_4 + 0.1 m NaF + 0.1 m NaBr.* *The results* show that Titanium Grade 7 and Grade 29 alloys maintain passivity at potential at least as high as 500 mV with no localized corrosion observed (SNL 2007a).

Hydride cracking of Titanium Grade 7

The uptake of hydrogen within titanium can lead to mechanically weak hydrides, which above a certain threshold value would lead to crack formation. Evidence suggests that hydrogen absorption in titanium could occur under repository relevant conditions. The palladium alloying element in Titanium Grade 7 acts to increase the critical hydrogen concentration value and decreasing the hydrogen absorption. Also in an unsaturated repository the atmospheric conditions would be oxidizing, which would also limit hydrogen uptake. Therefore, hydride cracking will not occur in the bulk plates. However, there is some concern of hydrogen uphill diffusion caused by stress gradients near welds between differing titanium alloys. The YMP mitigated and reduced this risk by adding an intermediate weld filler material, Titanium Grade 28, between the Titanium Grade 7 plates and the Titanium Grade 29 structural members (BSC 2008). Recent modeling (Mintz and He 2009) and noted that hydrogen concentrations would be minimal. The NRC staff reviewed the models and data and concluded that it was reasonable to exclude hydride cracking.

Thermal mechanical effects of Titanium Grade 7

Aging and Phase stability issues discussed for Alloy 22 are insignificant for Titanium Grade 7, because it is a single phase alloy and thus does not form intermetallics. No research is needed in this area.
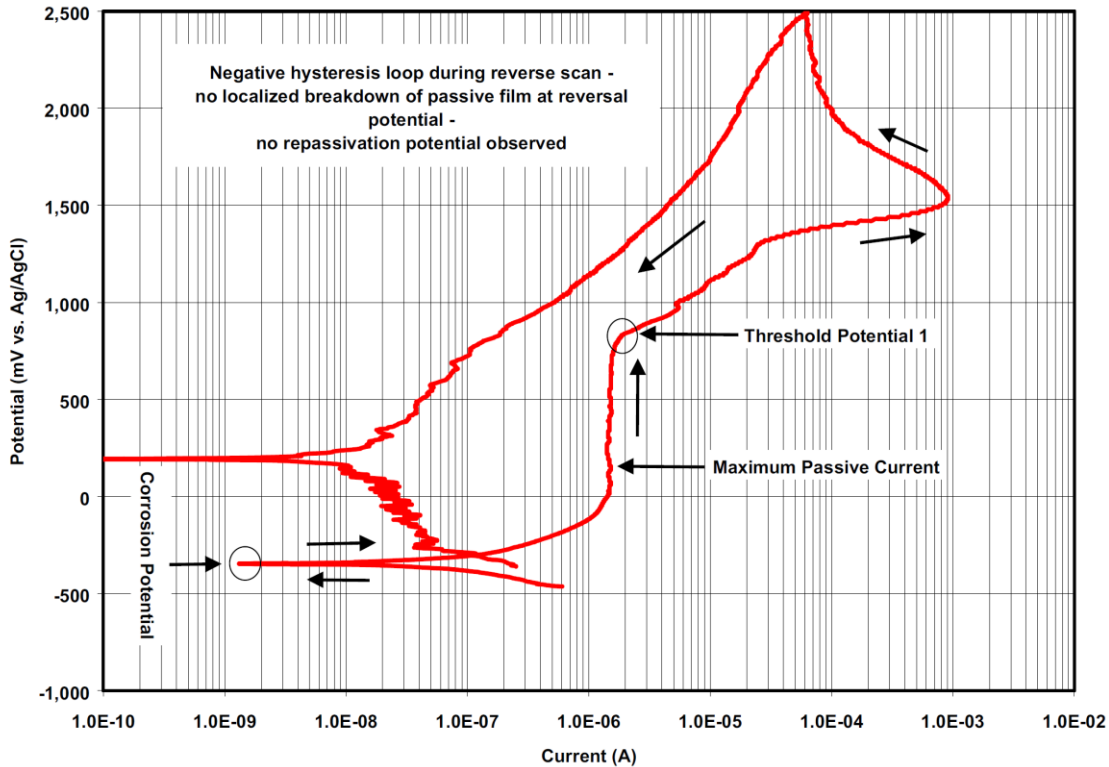
Source: SNL (2007a), Figure 14

Note: Negative hysteresis loop during reverse scan. No localized breakdown of passive film at reversal potential. No repassivation potential observed.

Figure 34.   Titanium Grade 7 in Simulated Saturated Water at 120°C

2.5.4.5   Titanium Grade 29

Titanium Grade 29 is a structural alloy owing to additions of aluminum and vanadium and thus has much higher mechanical strength and creep resistance than Titanium Grade 7. It has ruthenium as an alloying element to provide greater corrosion resistance under aggressive conditions and mitigate hydrogen uptake. However, the ruthenium is not as capable as the palladium added in Titanium Grade 7, and thus is not as corrosion resistant as Titanium Grade 7.

General corrosion of Titanium Grade 29

The passive film of Titanium Grade 29 is similar to that of Grade 7 (Andresen and Kim 2007). The corrosion rates for the two allows were also found to have negligible differences (Andresen and Kim 2007). Other researchers (Schutz 2005) noted that when exposed to chloride solutions with pH greater than 1 the corrosion rates of Titanium Grades 7 and 29 are similar, as shown in Figure 6. The NRC staff reviewed the Titanium Grade 29 general corrosion approach and found it reasonable (NRC 2011c).

Stress corrosion cracking of Titanium Grade 29

The SCC mechanism for Titanium Grade 29 is identical to that for Titanium Grade 7. As a result of additional alloying elements, Titanium Grade 29 has a much higher creep strength than Grade 7. The SCC crack initiation threshold for Titanium Grade 29 was set at 50% of the yield strength. This is based upon 6 month constant load tests under very aggressive conditions and U-bends exposed to 165°C SCW brine for over four months (SNL 2007a).

Localized corrosion of Titanium Grade 29

The localized corrosion behavior of Titanium Grade 29 is expected to be similar to Titanium Grade 7 due to similarities in the passive film. No further research is recommended at this time.

Hydride cracking of Titanium Grade 29

As discussed in regards to Titanium Grade 7, the alloying elements of palladium and ruthenium will act to reduce the amount of hydrogen uptake and increase the hydrogen critical concentration. Therefore, no research is recommended in this area at this time.

Thermal mechanical effects of Titanium Grade 29

Unlike Titanium Grade 7, Titanium Grade 29 consists of several phases and thus may be subjected to aging and phase stability issues. However, Titanium Grade 29 is a high temperature alloy and should be resistant to phase instabilities. No research is recommended at this time.

2.5.4.6   Titanium Grade 28

Titanium Grade 28 is expected to have lower corrosion resistance than Titanium Grade 7 (less palladium) and more alloying elements that would act to decrease corrosion resistance (aluminum, etc.) and have lower mechanical strength than Titanium Grade 29 less alloying elements which lead to strength (aluminum, etc.) and therefore, this material is unlikely to be used within a repository.

The only reason that Titanium Grade 28 would be used within a repository is as an intermediate weld filler material between Grade 7 and Grade 29. This should be effective at lowering hydrogen uptake from the Grade 29 to the Grade 7. Therefore, if a Titanium Grade 7/29 weld were planned, it would be prudent to conduct testing to determine if the Grade 29 helps in reducing hydrogen uptake.

No research in Titanium Grade 28 is recommended at this time.

2.5.4.7   Stainless Steels 304L and 316L

Stainless steels 304 L and 316L are possible corrosion allowance materials, and almost certainly would be used as structural members within a waste package. Both materials have been extensively studied.

General corrosion of stainless steels 304L and 316L

The materials get their corrosion resistance from chromium additions which result in a fairly adherent protective oxide film. Figure 35, Figure 36, and Figure 37 show the empirical cumulative distribution functions (ECDF) for the range of corrosion rates from numerous studies for both freshwater and hot and cold salt water (BSC 2006). As can be seen, the corrosion rates for freshwater (which includes many different well water compositions) are substantially lower than for saltwater. Therefore, knowledge of the expected environment would be extremely important for accurately modeling this material.

The general corrosion behavior of stainless steels is well understood. No further research is recommended at this time, except perhaps in support of spent fuel storage (not a subject of this section) or to gain greater understanding of corrosion products and their ability to sequester actinides. Finally, study of stainless steels may be appropriate to gain a greater understanding of the corrosion behavior of borated stainless steels (Section 2.5.4.9).

Stress corrosion cracking of stainless steels 304L and 316L

SCC of stainless steels is similar to that for the nickel based alloys and has been extensively studied. No research is recommended in this area at this time.

Localized corrosion of stainless steels 304L and 316L

Localized corrosion of stainless steels is similar to that for the nickel based alloys and has been extensively studied. No research is recommended in this area at this time.
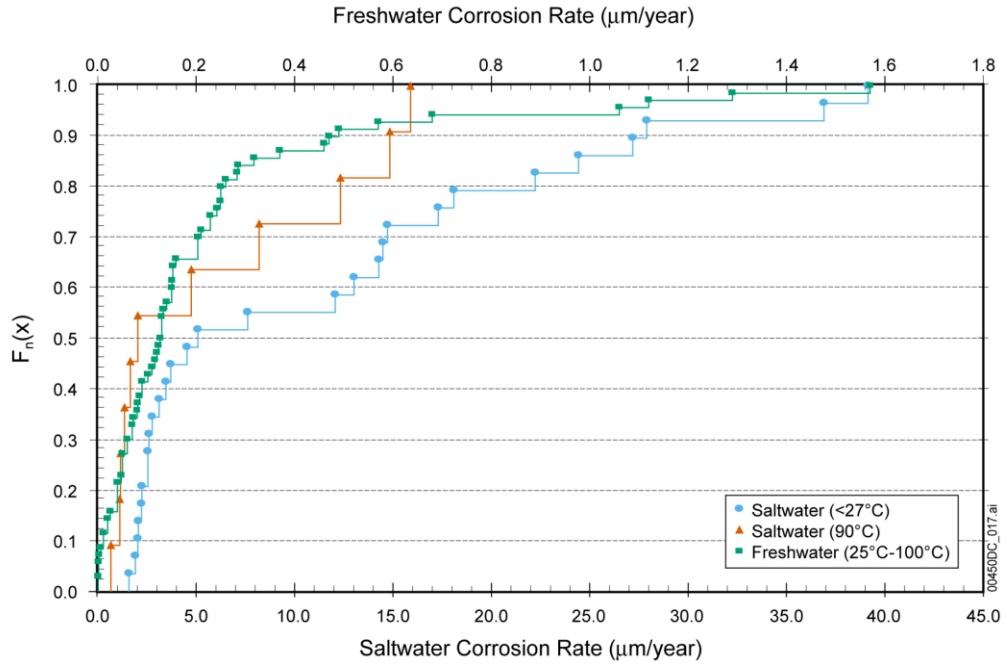
Source: BSC (2006), Figure 6-1

Figure 35.   ECDF for stainless steel types 302/304/304L in a range of freshwater and saltwater compositions
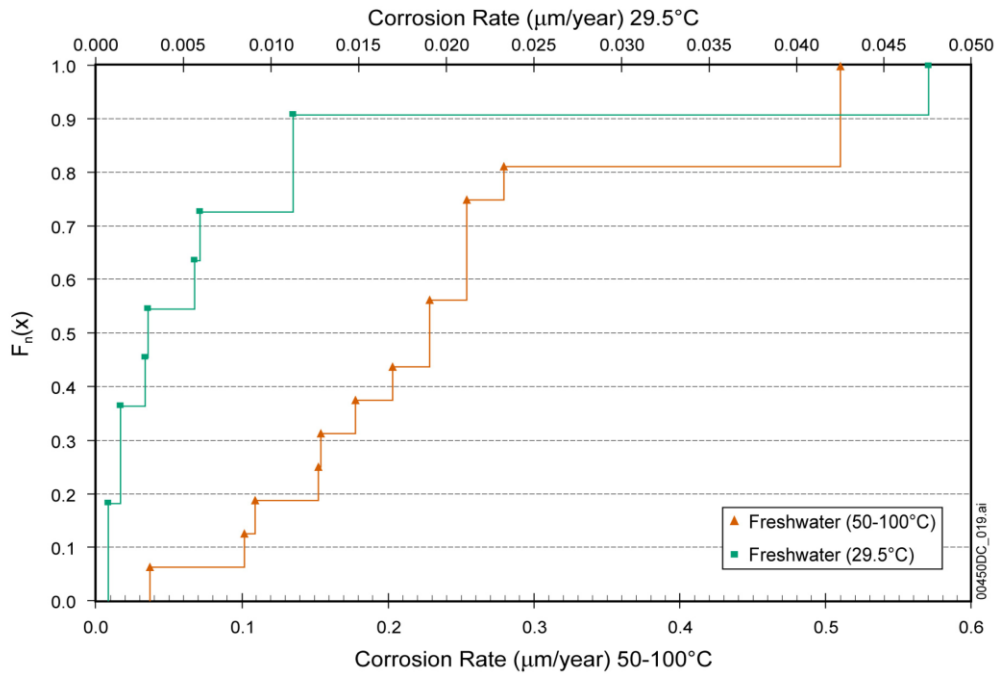
Source: BSC (2006), Figure 6-3

Figure 36.   ECDF for stainless steel types 316/316L/AM-350 in freshwater
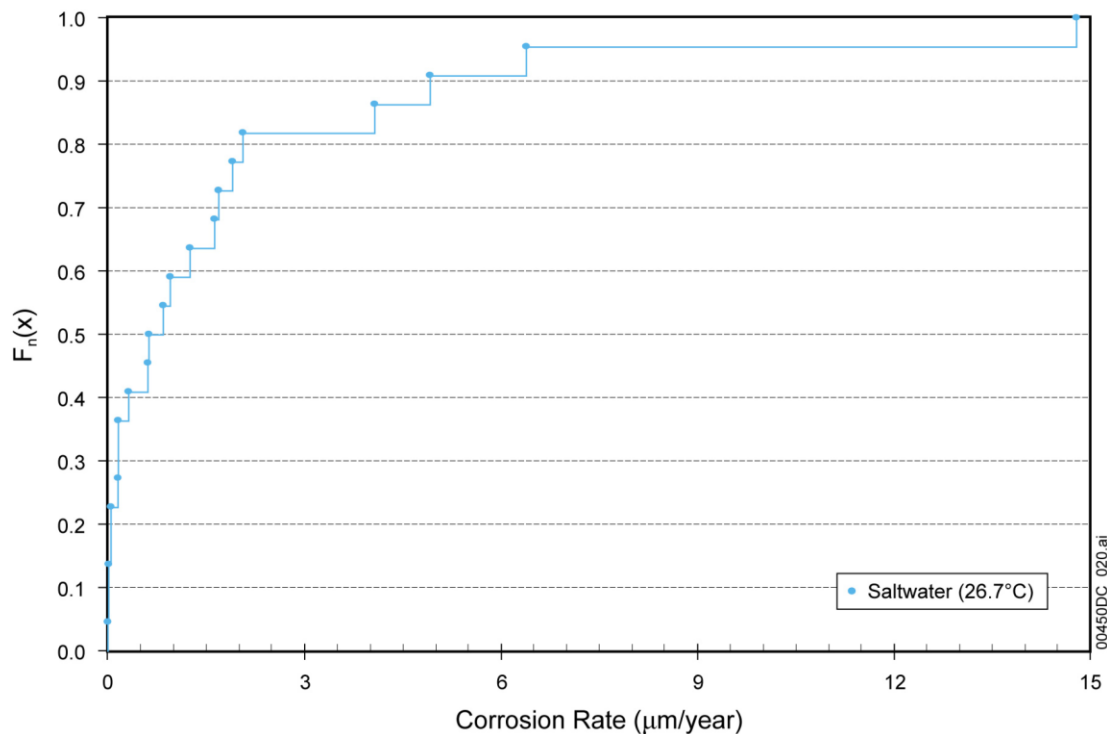
Source: BSC (2006), Figure 6-4

Figure 37.   ECDF for stainless steel types 316/316L/AM-350 in saltwater

Hydride cracking of stainless steels 304L and 316L

Hydrogen embrittlement of stainless steels may occur in aggressive environments. Data indicates essentially no change in mechanical properties of stainless steels at up to 40 ppm H (Graver 1984; Gdowski and Bullen 1988). There is no literature consensus on whether hydrogen uptake to the point of a critical threshold is possible in repository environments (Farmer et al. 1988; Gdowski and Bullen 1988). If stainless steel were considered as the waste package barrier material, this would need further investigation, but none is recommended at this time.

Thermal mechanical effects of stainless steels 304L and 316L

Due to their multi-phase nature, stainless steels may be subjected to aging and phase stability issues. Sensitization causes chromium rich carbides to precipitate from solid solution in the steel, producing chromium depleted zones around the carbides (Povich 1978). Reducing the carbon content improves the resistance to sensitization (Bullen and Gdowski 1988). Chromium carbide precipitation usually occurs in the temperature range of 500°C to 850°C, however, it is possible to occur over long periods of time at lower temperatures. One estimate states that at 200°C it would take over 4,000 years for stainless steel type 304L to become sensitized (Briant et al. 1982). As temperatures decrease, the rate of secondary phase formation drops off rapidly. Therefore, sensitization of stainless steels at repository conditions is unlikely and no further research is recommended at this time.

2.5.4.8   Alloy 825

As stated earlier, Alloy 825 is the most corrosion resistant of the corrosion allowance materials (or conversely the least corrosion resistant of the corrosion resistant alloys).

General corrosion of Alloy 825

Alloy 825 exhibits better corrosion resistance than Stainless Steels Types 304L and 316L. Alloy 825 exhibits corrosion rates of ~1 μm yr^{-1} after a 1 year exposure to 25ºC seawater, compared to 15 μm yr^{-1} for Type 304 and 36 μm yr^{-1} for Type 304 (Gdowski and Bullen 1988).

If Alloy 825 were to be considered as a candidate waste package material, it would be prudent to analyze the 9.5 year exposure samples from the LTCTF (Wall and Brown 2009).

Stress corrosion cracking of Alloy 825

The mechanism for SCC for Alloy 825 is the same as for Alloy 22. There is little data on SCC of Alloy 825 and if it were a likely waste package material, effort would be needed to establish a stress threshold under repository relevant conditions.

Localized corrosion of Alloy 825

Little data exists for localized corrosion of Alloy 825 under repository conditions and if it were a likely waste package material, effort would be needed to establish a localized corrosion model under repository relevant conditions.

Hydride cracking of Alloy 825

Hydrogen embrittlement of Alloy 825 may occur in aggressive environments. Data indicates essentially no change in mechanical properties of stainless steels at up to 40 ppm hydrogen (Graver 1984; Gdowski and Bullen 1988). There is no literature consensus on whether hydrogen uptake to the point of a critical threshold is possible in repository environments (Farmer et al. 1988; Gdowski and Bullen 1988). If stainless steel were considered as the waste package barrier material, this would need further investigation, but none is recommended at this time.

Thermal mechanical effects of Alloy 825

Similar to stainless steels Types 304L and 316L Alloy 825 could be subject to aging and phase stability issues. However, the Fe-Cr-Ni equilibrium phase diagram shows that Alloy 825 is compositionally more stable than 304L and 316L (Marshall 1984; Bullen and Gdowski 1988). No research is recommended at this time.

2.5.4.9   Borated Stainless Steels 304B4 and 304B5

Borated stainless steel plate is specified within ASTM A 887. Eight alloy types based upon 304 stainless steel with a boron addition are specified from 304B (0.2-0.29% B) to 304B7 (1.75-2.25% B). The ASTM A 887 specification does not explicitly state the manufacturing methods bus is based upon mechanical property minimums. To meet the requirements of the Grade A specifications the alloys have been manufactured by a powder metallurgy process and the Grade B materials are based on ingot metallurgy. Previous testing has shown that only the Grade A materials have sufficient corrosion resistance for disposal applications, with extensive localized corrosion occurring within fairly benign conditions (Fix et al. 2004). Also as the B content increases the corrosion rates increase rapidly and localized corrosion is more prevalent (Fix et al. 2004; Lister et al. 2007; He 2008; Lister et al. 2008). For these reasons, for the YMP Grade A 304B4 (1.1-1.2 wt% B) was specified (DOE 2008).

These materials may also be used for very long term storage, other repository conditions, and thus their study could benefit numerous possible fuel cycle alternatives.

General corrosion of borated stainless steels 304B4 and 304B5

Using expected in package conditions, corrosion rates for borated stainless steel 304B4 were measured at 27 nm yr^{-1} at 60°C, with a standard deviation of 10.1 nm yr^{-1} (Lister 2007), corrosion rates for 304B5 were found to be up of similar magnitude, except for one data point showing corrosion rates of 250 nm yr^{-1}. Considering data uncertainty and corrosion environment uncertainty, DOE established a corrosion

allowance of 2.5 mm (DOE 2008), which corresponds to a corrosion rate of approximately 9 times the average corrosion rate. This results in the necessary 6 mm thick plates (from a criticality standpoint) having to be 11 mm thick or almost twice as thick, resulting in less design freedom and greater cost.

Therefore, it is recommended that additional general corrosion studies be performed to reduce uncertainty. Furthermore, if uncertainty could be reduced, alloy 304B5 might be viable. This could increase the amount of B sufficiently that B10 enrichment would not be necessary, further reducing costs. In addition, the study of artificially aged material is recommended to determine if sensitization is likely and what its effects would be on general corrosion.

Stress corrosion cracking of borated stainless steels 304B4 and 304B5

SCC would not adversely affect the ability of the borated stainless steel to perform its functions and thus no study is warranted.

Localized corrosion of borated stainless steels 304B4 and 304B5

Additional localized corrosion research is recommended, particularly with (a) borated stainless steels in contact with other more noble waste package materials and (b) with artificially aged material to determine the effects of aging and phase stability has on localized corrosion.

Hydride cracking of borated stainless steels 304B4 and 304B5

The hydride cracking of borated stainless steels will be similar to that for stainless steel 304. Borated Stainless Steels would not serve as a structural element, and SCC would not affect the thermal neutron absorption capability. Therefore, no SCC research is recommended in this area.

Thermal mechanical effects of borated stainless steels 304B4 and 304B5

As discussed in Section 2.5.4.7, 304L is fairly susceptible to thermal sensitization. No studies of thermal sensitization of borated stainless steels have been located. Considering that the borated stainless steels could be used in storage casks, with young used fuels, prior to disposal, this issue is recommended for further research.

In-Package criticality borated stainless steels 304B4 and 304B5

Determining if the boron released from corrosion of the stainless steel remains soluble or precipitates out of solution would be of benefit to criticality analysis. Currently, it is assumed that all of the release boron leaves the package and thus would not be available to absorb neutrons in the degraded state. Carefully monitoring boron in corrosion solutions is recommended. Previous results were at best inconclusive due to experimental artifacts (Lister 2007).

2.5.4.10   Nickel Gadolinium Alloy N06464

DOE has developed a nickel alloy with gadolinium as a neutron absorber (Table 10), UNS N06464, which is specified within ASTM B932-04. Gadolinium is a more effective thermal neutron absorber than boron, and nickel alloys tend to be more corrosion resistant than stainless steels. Testing of N06464 has had mixed results with evidence that the material is somewhat susceptible to localized corrosion. This may be due in part to corrosion of the $(Ni,Cr)_5Gd$ (referred to as gadolinide) particles contained within, while the nickel matrix may remain passive (Lister et al. 2005; Mizia et al. 2005). However, the corrosion rates are fairly high (~30-500 nm yr^{-1}).

Research has shown that additional chromium (~21%) results in lower corrosion rates (Mizia et al. 2005). This could be due to chromium depletion as a result of the gadolinide particles. One advantage that Ni-Gd has over borated stainless steels is that the dissolved gadolinium will form GdF_3 and remain within the waste package to absorb thermal neutrons.

This alloy remains an interesting possibility for disposal, particularly for DOE Fuels with high enrichments. Research work for this alloy should include long term corrosion testing and determining the

corrosion rates of the Ni matrix (similar to C-4, UNS N06455) by itself to determine if the initial corrosion rates can be expected to drop as the gadolinide particles are consumed.

General corrosion of Nickel Gadolinium Alloy N06464

Long term testing of Ni-Gd has been performed in J-13 well water, a dilute groundwater from Yucca Mountain, and concentrated J-13 well water (concentrated by a factor of 50 relative to the dilute water). As expected, corrosion rates dropped with increasing time (Figure 38), particularly for the more relevant J-13 environment (Mizia et al. 2005) (note: general corrosion rates would be expected to be lower for the 21% Cr variant). Scanning electron microscopy examination showed preferential corrosion of the surface exposed gadolinides.

Stress corrosion cracking of Nickel Gadolinium Alloy N06464

As a neutron absorber, SCC would not affect the ability of Ni-Gd to perform its function and thus study of SCC is not recommended.

Localized corrosion of Nickel Gadolinium Alloy N06464

As discussed earlier, the localized corrosion behavior of the Ni-Gd alloy is complicated by the preferential corrosion of the gadolinide particles. A study where these particles were dissolved away through acid etching, followed by potentiodynamic scanning could shed light on whether the localized corrosion behavior of the matrix (which would dominate in the long-term) would be beneficial.

Hydride cracking of Nickel Gadolinium Alloy N06464

Nickel based alloys are essentially immune (particularly for repository relevant conditions) to hydride cracking and thus no research is needed in this area.

Thermal mechanical effects of Nickel Gadolinium Alloy N06464

The long term aging and phase stability of the Ni-Gd will be similar to its matrix composition, which is similar to Alloy C-4.

In-Package criticality Nickel Gadolinium Alloy N06464

Research should be performed to determine that the gadolinium coats nearby surfaces and does not remain within solution where it would be free to leave the waste package and thus not offer effective neutron absorption.
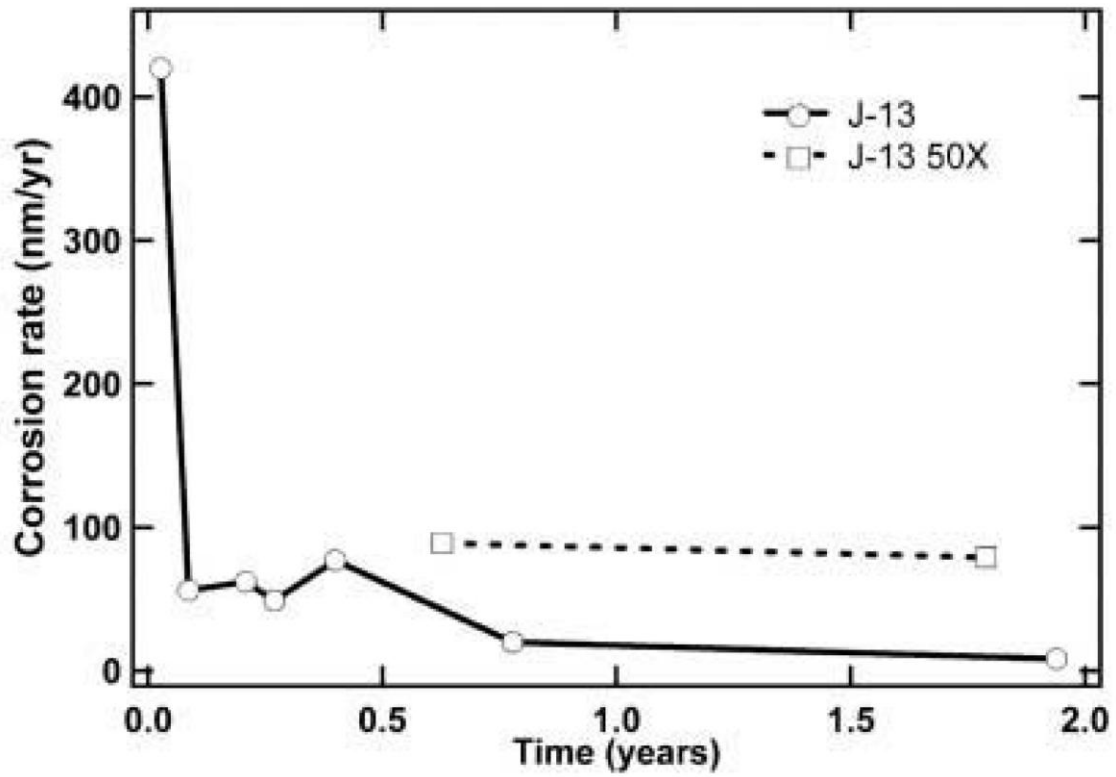
Source: Mizia et al. (2005), Figure 10

Figure 38.   Average corrosion rate for three Ni-Gd (15% Cr) specimens immersed in J-13 and J-13 50X solutions at 30°C

2.6   Deep Borehole Disposal

2.6.1   Introduction

The focus of this chapter is on the role of engineered materials under conditions relevant to deep borehole disposal (DBD) of nuclear waste. More specifically, this chapter is focused on the materials in the down hole environment; little is said with respect to the materials used to seal the well. The overall role of engineered materials in the DBD environment is significantly diminished relative to shallow geologic repository environments. The major barrier to radionuclide release and migration is depth and geology, while the materials used are far more critical in waste emplacement. There are few performance assessment type studies for DBD, and those that do exist range from simple diffusion equations to complex thermally driven water upwelling (Brady et al. 2009; Swift et al. 2011). However, in all of them, instantaneous failure of the waste package is assumed. No credit is taken for radionuclide containment or retardation because of the presence of the canister, casing or other materials present. Despite this, radionuclide release to the biosphere has been calculated to be orders of magnitude below even drinking water standards at the 10^6 year timeframe. More complex models that take into account material properties may give a different outcome, but as long as the materials do not in some way enhance the migration of radionuclides, it appears that the materials themselves do not need to be designed to specifically retard radionuclides.

This chapter starts with general background (Section 2.6.2) delineating what is known about the upper crust environment. Section 2.6.3 will introduce a conceptual model of the waste disposal environment, highlighting the role of engineered materials. Section 2.6.4 will discuss conceptual models for disposal variations on the DBD theme and the role of materials under each of these conditions. Section 2.6.5 is a summary of what has been presented and also contains some ideas for substantive forward movement in understanding the behavior of materials in DBD.

2.6.2   Background

DBD represents a significantly different conceptual model from other major proposed methods to dispose of nuclear waste. Most of the other disposal methods rely on a mined repository, forcing the repository to be in relatively shallow (<1000 m) geologically stable formations. It also forces repository design to encompass a large mined gallery into which the waste can be emplaced. Thus, large amounts of nuclear waste will be geologically entombed in a single location. DBD breaks with many of these design features. The basic conceptual model for DBD is to drill a deep borehole (3-5km) large enough for a string of waste canisters/packages approximately 1-2 km long. The canisters will be placed in the lower 1-2 km of the hole in crystalline basement rock (typically granite), and the remaining 2-3km shaft will be sealed with one or several materials including clay, asphalt, and/or cement (NIREX 2004). The minimum diameter varies, but is often dictated both by drilling technology and the size of nuclear fuel assemblies currently in use; the down hole diameter is typically in the range of 0.2-0.75 m and the surface diameter is approximately 1.5 m (Anderson 2004; Hoag 2006). It has been estimated that disposal of the entire US inventory of nuclear waste would require about 950 boreholes (Brady et al. 2009).

The radically different design of DBD opens a range of possibilities with respect to waste disposition. For example, DBD is semi-modular in nature. Instead of having a large single gallery, there can be many galleries much nearer to the point of production. This is advantageous from an environmental justice perspective in that the location of waste production may also be the location of waste disposal. Thus, those who benefit from nuclear energy must also bear the risk of waste release. It is also advantageous from a financial perspective in that the cost of disposal scales linearly with the amount of waste produced (Brady et al. 2009). And finally, in the ideal situation, waste transportation could be eliminated through the construction of an on-site waste handling plant. The waste would be produced in a reactor, stored for a pre-defined amount of time, and then emplaced in the deep borehole. Despite all of these arguments for DBD, much remains to be learned about the deep earth environment.

Although the DBD concept has been considered for decades, cost limitations have minimized experimental or directly applied work to characterize this disposal method compared to mined geologic repositories. To date there are approximately two dozen wells with readily available data that have been drilled to >2km as part of fundamental geologic research, geothermal or petroleum exploration, and nuclear waste disposal research. The information gleaned from these wells presents the following basic conceptual model of the upper crust (Juhlin and Sandstedt 1989; NIREX 2004; Sapiie and Driscoll 2009). From 0-1000 m depth, the lithology is dominated by relatively highly permeable rocks with a large degree of connection to meteoric waters. At greater depths, the rock becomes increasingly impermeable and the water becomes increasingly more saline leading to density stratification and separation from the surface. This general conceptual model has also been split into three distinct zones based on the salt concentration, thermal gradients and circulation rate of the pore water (NEDRA 1992). In Zone I, which can extend to 1-2 km below ground surface, the water is relatively fresh (50-60g L^{-1}) and continuously in contact with atmospheric waters (circulation rate ~10^4 years). The geothermal gradient is minimal. Zone II is transitional between Zones I and III. The upper reaches of Zone II are relatively well connected with Zone I, although the circulation rate is considerably slower than that of Zone I (~10^4-10^5 years). The lower reaches of Zone II are connected to Zone III, but the overall circulation rate between these two zones is extremely low. Zone II has salt concentrations in the range of 50-200 g L^{-1} which correlate with depth, and a geothermal gradient that also increases with depth. Zone III has salt concentrations >200 g L^{-1} and is characterized by little to no circulation of water due to exceedingly low permeability (circulation rate >10^5 years; permeability = 10^{-16} to 10^{-20} m^2) and density stratification. The geothermal gradient is essentially constant. This upper crust conceptual model is fairly basic and approximate due to the limited number of usable data points. However, even with the small number of data points, a fair amount of variability has been observed.

From a performance assessment perspective, the variability that has been observed creates a wide range of geochemical conditions which would need to be considered in waste disposal (Juhlin and Sandstedt 1989). For example, the temperature gradient in the experimental wells ranges from 13-90ºC km^{-1}. This translates to ambient temperatures ranging from about 60ºC at 3000m in well USA-11 to 204ºC at 2287 m in well USA-9. This large range in values in known wells, and the inability to predict local thermal gradients in new wells, means that corrosion data needs to be collected at a correspondingly large range of values. Another source of variability is the depth to highly saline water. This depth ranges from 1200 m (URS-1) to >6000 m (SWE-1). While the SWE-1 well appears to be an outlier having a TDS of only ~50g L^{-1} at depth (average depth to highly saline water ignoring SWE-1 = 2205 m, n=5), this does define a broad range of salinity in which the waste may be emplaced.

2.6.3   Conceptual Model of Waste Disposal Environment

Figure 39 shows a cartoon diagram representative of the waste environment in a semi-cross-sectional view. In the figure, the waste, in this case a fuel rod assembly, is placed inside a waste canister. The waste canister is filled with infill material. The canister itself is placed in the borehole, and is immediately surrounded with an outfill material. The outfill is between the canister and the casing, the casing is surrounded by well grout, and the well grout is in contact with the host rock formation. This diagram divides into two groups of material, engineered and natural or semi-natural. The engineered materials include the waste/fuel rods, the infill, the canister, and the casing. These engineered materials are all assumed to be designed with the goal of waste containment. The natural or semi-natural materials include the outfill, the grout and the host rock. The outfill will most likely be some sort of drilling mud used to maintain lithostatic pressure while drilling. Well grout generally takes the form of either pure forms or mixtures of cement and clay. Although it cannot be ruled out entirely, it is assumed that the natural materials used will not be engineered for waste isolation purposes, thus the material properties are determined by the natural state of the material. Though the natural materials are considered to have innate, non-engineered properties, they do interact with engineered materials. In Figure 39, there are six
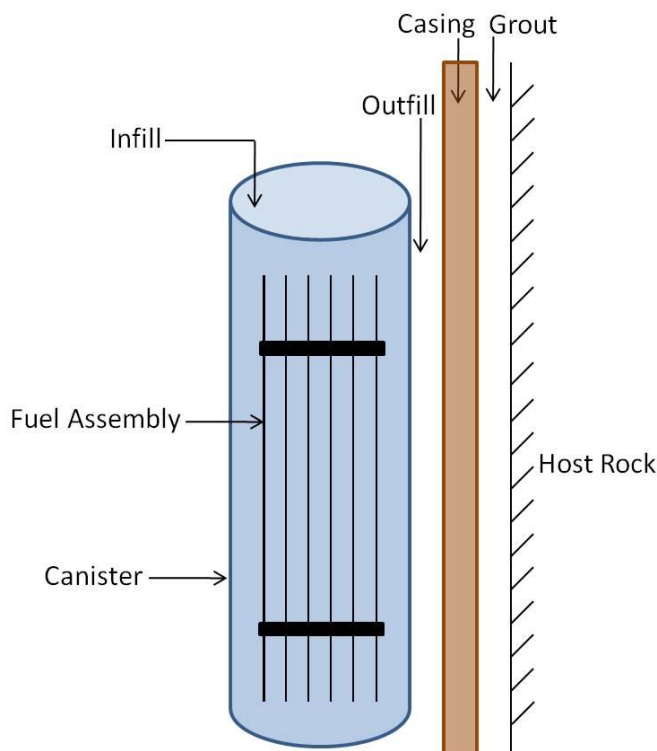
Figure 39.   Cartoon diagram of the waste disposal environment in a deep borehole

boundaries of concern between materials: 1. Waste/Infill, 2. Infill/Canister, 3. Canister/Outfill, 4. Outfill/Casing, 5. Casing/Grout, and 6. Grout/Host Rock.

This basic introduction to the materials present in the downhole environment allows for the generic desired characteristics of each material to be defined. The characteristics are summarized in Table 35. These characteristics are generic in the sense that they are consistent with the general conceptual model for disposal presented, and they do not account for the variations of DBD discussed in more detail in the following section. In the more specific disposal scenarios discussed below, the applicability of each of the desired characteristics becomes more conditional. However, this list of characteristics does have many items in common with shallow repository disposal methods. Resistance to thermal and radiation damage is universal in nuclear waste disposal, as is some level of reduced water flow and high retention of radionuclides. Because of these commonalities, much is already known with respect to materials' behavior in waste disposal scenarios. Some of this information will transfer directly to DBD, while certain conditions will require a reconsideration of the available information.

The conditions unique to DBD disposal compared to most shallow mined repository designs include: a consistently saturated, chemically reducing groundwater environment, very high TDS values (up to 350 g L^{-1}), the potential for a higher range of temperatures, and finally the presence of certain materials which would not be present in a shallow repository including the infill, outfill, casing and grout. Each of these issues will be considered in turn.

Table 35.   Desired properties of the natural and engineered materials in DBD

Material	Engineered/Natural	Desired Characteristics
Fuel Rods/Waste	Engineered	• Fuel rods: Design based on reactor core considerations • Fuel Rods/Waste: Waste form to minimize radionuclide release rates • Minimal damage from dynamic thermal/radiation sources
Infill	Engineered	• High degree of compressive strength • Some level of radiation shielding for above ground waste handling • Some level of radionuclide retention capability • Minimal damage from dynamic thermal/radiation sources
Canister	Engineered	• High resistance to cracking/deformation during emplacement • Low corrosion rates in high salt solutions (up to 350g L^{-1}) • Minimal damage from dynamic thermal/radiation sources • Some level of radionuclide retention capability
Outfill	Natural	• Drill bit cooling and lubrication while drilling • Removal of drill cuttings during drilling • Lubrication between canisters and casing during canister emplacement • Cushion between canisters once emplaced • Some level of radionuclide retention capability • Low permeability once waste is emplaced • Forms a water tight seal between canister and casing
Casing	Engineered	• Smooth internal surface for canister delivery • Sufficient strength to maintain borehole integrity • Minimal damage from dynamic thermal/radiation sources • Low corrosion rates in high salt solutions (up to 350g L^{-1})
Grout	Engineered/Natural	• Maintain a water tight seal between the casing and the host rock • Some level of radionuclide retention capability • Locally reduce the permeability of the host rock through pore plugging and cementation • Minimal damage from dynamic thermal/radiation sources
Host Rock	Natural	• Low permeability • Minimal damage from dynamic thermal/radiation sources • Some level of radionuclide retention capability

The Swedish nuclear waste program has long considered the emplacement of waste in a saturated granite environment; they have decided to use copper metal canisters to contain the waste. Other international designs have ranged from emplacement in the vadose zone (Yucca Mountain, USA) to the emplacement of the waste in a clay formation (Boom Clay, Mol site, Belgium). In many of these site types, the total amount of water is somewhat restricted, and heat produced from radiodecay is sufficient to dessicate the local environment sometimes for several hundred years (Landolt et al. 2009). In the DBD concept, the temperatures can be much higher, but the intense pressure at multi-kilometer depths is sufficient to maintain liquid water in contact with the waste canister. This constantly saturated environment reduces the prevalence of certain types of corrosion (e.g., deliquescence) while exacerbating others (e.g., chloride based stress corrosion cracking).

Another characteristic is the exceedingly high TDS values. With the exception of the SWE-1 well mentioned in the previous section, all other deep boreholes drilled to date eventually encounter highly saline water with TDS values of >200 g L^{-1}. Exact water compositions are not clear and may vary from well to well, but it can be surmised that there are appreciable amounts of sodium, calcium, and chloride. The chloride is especially problematic as there are many corrosion pathways that are caused or enhanced by chloride. While troubling, these large chloride concentrations are similar to those found in brine inclusions in salt beds and domes. Since many countries have considered salt based disposal, there are significant amounts of data on corrosion rates in such an environment.

The final defining characteristic of DBD which is not present in shallow mined repositories is the higher range of expected temperatures. As mentioned previously, ambient temperatures down hole may be as high as 200ºC. Performance assessment style calculations have shown temperature increases over ambient (110ºC) of 120ºC for vitrified high level waste, and 30ºC for spent fuel (Brady et al. 2009). So even in boreholes with non-extreme ambient temperatures, the decay heat can drive system temperatures much higher than is generally expected in shallower repositories. For comparison, at Yucca Mountain, both 'cold' and 'hot' designs have been put forward. The maximum predicted temperatures of the waste packages themselves in the 'hot' scenario have been calculated to be ~180^{0}C (Buscheck et al. 2003). The maximum temperatures in the surrounding waste gallery and rock would be considerably lower but are still anticipated to be >100ºC.

DBD is somewhat unique due to these three, co-occurring aqueous conditions which would probably not be present in shallow repositories. While pieces of information may exist to address each of the aqueous conditions in turn, these pieces may not combine to accurately describe material behaviors under conditions when all three pieces are present. Corrosion studies are needed on the materials of interest where all three of these conditions are present. Many such studies already exist (e.g., Braithwaite and Molecke 1980; Nagies and Heusler 1998; Wang et al. 2001); however, the focus in these studies is generally on a material for a waste canister. While useful in DBD design, there is also a need for information on the other materials associated with DBD such as the drill casing, the outfill, and the grout materials. If the casing is being relied upon for radionuclide containment, then either the corrosion rate of the casing needs to be known, or the casing must be made out of a previously developed corrosion resistant alloy. The ability to make casing out of a previously developed alloy depends on the structural properties of the alloys themselves.

The other major difference between DBD and shallow repositories is the presence of interfaces between materials unique to DBD relative to shallow repositories. The most notable of these interfaces are at the canister/infill, canister/outfill, outfill/casing, and casing/grout interfaces. These boundaries are of interest due to the fact that they include the engineered materials and represent the only tunable materials present. Possible infill materials that have been proposed include: metallic lead or lead alloy (Gibb et al. 2008), graphite, silicon carbide, and boron carbide (Hoag 2006). The major required characteristic of the infill is compressive strength, and secondary characteristics are thermal and radiation shielding properties to minimize energy transfer from the waste. The infill will be in direct contact with the waste on the inside, and the canister on the outside. The outfill material will most likely be a drilling mud consisting of a bentonite slurry. This is standard practice in current oil well drilling technology (Bram et al. 1995). Because clays have applications in almost any nuclear waste repository, and the common use of drilling mud in drilling wells, data abounds on clay interactions with engineered materials and on the corrosion susceptibility at clay boundaries. Similarly, the grout material is typically a mixture of clay and/or cement and is an industry standard. Thus, the major boundaries that are unique to DBD mostly involve the infill. It is currently unknown what this material will be. An additional secondary design constraint may be corrosion resistance at the waste/infill and infill/canister boundaries.

To this point, this chapter has focused on the desired design constraints of materials present in a generic DBD repository. In the following section, more advanced DBD scenarios will be considered. The

advanced scenarios center on whether there are plans for waste retrieval, and whether melting of the surrounding waste emplacement zone is feasible/desired.

2.6.4   Advanced Deep Borehole Disposal Considerations

Current legislation in the US requires that nuclear waste be retrievable. It also names Yucca Mountain as the only possible civil nuclear waste disposal site. For DBD to be implemented, dramatic shifts in nuclear waste policy are needed. From a design perspective, the assumption of major changes in policy allows for the consideration of non-retrieval based scenarios. DBD then breaks down into the three major designs shown in Table 36. These include: retrieval based DBD, permanent disposal/non-melting, and permanent disposal/melting. These three separate methods may have separate application as the waste stream changes. For example in retrieval based wells, un-processed spent fuel could be emplaced. As re-processing of nuclear fuels advances, this waste could be retrieved to be re-processed instead of finding virgin material. For wastes coming from re-processing, especially separated fission products, there is no predicted practical need for these materials. Permanent disposal may be the best option due to the simpler design of one time disposal and sequestration. Rock melting scenarios are only applicable to high heat producing waste, and it may offer added protection from release. It may also allow for added protection from proliferation concerns by making the waste even more isolated and difficult to recover.

Table 36.   Materials considerations from advanced DBD conceptual models

Conceptual Model	Conditions	Unknowns
Retrieval Scenario	1. Melting options not valid 2. Casing must be left in place 3. Casing must have minimal corrosion rates to maintain hole integrity 4. Canister must have minimal corrosion rates 5. Canister must be able to travel up and down well casing without rupture even after being exposed to a corrosive environment	1. How long will waste be recoverable? 2. Will canister and casing co-corrode into a single non-retrievable mass? 3. Consistently saturated, high salt and temperature combined corrosion rates
Permanent Disposal/Non-Melting	1. Casing may or may not be left 2. Canister can be less robust, traveling only down hole.	1. Does the casing present a preferential flowpath or does it offer a protective effect? 2. Are the financial savings on less robust canisters worth the risk of earlier release? 3. Should the sealing material change based on disposal conceptual model?
Permanent Disposal/Melting	1. Casing will most likely be removed 2. Canister may or may not survive the melting process 3. Special materials may need to be developed to achieve a certain melting/solidification regime	1. Is melting necessary to ensure waste segregation? 2. Mechanical properties of metal/rock melt mixtures 3. Corrosion properties of metal/rock melt mixtures 4. General nature of special melting materials

As each of these different models is considered, it changes the general disposal environment shown in Figure 39. For the retrieval scenario, the figure remains as is. For the permanent disposal/non-melting scenario, the casing may be removed and if there is no casing, there is no need for grout. So the outfill will most likely be in direct contact with the host rock. For the permanent disposal/melting model, Figure 1 nearly loses relevance completely. Using a previously defined conceptual model (Gibb 2000) melting based disposal is described by concentric circles surrounding the waste emplacement zone. Moving out from the waste package, there exists a zone of partially melted and eventually re-crystallized host rock, a zone of sub-solidus metamorphic re-crystallization, a zone of hydration reactions leading to fracture filling precipitation, and the final zone is that of unaltered host rock. In the Gibb model, the canister survives the 800-900°C required, but the well casing would have been removed. In other models, the temperature is too high for canister survival. In still other models, the area immediately surrounding the waste is filled with a non-granitic material with a much lower melting point (Gibb et al. 2008). This allows for lower temperatures to achieve nearly the same entombment, but creates a boundary between the non-granitic material (potentially lead or lead alloys) and the host rock. Predicting behavior in each of these melting scenarios is quite difficult given the range of materials and boundaries potentially involved. However, if it works as envisioned the combined aspects of localized waste entombment and larger scale geologic seclusion may represent the most conservative isolation method conceivable for continental disposal.

2.6.5   Perspectives

As mentioned in the introduction, no performance assessment type of calculations which have been performed to date show significant releases to the biosphere from DBD. The most elaborate of these includes thermally driven water upwelling directly back up the drill shaft (Brady et al. 2009). Flow is impeded in the drill shaft by a bentonite/asphalt/cement seal, and flow is only significant for the first 10,000 years. When the thermal upwelling model is connected to a groundwater pumping model, where the groundwater is being pumped at the ground surface from a location over the borehole and is used as a drinking water source, the total peak dose occurs at 8,200 years and is 1.42×10^{-10} mrem yr^{-1} caused exclusively by ^{129}I. The model as presented assumes instantaneous dissolution of waste within the container, an intact but sealed borehole, and does not account for radionuclide sorption or decay during migration. Correspondingly long particle travel times were also found in a separate modeling study with a much finer discretization (Marsic et al. 2006). While more modeling studies are needed with a wider array of conditions, these preliminary studies suggest that the role of the downhole materials in radionuclide segregation from the biosphere is somewhat limited.

In order to further constrain the type of materials which lead to the highest degree of segregation, future modeling studies need to focus on the role of materials in disposal scenarios. For example, are there any conditions where material behavior can increase the permeability of the overlying seal? Reactions at boundaries between the casing and well grout or seal material may lead to preferential flow paths along either the outer or inner boundary of the casing. Information gained from such a study would likely inform many of the questions in Table 2 regarding whether the casing should be left, and thus whether retrieval is feasible or not. Another example is to model how the release would change assuming some level of containment within the canister or the deep well environment. Despite data gaps, usable data exists to give bounding estimates on corrosion rates in a DBD environment, which would in turn give a generalized picture of how corrosion rates relate to radionuclide release to the biosphere. High level modeling studies such as these may lead to a more enlightened experimental path forward. In the end, the conservative nature of nuclear waste disposal may well require corrosion resistant materials for the DBD environment regardless what performance assessments may dictate. Due to much of the overlap between the materials involved and the partial overlap of many geochemical conditions in both shallow and deep disposal environments, there already exists a large database to draw from when considering materials for DBD. The major challenges remain understanding and describing materials behavior in an environment

where there are several co-occurring conditions which may exacerbate corrosion pathways for long periods of time.

In shallow repositories the traditional role for materials in terms of long term sequestration is related to the corrosion of the canister and waste packages. In DBD, if the performance assessments completed to date can be believed, the risk profile once the waste is emplaced is dramatically low. However, during emplacement the risk profile spikes as the risk of a canister breaking, getting stuck, or being dropped down hole is at its highest. During drilling, down hole losses of drilling materials are common and can require a re-direct of the hole trajectory (Bram et al. 1995). With the exception of drill parts and other small instrumentation, very few items are routinely placed at depth in deep boreholes. Thus the behavior of both well materials and waste canisters as hundreds of canisters are placed down hole is completely unknown. Canister design largely focuses on the static characteristics once the waste is emplaced (Hoag 2006), but another important design criteria is material resistance to the dynamic stresses and strains caused during down hole emplacement. As the canister is lowered, there will undoubtedly be repeated scratching, indentations, and other deformities caused by the interaction between the casing and the canister. Will this have an effect on the down hole canister behavior? Is there any way to predict canister behavior downhole based on a random distribution of imperfections? Do interactions of imperfections between the well casing and the canister increase the probability of a canister getting stuck, and if so, how can this risk be managed? Both experimental and modeling work could start on this topic immediately. Well casing and drilling materials are well constrained by oil industry experience and as a first order consideration the canister materials will most likely be similar if not identical to the canisters in other repositories, including: steel, copper, zirc-alloy, or possibly titanium (SKB 1993). Understanding canister/casing interactions during emplacement will be critical to waste emplacement strategies as well as overall risk profiles of DBD. The uniqueness of the DBD environment also means a unique delivery system. The role of materials in this system and the overall effect on the risk profile have yet to be considered.

Despite the longevity of the DBD idea, it remains dramatically understudied relative to the shallow repository designs. While there is plenty of room for more mechanistic understanding of corrosion processes, conceptual models of DBD are still far too simplistic and generalized to incorporate them. Thus for a first step, a broader range of DBD conceptual models need to be developed and evaluated to better constrain the role of materials in such a disposal system. As this occurs, the level of corrosion resistance and other design criteria required will become clearer, and then a re-consideration of available materials can begin.

2.7   Interim storage

2.7.1   Introduction

This section summarizes the results of the initial dry storage knowledge gap analysis performed in FY11 (Hanson et al. 2011) to identify data and modeling needs for developing the desired technical bases to enable the extended storage of used nuclear fuel (UNF) (UNF becomes SNF once it is determined that it will not be recycled and is of no further value). The aforementioned report dealt with all aspects of a dry storage installation, including the fuel and support structure, as well as the container and (if present) overpack used to maintain confinement of the spent nuclear fuel. In this document, only the issues specific to the engineered barriers – in this case the container/storage cask along with the overpack (if present) are addressed. While a wide variety of issues were identified for both the container and the overpack, the only summaries presented in this document are for those research areas whose importance towards licensing was determined to be high or medium in Hanson et al. (2011). Areas determined to be of low priority will be mentioned in tables, but the discussion in the parent report will not be summarized here. The reader is directed to the parent report for additional discussion on the topics covered here, as well as any concerns involving the actual spent nuclear fuel, storage baskets, channels, neutron poisons, etc.

Until a disposition pathway, either recycling or geologic disposal, is chosen and implemented, the storage periods for UNF will likely be longer than were originally intended. The ability of the important-to-safety structures, systems, and components (SSCs) to continue to meet safety functions over extended times must be determined. In addition, it needs to be determined if these SSCs can also meet applicable safety functions when the used nuclear fuel is transported to its final location.

Without an operating repository, centralized storage facility, or reprocessing facility, the commercial nuclear industry has been actively pursuing dry storage to meet its fuel storage needs. Because dry storage systems are designed to allow passive cooling, their overall cost and maintenance are expected to be less than the cost and maintenance for an additional pool. Dry storage systems include the necessary SSCs to facilitate loading, maintain an inert environment, ensure eventual retrieval, and, for dual-purpose systems, enable transportation of used nuclear fuel. Dry storage systems include an overpack, container, and fuel basket SSCs to meet safety required safety functions. A concrete or metal overpack provides protection for a welded or bolted confinement barrier from environmental conditions and natural phenomena. The overpack also provides radiation shielding. The container consists of a welded or bolted confinement barrier that prevents release of radioactive material and maintains an inert atmosphere. Finally, fuel baskets, including fixed neutron poisons, hold the fuel assemblies in a set geometry to facilitate loading and retrieval of used nuclear fuel, transfer heat, and maintain subcriticality.

Dry storage systems were originally designed for a 20-year period. Although, three independent spent fuel storage installations (ISFSIs) and associated dry storage systems were granted license extensions for an additional 40 years, other ISFSIs and storage systems may not receive similar extensions. Many site-specific factors including environmental conditions (e.g., marine environments) and natural phenomena (e.g., seismicity) could impact the performance of the dry storage systems such that extensions may be more limited. With extended dry storage beyond 60 years, demonstrating continued efficacy of the various SSCs of dry storage systems becomes challenging.

Some of the storage systems were designed to serve a dual purpose of storage and transportation. However, transportation of these systems after a period of storage is required to be licensed separately to demonstrate compliance with applicable transportation safety requirements. To meet transportation confinement and subcriticality requirements, the used nuclear fuel, fuel baskets, neutron poisons, and the confinement barrier for transportable storage casks must remain intact during normal conditions of transport and hypothetical accident conditions. Although alternative transportation approaches and safety

bases may be pursued to demonstrate subcriticality, such as moderator exclusion, there are regulatory and technical hurdles that must be overcome before they can be adopted.

The purpose of this study is to identify data gaps associated with the extended storage capability of the container and overpack in DCSSs. This evaluation focuses on determining the conditions that could potentially lead to failure of dry storage SSCs and the material and structural properties of these SSCs as a function of storage conditions. Thermal performance, radiological protection, confinement, subcriticality, and retrievability safety functions are analyzed for both the container and overpack. A literature review and degradation mechanism analysis is used as the basis for prioritizing additional research and development in the identified areas.

2.7.2   Background

The container is the primary confinement component of the DCSS. It provides a physical barrier to prevent release of radionuclides, maintains an inert atmosphere of helium for the container internals to prevent chemical degradation and enhance heat transfer, and prevents ingress of moderator (water) to provide additional criticality protection. There are two generic types of storage confinement containers currently in use—bolted metal casks and welded metal canisters. Currently, 13% of the storage containers in use are the bolted direct-load casks and 87% are welded steel canisters. There are a number of key differences between the two varieties of storage systems. Welded canisters are stored or transported within a separate, air-ventilated overpack that provides both neutron shielding and physical protection. In contrast, bolted direct-load casks have integral gamma and neutron shielding with a thick metal body and polymer–resin neutron shields. The bolted direct-load casks are mechanically sealed via a combination of lids, bolts, and physical seals (e.g., gaskets to maintain the pressure boundaries). In addition, a weather cover is positioned over the bolts and seals to protect them from rainwater. The older bolted casts were thick-walled vessels (10 to 12 inches thick) made of a variety of ferrous alloys including nodular cast iron, carbon steel, and low-alloy steel, while the more recent welded canisters have been constructed with stainless steels.

The external environment to which the container is exposed will impact its long-term performance. In marine environments, the chloride-containing atmospheric aerosols that are ubiquitous under such conditions, combined with high relative humidity levels, can lead to corrosion of the container itself, along with the sealing system (i.e., welds, bolts, or metallic seals). Localized corrosion (i.e., pitting or crevice corrosion) may take place whenever sufficient moisture and contamination are present. In addition, in locations where dissimilar metals are in contact, such as where a metallic seal contacts the container body or lid, galvanic corrosion could potentially take place. In regions where sufficient stress is present, such as within bolts or in the heat-affected zone around welds, SCC may take place. In all cases, the actual corrosion mechanisms, if any, that become active will be dictated by the environment and the materials under consideration. The potential impact of corrosion on a storage container will be controlled by the operative corrosion mechanisms over the period of performance of the storage system as well as the period over which they occur.

While the container is the primary confinement component of the dry cask storage system, it is housed within an overpack or storage module, typically constructed of steel-reinforced concrete. As a result, although the overpack or storage module does not provide primary containment of used nuclear fuel, it does dictate the environment to which the storage container is exposed. Understanding the aging characteristics of the storage module is a critical factor in determining the long-term performance of a DCSS as it defines the container environment.

There are many different dry cask storage systems, and most fall into two main categories based on how they are loaded. The first is the bare fuel, or direct-load cask, where the UNF assemblies are loaded directly into a basket that is integrated into the cask. The second is the canister-based system, in which UNF assemblies are loaded into a basket inside a relatively thin-walled cylinder (canister) that is contained within a transfer cask before it is transferred into a storage overpack. A second characterizing

feature is whether the closure system (for confinement barrier) is bolted or welded. Direct-load casks are generally bolted. For canister-based systems, the canister is welded but is placed in a concrete or a bolted overpack. Cask systems can also be categorized as to whether their main shielding is metal or concrete. Bare fuel casks tend to be all metal casks that are stored vertically. Canister-based systems can have the canister go into either a metal or a concrete overpack.

Another means of characterizing dry cask storage systems is whether they are licensed for storage only or for storage and transportation. Casks licensed for both are generally referred to as dual-purpose casks, and canisters intended for both storage and transportation are referred to as dual purpose canisters (DPCs). Some vendors refer to their DPCs as multi-purpose canisters (MPCs). Under the Yucca Mountain Project (YMP), a true MPC was designed to store, transport, and dispose of the fuel. Canister-based systems that are considered dual-purpose usually have different overpacks for loading, storage, and transportation. Throughout this document, DPC and MPC may refer to both casks and canisters.

Bare fuel casks are placed into the spent fuel pool for loading. Once loaded, the bare fuel cask is sealed and lifted out of the pool. Water is removed through a drain tube, the outer surfaces are decontaminated, and the cask is then transferred to the drying location. For the canister-based systems, the empty canister is loaded into the transfer cask and the two are lowered into the spent fuel pool for loading. Once loaded, the canister and cask are removed from the pool and the water is drained enough to weld the top onto the canister. Like the bare fuel casks, the system is then drained, decontaminated and dried. Most systems use vacuum drying (e.g., (ASTM.C1553-08 2008)) in which the decay heat of the fuel is used to help drive off water. Other systems, such as some of the Holtec International systems, use a flow of dry helium to remove residual water. The vacuum drying process often produces the highest cladding temperatures experienced during the dry storage process, and NRC guidance limits the peak clad temperature to 400°C under normal conditions (NRC 2010) to meet the regulations in 10 CFR 72.122. When vacuum drying is complete, the cask is then transported to the storage location. In the case of a canister system, the canister is transferred from the transfer cask into the storage overpack. While the majority of dry storage modules are above ground, some are designed for underground storage.

Modern cask systems are designed to hold about 10 to 15 metric ton of UNF, equivalent to about 32 PWR assemblies or 68 BWR assemblies. As a means of cost savings, the trend has been to increase the size of casks to hold more fuel. Because a typical assembly is about 12–15 feet long (without considering control components), the dry casks are about 15–19 feet high and 8 feet in diameter. When fully loaded and dried, casks generally weigh between 100 to 120 tons. The quantity of welded and bolted containers in use as of May 2011 (StoreFUEL 2011) is shown in Table 37. As illustrated in Figure 40, while dry storage installations are either presently located, or currently planned throughout the country, a large number of them are located in close proximity to the coast. Due to the abundance of chloride-containing aerosols produced by the marine environment, a significant quantity of aggressive salts may be deposited on the surface of the storage containers and/or overpack. This is illustrated by the National Atmospheric Deposition Program (NADP) rainout data, also shown in the figure (specifically for chloride). Thus, while the locations themselves may appear to be dry most of the time, there will be instances where chloride-bearing solutions may be present, and as such, corrosion of these structures is a plausible concern.

Table 37.   Dry storage designs in use (May 2011)

Closure Type	Vendor	Cask	Overpack	Orientation	Number In Use
Welded Metal Container	BNG Fuel Solutions	VSC, W150	Reinforced Concrete	Vertical	65
	NAC	UMS, MPC	Reinforced Concrete	Vertical	243
	NAC	MAGNASTOR	Reinforced Concrete	Vertical	0
	Holtec	TranStor	Bolted Metal	Vertical	34
	Holtec	HI-STAR 100	Metal/Concrete	Vertical	11
	Holtec	HI-STORM	Metal/Concrete	Vertical	343
	TN	NUHOMS	Concrete Module	Horizontal	527
Bolted Metal Cask	NAC	I28		Vertical	2
	TN	TN-32, TN-40, TN-68		Vertical	141
	CASTOR	V/21, X33		Vertical	26
	Westinghouse	MC-10		Vertical	1

Source: (Hanson et al. 2011, Table 2-1)
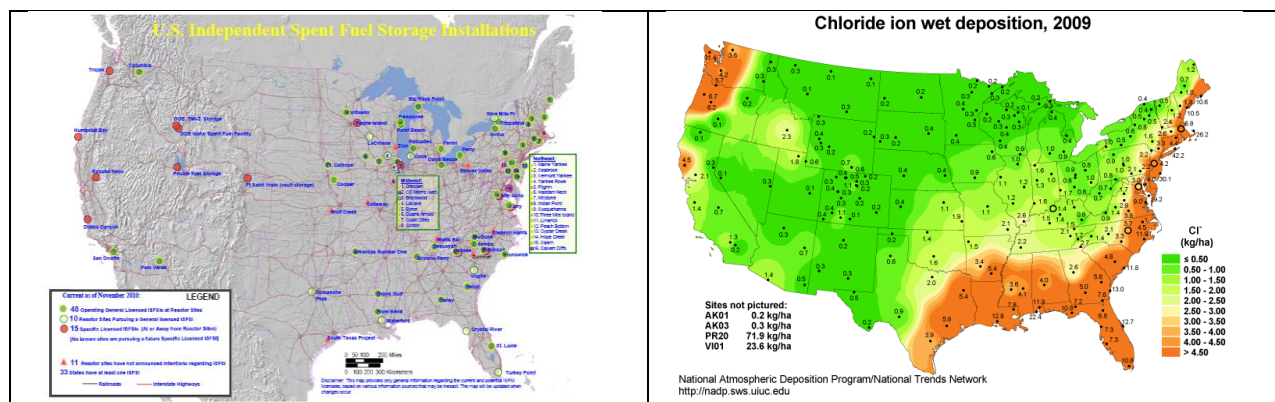
Figure 40.   Location of current and planned dry storage locations, as well as the NADP rainout data for chloride as a function of location within the continental USA

2.7.3   Gap Analysis Methodology

A systematic approach is used to identify data gaps in the technical bases for extended storage of used nuclear fuel in independent spent fuel storage installations (ISFSIs):

1. Determine which safety functional areas are directly impacted or supported. Dry storage functional areas are retrievability, thermal performance, confinement, radiation protection and subcriticality.

2. For those functional areas for which the failure does not result in a direct impact, determine whether failure or chemical and physical property changes could cause changes in other DCSS SSCs, which in turn could impact other safety functional areas.

3. Define the safety function for each impacted safety functional area.

4. For each degradation definition, determine the specific degradation modes.

5. For each of the four stressors that contribute to the specific degradation mode identified in step 4, list the specific degradation mechanisms.

6. For each degradation mechanism, summarize what is known, what needs to be done, and the importance of new research for extended dry storage based on the established research and development priorities.

Identified data gaps are categorized to best direct research and development efforts for UFD extended storage. Several factors influence the basis for prioritizing research and development to address the data gaps in evaluating the impact of a specific degradation mechanism on the container and overpack performance during extended storage. Priorities of the data needs are established based on four primary criteria:

7. Whether existing data are sufficient to evaluate the degradation mechanism and its impact.

8. The likelihood of occurrence of the degradation mechanism during extended storage.

9. Ease of remediation of the degradation such that it continues to provide its safety function

10. Significance of the potential consequences that may result from the degradation mechanism.

These four criteria draw their relative importance to meet objectives for current regulatory compliance, future regulatory drivers, design and operational efficiency, and future waste management needs. Table 38 lists the specific set of questions applied to each degradation mechanism for R&D prioritization. The prioritization of identified data gaps will be used to drive R&D efforts on evaluation of specific degradation mechanisms, their impact on the container or overpack, and their effect on associated storage safety functional areas.

Table 38.   Research and development prioritization criteria

Data Needs	Is there sufficient data to evaluate the degradation mechanism and container or overpack performance?
Regulatory Considerations	What are the current regulatory considerations that cannot be addressed based on existing data and can be addressed with additional data?
Likelihood of Occurrence	What is the likelihood of occurrence of the degradation mechanism during extended storage?
Consequences	What are the consequences of the degradation mechanism?
Remediation	Can the issue be remediated or managed in an aging management program (AMP)?
Cost and Operations	Would any costly design and operational difficulties be endured due to the degradation mechanism?
Future Waste Management Strategies	Would the degradation mechanism limit or complicate future waste management strategies?

2.7.4   Container Gap Analysis

2.7.4.1   Introduction

As noted previously (Section 2.7.1), the container is the primary confinement component of the dry cask storage system (DCSS). It has several functions, including providing a physical barrier to prevent release of radionuclides, maintaining an inert atmosphere of helium for the container internals to prevent chemical degradation and enhance heat transfer, and preventing ingress of moderator (water) to provide additional criticality protection. There are two generic types of storage confinement containers currently in use—bolted metal casks and welded metal canisters. There are a number of key differences between the two varieties of storage systems (Section 2.7.2). Welded canisters are stored or transported within a separate, air-ventilated overpack that provides both neutron shielding and physical protection. Bolted direct-load casks have integral gamma and neutron shielding with a thick metal body and polymer–resin neutron shields. The bolted direct-load casks are mechanically sealed via a combination of lids, bolts, and physical seals (e.g., gaskets to maintain the pressure boundaries). In addition, a weather cover is positioned over the bolts and seals to protect them from rainwater. Older bolted casts were thick-walled vessels (10 to 12 inches thick) made of a variety of ferrous alloys including nodular cast iron, carbon steel, and low-alloy steel, while more recent welded canisters have been constructed with stainless steels.

As noted in Section 2.7.1, the external environment to which the container is exposed will impact its long-term performance, and in aggressive environments, such as marine environments, corrosion of the container or seals is likely to occur. Localized corrosion, galvanic corrosion, SCC may occur, depending upon the environment and the materials under consideration. The potential impact of corrosion on a storage container will be controlled by the operative corrosion mechanisms over the period of performance of the storage system as well as the period over which they occur.

2.7.4.2   Analysis of Safety Functions

The container plays a role in all five key safety functions as described in Table 39.

Table 39.   Container safety functions

Safety Function	Impact
Retrievability	The container ensures the retrievability of the fuel by maintaining its physical and chemical integrity. It provides a substantial physical barrier to alleviate potential structural damage and prevents chemical damage by maintaining an inert atmosphere around the fuel assemblies.
Thermal Performance	Mitigation of the heat generated by the used nuclear fuel within the waste container is enhanced by the use of a helium backfill.
Radiological Protection	The container provides some radiation shielding, especially in the direct-load bolted casks that are made with integral gamma and neutron shielding. For the welded canisters, the steel provides some shielding, although its contribution is minor when compared to that of the transfer or storage overpacks.
Confinement	The container is the primary physical barrier of the DCSS, providing a pressure boundary that holds an inert atmosphere and isolates radionuclides from the external environment.
Subcriticality	During storage, subcriticality is maintained by the exclusion of moderator (water) from the interior of the container.

2.7.4.3   Discussion of Selected Container Issues

The welded canisters differ from the bolted, direct-load casks in both their materials of construction and the method of closure. Their degradation methods are discussed separately.

Welded canisters are robust, with little degradation due to thermal, mechanical, or radiation stressors. However, the canisters are exposed to the atmosphere and may undergo atmospheric or aqueous corrosion in some situations. For this reason, newer welded canisters are made of a corrosion-resistant stainless steel. The areas of welded canisters most susceptible to environmentally induced degradation are the closure welds. These welds are neither annealed nor stress-mitigated, and thus have significant residual stress that may lead to stress corrosion cracking when exposed to sufficiently aggressive environments.

The degradation of bolts and seals in containment systems is discussed in Sections A3.3.3.2 and A3.3.3.3 of ASTM C1562-10. For bolted casks, the features most susceptible to degradation are the closure bolts and seals. Although the seals are normally dry and protected by a weather cover, there may be residual borated water trapped within the seals due to incomplete drying after being loaded in the pool or water from the external environment deposited via capillary condensation. While more modern bolted casks have a double metallic O-ring seal, some older designs had a metallic inner and elastomeric O-ring secondary seal. In such older designs, primary containment is achieved with a metal seal, and secondary containment either with an elastomeric seal or a second metal seal. The elastomeric seal is never the primary containment seal.

The conditions to which the environmental seals are exposed can have a detrimental impact on their performance. In the case of the metal seals, although radiation generally does not impact their performance, the thermal excursions to which they are exposed can compromise the seal by causing the material to creep, thermally fatigue, or otherwise change in mechanical properties. In addition to impacting the performance of metal seals, the thermal and radiation exposure can degrade the physical properties of the bolts used to secure the lid. As with the seals, creep may lead to eventual unloading of the bolts and the loss of an effective seal. In addition, thermomechanical fatigue due to temperature cycling may lead to crack initiation at threads or other stress raisers. The temperature excursions themselves may result in changes in the mechanical properties of the fasteners.

In Appendix D of NUREG-1927 (NRC 2011a), the NRC outlines the aging effects and possible degradation mechanisms for the structural steel members (such as the storage container) that they consider important for an ISFSI or DCSS. These are listed in Table 40. While a number of areas have been identified, we are only reviewing those where the importance of new R&D was identified as being high or medium. The reader should refer to Hanson et al. (2011) for details on other areas.

Specific guidance is given with respect to an AMP for canisters in Appendix E of NUREG-1927. It is noted that material selection is done such that corrosion-resistant materials are used. To ensure that the canister is functioning properly at license renewal, the applicant will have to demonstrate that the canisters have not undergone any unanticipated degradation. An acceptable approach to verify this is via remote visual inspection of one or more canisters, with the selected canisters being identified on the basis of the longest exposure time, highest thermal load, and/or other key parameters that might contribute to degradation of the canister.

Table 40.   Aging effects and possible degradation mechanisms per NUREG-1927

Aging Effects of SSCs	Possible Aging Mechanism
Loss of material	Corrosion (general or localized)
Loss of strength and modulus	Elevated temperature
Loss of fracture toughness	Irradiation
Crack initiation and growth	Stress corrosion cracking

2.7.4.4   Identified Degradation Mechanisms for Containers

Gap analysis identified numerous degradation mechanisms that could feasibly affect the container for UNF extended storage. The R&D importance of these degradation mechanisms has been assigned a High, Medium or Low priority based on the criteria outlined in the gap analysis methodology section. Table 41 shows the various degradation mechanisms identified for both welded containers and bolted casks. The mechanisms identified as a High or Medium R&D priority are discussed in detail. Refer to the comprehensive gap analysis report (Hanson et al. 2011) for a detailed consideration of low R&D priority degradation mechanisms.

Table 41.   Summary of container degradation mechanisms

Stressor	Degradation Mechanism	Influenced by Extended Storage or Higher Burnup	Additional Data Needed	R&D Importance
Welded Containers				
Chemical	Atmospheric corrosion (including marine environment)	Yes	Yes	High
	Aqueous corrosion: general, localized (pitting, crevice), SCC, galvanic	Yes	Yes	High
Bolted Casks				
Chemical	Atmospheric corrosion (including marine environment)	Yes	Yes	High
	Aqueous corrosion: general, localized (pitting, crevice), SCC, galvanic	Yes	Yes	High
Thermal and Mechanical	Embrittlement of elastomer seals	Yes	Yes	Low
	Thermo mechanical fatigue of seals and bolts	Yes	Yes	Medium
Radiation	Embrittlement of elastomer seals	Yes	Yes	Low

2.7.4.5   Atmospheric Corrosion of Welded Containers

Welded canisters are typically stored in ventilated concrete overpacks. The overpacks protect storage containers from direct contact with rainwater but not from exposure to the atmosphere. Atmospheric corrosion is therefore considered a potential degradation mechanism. Corrosion resistant materials such as stainless steels are largely immune to the effects of atmospheric corrosion under all but the most severe exposure conditions. Because recently produced welded containers have thick (0.5-inch to 0.625-inch) stainless steel walls (e.g., the NUHOMS DSC, NAC MPC, and HI-STORM MPC), it is unlikely that either atmospherically induced general or localized corrosion would compromise the structural integrity of the container. Stress corrosion cracking of the welds in humid environments is the most likely atmospheric degradation mechanism for welded stainless steel containers, although the risk of canister breach is relatively low unless salt deposition is high.

Less corrosion-resistant materials, such as the carbon steels used in early welded container designs, are more likely to undergo atmospheric corrosion to a measureable degree. Atmospheric corrosion is a concern in environments where a combination of high moisture content and aggressive ion-containing contamination are present that could lead to enhanced corrosion, such as in polluted industrial areas and in marine environments. For marine exposure, the dominant form of aggressive ions comes from salt particles formed from seawater aerosols. Depending on the relative humidity of the environment and the

size of the particulates, these salt particles can be either actual droplets of seawater, droplets of evaporatively concentrated brine, or solid salt particulates (Blanchard and Woodcock 1980). Irrespective of their physical form, all result in the delivery of chloride-rich contaminants onto the metal surface. The mechanisms observed for atmospheric corrosion are similar to those observed in bulk aqueous solutions—namely general and localized corrosion of various forms, including pitting, crevice corrosion, and stress corrosion cracking. Atmospheric corrosion processes are profoundly impacted by the morphology and physical configuration of the corroding surfaces as well as their position relative to any potential sources of moisture or solid contamination.

Morphology is determined by surface roughness (scratches) and presence of contaminants (e.g., chloride-bearing salts). As such, it is imperative to assess the environment to which the containers at a specific site are exposed. The analysis should capture seasonal variations in temperature, moisture content, and contamination deposition (particularly for marine environments). The result of this effort will establish both which materials of construction are appropriate for a particular location and the conditions under which the acceptable performance materials of construction must be verified.

Three factors are necessary for SCC: stress (either residual or applied), a susceptible material, and a sufficiently aggressive environment. In marine locations, some austenitic stainless steels have been demonstrated to be susceptible to such degradation. SCC of sensitized stainless steels in marine exposure was been observed for 201, 301, 302, 304, 309, and 316 stainless steel when exposed at the LaQue Kure beach site (Kain 1990). It was observed that annealed and moderately cold-worked stainless steels were largely immune to SCC unless a crevice was present. Also, it was determined the susceptibility of the steels to SCC and hence the extent to which cracking occurred correlated with the carbon content of the steel. In other words, "L" grade stainless steels were far less susceptible than their normal carbon level counterparts. In a more recent Japanese study (Tani et al. 2008; Tani et al. 2009; Shirai et al. 2011), the SCC susceptibility of stainless steel canisters for dry storage of used nuclear fuel in marine environments has been explored. In that work, the performance of more commonly applied stainless steels (304L and 316L) was evaluated, alongside several 6% Mo stainless steels designed for increased resistance to localized attack (UNS S31260 (duplex) and UNS S31254 (austenitic)). As with the earlier LaQue study, Tani and Shirai et al. observed that the standard stainless steels (i.e., 304L and 316L in this case) were susceptible, but the more highly alloyed materials (i.e., a 6% Mo duplex and a 6% Mo austenitic stainless steel) were effectively immune.

Although the more modern 6% Mo alloys were immune, they carry with them a substantial increase in cost. As a result, Japanese current research is aimed at evaluating stress mitigation techniques to improve the performance of less costly materials such as 304L stainless steel, as well as developing means to reduce the deposition of chloride-bearing salt particles onto the canister surface. Other similar studies include the work of (Caseres and Mintz 2010) who also evaluated atmospheric stress corrosion cracking in austenitic stainless steels to investigate this degradation mechanism in dry cask storage containers in marine environments. Their work, which evaluated the performance of a number of stainless steels at a range of temperatures, found that SCC did not occur at temperatures in excess of 85°C. This work suggests that SCC is not likely to be a problem during the early years of storage when the containers are above 85ºC but could become a viable degradation mechanism for extended storage times if the circulating air contains significant chloride-containing particulate.

For any important-to-safety (ITS) metal exposed to the external environment, it must be demonstrated that atmospheric corrosion will not significantly degrade its safety functions within the license period. Such demonstration includes the basic materials of construction, as well as any specific geometries associated with the storage system or microstructural changes brought about by assembly processes such as welding. This requires the characterization of both the environment to which the system will be exposed and the atmospheric corrosion performance of the container materials when exposed to relevant environments. In the case of marine environments, key variables that must be understood include the deposition rate of salt particulates on a relevant material surface and the typical chemistry of those

aerosols. Most initial safety analysis reports for welded containers simply state that for non-marine environments, the interior of the overpack will be relatively mild (warm and dry) and the stainless steel alloys used have a proven history of material integrity under these conditions (Holtec-International 2000; Transnuclear 2001; NAC 2004).

The Nuclear Waste Technical Review Board (NWTRB) identified atmospheric corrosion as a potential degradation mechanism for the container (NWTRB 2010). They stressed the importance of all chemical species in the atmosphere and in dust, as well as the effects of gamma radiation on these contaminants, such as production of nitric acid in irradiated moist air or halogen from irradiated halide salts.

Table 42 presents the impact of degradation mechanisms on various criteria used in prioritizing additional research and development activities. Additional research and development for environmentally induced degradation (e.g., atmospheric corrosion or SCC) of the welded canisters is assigned a High priority.

Table 42.   Impact from atmospheric corrosion of welded containers

Criteria	Impact
Data Needs	There is sufficient data available to evaluate the potential for atmospheric corrosion to occur during the licensing period, given that the materials and environment are known. However, predictions of the environment for extended storage are required.
Regulatory Considerations	The ability of a container to maintain its integrity and provide waste containment is a critical aspect of the DCSS. Environmentally induced degradation of the welded canisters, especially the more rapid modes of corrosion such as SCC, can lead to loss of confinement during the license period.
Likelihood of Occurrence	The likelihood of the atmospheric corrosion of the older-design casks can be significant if the coatings on the older casks are not adequately maintained. The likelihood of marine atmosphere SCC for extended storage is also significant.
Consequences	The impact of atmospheric general corrosion likely will be minimal because the newer stainless containers are effectively immune and older corrosion-allowance materials are sufficiently thick walled. Localized corrosion of metallic seals in bolted containers or SCC of the weldments in newer containers could result in a potential breach of the container and is an unacceptable consequence.
Remediation	AMPs are hindered by the overall construction of the DCSS, where many of the areas that must be monitored (e.g., welds on newer containers) are obscured by the overpack. Remediation of a cracked weldment could require either repair or replacement of the canister, depending on the assessment of the extent of damage.
Cost and Operations	Replacement of the canister would involve relocation of the used nuclear fuel to a new canister, which would have high cost and the potential for significant worker dose.
Future Waste Management Strategies	No impact.

2.7.4.6   Aqueous Corrosion of Welded Containers

With time waste container temperatures will decrease, allowing for the formation of condensation on the inside of the overpack and on the container surface. Water may also be present if there is inadequate drying or the overpack fails to protect the container from rainwater. Unlike the atmospheric corrosion scenarios discussed previously, the environment present when condensation takes place is effectively a bulk aqueous environment. As with atmospheric corrosion conditions, the chemical composition of the aqueous phase will be a strong function of solid and liquid contamination delivered from the environment to the metal surface. If the solution chemistry is sufficiently aggressive, aqueous corrosion of the storage containers may occur. While the active corrosion mechanisms will be determined by the combination of material and environment (e.g., chloride concentration, presence of occluded geometries, concrete), they can include general corrosion, localized corrosion (i.e., pitting and crevice corrosion), SCC, and galvanic corrosion.

The ability of a welded container to maintain its integrity and provide waste containment is a critical aspect of the DCSS. Any plausible degradation processes that may directly impact the structural integrity of the container must be well understood such that appropriate materials and processing techniques can be selected. While appropriate material selection can minimize the impact of any potential aqueous corrosion, existing designs contain many materials, such as carbon and low alloy steels, which are highly susceptible to general and/or localized corrosion under inundated conditions.

The NWTRB identified pitting, crevice, and galvanic corrosion, as well as SCC as potential degradation mechanisms for the container: "There is an insignificant risk of canister wall failure due to pitting or crevice corrosion unless the duration of storage is very long. A metal canister's corrosion lifetime for pitting and crevice corrosion can be estimated as the time needed for the canister to decline to a temperature where corrosive aqueous environments are possible (i.e., below about 100°C), plus the time for electrochemical corrosion to propagate through canister wall thickness" (NWTRB 2010, p. 106). The NWTRB cites Kosaki (2008), who predicts the failure of a 13-mm canister between 430 and 650 years after the temperature on the canister has dropped sufficiently to allow condensation. Galvanic corrosion can occur whenever dissimilar metals are in contact with each other in the presences of an electrolyte.

Table 43 presents the impact of degradation mechanisms on various criteria used in prioritizing additional research and development activities. Additional research and development for aqueous corrosion of the welded canisters is assigned a High priority.

Table 43.   Impact from aqueous corrosion of welded containers

Criteria	Impact
Data Needs	While there is sufficient data to evaluate aqueous corrosion and container performance, the likelihood of aqueous corrosion is currently unknown. Aqueous corrosion will depend on the temperature at the container surface and the degradation state of the overpack. Data needs include a thermal analysis of the container surface for a variety of DCSSs.
Regulatory Considerations	The ability of a container to maintain its integrity and provide waste containment is a critical aspect of the DCSS. Aqueous corrosion can lead to loss of confinement during the license period, particularly if localized corrosion or SCC become operative mechanisms.
Likelihood of Occurrence	Unknown.
Consequences	The consequences of aqueous corrosion range from minimal for the generalized corrosion of the corrosion allowance materials used in the older designs to unacceptable for breach of the newer stainless steel containers by localized corrosion or SCC.
Remediation	Aging management programs are hindered by the overall construction of the DCSS, where many of the areas that must be monitored (e.g., welds) are obscured by the overpack. Remediation involves ensuring the weather protection is functioning correctly and condensation is not occurring, and can be accomplished with an aging management program.
Cost and Operations	If aqueous corrosion is prevented through an aging management program, then the cost is small. However, if corrosion is significant enough to require canister replacement, relocation of the used nuclear fuel to a new canister will be required. This would be a high cost process that has the potential for significant worker dose.
Future Waste Management Strategies	No impact.

2.7.4.7   Thermal Degradation of Fasteners and Metallic Seals in Bolted Casks

For the seal to remain intact the stress imposed by the fasteners used to press the cover onto the metallic and elastomeric seals must be maintained. Degradation of the elastomeric seals is considered a Low R&D priority and is discussed in the comprehensive gap analysis report (Hanson et al. 2011). If sufficiently large, thermal excursions can support creep of both the metallic seal and the bolts. This creep results in stress relaxation of the sealing system and could compromise the integrity of the seal. In addition to creep, fluctuations in temperature can result in thermomechanical fatigue of the fasteners, potentially leading to crack initiation and eventual fastener failure.

Analyses of the temperature profiles (axial and radial) of low and high burnup fuels over the entire period of dry storage (from the start of drying operations to transfer to the ISFSI to extended dry storage) are needed to determine the exposure conditions under which the mechanical seal must remain intact. Once temperature histories are calculated, an analysis of seals and bolts metal fatigue caused by temperature fluctuations can be performed. In the meantime, BAM (Germany), CRIEPI (Japan), and the French Atomic Energy Commission have been studying metal seals for thermal degradation and corrosion due to inadequate drying (Volzke and Wolff 2011). The French have found no significant changes in seals in a testing program started in 1973. The Germans have measured the creep of Helicoflex® seals with aluminum or silver jackets at 150°C but as yet have found no loss of seal tightness due to the improved contact between the weak outer jacket material and the sealing flange surface. The Japanese studied Helicoflex® metal seals kept at 160°C from 1990 to 2010. Shirai et al. (2011) measured the relationship between the leak rate and the Larson–Miller parameter. They concluded that as long as aluminum-covered gaskets had initial temperatures of below 134°C, or silver-covered gaskets had initial temperatures below 125°C, sealing performance would be ensured for 60 years.

The NWTRB identified some component specific degradation mechanisms including those of bolts and metallic seals: "Bolts are subject to high stress. Under both thermal accident events and mechanical impact events, relatively brittle welds can fracture. Under accident thermal events, creep rupture failures also are possible. Metallic seals and gaskets under high loads can degrade through stress relaxation of the metal, plastic deformation, and creep" (NWTRB 2010, p. 108).

Table 44 presents the impact of degradation mechanisms on various criteria used in prioritizing additional research and development activities. While issues with fastener or metal seal creep can be avoided by proper materials selection and system design (provided the environment can be adequately characterized), the ability to maintain waste isolation/confinement is a critical aspect of any container. The importance of new research and development in this area is categorized as Medium.

Table 44.   Impact from thermal degradation of fasteners and metallic seals in bolted casks

Criteria	Impact
Data Needs	Until there are validated calculations of representative temperature histories of extended storage, there is insufficient data to evaluate the thermal degradation of seals and bolts, and the likelihood of this degradation mechanism is unknown.
Regulatory Considerations	Thermal degradation of seals and bolts can lead to loss of confinement.
Likelihood of Occurrence	Unknown.
Consequences	The consequence of seal or bolt failure is loss of regulatory-required confinement. Because the pressure of the space between the redundant seals is monitored, loss of confinement may be easily detected.
Remediation	Remediation can range from retightening the bolts to returning the cask to the pool for replacement of the seals.
Cost and Operations	Cost ranges from minimal (bolt tightening) to high (seal replacement).
Future Waste Management Strategies	No impact.

2.7.4.8   Atmospheric Corrosion of Bolted Casks

Atmospheric corrosion is a potential degradation mechanism for bolted casks because, like the welded canisters, the outer surface is exposed to the external environment. The bolts and seals are normally protected from rainwater and humidity by a weather cover, but if this cover fails, the bolts and seals would be subject to corrosion. Bolted casks have occluded geometries around the bolts and seals, which can result in capillary condensation where liquid water deposits are formed within the occluded environment. The resulting liquid layer can enable traditional crevice corrosion to take place at relative humidities where an aqueous surface layer was not anticipated.

While atmospheric corrosion is not typically a concern for many corrosion-resistant materials such as stainless steels, it is more likely for corrosion-allowance materials (e.g., carbon or low-alloy steels), particularly in marine environment installations. For this reason, most corrosion-allowance materials have a protective organic coating applied. It must be demonstrated that any viable degradation mechanism such as atmospheric corrosion will not significantly compromise the safety function of the bolted container within the license period. Such demonstration includes the basic materials of construction, as well as any specific geometries associated with the storage system or microstructural changes brought about by assembly processes such as welding. As such, both the environment to which the system will be exposed and the atmospheric corrosion performance of the container materials when exposed to relevant environments must be characterized.

The ability of a container to maintain its integrity and provide waste containment is a critical aspect of the DCSS. Any plausible degradation processes that may directly impact the structural integrity of the

container must be well understood, such that appropriate materials and processing techniques can be selected. While appropriate material selection can prevent atmospheric corrosion, existing designs contain many materials such as carbon and low-alloy steels, which can readily undergo atmospheric corrosion. As such, the importance of new research in this area is categorized as High.

The NWTRB identified atmospheric chemistry corrosion environment as a potential degradation mechanism for the container (NWTRB 2010). Table 45 presents the impact of degradation mechanisms on various criteria used in prioritizing additional research and development activities. Until susceptible containers are replaced, the priority of new research and development is High.

Table 45. Impact from atmospheric corrosion of bolted casks

Criteria	Impact
Data Needs	The atmospheric corrosion of bolted casks is well understood, and there is sufficient data to indicate that the less corrosion-resistant metals used in bolted cask may undergo atmospheric corrosion.
Regulatory Considerations	If atmospheric corrosion is significant, the container may be breached, which is an unacceptable regulatory consequence.
Likelihood of Occurrence	The likelihood of significant atmospheric corrosion (i.e., sufficient attack to compromise the performance of the container) is low.
Consequences	Unless the corrosion involves a critical structure such as bolts, superficial corrosion will not degrade the safety functions of the casks, which are often quite thick.
Remediation	The remediation may be simply maintaining the weather cover and surface coating of the casks, but under extreme conditions it could also involve replacement of the container.
Cost and Operations	Canister replacement would involve relocation of the used nuclear fuel to a new canister, which would have high cost and the potential for significant worker dose.
Future Waste Management Strategies	No impact.

2.7.4.9   Aqueous Corrosion of Bolted Casks

Unlike the welded containers, the bolted casks are not protected from the rain except over the bolts and seals. As with atmospheric corrosion conditions, the chemical composition of the aqueous phase that forms due to condensation or rain will be a strong function of solid and liquid contamination delivered from the environment to the metal surface. If the solution chemistry is sufficiently aggressive, aqueous corrosion of the outer surfaces of the storage containers may occur. While the active corrosion mechanisms will be determined by the combination of material and environment (e.g., chloride concentration, presence of occluded geometries), they can include general corrosion, localized corrosion (i.e., pitting and crevice corrosion), SCC, and galvanic corrosion.

Corrosion is particularly problematic in situations where the structural integrity of the container could be threatened, such as when the weather cover over the seals and bolts fails. Seals and bolts are under stress and thus subject to SCC if wetted. There are examples in the field where corrosion has led to an unanticipated breach of the storage containers, highlighting the importance of proper consideration of potential failure mechanism prior to utilizing a system for waste containment. For example, EPRI reports "Recently, six casks at Surry were determined to have leaking outside seals by monitoring. A CASTOR-X cask had galvanic corrosion of the secondary metallic seal due to the presence of chloride probably from residual cleaning fluid. Five TN-32 casks experienced galvanic corrosion of the secondary metallic seal due to water leakage through the protective cover. Based on the monitoring and subsequent examinations of the seals, corrective actions were taken to prevent a recurrence. The design of the protective cover was improved and aluminum was replaced by silver secondary seals on new loadings" (EPRI 2002a, p. 4-3). Another example was reported by Aida et al. (2010) in which corrosion of metal seals due to residual water from insufficient drying was observed in 2000. "The Procedure manual was updated so that residual water could be completely removed." Corrosion of metal seals was primary lid. Procedure manual will be additionally updated in order to reduce the immersion duration."

For any ITS metal exposed to conditions where condensation or rainwater leakage is possible, it must be demonstrated that any potential aqueous corrosion processes (general, localized, or SCC) will not significantly degrade its safety functions within the license period. Demonstration includes the basic materials of construction, as well as any specific geometries associated with the storage system or microstructural changes brought about by assembly processes such as bolting. Both the environment to which the system will be exposed and the atmospheric corrosion performance of the container materials in relevant environments require characterization. In the case of marine environments, key variables that must be understood include the deposition rate of salt particulates on a relevant material surface and the typical chemistry of those aerosols.

The ability of a container and its subcomponents (e.g., welds, fasteners) to maintain their integrity and provide waste containment is a critical aspect of the DCSS. Any plausible degradation processes that may directly impact the structural integrity of the container must be well understood, such that appropriate materials and processing techniques can be selected. While appropriate material selection can minimize the impact of any potential aqueous corrosion, existing designs contain many materials such as carbon and low alloy steels, which are susceptible to significant corrosion under inundated conditions.

The NWTRB identified pitting, crevice, galvanic corrosion, and SCC as potential degradation mechanisms for the container (NWTRB 2010). Table 46 presents the impact of degradation mechanisms on various criteria used in prioritizing additional research and development activities. Until it can be demonstrated that aqueous corrosion can be reliably prevented by an AMP, the priority of new research and development remains High.

Table 46.   Impact from aqueous corrosion of bolted casks

Criteria	Impact
Data Needs	While there is sufficient data to evaluate aqueous corrosion of bolted casks, this data indicates that the likelihood of occurrence of the aqueous corrosion has been high (it has occurred due to failure of a weather cover and due to insufficient drying).
Regulatory Considerations	Failure of bolts or seals can lead to loss of confinement.
Likelihood of Occurrence	As remedial measures are taken, the likelihood of occurrence should decrease.
Consequences	If failure of the weather protection of the container is undetected, or condensation occurs, the container may be breached, which is an unacceptable regulatory consequence.
Remediation	Remediation involves ensuring the weather protection is functioning correctly and condensation is not occurring under the weather cover. This can be accomplished with an aging management program. Remediation also includes inspecting any external coatings and repairing them as necessary.
Cost and Operations	An aging management program is cost effective and should prevent the need to return the cask to the pool.
Future Waste Management Strategies	No impact.

2.7.4.10   *Approach to Closing Container Gaps*

Degradation processes that directly impact the ability of the system to maintain its environmental seal have been given a high priority. These include phenomena such as localized corrosion, galvanic corrosion, and stress corrosion cracking of key components of the sealing system (e.g., metallic O-ring seals, weldments). Understanding the environments to which the containers are subjected is critical in order to ensure that the degradation processes of concern are evaluated under a relevant set of environmental parameters (e.g., temperature, humidity, surface contamination). To address these concerns, a program that encompasses a variety of research areas is needed. The proposed approach would begin with the experimental evaluation of relevant environmental parameters and corrosion degradation processes. The experimental results would then be used to generate a predictive model that could in turn be utilized to establish the time dependent potential for seal failure, given the design of the storage container and relevant environmental parameters. This model would then provide input to an AMP with the goal of assessing the time-dependent risk of seal failure associated with a specific storage system. The experimental program and development of this model will be done in collaboration with the disposal research being done in the Used Fuel Disposition Campaign. Also, the Japanese (CRIEPI) and Germans (BAM) have been studying the degradation of seals for many years. The DOE will explore how to best use its resources to collaborate with international researchers through the ESCP.

2.7.5   Overpack Gap Analysis

2.7.5.1   Introduction

Typically constructed of steel-reinforced concrete, overpacks and storage modules (hereafter referred to as "overpacks") house the primary UNF storage container. Understanding overpack aging characteristics is critical in determining long term DCSS performance as the overpack dictates the environment to which the container is exposed. This section focuses on reinforced concrete overpack designs. Some designs have steel components not imbedded in concrete and have the same degradation mechanisms as steel containers.

2.7.5.2   Analysis of Safety Functions

The primary functions of overpack/storage module are to:

1. Protect the canister from direct contact with the environment under both normal and abnormal (i.e., accident) conditions.

2. Provide radiation shielding, thereby minimizing the exposure to workers and other surrounding objects/structures.

3. Provide thermal management for the storage cask by facilitating heat removal, thereby minimizing temperature excursions.

The overpack directly supports three of the five key safety functions of the DCSS: thermal performance, radiological protection, and retrievability. The overpack also indirectly supports the confinement function of the canister. The overpack is generally on the outside of the DCSS, and any issues associated with degradation processes can typically be addressed through an AMP that can include inspection, repair, or replacement with fairly minimal dose exposure or risk of damaging fuel or the rest of the DCSS. Degradation of the concrete overpack affects the five storage safety functional areas as described in Table 47.

Table 47.   Overpack safety function descriptions

Criteria	Impact
Retrievability	Gross degradation of the overpack may hinder retrievability.
Thermal Performance	Because concrete is a thermal insulator, it is important to the thermal management of the DCSS that any structural features such as air cooling channels remain free of debris.
Radiological Protection	The concrete overpack provides significant radiation shielding during storage.
Confinement	The concrete overpack indirectly supports confinement by protecting the container.
Subcriticality	Other than indirect support by providing protection for the container, the overpack has no direct subcriticality function.

2.7.5.3   Discussion of Selected Concrete Overpack Issues

Concrete properties are a strong function of the mix design from which they are formulated. Water fraction, aggregate type and quantity, and other mixture characteristics combine to determine the ultimate concrete mechanical properties. These mixture characteristics can also impact pore structure, which can in turn affect concrete permeability. Numerous admixtures can have a significant impact on the properties of the concrete and its resistance to specific degradation processes. For these reasons, care must be taken to tailor the concrete mix design and curing process for the specific application. For example, if the application requires high compressive strength, the mixture must be cured in a comparatively reduced timeframe. The American Concrete Institute (ACI) has issued numerous specifications that attempt to capture and control the key aspects of concrete mix design for different applications. These specifications should be followed closely as deviations may result in undesirable changes in the concrete properties.

An overview of the factors impacting the durability of concrete for nuclear power plant structures, many of which are of equal relevance to a DCSS, is presented in NUREG/CR-6927 (Naus 2007). The degradation mechanisms for concrete structures of relevance to a DCSS are also described in Section A5.4 in ASTM.C1562-10 (2010) and are summarized below. All of these areas have been heavily investigated by previous researchers, so a thorough literature review should be completed prior to constructing a detailed research plan for any of them.

2.7.5.4   Identified Degradation Mechanisms for Overpacks

Gap analysis identified numerous degradation mechanisms that could feasibly affect the overpack for UNF extended storage. The R&D importance of these degradation mechanisms has been assigned a High, Medium or Low priority based on the criteria outlined in the gap analysis methodology section. Table 48 shows the various degradation mechanisms identified. As the degradation processes associated with overpack construction materials of construction are well understood, most areas are assigned a Low R&D priority. Only monitoring activities for freeze-thaw and embedded steel corrosion degradation mechanisms were assigned a Medium priority. No overpack issues were deemed a High R&D priority. The Medium priority degradation mechanisms are discussed in detail. Refer to the comprehensive gap analysis report (Hanson et al. 2011) for information on the low R&D priority overpack degradation mechanisms.

Table 48.   Summary of overpack degradation mechanisms

Stressor	Degradation Mechanism	Influenced by Extended Storage or Higher Burnup	Additional Data Needed	New R&D Priority
Thermal	Dry-out	Yes	Yes	Low
	Fatigue	Yes	Yes	Low
	Freeze-thaw	Yes	Yes	Medium
	Aggregate growth	Yes	Yes	Low
Radiation	Water decomposition	Yes	Yes	Low
	Aggregate reaction	Yes	Yes	Low
Chemical	Calcium leaching	Yes	Yes	Low
	Chemical attack	Yes	Yes	Low
	Embedded steel corrosion	Yes	Yes	Medium
Mechanical	Blocked air flow	Yes	No	Low
	Creep	Yes	No	Low
	Shrinkage	No	No	Low

2.7.5.5   *Freeze–Thaw Damage*

Concrete is a highly porous material, containing a fine network of both macroscopic and microscopic pores. Under conditions in which water is readily available, either through ponding on the surface of a concrete structure or in the form of a high relative humidity, this pore structure can become saturated/filled with water. As the water within the pores repetitively freezes and thaws, the mechanical stress placed upon the concrete by the expansion and contraction of the water within the pores (i.e., transition to ice [expansion] then back to liquid [contraction]) can result in degradation of the physical properties of the concrete. In general, freeze–thaw damage occurs on flat surfaces upon which water may pond, remaining in contact with the concrete. The resulting damage typically initiates at the surface of the concrete and, as such, can be discovered readily through visual inspection. It should also be noted that freeze–thaw damage is of concern only under environmental conditions that result in significant freeze–thaw cycling combined with a high availability of water. Thus, the geographical location of a DCSS will largely dictate whether this type of damage is even possible. However, even under conditions that tend to exacerbate this damage process, proper design and construction practices (e.g., ACI specifications ACI.318-63 1963; ACI.301-66 1966; ACI.345-85 1985 [or later versions of each]) will result in the production of a structure that is effectively immune to this damage mode.

Although best construction practices should preclude freeze–thaw damage, this degradation mode has been observed at the Three Mile Island (TMI) ISFSI at Idaho National Laboratory (INL); the degradation has been attributed to freeze–thaw of water in roof bolt holes (NRC 2011b). This implies that in addition to the nature of the concrete itself, geometric features of the overpack within which water could collect (e.g., bolt holes) must also be carefully considered.

In 1994, EPRI concluded that with good practices, there will be no significant damage from freeze–thaw in the licensing period. In 1995, the NUHOMS module designs were approved for general use by the NRC. By design, these modules have roof bolt holes that should be sealed when deployed in an environment subject to freeze-thaw. As the licensing period is extended the validity of EPRI's conclusion

should be confirmed. The NWTRB identified freeze–thaw as a potential degradation mechanism for concrete (NWTRB 2010).

Table 49 presents the impact of degradation mechanisms on various criteria used in prioritizing additional research and development activities. Freeze–thaw damage of concrete is an extensively researched and well-understood damage mechanism. Proper design procedures should eliminate situations having the potential to exacerbate freeze–thaw damage, such as low spots or bolt holes where water may collect/pool. Therefore, additional research and development for freeze–thaw damage is assigned a Low priority. However, this low priority is contingent on proper remediation of roof bolt holes, adequate monitoring and an adequate AMP as outlined in NUREG-1927 (NRC 2011a). This remediation, monitoring, and AMP have a Medium priority.

Table 49.   Freeze-Thaw damage impact

Criteria	Impact
Data Needs	Freeze–thaw degradation of concrete is a well-studied mechanism.
Regulatory Considerations	If freeze–thaw results in loss of protection of the canister, it may indirectly compromise confinement.
Likelihood of Occurrence	Freeze–thaw damage is a concern only in regions where weather conditions are conducive and the concrete is relatively porous or has places for water to collect. When appropriate ACI specifications are followed, the resulting concrete is highly resistant to this degradation mode, and no significant damage is anticipated during the licensing period. Freeze–thaw damage has occurred at the NUHOMS-12T (with TMI fuel) ISFSI at the INL, where roof bolt holes were not sealed.
Consequences	If freeze–thaw results in loss of protection of the canister, it may indirectly compromise confinement.
Remediation	Inspection and replacement of damaged concrete and the elimination of locations that may collect water are straightforward engineering solutions to freeze–thaw damage.
Cost and Operations	Cost is minimal, but will scale with the extent of damage incurred before detection.
Future Waste Management Strategies	No impact.

2.7.5.6   Corrosion of Concrete Metal Reinforcement

To function as a structural member when tensile loads are present, steel reinforcement is typically used within the concrete. In general, the material used to reinforce concrete is carbon steel. Because the environment within concrete is highly alkaline (pH > 12.5), the carbon steel is passive, and corrosion does not take place. However, if this alkaline environment is altered due to leaching of calcium hydroxide, reaction of calcium hydroxide with atmospheric carbon dioxide (i.e., carbonation), or infiltration of the

concrete with an acidic solution, this passivity may be lost and corrosion of the steel reinforcement may result. Similarly, if a solution rich in aggressive anions such as chloride reaches the reinforcement, corrosion may initiate despite the pH being highly alkaline.

Irrespective of how it initiates, corrosion of the steel results in the metallic reinforcement being transformed to corrosion products (e.g., iron oxides). The resulting corrosion product is vastly more voluminous than the metal it replaces. As a result, corrosion that is insignificant in terms of the loss of cross section of the reinforcement can cause large internal expansion stresses within the concrete, causing it to crack. Once cracked, transport of aggressive solutions to the reinforcement becomes increasingly rapid, resulting in corrosion acceleration and damage to the concrete.

The risk of reinforcement corrosion can be minimized by ensuring an adequately thick, low permeability concrete layer exists between the reinforcement and the external environment. Low-permeability concrete reduces the quantity of electrolyte available to the concrete, as well as minimizing the migration rate of cathodic reactants (i.e., oxygen) or aggressive species (e.g., chlorides) to the reinforcement.

The characteristics of concrete required to minimize the risk of reinforcement corrosion are fairly well defined. Following standards such as ACI 201.2R-67 when designing/constructing a concrete overpack minimizes the risk of corrosion (ACI.201.2R-67 1967). Furthermore, if exposure to aggressive environments is likely to occur, or if the design life of the overpack is to be very long, more corrosion-resistant reinforcement can be used, such as stainless steels, which, although significantly increasing materials cost, will effectively alleviate any concerns over corrosion of the reinforcement. Other potential solutions to corrosion of the reinforcing steel include the use of corrosion-inhibitor admixtures during construction or the application of a cathodic protection system.

In addition to being used as an embedded reinforcement, some storage systems (e.g., the Holtec HI-STORM system) use steel reinforcement in the form of an external shell. As with the outer surface of carbon steel storage containers such as the CASTOR V/21, the steel shell is coated with a protective polymeric material to prevent corrosion. If this coating is breached and corrosion of the underlying steel takes place, the presence of damage would be easily detected via visual examination.

The NWTRB identified corrosion of reinforcing steel as a potential degradation mechanism for concrete (NWTRB 2010). Table 50 presents the impact of degradation mechanisms on various criteria used in prioritizing additional research and development activities. Because the corrosion of steel in concrete is a well-documented degradation mode, and because following proper construction practices (e.g., ACI.201.2R-67 1967) minimizes the risk of reinforcement corrosion, the priority of new research in this area is Low. However, this low priority is contingent on adequate monitoring and an adequate AMP as outlined in NUREG-1927. Preventing damage to the overlying concrete is critical in preventing corrosion of embedded steel. Monitoring and an AMP are assigned a Medium priority.

Table 50.   Metal reinforcement corrosion impact

Criteria	Impact
Data Needs	The degradation of embedded steel in concrete is a well-known and extensively studied phenomenon.
Regulatory Considerations	The ability of the overpack to protect the container must not be compromised.
Likelihood of Occurrence	Under conditions in which significant aggressive ion exposure occurs, corrosion of the reinforcement is inevitable, although the induction time prior to corrosion initiation can be significant.
Consequences	Corrosion of the reinforcement can result in significant structural damage to the overpack, requiring repair or replacement
Remediation	Adequate engineering and aging management solutions exist for this degradation mechanism.
Cost and Operations	If corrosion of the reinforcement takes place, the overpack may be repaired (if the damage is minor) or replaced. If replacement of the overpack is required, the cost and operations involved would be significant.
Future Waste Management Strategies	No impact.

2.7.5.7   *Approach to Closing Overpack Gaps*

The overpack plays a critical role in the overall performance of many storage systems. Fortunately, the degradation processes associated with the materials of construction are well understood, and thus the priority of research in those areas has been ranked Low. While the mechanisms themselves are well understood, the means to effectively monitor and maintain the overpack throughout the service life of the storage system as part of an active AMP is still being pursued by utilities. The continued development of an active AMP has been given a Medium priority.

2.8   Summary of Gap Analysis

The previous sections have described the current state of knowledge for the performance of engineered materials in several potential disposal environments, including: clay, crystalline rock, and salt repositories that are in the long term, water/brine-saturated and anaerobic; unsaturated, oxic crystalline rock repositories; and deep boreholes in crystalline rock. Also considered are the conditions and materials that are relevant to interim storage for spent nuclear fuel for extended periods of time. In this section, additional research needs are summarized, and a priority is assigned to each, along with a status or recommendation for future work on the topic by the Engineered Materials Performance work package.

Table 51 summarizes the additional research needs that have been identified, and provides a relative ranking of each topic. Research needs for interim storage have already been ranked in Section 2.7, and only a small fraction of those topics are repeated here; Table 51 contains the only two research needs that have been identified as high priority in Section 2.7. Shaded cells indicate that the topic is currently being evaluated by another work package (green), or is either currently or in FY12 being addressed by the Engineered Materials Performance work package (orange).

Table 51.   Summary and ranking of additional research needs

Repository/ Storage setting	Additional research needs	Priority	Recommendation
Clay	Carbon steel interactions with backfill, including: (1) Diffusion of corrosion-active species through backfill (2) Backfill effects on H_2 transport, H_2 buildup, and potential feedbacks on corrosion. (3) Interactions between aqueous Fe and backfill, and potential changes in backfill ion exchange and swelling capacity.	High	Some aspects of this are currently being evaluated by the UFD Engineered Barrier System work package.
	Verification of the localized corrosion behavior of carbon steel in alkaline environments.	Low	Although identified in several recent evaluations as an additional research need relative to the Belgian supercontainer, recent work by ONDRAS/NIRAS has largely addressed this. No further work is necessary
Granite	"The Copper Controversy." Additional research to evaluate processes occurring in the controversial hydrogen generation experiments, and to evaluate rates of copper corrosion under anoxic conditions.	High	Will be evaluated starting in FY12 by this work package. See Appendix A.
	Additional evaluation of copper localized corrosion and stress corrosion cracking under repository-relevant conditions, to understand the potential effects of environmental variables (chloride, sulfide).	Medium	Although identified as a potential issue in some summaries of European corrosion work, copper is not believed to be susceptible to these under relevant conditions.

Repository/ Storage setting	Additional research needs	Priority	Recommendation
Salt	Brine migration. Accurate estimates of brine volume/composition are required to estimate performance of both corrosion allowance and corrosion resistant materials in a salt repository.	High	Already a target for proposed work: field-scale heater test proposed by Salt Disposal Investigations program.
	Evaluation of the localized corrosion behavior of Ti99.8-Pd (Ti grade 7) in bedded salt brines.	Medium	Evaluation of Ti Grade 7 behavior in bedded salt brines would be useful, if a corrosion-resistant material were to be considered. However, existing repository concepts in salt rely mostly on the natural barrier, and consider only corrosion allowance materials, intended to last only the duration of the thermal pulse.
	Evaluation of BSK-3 waste package lifetimes.	Low	Specific to the German disposal concept. Also, it is not clear that the specific alloy to be used for BSK-3 has yet been chosen.
Unsat. xtln.	Localized corrosion of Alloy 22 under conditions of dust deliquescence: • Evaluation of conditions of LC initiation • Evaluation of stifling (is extent of corrosion limited by mass of corrosive agent?)	High	Being addressed by experiments already in progress by the Engineered Materials Performance work package. See Section 3.
	General corrosion of Alloy 22 in concentrated brines at elevated temperature • Corrosion rate as a function of brine composition • Temperature dependence	High	Being addressed by experiments already in progress by the Engineered Materials Performance work package (these experiments will be completed in FY12). See Section 3.
Unsat. xtln., Interim Storage	Corrosion of borated stainless steel • general corrosion rates • localized corrosion (particularly in contact with other, more noble metals) • thermal susceptibility (aging and phase stability) • fate of boron during corrosion	High	Will be evaluated in FY 12 by the Engineered Materials Performance work package. See Appendix A.
Interim storage	Atmospheric corrosion (including marine environment)	High	Will be evaluated in FY 12 by the Engineered Materials Performance work package. See Appendix A.
	Aqueous corrosion: general, localized (pitting, crevice), SCC, galvanic	High	Will be evaluated in FY 12 by the Engineered Materials Performance work package. See Appendix A.

Repository/ Storage setting	Additional research needs	Priority	Recommendation
Clay Granite Salt Unsat. xtln.	Improved use of archaeological analogs: • better characterization of corrosion rate (corrosion layer thickness), corrosion product mineralogy and structure • combination of analog data with thermodynamic calculations to better understand environmental factors	Medium	Insufficient resources to pursue at this time.
All	Model development: • Mechanistic models are required to enable accurate extrapolation of experimentally-determined corrosion rates to repository-relevant time scales. • More mechanistically-based corrosion models require a better understanding of corrosion processes.	High	Aspects will be addressed indirectly by Engineered Materials Performance work package planned FY 12 work (e.g., anoxic copper corrosion studies). See Appendix A.
	Effect of container fabrication and design on corrosion (e.g., SCC, LC of welded regions)	High	Some of this may be addressed in dust deliquescence and brine studies relevant to storage and unsaturated repository settings
	Determining the evolutionary path of the near-field environment through time, and its impact on corrosion.	High	Already being addressed by existing and planned work, by the Engineered Barrier System and Natural System near-field work packages.
	Radiolysis and radiation effects	Medium	Will not be pursued at this time. In anoxic repositories, reactive radicals generated by radiolysis may have a significant effect on corrosion rate. Under storage conditions, fluxes at the package surface can very high, and quite variable. However, radiolysis has not yet been identified as a major contributor to corrosion in any environment.

3.   Status Report on Existing Experimental Work

Existing experimental work at Sandia National Laboratories consists of two sets of experiments. The first consists of immersion tests, evaluating the long-term corrosion performance of Alloy 22 in hot brines. The second set of experiments evaluates the potential for corrosion due to brines formed by dust deliquescence, and also, the potential dependence of extent of corrosion on the mass of the active species present (e.g., the chloride deposited as salts on the metal surface). Both sets of experiments were initiated under the Yucca Mountain Program, but provide information relevant to repository disposal and interim storage conditions, and have been continued under the aegis of the Used Fuel Disposition/Radioactive Waste (RW) Science program.

3.1   Long Term Corrosion Performance of Alloy 22

Concerns exist as to the quality of the corrosion data collected at in the long term corrosion test facility (LTCTF) at Lawrence Livermore national Labs (LLNL), which were used to determine both the general corrosion rate as well as the temperature dependence of the general corrosion rate of Alloy 22 when exposed to repository relevant brines. To validate the results of that experimental program, a series of exposure tests were initiated at SNL. In these tests, Alloy 22 samples were prepared and then placed in solutions identified in the Yucca Mountain model report *General and Localized Corrosion of the Waste Package Outer Barrier* (SNL 2007b). These environments included 0.6M NaCl, simulated acidified water (SAW), and simulated concentrated water (SCW). Care was taken to insure each sample had a nominally identical surface finish, and had been chemically cleaned/passivated in the same manner prior to exposure. Exposure tanks consisted of glass vessels with appropriate heating controls, condensers to prevent water loss, etc., as illustrated in Figure 41.

The test program itself was initiated prior to the shutdown of the Yucca Mountain Project under Yucca Mountain QA procedures. The governing QA document is *Technical Work Plan: General and Localized Corrosion Testing of Waste Package and Drip Shield Materials* (SNL 2008b), and testing has been consistent with the procedures described in that document, with the exception of planned sampling times. As a result of the shutdown, funding was not available to remove samples at the prescribed time periods, and new time intervals have been chosen. Specimens will be removed after 3, 9, 18, and 24 months of exposure.
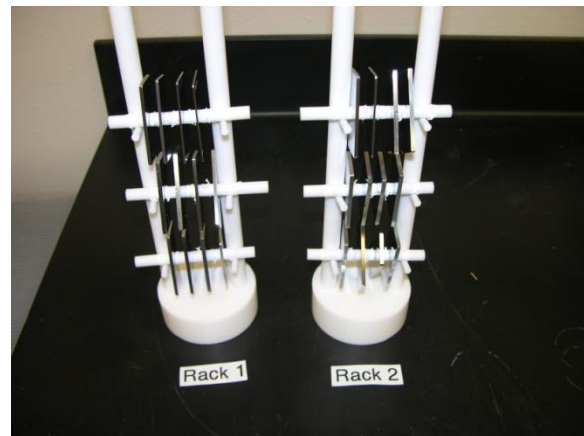
Figure 41.   Experimental configuration for long term corrosion performance testing, and polytetrafluoroethylene (Teflon®) sample racks used to suspend coupons within each container

The first set of coupons was removed at 9 months, and has been analyzed, for the most part, at this time. Analyses were performed following the methods defined in technical procedure *Cleaning Corrosion Resistant Metals Using a Hydrochloric Acid Bath* (SNL 2008a). The data are very reproducible, with little statistical variation from sample to sample. Figure 42 shows the weight changes observed for the specimens immersed in SAW at three different temperatures. Samples from the SCW solution are still being prepared, as a considerable quantity of precipitate formed on their surface. This precipitation was unexpected as the SCW formulation was recalculated after the LTCTF experiments (which had extensive precipitation). The precipitate composition is being analyzed, and a procedure to remove it without impacting the underlying metal substrate developed.

Future Direction

The 3 month samples will be backfilled into the solutions as space becomes available, and will be completed prior to FY12Q3. The 18 month samples are being removed at the beginning of FY12Q1, and the 24 month samples will be removed at the beginning of FY12Q3. This experimental program will then be concluded, and the results documented. A final report will be issued at the end of FY12Q3.
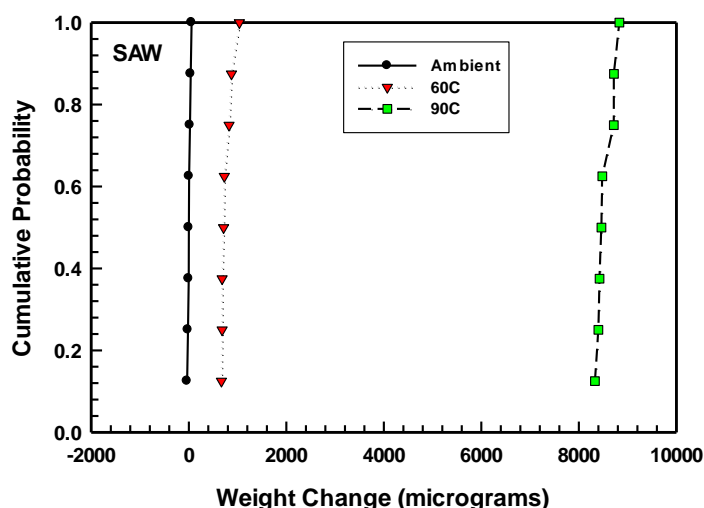
Figure 42.   Cumulative distribution plot of the weight change measured for coupons exposed to SAW for a period of 9 months

3.2   Evaluating the potential for corrosion due to brines formed by dust deliquescence

Any waste package or interim storage container which is exposed to the atmosphere will have particulates (i.e., dust) carried by the atmosphere deposited on its surface. A portion of most atmospheric dusts consists of soluble salts. It has been suggested by several researchers that these salts may combine to form deliquescent brines on the surface of a waste package at temperatures well above the boiling point of water, and further, that these brines might be corrosive depending on the material used to construct the package. Other researchers have suggested that for highly corrosion resistant/passive materials, several factors will prevent extensive localized corrosion due to deliquescence, including electrochemical limitations (e.g., insufficient cathode reaction area) and physical (e.g., limited amount of brine coupled with consumption or sequestration of aggressive species in the corrosion product).

In an effort to determine if there is indeed a potential for deliquescent brines to result in localized corrosion, a series of experiments have been (and continue to be) performed. Materials of interest have

been decorated with thin layers of salt in the presence of an occluded geometry in an effort to establish if localized corrosion (i.e., crevice corrosion) could initiate and propagate under such conditions. In these experiments, no inert species were added, and as such physical sequestration of the brine by the dust layer due to capillary forces have been eliminated, allowing all of the material deposited on the metal surface to participate in the corrosion reaction.

The chemical composition of the brines which can form is a function of temperature, as well as the available constituent materials. At very high temperatures, brines can only persist if they are very nitrate-rich, whereas at lower temperatures, the composition can be dominated by other species, such as chloride. In terms of the corrosiveness of the brine, both the chemistry (e.g., concentration of aggressive species) and the exposure temperature have a strong impact on corrosion processes.

This experimental program was conducted in accordance YMP QA procedures, under the following technical documents:

- *Technical Work Plan: Experimental Work to Support Evaluation of Dust-Deliquescence-Induced Screening Localized Corrosion of Alloy 22* (SNL 2006)

- *Technical Work Plan: General and Localized Corrosion Testing of Waste Package and Drip Shield Materials* (SNL 2008b).

Experiments have been performed in a multi-salt assemblage consisting of $NaCl$, $NaNO_3$, KNO_3, and $Ca(NO_3)_2$ with an overall nitrate to chloride ratio of 18. Samples of Hastelloy C22, Inconel 625, Hastelloy C276, and an 80:20 Ni:Cr alloy were evaluated. Each sample was polished to a mirror finish, loaded with salt to over 350 μg cm^{-2} on top of which a multi-crevice assembly was placed (Figure 43). Samples were then exposed to an environment at 180°C with a dewpoint of 94.5°C (tests were performed in Albuquerque, NM, and as such the boiling point of water is approximately 94.5°C and the environment was pure steam). After 30 days exposure, the samples were removed, the crevice formers taken off, and the extent of any crevice corrosion measured. In all cases, localized corrosion did not initiate on any of the materials. The experiment was then repeated at the same temperature with a slightly lower dewpoint (92°C) to determine if atmospheric oxygen was required for corrosion initiation. The test was run for 30 days, and again, no crevice corrosion initiation was observed on any of the materials.

At lower temperatures, closer to 100°C, it is possible to form a concentrated brine containing only chloride species. Mixtures of KCl and NaCl are capable of forming a brine at temperatures as high as 105°C. Experiments were performed in the same manner as those described above at a dewpoint of 94.5°C, only with a brine consisting only of KCl and NaCl at a temperature of 101°C for 100 days. In addition to the materials used in the four component, nitrate-chloride brine, 303SS was added to the test matrix. This is a free-machining stainless steel which is extremely susceptible to localized corrosion, and was selected to demonstrate that the test procedure could support localized corrosion for a sufficiently susceptible material. The test was run for a total of 100 days, and for the nickel based alloys, no discernable crevice corrosion was observed. The 303SS, however, did initiate localized corrosion for many of the teeth on the multiple crevice assembly (Figure 44).

Future Direction

Now that a system has been identified where localized corrosion can be readily initiated in a deliquescence formed brine, additional work is in progress to determine if the extent of attack is a function of the quantity of brine present on the metal surface. 303 and 304SS samples have been loaded with the NaCl:KCl salt mixture at 50, 100, and 200 μg cm^{-2} and placed again in an environment with a dewpoint of 94.5°C and a system temperature of 101°C. Upon completion of the exposure period (100 days, will complete in early FY12Q1), samples will be evaluated and it will be determined if the degree of attack is indeed a function of the quantity of reactant present at the onset of the experiment.
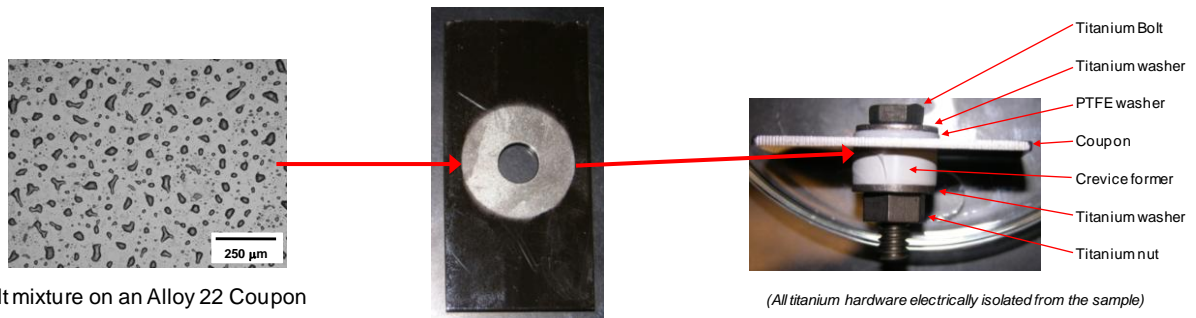
Figure 43.   Configuration of salt coated specimens used for crevice corrosion initiation studies
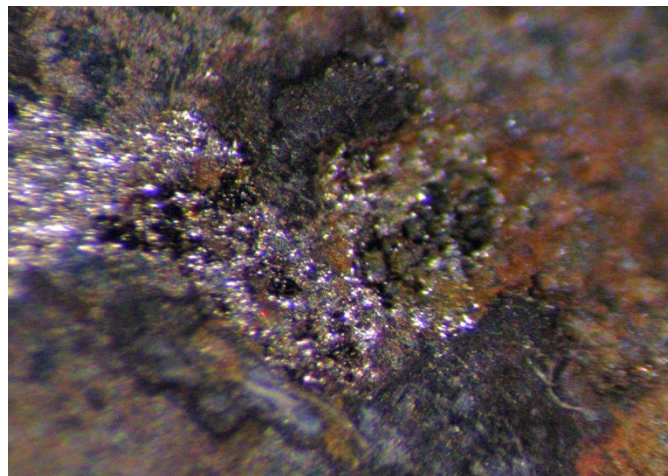
Figure 44.   Crevice corrosion initiated beneath the crevice former on a 303SS specimen. Sample had approximately 250 µg cm^{-2} NaCl/KCl deposited on the surface and was exposed to an environment with a temperature of 101°C and a dewpoint of 94.5°C for a period of 100 days

4. References

ACI.201.2R-67 (1967) *Guide to durable concrete.* Farmington, MI: American Concrete Institute.

ACI.301-66 (1966) *Standard specifications structural concrete for buildings.* Farmington, MI: American Concrete Institute.

ACI.318-63 (1963) *Building code requirements for reinforced concrete.* Farmington, MI: American Concrete Institute.

ACI.345-85 (1985) *Code requirements for nuclear safety related concrete structures.* Farmington, MI: American Concrete Institute.

Ahn, T. M. and Soo, P. (1982a) *Container assessment-corrosion study of HLW container materials: Quarterly progress report, July-September 1981*. NUREG/CR-2317, BNL NUREG-51449, Volume 1, no. 3, Upton, NY: Brookhaven National Laboratory.

Ahn, T. M. and Soo, P. (1982b) *Container assessment-corrosion study of HLW container materials: Quarterly progress report, October-December 1981*. NUREG/CR-2317, BNL NUREG-51449, Vol. 1, no. 4, Upton, NY: Brookhaven National Laboratory.

Ahn, T. M. and Soo, P. (1982c) *Container assessment-corrosion study of HLW container materials: Quarterly progress report, January-March 1982*. NUREG/CR-2317, BNL NUREG-51449, Vol. 2, no. 1, Upton, NY: Brookhaven National Laboratory.

Aida, T., Hara, T. and Kumanao, Y. (2010) *Operating experience in spent fuel storage casks*. IAEA-CN-178/KN27, Vienna: International Atomic Energy Agency.

Anderson, V. K. (2004) *An Evaluation of the Feasibility of Disposal of Nuclear Waste in Very Deep Boreholes*. M.Sc. M.Sc., Massachusetts Institute of Technology.

Andersson, J., Ahokas, H., Hudson, J. A., Koskinen, L., Luukkonen, A., Löfman, J., Keto, V., Pitkänen, P., Mattila, J., Ikonen, A. T. K. and Ylä-Mella, M. (2007) *Olkiluoto site description 2006*. POSIVA 2007-03, Olkiluoto: Posiva Oy.

ANDRA (2005a) *Dossier 2005 argile: Synthesis. Evaluation of the feasibility of a geological repository in an argillaceous formation. Meuse/Haute-Marne site*. France: ANDRA.

ANDRA (2005b) *Dossier 2005 argile: Tome. Architecture and management of a geological repository*. France: ANDRA.

ANDRA (2005c) *Dossier 2005 argile: Tome. Phenomenological evolution of a geological repository*. France: ANDRA.

ANDRA (2005d) *Dossier 2005 argile: Tome. Safety evaluation of a geological repository*. France: ANDRA.

ANDRA (2005e) *Dossier 2005 granite: Synthesis. Assets of granite formations for deep geological disposal*. France: ANDRA.

ANDRA (2005f) *Dossier 2005 granite: Tome: Architecture and management of a geological repository*. France: ANDRA.

ANDRA (2005g) *Dossier 2005 granite: Tome: Phenomenological evolution of a geological repository*. France: ANDRA.

ANDRA (2005h) *Dossier 2005 granite: Tome: Safety analysis of a geological repository*. France: ANDRA.

Andresen, P. L. (1991) Fracture mechanics data and modeling of environmental cracking of nickel-base alloys in high temperature water. Paper No. 44. *In: CORROSION 91 Conference*: Houston, TX: NACE International.

Andresen, P. L. and Ford, F. L. (1994) Fundamental modeling of environmental cracking for improved design and lIfetime evaluation in BWRs. *International Journal of Pressure Vessels and Piping* **59**(1-3)**,** 61-70.

Andresen, P. L. and Kim, Y. J. (2007) *Stress corrosion crack initiation and growth measurements in environments relevant to high-level nuclear waste packages: Final report for October 1, 2006-September 30, 2007*. GE-GRC-Sandia-2007-3, Niskayuna, NY: General Electric Global Research Center.

Andresen, P. L. and Kim, Y. J. (2010) *Stress corrosion crack initiation and growth measurements in environments relevant to high level nuclear waste packages: Status report on specimens tested and completion of experiments, August 23, 2010*. Niskayuna, NY: General Electric Global Research Center.

Anonymous. 2005. *Radioactive waste management programs in OECD/NEA member countries: Germany* [Online]. Available: www.oecd-nea.org/rwm/profiles. Downloaded June 22, 2011.

Anthony, T. R. and Cline, H. E. (1971) Thermal migration of liquid droplets through solids. *Journal of Applied Physics* **42**(9)**,** 3380-3387.

Anthony, T. R. and Cline, H. E. (1972) The thermomigration of biphase vapor-liquid droplets in solids. *Acta Metallurgica* **20**(2)**,** 247-255.

Anthony, T. R. and Cline, H. E. (1973) The stability of migrating droplets in solids. *Acta Metallurgica* **21**(2)**,** 117-122.

Arcos, D., Grandia, F. and Domènech, C. (2006) *Geochemical evolution of the near field of a KBS-3 repository*. SKB TR-06-16, Stockholm: Svensk Karnbranslehantering AB.

Ashida, Y., McMillion, L. G. and Misra, M. (2008) Communication C: A heated electrode test system for studying corrosion behavior of Alloy 22. *In:* Lattefer, A. P. (ed.) *Nuclear waste research: Siting, technology and treatment.* Hauppauge, NY: Nova Science Publishers, Inc. pp. 25-36.

ASM International (1987) Corrosion. *ASM handbook. Formerly 9th edition, metals handbook.* **13**. Materials Park, OH: ASM International.

ASTM.C1553-08 (2008) *Standard guide for drying behavior or spent nuclear fuel* American Society for Testing and Materials.

ASTM.C1562-10 (2010) *Standard guide for the evaluation of materials used in extended service of interim spent nuclear fuel dry storage.* American Society for Testing and Materials.

Baes, C. F., Jr. and Mesmer, R. E. (1976) *The hydrolysis of cations.* New York, NY: John Wiley and Sons.

Belonoshko, A. B. and Rosengren, A. (2010) Ab initio study of water interaction with a Cu surface. *Langmuir* **26**(21)**,** 16267-16270.

Bennett, D. G. and Gens, R. (2008) Overview of European concepts for high-level waste and spent fuel disposal with special reference waste container corrosion. *Journal of Nuclear Materials* **379**(1-3)**,** 1-8.

Bildstein, O., Trotignon, L., Perronnet, M. and Jullien, M. (2006) Modelling iron-clay interactions in deep geological disposal conditions. *Physics and Chemistry of the Earth* **31**(10-14)**,** 618-625.

Bischoff, J. L. and Seyfried, W. E. (1978) Hydrothermal chemistry of from 25° to 350 °C. *American Journal of Science* **278**(6)**,** 838-860.

Blanchard, D. C. and Woodcock, A. H. (1980) The production, concentration, and vertical distribution of sea-salt aerosol. *Annals of the New York Academy of Sciences* **338,** 330-347.

Boegly, W. J., Jr., Bradshaw, R. L., Empson, F. M., W.F. Schaffer, J., Parker, F. L. and Blomeke, J. O. (1966) Project Salt Vault: A demonstration disposal of high-level radioactive solids in Lyons, Kansas, salt mine. *Health Physics* **12,** 417-424.

Bollingerfehr, W., Filbert, W., Wehrmann, J. and Bosgiraud, J.-M. (2008) New transport and emplacement technologies for vitrified waste and spent fuel canisters. 20-23 October. *In: Euradwaste '08*, Luxembourg.

Bollingerfehr, W., Filbert, W., Bosgiraud, J.-M. and Haverkate, B. (2009) *Deliverable 8 of module 2-WP7 evaluation and final report*. FI6W-CT-2003-508851:

Bottomley, D. J., Gregoire, D. C. and Raven, K. G. (1994) Saline groundwaters and brines in the Canadian Shield - geochemical and isotopic evidence for a residual evaporite brine component. *Geochimica et Cosmochimica Acta* **58**(5)**,** 1483-1498.

Bradbury, M. H. and Baeyens, B. (2002) *Porewater chemistry in compacted re-saturated MX-80 bentonite: Physico-chemical characterisation and geochemical modelling*. Nr. 02-10: PSI Bericht/NAGRA.

Bradshaw, R. L. and Sanchez, F. (1969) Migration of brine cavities in rock salt. *Journal of Geophysical Research* **74**(17)**,** 4209-4212.

Bradshaw, R. L. and McClain, W. C. (eds.) (1971) *Project Salt Vault: A demonstration of the disposal of high-activity solidified wastes in underground salt mines.* Oak Ridge, TN: Oak Ridge National Laboratory. ORNL 4555.

Brady, P. V., Arnold, B. W., Freeze, G. A., Swift, P. N., Bauer, S. J., Kanney, J. L., Rechard, R. P. and Stein, J. S. (2009) *Deep borehole disposal of high-level radioactive waste*. SAND2009-4401, Albuquerque, NM: Sandia National Laboratories.

Braithwaite, J. W., Magnani, N. J. and Munford, J. W. (1979) Titanium alloy corrosion in nuclear waste environments. SAND79-2023C. March 3-7, 1980. *In: Corrosion '80*, Chicago, IL.

Braithwaite, J. W. and Molecke, M. A. (1980) Nuclear waste canister corrosion studies pertinent to geologic isolation. *Nuclear and Chemical Waste Management* **1,** 37-50.

Bram, K., Draxler, J., Hirschmann, G. and Zoth, G. (1995) The KTB Borehole- Germany's Superdeep Telescope into the Earth's Crust. *Oilfield Review.* Schlumberger.

Briant, C. L., Mulford, R. A. and Hall, E. L. (1982) Sensitization of austenitic stainless-steels.1. Controlled purity alloys. *Corrosion* **38**(9)**,** 468-477.

Brossia, C. S. and Cragnolino, G. A. (2000) *Effects of environmental, electrochemical, and metallurgical variables on the passive and localized dissolution of Ti Grate 7*. CORROSION/2000. Paper No. 00211, Houston, TX: NACE International.

Brossia, C. S., Browning, L., Dunn, D. S., Moghissi, O. C., Pensado, O. and Yang, L. (2001) *Effect of environment on the corrosion of waste package and drip shield materials*. CNWRA 2001-003, San Antonio, TX: CNWRA.

Brush, L. H., Grbic-Galic, D., Reed, D. T., Tong, X., Vreeland, R. H. and Westerman, R. E. (1990) Preliminary predictions of repository chemistry for the Waste Isolation Pilot Plant. *Abstracts with Programs, Geological Society of America 1990 Annual Meeting, Dallas, TX, October 29-November 1, 1990.* A100. ERMS 224891. SAND90-1695A.

Brush, L. H. (1990) *Test plan for laboratory and modeling studies of repository and radionuclide chemistry for the Waste Isolation Pilot Plant*. SAND90-0266, Albuquerque, NM: Sandia National Laboratories.

Brush, L. H. (1995) *Systems prioritization method - iteration 2 baseline position paper: Gas generation in the Waste Isolation Pilot Plant*. March 17, 1995. ERMS 228740, Albuquerque, NM: Sandia National Laboratories.

Brush, L. H., Garner, J. W. and Storz, L. J. (1994) Development of a gas generation model for the Waste Isolation Pilot Plant. SAND93-1145C. *In:* Barkatt, A. and Konynenburg, R. A. V. (eds.) *Scientific Basis for Nuclear Waste Management XVII.* **333**. Pittsburgh, PA: Materials Research Society. 214-246.

Brush, L. H., Molecke, M. A., Lappin, A. R., Westerman, R. E., Tong, X., Black, J. N. P., Grbic-Galic, D., Vreeland, R. E. and Reed, D. T. (1991b) Laboratory and bin-scale tests of gas generation for the Waste Isolation Pilot Plant. SAND91-2378. *In:* Davies, P. B., Brush, L. H., Molecke, M. A., Mendenhall, F. T. and Webb, S. W. (eds.) *Waste-generated gas at the Waste Isolation Pilot Plant: Papers presented at the Nuclear Energy Agency Workshop on Gas Generation and Release from Radioactive Repositories.* Albuquerque, NM: Sandia National Laboratories. 2-1 to 2-14.

Brush, L. H., Molecke, M. A., Westerman, R. E., Francis, A. J., Gillow, J. B., Vreeland, R. H. and Reed, D. T. (1993) Laboratory studies of gas generation for the Waste Isolation Pilot Plant. SAND92 2160C. *In:* Interrante, C. G. and Pabalan, R. T. (eds.) *Scientific Basis for Nuclear Waste Management XIV.* **294**. Pittsburg, PA: Materials Research Society. 335-340.

Brush, L. H., Grbic-Galic, D., Reed, D. T., Tong, X., Vreeland, R. H. and Westerman, R. E. (1991a) Preliminary results of laboratory studies of repository chemistry for the Waste Isolation Pilot Plant. SAND90-1031C. *In:* T. Abrajano, J. and Johnson, L. H. (eds.) *Scientific Basis for Nuclear Waste Management XIV.* **212**. Pittsburg, PA: Materials Research Society. 893-900.

BSC (2004) *Aging and phase stability of waste package outer barrier*. ANL-EBS-MD-000002 Rev 02 September 2004, Las Vegas, NV: Bechtel SAIC Company.

BSC (2005) *Analysis of dust deliquescence for FEP screening*. ANL-EBS-MD-000074 Rev 01, Las Vegas, NV: Bechtel SAIC Company.

BSC (2006) *Aqueous corrosion rates for waste package materials*. ANL-DSD-MD-000001 Rev 01, Las Vegas, NV: Bechtel SAIC Company.

BSC (2008) *Postclosure modeling and analyses design parameters*. TDR-MGR-MD-000037 Rev 02, Las Vegas, NV: Bechtel SAIC Company.

Bullen, D. B. and Gdowski, G. E. (1988) *Survey of degradation modes of candidate materials for high-level radioactive-waste disposal containers- Volume 1 phase stability*. UCID-21362 Vol. 1:

Buscheck, T. A., Rosenberg, N. D., Blink, J. A., Sun, Y. and Gansemer, J. (2003) Analysis of thermohydrologic behavior for above-boiling and below-boiling thermal-operating modes for a repository at Yucca Mountain. *Journal of Contaminant Hydrology* **62**(3)**,** 441-457.

Carter, N. L. and Hansen, F. D. (1983) Review: Creep of rocksalt. *Tectonophysics* **92**(4)**,** 275-333.

Caseres, L. and Mintz, T. S. (2010) *Atmospheric stress corrosion cracking susceptibility of welded and unwelded 304, 304L, and 316L austenitic stainless steels commonly used for dry cask storage containers exposed to marine environments* NUREG/CR-7030, Washington, DC: Office of Nuclear Regulatory Research, U.S. Nuclear Regulatory Commission.

Chivot, J. (2004) Thermodynamique des produits de corrosion: Fonctions thermodynamiques, diagrammes de solubilité, diagrammes E-pH des systèmes Fe-H2O, Fe-CO2-H2O, Fe S H2O, Cr-H2O, et Ni-H2O en fonction de la température. *Collection sciences et techniques.* Châtenay-Malabry, France: Agence National pour la Gestion des Déchets Radioactifs.

Claret, F., Sakharov, B. A., Drits, V. A., Velde, B., Meunier, A., Griffault, L. and Lanson, B. (2004) Clay minerals in the Meuse-Haute marne underground laboratory (France): Possible influence of organic matter on clay mineral evolution. *Clays and Clay Minerals* **52**(5)**,** 515-532.

Cline, H. E. and Anthony, T. R. (1972) Effects of the magnitude and crystallographic direction of a thermal gradient on droplet migration in solids. *Journal of Applied Physics* **43**(1)**,** 10-15.

Cline, H. E. and Anthony, T. R. (1977) Nonequilibrium morphology of liquid inclusions migrating in solids. *Journal of Applied Physics* **48**(12)**,** 5096-5104.

Costa, D. and Marcus, P. (1993) Modification of passive films formed on Ni-Cr-Fe alloys with choromium content in the alloy and effects of adsorbed or segregated sulphur. *In: European Symposium on Modifications of Passive Film*, Paris, France. London, England: Institute of Materials, Minerals, and Mining. 17-25.

Craeye, B., De Schutter, G., Van Humbeeck, H. and Van Cotthem, A. (2009) Early age behaviour of concrete supercontainers for radioactive waste disposal. *Nuclear Engineering and Design* **239**(1)**,** 23-35.

Cragnolino, G. A., Dunn, D. S., Brossia, C. S., Jain, V. and Chan, K. S. (1999) *Assessment of performance issues related to alternate engineering barrier system materials and design options*. CNWRA 99-003, San Antonio, TX: Center for Nuclear Waste Regulatory Analyses.

Curti, E. and Wersin, P. (2002) *Assessment of porewater chemistry in the bentonite backfill for the Swiss SF / HLW repository*. Nagra Technical Report NTB 02-09, Wettingen, Switzerland: NAGRA.

Davies, P. B., Brush, L. H. and Mendenhall, F. T. (1991) Assessing the impact of waste generated gas from the degradation of transuranic waste at the Waste Isolation Pilot Plant (WIPP): An overview of strongly coupled chemical, hydrologic, and structural processes. SAND91-2378. *In:* Davies, P. B., Brush, L. H., Molecke, M. A., Mendenhall, F. T. and Webb, S. W. (eds.) *Waste-generated gas at the Waste Isolation Pilot Plant: Papers presented at the Nuclear Energy Agency Workshop on Gas Generation and Release from Radioactive Repositories.* Albuquerque, NM: Sandia National Laboratories. 1-1 to 1-24.

DBE. 2011. German Company for the Construction and Operation of Waste Repositories. Available: http://www.dbe.de/en/sites/index.php. Downloaded June 15, 2011.

De Las Cuevas, C. and Pueyo, J. J. (1995) The influence of mineralogy and texture in the water content of rock salt formations. Its implication in radioactive waste disposal. *Applied Geochemistry* **10**(3)**,** 317-327.

Dillmann, P., Béranger, G., Piccardo, P. and Matthieson, H. (2007) *Corrosion of Metallic Heritage Artefacts: Investigation, Conservation, and Prediction of Long-term Behavior.* Woodhead Publishing Limited.

Dixit, S., Roberts, S., Evans, K., Wolery, T. and Carroll, S. (2006) *General corrosion and passive film stability-FY05 summary report*. UCRL-TR-217393, Livermore, CA: Lawerence Livermore National Laboratory.

DOE (1986) *Recommendation by the Secretary of Energy of candidate sites for site characterization for the first radioactive-waste repository*. DOE/S-0048, Washington, DC: U.S. Department of Energy.

DOE (1996) *Title 40 CFR Part 191 compliance certification application for the Waste Isolation Pilot Plant, Vol. 1-21*. DOE/CAO-1994-2184, Carlsbad, NM: Carlsbad Area Office, U.S. Department of Energy.

DOE (2004) *Title 40 CFR part 191 subparts B and C compliance recertification application for the Waste Isolation Pilot Plant, vols. 1-8*. DOE/WIPP 2004-3231, Carlsbad, NM: Carlsbad Field Office, U.S. Department of Energy.

DOE (2008) *Transportation, aging and disposal canister system performance specification*. DOE/RW-0585 WMO-TADCS-000001Rev1/ICN1 March 2008: US Department of Energy Office of Civilian Radioactive Waste Management.

DOE (2009) *Title 40 CFR Part 191 Subparts B and C Compliance Recertification Application for the Waste Isolation Pilot Plant*. DOE/WIPP 09-3424, Carlsbad, NM: Department of Energy Carlsbad Field Office.

DOE (2011) *A management proposal for salt disposal investigations with a field scale heater test at WIPP*. DOE/CBFO-11-3470, Carlsbad, NM: Carlsbad Field Office, U.S. Department of Energy.

Dosch, R. G. (1976) *Analytical work in development of synthetic brine compositions. Memorandum to M.A. Molecke, October 12, 1976*. Albuquerque, NM: Sandia National Laboratories.

Drake, H. and Tullborg, E.-L. (2009) *Fracture Mineralogy Laxemar. Site descriptive modelling SDM-Site Laxemar*. SKB-R-08-99, Stockholm: Svensk Karnbranslehantering AB.

Dunn, D. S., Cragnolino, G. A. and Sridhar, N. (2000) An electrochemical approach to predicting long-term localized corrosion of corrosion-resistant high-level waste container materials. *Corrosion* **56,** 90-104.

Dunn, D. S., Pensado, O., Pan, Y.-M., Pabalan, R. T., Yang, L., He, X. and Chiang, K. T. (2005) *Passive and localized corrosion of alloy 22- modeling and experiments Rev. 01*. CNWRA 2005-002, San Antonio, TX: Center for Nuclear Waste Regulatory Analyses.

Dunn, D. S., Pensado, O., Pan, Y. M., Yang, L. T. and He, X. (2006) Modeling corrosion processes for alloy 22 waste packages. *In:* VanIseghem, P. (ed.) *Scientific Basis for Nuclear Waste Management XXIX*. **932**. pp. 853-860.

Elbiache, A. and Marcus, P. (1992) The role of molybdenum in the dissolution and the passivation of stainless-steels with adsorbed sulfur. *Corrosion Science* **33**(2)**,** 261-269.

Emmerich, R., Ensinger, W. and Enders, B. (2004) Corrosion behavior or borated aluminium used as a neutron absorber. 20-24 September 2004. *In: PATRAM*, Berlin, Germany.

EPA (1998) 40 CFR 194, Criteria for the certification and recertification of the Waste Isolation Pilot Plant's compliance with the disposal regulations: Certification decision: Final rule. *Federal Register* **63,** 27354-27406.

EPA (2006) 40 CFR 194, Criteria for the certification and recertification of the Waste Isolation Pilot Plant's compliance with the disposal regulations: Recertification decision: Final notice. *Federal Register* **71**(68)**,** 18010-18021.

EPA (2010a) 40 CFR 194, Criteria for the certification and recertification of the Waste Isolation Pilot Plant's compliance with the disposal regulations: Recertification decision. *Federal Register* **75**(222)**,** 70584-70595.

EPRI (2002a) *Technical bases for extended dry storage of spent nuclear fuel*. TR-1003416, Palo Alto, CA: EPRI.

EPRI (2002b) *Evaluation of the proposed high-level radioactive waste repository at Yucca Mountain using total system performance assessment, phase 6*. EPRI-TR-1003031, Palo Alto, CA: Electric Power Research Institute.

Everitt, R. A. and Lajtai, E. Z. (2004) The influence of rock fabric on excavation damage in the Lac du Bonnett granite. *International Journal of Rock Mechanics and Mining Sciences* **41**(8)**,** 1277-1303.

Farmer, J. C., McCright, R. D. and Kass, J. N. (1988) *Survey of degradation modes of candidate materials for high-level radioactive-waste disposal containers- vol. 3 overview*. UCID-21362 Overview:

Féron, D. and Macdonald, D. D. (eds.) (2003) *Prediction of long term corrosion behavior in nuclear waste systems.* European Federation of Corrosion and Maney Publishing.

Féron, D., Crusset, D., Gras, J. M. and Macdonald, D. D. (eds.) (2005) *Second International Workshop 'Prediction of Long Term Corrosion Behaviour in Nuclear Waste Systems.* Chatenay-Malabry: ANDRA.

Féron, D., Crusset, D. and Gras, J. M. (2008) Corrosion issues in nuclear waste disposal. *Journal of Nuclear Materials* **379**(1-3)**,** 16-23.

Féron, D., Crusset, D. and Gras, J. M. (2009) Corrosion Issues in the French High-Level Nuclear Waste Program (reprinted from proceedings of the CORROSION/2008 Research Topical Symposium). *Corrosion* **65**(3)**,** 213-223.

Fix, D. V., Estill, J. C., Wong, L. L. and Rebak, R. B. (2004) *General and localized corrosion of austenitic and borated stainless steels in simulated concentrated ground waters*. San Diego, CA: ASME-Pressure Vessels and Piping.

Ford, F. L. and Andresen, P. L. (1998) Development and use of a predictive model of crack propagation in 304/316L, A533B/A508, and Inconel 600/182 alloys in 288°C water. 30 August - 3 September. *In:* Weeks, J. R. and Theus, G. J., eds. *Third International Symposium on Environmental Degradation of Materials in Nuclear Power Systems—Water Reactors*, Traverse City, MI. Warrendale, PA: The Metalurgical Society. 789-800.

Francis, A. J. and Gillow, J. B. (1994) *Effect of microbial processes on gas generation under expected Waste Isolation Pilot Plant repository conditions: Progress report through 1992*. SAND93-7036, Albuquerque, NM: Sandia National Laboratories.

Francis, A. J. and Gillow, J. B. (1997) *Microbial gas generation under expected Waste Isolation Pilot Plant repository conditions*. SAND96-2582, Albuquerque, NM: Sandia National Laboratories.

Francois, B., Laloui, L. and Laurent, C. (2009) Thermo-hydro-mechanical simulation of ATLAS in situ large scale test in Boom Clay. *Computers and Geotechnics* **36**(4)**,** 626-640.

Freeze, G., Mariner, P., Houseworth, J. E. and Cunnane, J. C. (2010) *Used Fuel Disposition Campaign features, events, and processes (FEPs): FY10 progress report*. SAND2010-5902, Albuquerque, NM: Sandia National Laboratories.

Freeze, G. A., Larson, K. W. and Davies, P. B. (1995a) *Coupled multiphase flow and closure analysis of repository response to waste-generated gas at the Waste Isolation Pilot Plant (WIPP)*. SAND93-1986, Albuquerque, NM: Sandia National Laboratories.

Freeze, G. A., Larson, K. W. and Davies, P. B. (1995b) *A summary of methods for approximating salt creep and disposal room closure in numerical models of multiphase flow*. SAND94-0251, Albuquerque, NM: Sandia National Laboratories.

Garisto, F., Kempe, T. and Gierszewski, P. (2009) *Technical Summary of the Safety Aspects of the Deep Geological Repository Concept for Used Nuclear Fuel*. NWMO TR-2009-12, Toronto: Nuclear Waste Management Organization.

Gascoyne, M. and Manineni, D. C. (1994) The hydrogeochemistry of fractured plutonic rocks in the Canadian Shield. *Applied Hydrogeology* **2,** 43-49.

Gascoyne, M. (2004) Hydrogeochemistry, groundwater ages and sources of salts in a granitic batholith on the Canadian Shield, southeastern Manitoba. *Applied Geochemistry* **19**(4)**,** 519-560.

Gaudin, A., Gaboreau, S., Tinseau, E., Bartier, D., Petit, S., Grauby, O., Foct, F. and Beaufort, D. (2009) Mineralogical reactions in the Tournemire argillite after in-situ interaction with steels. *Applied Clay Science* **43**(2)**,** 196-207.

Gdowski, G. E. and Bullen, D. B. (1988) *Oxidation and corrosion – vol 2*. UCID-21362.

Gibb, F. G. F. (2000) A new scheme for the very deep geological disposal of high-level radioactive waste. *Journal of the Geological Society, London* **157,** 27-36.

Gibb, F. G. F., McTaggart, N. A., Travis, K. P., Burley, D. and Hesketh, K. W. (2008) High-density support matrices: Key to the dee borehole disposal of spent fuel. *Journal of Nuclear Materials* **374**370-377.

Gillow, J. B. and Francis, A. J. (2003) *Microbial gas generation under expected Waste Isolation Pilot Plant repository conditions: Draft final report, rev. 0, October 6, 2003*. ERMS 532877, Upton, NY: Brookhaven National Laboratory.

Gmal, B., Hummelsheim, K., Kilger, R., Moser, E. F. and Thiel, J. (2003) Current activities in criticality analyses for final disposal of spent fuel and fissile material containing waste in Germany. 20-24 October. *In: 7th International Conference on Nuclear Criticality Safety*, Tokai-mura, Japan.

Grambow, B., Loida, A. and Smailos, E. (1998) Long-term stability of spent nuclear fuel waste packages in Gorleben salt repository environments. *Nuclear Technology* **121,** 174-188.

Grauer, R., Knecht, B., Kreis, P. and Simpson, J. P. (1991) Hydrogen evolution from corrosion of iron and steel in intermediate level waste repositories. *In:* T.A. Abrajano, J. and Johnson, L. H. (eds.) *Scientific Basis for Nuclear Waste Management XIV.* **44**. Pittsburgh, PA: Materials Research Society. 295-302.

Graver, D. L. (1984) Hydrogen permeation and embrittlement of some nickel alloys. *In: Corrosion of Nickel-Based Alloys*, Metals Park, OH. American Society for Metals. 79-85.

Gray, J. J., Hayes, J. R., Gdowski, G. E., Viani, B. E. and Orme, C. A. (2006) Inhibiting effects of nitrates on the passive film breakdown of Alloy 22 in chloride environments. *Journal of the Electrochemical Society* **153**(5)**,** B156-B161.

Groat, C. G. (1981) Rig lost; lake fills salt mine. *Geotimes* **26**(3)**,** 14.

Haberman, J. H. and Frydrych, D. J. (1988) Corrosion studies of A216 grade WCA steel in hydrothermal magnesium-containing brines. *In:* Apted, M. J. and Westerman, R. E. (eds.) *Scientific Basis for Nuclear Waste Management XI.* **112**. Pittsburgh, PA: Materials Research Society. 761-772.

Hadley, G. R. (1981) *SALT BLOCK II: Brine migration modeling*. SAND81-0433, Albuquerque, NM: Sandia National Laboratories.

Hadley, G. R. and Faris, G. W. (1981) *Revised theory of water transport in rock salt*. SAND80–2398, Albuquerque, NM: Sandia National Laboratories.

Hanson, B., Stockman, C., Alsaed, H., Enos, D., Meyer, R. and Sorenson, K. (2011) *Gap analysis to support extended storage of used nuclear fuel*. FCRD-USED-2011-000136: U.S. Department of Energy.

Hautevelle, Y., Michels, R., Malartre, F., Elie, M. and Trouiller, A. (2007) Tracing of variabilities within a geological barrier by molecular organic geochemistry. Case of the Callovo-Oxfordian sedimentary series in the East of the Paris Basin (France). *Applied Geochemistry* **22**(4)**,** 736-759.

He, X. and Dunn, D. S. (2006) *Crevice corrosion penetration rates of Alloy 22 in chloride-containing waters–progress report*. CNWRA 2006-001, San Antonio, TX: Center for Nuclear Waste Regulatory Analyses.

He, X. (2008) Corrosion performance of neutron-absorbing borated stainless steel. 24 June, 2008. *In: Presented to ASTM C26 – nuclear fuel cycle C260300 subcommittee on neutron absorber materials*.

He, X., Brettmann, B. and Jung, H. (2009) Effects of test methods on crevice corrosion repassivation potential measurements of Alloy 22. *Corrosion* **65**(7)**,** 449-460.

Hoag, C. I. (2006) *Canister design for deep borehole disposal of nuclear waste*. M.Sc., Massachusetts Institute of Technology.

Hoekstra, P., Osterkamp, T. E. and Weeks, W. F. (1965) The migration of liquid inclusions in single ice crystals. *Journal of Geophysical Research* **70**(20)**,** 5035-5041.

Hohlfelder, J. J. and Hadley, G. R. (1979) Laboratory studies of water transport in rock salt. *Letters in Heat and Mass Transfer* **6**(4)**,** 271-279.

Holtec-International (2000) *Final safety analysis report for the HI-STORM 100 cask system*. USNRC Docket No. 72-1014, Holtec Report Number HI-2002444, Marlton, NJ: U.S. Nuclear Regulatory Comission.

Hua, F. and Gordon, G. (2004) Corrosion behavior of alloy 22 and Ti Grade 7 in a nuclear waste repository environment. *Corrosion* **60**(8)**,** 764-777.

Hultquist, G. (1986) Hydrogen evolution in corrosion of copper in pure water. *Corrosion Science* **26**(2)**,** 173-177.

Hultquist, G., Szakálos, P., Graham, M. J., Sproule, G. I. and Wikmark, G. (2008) Detection of hydrogen in corrosion of copper in pure water. *In: 17th International Corrosion Conference*.

Hultquist, G., Szakalos, P., Graham, M. J., Belonoshko, A. B., Sproule, G. I., Grasjo, L., Dorogokupets, P., Danilov, B., Aastrup, T., Wikmark, G., Chuah, G. K., Eriksson, J. C. and Rosengren, A. (2009) Water corrodes copper. *Catalysis Letters* **132**(3-4)**,** 311-316.

Hultquist, G., Szakalos, P., Graham, M. J., Belonoshko, A. B. and Rosengren, A. (2010) Reply to Lars O. Werme et al.: "Comments on 'water corrodes copper'". *Catalysis Letters* **135**(3-4)**,** 167-168.

Hultquist, G., Graham, M. J., Szakalos, P., Sproule, G. I., Rosengren, A. and Grasjo, L. (2011) Hydrogen gas production during corrosion of copper by water. *Corrosion Science* **53**(1)**,** 310-319.

Hunkeler, F. and Boehni, H. (1983) Pit growth measurements on stainless steels. 30 May- 3 June. *In:* Froment, M., ed. *Fifth International Symposium on Passivity*, Bombannes, France. New York City, NY: Elsevier. 655-660.

Hur, D. H. and Park, Y. S. (2006) Effect of temperature on the pitting behavior and passive film characteristics of alloy 600 in chloride solution. *Corrosion* **62**(9)**,** 745-750.

Husain, A. and Choi, K. (2003) *Status of storage, disposal and transportation containers for the management of used nuclear fuel*. Nuclear Waste Managment Organization. Organization, N. W. M.

Hwang, Y., Chambré, P. L., Pigofrd, T. H. and Lee, W. W.-L. (1990) Brine migration in a salt repository. *Nuclear Technology* **90,** 205-214.

Janberg, K. and Spilker, H. (1998) Status of the development of final disposal casks and prospects in Germany. *Nuclear Technology* **121,** 136-147.

Janecky, D. R. and Seyfried, W. E. J. (1983) The solubility of magnesium-hydroxide-sulfate-hydrate in seawater at elevated temperatures and pressures. *American Journal of Science* **283**(8)**,** 831-860.

Jenks, G. H. and Claiborne, H. C. (1981) *Brine migration in salt and its implications in the geologic disposal of nuclear waste*. ORNL 5318, Oak Ridge, TN: Oak Ridge National Laboratory.

Jockwer, N. (1981) Laboratory investigations of water content within rock salt and its behavior in a temperature field of disposed high level waste. *In:* Moore, J. G. (ed.) *Scientific Basis for Nuclear Waste Management, Proceedings of the Third International Symposium on the Scientific Basis for Nuclear Waste Management, as part of the Annual Meeting of the Materials Research Society.* **3**. New York, NY: Plenum Press. 35-40.

Johansson, L. G. (2008) Comment on "Corrosion of copper by water" Electrochem. Solid-State Lett., 10, C63, (2007). *Electrochemical and Solid State Letters* **11**(4)**,** S1-S1.

Jones, R. H. (1992) *Stress-corrosion cracking.* Materials Park, OH: ASM International.

Jove-Colon, C. (2011) *Disposal systems evaluations and tool development – engineered barrier tool system (EBS) evaluation*. SAND2010-8200:

Juhlin, C. and Sandstedt, H. (1989) *Storage of nuclear waste in very deep boreholes: Feasibility study and assessment of economic potential*. 89-39: Svensk Karnbranslehantering AB.

Jung, H., Mintz, T. S., Yang, L. and Ahn, T. (2008) *Long-term persistence of the passive film on Alloy 22 at elevated temperatures in the potential Yucca Mountain repository environment*. ML090220175 and ML090220186, Washington, DC: Nuclear Regulatory Commission.

Kain, R. M. (1990) Marine atmosphere corrosion cracking of austenic stainless steels. *Materials Performance* **29**(12)**,** 60-62.

Karnland, O. (2010) *Chemical and mineralogical characterization of the bentonite buffer for the acceptance control procedure in a KBS-3 repository*. SKB TR-10-60, Stockholm: Svensk Kärnbränslehantering AB.

King, F., Litke, C. D., Quinn, M. J. and Leneveu, D. M. (1995) The measurement and prediction of the corrosion potential of copper in chloride solutions a a function of oxygen concentration and mass-transfer coefficient. *Corrosion Science* **37**(5)**,** 833-851.

King, F. (2010) *Stress Corrosion Cracking of Carbon Steel Used Fuel Containers in a Canadian Deep Geological Repository in Sedimentary Rock*. NWMO TR-2010-21, Toronto: Nuclear Waste Management Organization.

King, F., Kolar, M., Vahanen, M. and Lilja, C. (2011) Modelling long term corrosion behaviour of copper canisters in KBS-3 repository. *Corrosion Engineering Science and Technology* **46**(2)**,** 217-222.

King, F., Ahonen, L., Taxén, C., Vuorinen, U. and Werme, L. (2001) *Copper corrosion under expected conditions in a deep geologic repository*. SKB TR-01-23, Stockholm: Svensk Kärnbränslehantering AB.

King, F., Lilja, C., Pedersen, K., Pitkänen, P. and Vähänen, M. (2010) *An update of the state-of-the-art report on the corrosion of copper under expected conditions in a deep geologic repository*. SKB TR-10-67, Stockholm: Svensk Kärnbränslehantering AB.

Kinnunen, P. (2006) *Stress corrosion cracking investigation of copper in groundwater with acetate ions*. Working Report 2006-18, Olkiluoto: Posiva Oy.

Knauth, L. P., Kumar, M. B. and Martinez, J. D. (1980) Isotope geochemistry of water in Gulf Coast salt domes. *Journal of Geophysical Research* **85**(B9)**,** 4863-4871.

Knauth, L. P. and Kumar, M. B. (1981) Trace water content in Louisiana salt domes. *Science* **213**(4511)**,** 1005-1007.

Knauth, L. P. and Kumar, M. B. (1983) Isotopic character and origin of brine leaks in the Avery Island Salt Mine, South Louisiana, U.S.A. *Journal of Hydrology* **66,** 343-350.

Korzhavyi, P. A. and Johansson, B. (2010) *Thermodynamic properties of copper compoounds with oxygen and hydrogen from first principles*. SKB TR-10-30, Stockholm: Svensk Kärnbränslehantering AB.

Kosaki, A. (2008) Evaluation method of corrosion lifetime of conventional stainless steel canister under oceanic air environment. *Nuclear Engineering and Design* **238**(5)**,** 1233-1240.

Krause, W. B. (1983) *Avery Island brine migration tests: installation, operation, data collection, and analysis*. ONWI-190(4), Columbus, OH: Office of Nuclear Waste Isolation, Battelle Project Management Division.

Krumhansl, J. L. (1989) *A review of near-field seawater-sediment interactions with application to subseabed disposal of nuclear waste*. SAND88-1156, Albuquerque, NM: Sandia National Laboratories.

Krumhansl, J. L., Kimball, K. M. and Stein, C. L. (1991) *Intergranular fluid compositions from the Waste Isolation Pilot Plant (WIPP), Southeastern New Mexico*. SAND90-0584, Albuquerque, NM: Sandia National Laboratories.

Kumar, M. B. and Martinez, J. D. (1981) Character of brines from the Belle Isle and Weeks Island salt mines, Louisiana, U.S.A. *Journal of Hydrology* **54,** 107-140.

Kumar, M. B. (1983) Character of meteoric leaks in the salt mines of South Louisiana, U.S.A. *Journal of Hydrology* **66**(4)**,** 351-368.

Kursten, B., Smailos, E., Azkarate, I., Werme, L., Smart, N. R. and Santarini, G. (2004a) *COBECOMA: State-of-the-art document on the COrrosion BEhaviour of COntainer MAterials. European Commission 5th Euratom Framework Programme, 1998-2002*. Contract no. FIKW-CT-20014-20138 Final Report: European Commission.

Kursten, B., Druyts, F. and Feron, D. (2011a) Long term prediction of corrosion damage in nuclear waste systems. *Corrosion Engineering Science and Technology* **46**(2)**,** 81-81.

Kursten, B., Druyts, F., MacDonald, D. D., Smart, N. R., Gens, R., Wang, L., Weetjens, E. and Govaerts, J. (2011b) Review of corrosion studies of metallic barrier in geological disposal conditions with respect to Belgian Supercontainer concept. *Corrosion Engineering Science and Technology* **46**(2)**,** 91-97.

Kursten, B., Smailos, E., Azkarate, I., Werme, L., Smart, N. R., Marx, G., Cuñado, M. A. and Santarini, G. (2004b) Corrosion evaluation of metallic materials for long-lived HLW/spent fuel disposal containers: Review of 15-20 years of research. *In:* Davies, C., ed. *Euradwaste '04 Radioactive Waste Management— Community Policy and Research Initiatives*, Luxembourg. European Commission.

Kursten, B. and Druyts, F. (2006) A review of corrosion considerations of container materials relevant to underground disposal of high-level radioactive waste in Belgium. *In:* VanIseghem, P. (ed.) *Scientific Basis for Nuclear Waste Management XXIX*. **932**. 805-812.

Kwong, G. M. (2011) *Status of corrosion studies for copper fuel containers under low salinity conditions*. NWMO TR-2011-14, Toronto: Nuclear Waste Management Organization.

Laaksoharju, M., Smellie, J., Tullborg, E.-L., Wallin, B., Drake, H., Gascoyne, M., Gimeno, M., Gurban, I., Hallbeck, L., Molinero, J., Nilsson, A.-C. and Waber, N. (2009) *Bedrock hydrogeochemistry Laxemar. Site descriptive modelling SDM-Site Laxemar*. SKB R-08-93, Stockholm: Svensk Karnnranslehantering AB.

Lagrou, D., Vandenberghe, N., Van Simaeys, S. and Hus, J. (2004) Magnetostratigraphy and rock magnetism of the Boom Clay (Rupelian stratotype) in Belgium. *Netherlands Journal of Geosciences-Geologie En Mijnbouw* **83**(3)**,** 209-225.

Lambert, S. J. (1979) *Mineralogical aspects of fluid migration in the Salt Block II Experiment*. SAND79–2423, Albuquerque, NM: Sandia National Laboratories.

Landolt, D., Davenport, A., Payer, J. and Shoesmith, D. (2009) *A review of materials and corrosion issues regarding canisters for disposal of spent fuel and high-level waste in Opalinus clay*. Technical Report 09-02, Wettingen: National Cooperative for the Disposal of Radioactive Waste

Lister, T. E., Mizia, R. E. and Birk, S. M. (2005) *Electrochemical testing of Ni-Cr-Mo-Gd alloys*. EXT-05-00713: INL.

Lister, T. E., Mizia, R. E., Ericksen, A. and Birk, S. M. (2007) *Electrochemical corrosion testing of borated stainless steel alloys*. EXT-07-12633: INL.

Lister, T. E., Mizia, R. E., Erickson, A. W. and Matteson, B. S. (2008) General and localized corrosion of borated stainless steel. *In: CORROSION*. NACE.

Litke, C. D. and Ikeda, B. M. (2011) *Status report on stress corrosion cracking behaviour of OFP copper in nitrite and ammonia solutions*. NWMO TR-2011-06, Toronto: Nuclear Waste Management Organization.

Lloyd, A. C., Shoesmith, D. W., McIntyre, N. S. and Noel, J. J. (2003) Effects of temperature and potential on the passive corrosion properties of alloys C22 and C276. *Journal of the Electrochemical Society* **150**(4)**,** B120-B130.

Lloyd, A. C., Noel, J. J., McIntyre, S. and Shoesmith, D. W. (2004) Cr, Mo and W alloying additions in Ni and their effect on passivity. *Electrochimica Acta* **49**(17-18)**,** 3015-3027.

Lorenzo de Mele, M. F. and Cortizo, M. C. (1999) Electrochemical behaviour of titanium in fluoride-containing saliva. *Journal of Applied Electrochemistry* **30**(1)**,** 95-100.

Maak, P., Birch, K. and Simmons, G. R. (2010) *Evaluation of Container Placement Methods for the Conceptual Design of a Deep Geological Repository*. NWMO TR-2010-20, Toronto: Nuclear Waste Management Organization.

Macdonald, D. D. and Urquidi-Macdonald, M. (1991) A coupled environment model for stress-corrosion cracking in sensitized Type-304 stainless-steel in LWR environments. *Corrosion Science* **32**(1)**,** 51-81.

MacDonald, D. D., Urquidi-MacDonald, M. and Lu, P.-C. (1994) The coupled environmental fractural model—a deterministic method for calculating crack growth rates. Paper No. 246. *In: CORROSION/1994*, Houston, TX. NACE International.

Macdonald, D. D., Saleh, A., Lee, S. K., Azizi, O., Rosas-Camacho, O., Al-Marzooqi, A. and Taylor, M. (2011) The electrochemistry of carbon steel in simulated concrete pore water in boom clay repository environments. *EPJ Web of Conferences* **12,** 04003.

Maes, A., Bruggeman, C., Van Geet, M., Deniau, I. and Largeau, C. (2004) Methodologies Developed to Identify the Source of Mobile Boom Clay Organic Matteer. *In:* Davies, C., ed. *Proceedings of the Sixth European Commission Conference on the Management and Disposal of Radioactive Waste, Euradwaste '04*, 417-424. Luxembourg: European Commission.

Manjanna, J., Kozaki, T. and Sato, S. (2009) Fe(III)-montmorillonite: Basic properties and diffusion of tracers relevant to alteration of bentonite in deep geological disposal. *Applied Clay Science* **43**(2)**,** 208-217.

Marcus, P. and Moscatelli, M. (1989) The role of alloyed molybdenum in the dissolution and the passivation of nickel-molybdenum alloys in the presence of adsorbed sulfur. *Journal of the Electrochemical Society* **136**(6)**,** 1634-1637.

Marcus, P. and Grimal, J. M. (1990) The antagonistic roles of chromium and sulfur in the passivation of Ni-Cr-Fe alloys studied by Xps and radiochemical techniques. *Corrosion Science* **31,** 377-382.

Marcus, P. (2001) Long-term extrapolation of passive behavior: Proceedings from an International Workshop on Long-Term Extrapolation of Passive Behavior. 19-20 July. *In: Nuclear Waste Technical Review Board Meeting*, Arlington, VA. 55-60.

Marshall, P. (1984) *Austenitic stainless steels*. London: Elsevier Publishers.

Marsic, N., Grundfelt, B. and Wiborgh, M. (2006) *Very deep hole concept thermal effects on groundwater flow*. SKB R-06-59, Stockholm, Sweden: Svensk Karnbranslehantering AB.

Martinez, J. D., et al., (1980) *An investigation of the utility of Gulf Coast salt domes for the storage or disposal of radioactive wastes: Technical progress report for the quarter, 1 July 30 September, 1980*. ONWI-9(4), Columbus, OH: Office of Nuclear Waste Isolation, Battelle Memorial Institute.

Matalucci, R. V., Christensen, C. L., Hunter, T. O., Molecke, M. A. and Munson, D. E. (1982) *Waste Isolation Pilot Plant (WIPP) research and development program in situ testing plan*. SAND81-2628, Albuquerque, NM: Sandia National Laboratories.

Mazurek, M. (2004) *Long-term used nuclear fuel waste management - geoscientific review of the sedimentary sequence in southern Ontario*. NWMO Background Papers 6. Technical Methods: Nuclear Waste Managment Organization.

Mendenhall, F. T., Butcher, B. M. and Davies, P. B. (1991) Investigations into the coupled fluid flow and mechanical creep closure behavior of waste disposal rooms in bedded salt. SAND91-2378. *In:* Davies, P. B., Brush, L. H., Molecke, M. A., Mendenhall, F. T. and Webb, S. W. (eds.) *Waste-generated gas at the Waste Isolation Pilot Plant: Papers presented at the Nuclear Energy Agency Workshop on Gas Generation and Release from Radioactive Repositories.* Albuquerque, NM: Sandia National Laboratories. 3-1 to 3-15.

Mintz, T. S. and Devine, T. M. (2004) Influence of surface films on the susceptibility of Inconel 600 to stress corrosion cracking. *Key Engineering Materials* **261-263,** 875-884.

Mintz, T. S. and He, X. (2009) Modeling of hydrogen uphill diffusion in dissimilar titanium welds. Paper No. 09430. *In: CORROSION/2009*, Houston, TX. NACE International.

Miserque, F., Huet, B., Azou, G., Bendjaballah, D. and L'Hostis, V. (2006) X-Ray photoelectron spectroscopy and electrochemical studies of mild steel FeE500 passivation in concrete simulated water. *Journal de Physique IV Proceedings* **136,** 89-97.

Mizia, R. E., Lister, T. E., Pinhero, P. J. and Trowbridge, T. L. (2005) *Localized corrosion of a neutron absorbing Ni-Cr-Mo-Gd Alloys*. Con-02578: INEEL.

Molecke, M. A. (1976) *Revised representative brines/solutions for WIPP experimentation. Memorandum to distribution, October 8, 1976*. Albuquerque, NM: Sandia National Laboratories.

Molecke, M. A., Schaefer, D. W., Glass, R. S. and Ruppen, J. A. (1981) *Sandia HLW canister/overpack studies applicable to a salt repository*. SAND81-1585, Albuquerque, NM: Sandia National Laboratories.

Molecke, M. A., Ruppen, J. A. and Diegle, R. B. (1982) *Materials for high level waste canister/overpacks in salt formations*. SAND82-0429, Albuquerque, NM: Sandia National Laboratories.

Molecke, M. A., Ruppen, J. A. and Diegle, R. B. (1983) Materials for high level waste canister/overpacks in salt formations. *Nuclear Technology* **63,** 476-506.

Molecke, M. A. (1983) *A comparison of brines relevant to nuclear waste experimentation*. SAND83-0516, Albuquerque, NM: Sandia National Laboratories.

Molecke, M. A. (1984) *Test plan: Waste package performance technology experiments for simulated DHLW*. Albuquerque, NM: Sandia National Laboratories.

Molecke, M. A. (1986) *Test plan: WIPP Materials Interface Interactions Test (MIIT)*. Albuquerque, NM: Sandia National Laboratories.

Molecke, M. A. and Avyle, J. V. D. (1988) *FY 1985 summary of WIPP waste package corrosion and metallurgy laboratory research*. SAND86-2636, Albuquerque, NM: Sandia National Laboratories.

Molecke, M. A., Sorensen, N. R. and Krumhansl, J. L. (1988) *Summary of WIPP materials interface interactions test data on metals interactions and leachate brine analyses*. SAND88-2023C, Albuquerque, NM: Sandia National Laboratories.

Molecke, M. A., Sorensen, N. R. and Wicks, G. G. (1993) *Waste Isolation Pilot Plant materials interface interactions test: Papers presented at the Commission of the European Communities Workshop on In Situ Testing of Radioactive Waste Forms and Engineered Barriers*. SAND93-1055, Albuquerque, NM: Sandia National Laboratories.

Montemor, M. F., Ferreira, M. G. S., Walls, M., Rondot, B. and Belo, M. C. (2003) Influence of pH on properties of oxide films formed on type 316L stainless steel, alloy 600, and alloy 690 in high-temperature aqueous environments. *Corrosion* **59**(1)**,** 11-21.

Moody, N. R., Robinson, S. L. and Greulich, F. A. (1985) *Hydrogen effects on TiCode-12 properties and microstructure*. SAND85–8203, Albuquerque, NM: Sandia National Laboratories.

Moody, N. R. and Robinson, S. L. (1986) *Compositional and microstructural effects on hydrogen embrittlement of ASTM grade 12 titanium (Ti—0.3 Mo—0.8 Ni)*. SAND85 8247, Albuquerque, NM: Sandia National Laboratories.

Mora, C. J. (1999) *Sandia and the Waste Isolation Pilot Plant, 1974-1999*. SAND99-1482, Albuquerque, NM: Sandia National Laboratories.

Mosser-Ruck, R., Cathelineau, M., Guillaume, D., Charpentier, D., Rousset, D., Barres, O. and Michau, N. (2010) Effects of temperature, pH, and iron/clay and liquid/clay ratios on experimental conversion of dioctahedral smectite to berthierine, chlorite, vermiculite, and saponite *Clays and Clay Minerals* **58**(2)**,** 280-291.

Muller, E. (1985) The transportation of brine inclusions in rock salt in a temperature field of a heat source. *Crystal Research Technology* **20**(5)**,** 677-682.

NAC (2004) *NAC-UMS, NAC universal MPC system final safety analysis report, rev. 4*. Docket Number 72-1025, Norcross, GA: Nuclear Assurance Corporation International.

Nagies, F. and Heusler, K. E. (1998) Corrosion of metallic materials in hot salt brines. *Electrochimica Acta* **43**(1-2)**,** 41-51.

NAGRA (2002a) *Project Opalinus Clay Safety Report: Demonstration of disposal feasibility for spent fuel, vitrified high-level waste and long-lived intermediate-level waste (Entsorgungsnachweis)*. **Technical Report 02-05**Wettingen, Switzerland: NAGRA (National Cooperative for the Disposal of Radioactive Waste). Waste), N. N. C. f. t. D. o. R.

NAGRA (2002b) *Project Opalinus Clay safety report: Demonstration of disposal feasibility for spent fuel, vitrified high-level waste and long-lived intermediate-level waste (Entsorgungsnachweis)*. Technical Report 02-05, Wettingen, Switzerland: NAGRA (National Cooperative for the Disposal of Radioactive Waste).

Naus, D. J. (2007) *Primer on durability of nuclear power plant reinforces concrete structures- a review of pertinent factors*. NUREG/CR-6927, ORNL/TM-2006/529, Washington, DC: U.S. Nuclear Regulatory Commission.

NEDRA (1992) *Characterization of crystalline rocks in deep boreholes. The Kola, Krivoy Rog and Tyrnauz boreholes*. 92-39, Stockholm: Svensk Karnbranslehantering AB.

NIREX (2004) *A review of the deep borehole disposal concept for radioactive waste*. N/108: NIREX.

Nowak, E. J. (1986) *Preliminary results of brine migration studies in the Waste Isolation Pilot Plant (WIPP)*. SAND86-0720, Albuquerque, NM: Sandia National Laboratories.

Nowak, E. J. and McTigue, D. F. (1987) *Interim results of brine transport studies in the Waste Isolation Pilot Plant (WIPP)*. SAND87-0880, Albuquerque, NM: Sandia National Laboratories.

NRC (2010) *Standard review plan for spent fuel dry storage systems at a general license facility - final report*. NUREG 1536, Washington, DC: U.S. Nuclear Regulatory Committee.

NRC (2011a) *Standard review plan for renewal of spent fuel dry cask storage system licenses and certificates of compliance*. NUREG-1927, Washington, DC: U.S. Nuclear Regulatory Commission.

NRC (2011b) *Three Mile Island Unit-2 ISFSI-NRC inspection report 070-020/2011-001 and notice of deviation*. Washington DC: U.S. Nuclear Regulatory Commission.

NRC (2011c) Technical evaluation report on the content of the U.S. Department of Energy's Yucca Mountain repository license application – postclosure volume: Repository safety after permanent closure.

NRC Committee on Radioactive Waste Management (1970) *Disposal of solid radioactive wastes in bedded salt deposits*. Washington, DC: National Academy Press.

NWTRB (2010) *Evaluation of the technical basis for extended dry storage and transportation of used nuclear fuel*. Arlington, VA: U.S. Nucelar Waste Technical Review Board.

Olander, D. R., Machiels, A. J., Balooch, M. and Yagnik, S. K. (1982) Thermal gradient migration of brine inclusions in synthetic alkali halide single crystals. *Journal of Applied Physics* **53**(1)**,** 669-681.

Olander, D. R. (1982) A model of brine migration and water transport in rock salt supporting a temperature gradient. *Nuclear Technology* **58,** 256-270.

Olander, D. R. (1984) *A study of thermal-gradient-induced migration of brine inclusions in salt: Final report*. BMI/ONWI-538, Columbus, OH: Office of Nuclear Waste Investigations, Battelle Memorial Institute.

Orme, C. A. (2005) *The passive film on Alloy 22*. UCRL–TR–215277, Livermore, CA: Lawrence Livermore National Laboratory.

Pastina, B. and Hellä, P. (2006) *Expected evolution of a spent nuclear fuel repository at Olkiluoto*. POSIVA 2006-05, Olkiluoto: Posiva Oy.

Pearson, F. J., Arcos, D., Bath, A., Boisson, J.-Y., Fernández, A. M., Gäbler, H.-E., Gaucher, E., Gautschi, A., Griffault, L., Herná, P. and Waber, H. N. (2003) *Mont Terri Project – geochemistry of water in the Opalinus Clay formation at the Mont Terri Rock Laboratory*. **5,** Bern

Peiffer, F. and Weber, S. (2010) Robustness, a design principle for the operation of a repository for heat-generating waste? March 7-11. *In: Waste Management 2010*, Phoenix, AZ.

Pensado, O., Dunn, D. S., Cragnolino, G. and Jain, V. (2002) *Passive dissolution of container materials—modeling and experiments*. CNWRA 2003-01, San Antonio, TX: Center for Nuclear Waste Regulatory Analyses.

Pigford, T. (1982) Migration of brine inclusions in salt. *Nuclear Technology* **56,** 93-101.

Pourbaix, M. (1974) *Atlas of electrochemical equilibria in aqueous solutions.* Houston, TX: NACE International.

Povich, M. J. (1978) Low-temperature sensitization of Type 304 stainless-steel. *Corrosion* **34**(2)**,** 60-65.

Poyet, S. (2006) The Belgian supercontainer concept: Study of the concrete buffer behaviour in service life. *Journal De Physique IV* **136,** 167-175.

Rebak, R. B. (2005) Factors affecting the crevice corrosion susceptibility of Alloy 22. Paper No. 05610. *In: CORROSION/2005* Houston, Texas. NACE International.

Roedder, E. and Belkin, H. E. (1979) *Fluid inclusions in salt from the Rayburn and Vacherie Domes, Louisiana*. Open-File Report no. 79-1675: U.S. Geological Survey.

Roedder, E. and Bassett, R. L. (1981) Problems in determination of the water content of rock salt samples and its significance in nuclear-waste storage siting. *Geology* **9**(11)**,** 525-530.

Roedder, E. (1984) The fluids in salt. *American Mineralogist* **69,** 413-439.

Roedder, E. and Belkin, H. E. (1980) Thermal gradient migration of fluid inclusions in single crystals of salt from the Waste Isolation Pilot Plant Site (WIPP). *In:* C.J.M. Northrup, J. (ed.) *Scientific Basis for Nuclear Waste Management, proceedings of the International Symposium on the Scientific Basis for Nuclear Waste Management, sponsored by the Materials Research Society.* **2**. New York, NY: Plenum Press. 453-464.

Roselle, G. T. (2009) *Iron and lead corrosion in WIPP-relevant conditions: Six month results. Milestone report, October 7, 2009*. ERMS 546084, Carlsbad, NM: Sandia National Laboratories.

Roselle, G. T. (2010) *Iron and lead corrosion in WIPP-relevant conditions: 12 Month Results. Milestone report, October 14, 2010*. ERMS 554383, Carlsbad, NM: Sandia National Laboratories.

Roselle, G. T. (2011a) *Iron and lead corrosion in WIPP-relevant conditions: 18 Month Results. Milestone report, January 5, 2011*. ERMS 554715, Carlsbad, NM: Sandia National Laboratories.

Roselle, G. T. (2011b) *Iron and lead corrosion in WIPP-relevant conditions: 24 Month Results. Milestone report, May 3, 2011*. ERMS 555426, Carlsbad, NM: Sandia National Laboratories.

Rothfuchs, T. (1986) In situ investigations on the impact of heat production and gamma radiation with regard to high-level radioactive waste disposal in rock salt formations. *Nuclear Technology* **58,** 256-270.

Rothfuchs, T., Wieczorek, K., Feddersen, H. K., Staupendahl, G., Coyle, A. J., Kalia, H. and Eckert, J. (1988) *Brine migration test: Asse salt mine, Federal Republic of Germany. Final report*. GSF-Bericht 6/88, Munich, Germany: Society for Radiation and Environmental Research.

Russell, S., Garisto, F., Gierszewski, P., Hobbs, M., Jensen, M., Kempe, T., Lam, T., Maak, P., Simmons, G., Vorauer, A. and Wei, K. (2007) *Technical Research and Development Program for Long-term Management of Canada's Used Nuclear Fuel - Annual Report 2006*. Report No: 06819-REP-01200-10163-R00, Toronto: Ontario Power Generation.

Salas, J., Gimeno, M. J., Auqué, L., Molinero, J., Gómez, J. and Juárez, I. (2010) *SR-Site–hydrogeochemical evolution of the Forsmark site*. SKB TR-10-58, Stockholm: Svensk Karnbranslehantering AB.

Sandström, B. and Tullborg, E.-L. (2006) *Forsmark site investigation. Mineralogy, geochemistry, porosity and redox capacity of altered rock adjacent to fractures*. SKB P-06-209, Stockholm: Svensk Kärnbränslehantering AB.

Sapiie, B. and Driscoll, M. J. (2009) *A review of geology-related aspects of deep borehole disposal of nuclear wastes*. MIT-NFC-TR-109, Cambridge: Massachusetts Institute of Technology.

Savage, D., Watson, C., Benbow, S. and Wilson, J. (2010) Modelling iron-bentonite interactions. *Applied Clay Science* **47**(1-2)**,** 91-98.

Schlegel, M. L., Bataillon, C., Benhamida, K., Blanc, C., Menut, D. and Lacour, J. L. (2008) Metal corrosion and argillite transformation at the water-saturated, high-temperature iron-clay interface: A microscopic-scale study. *Applied Geochemistry* **23**(9)**,** 2619-2633.

Schlich, M. and Jockwer, N. (1985) Simulation of water transport in heated rock salt. *In:* Apted, M. J. and Westerman, R. E. (eds.) *Scientific Basis for Nuclear Waste Management IX, International Symposium.* **50**. Pittsburgh, PA: Materials Research Society. 577-585.

Schutz, R. W. and Thomas, D. E. (1987) *Corrosion of titanium and titanium alloys.* Materials Park, OH: ASM International.

Schutz, R. W. and Hall, J. A. (1988) *Optimization of mechanical/corrosion properties of Ti Code 12 plate and sheet part II: Thermomechanical processing effects (Stage II final report)*. SAND87-7171, Albuquerque, NM: Sandia National Laboratories.

Schutz, R. W. (2005) *Corrosion of titanium and titanium alloys.* Materials Park, OH: ASM International.

Schwarzkopf, W., Smailos, E. and Köster, R. (1989) In-situ corrosion studies on cast steel for a high-level waste packaging in a rock salt repository. *In:* Lutze, W. and Ewing, R. C. (eds.) *Scientific Basis for Nuclear Waste Management XII.* **127**. Pittsburgh, PA: Materials Research Society. 411-418.

Schwarzkopf, W., Smailos, E. and Köster, R. (1992) In-situ corrosion studies on cast steel high-level waste containers plated with titanium/nickel-alloys. *In:* Sombret, C. G. (ed.) *Scientific Basis for Nuclear Waste Management XV*. **257**. Pittsburgh, PA: Materials Research Society. 423-430.

Seidensticker, R. G. (1966) Comment on paper by P. Hoekstra, T.E. Osterkamp, and W.F. Weeks, The migration of liquid nclusions in single ice crystals. *Journal of Geophysical Research* **71**(8)**,** 2180-2181.

Selnert, E., Byegård, J. and Widestrand, H. (2008) *Forsmark site investigation: Laboratory measurements within the site investigation programme for the transport properties of the rock. Final report*. SKB P-07-139, Stockholm: Svensk Kärnbränslehantering AB.

Shan, X. and Payer, J. (2007) Comparison of ceramic and polymer crevice formers on the crevice corrosion behavior of Ni-Cr-Mo Alloy C-22. Paper No. 07582. *In: CORROSION/2007*, Houston, TX. NACE International.

Shirai, K., Tani, J., Arai, T., Wataru, M., Takeda, H. and Saegusa, T. (2011) SCC evaluation test of a multi-purpose canister. 10-14 April. *In: 13th International High-Level Radioactive Waste Management Conference (IHLRWMC)*, 824-831. American Nuclear Society.

Simpson, J. P. and Schenk, R. (1987) Hydrogen evolution from corrosion of pure copper. *Corrosion Science* **27**(12)**,** 1365-1370.

Simpson, J. P. and Schenk, R. (1989) Corrosion induced hydrogen evolution on high level waste overpack materials in synthetic groundwaters and chloride solutions. *In:* Lutze, W. and Ewing, R. C. (eds.) *Scientific Basis for Nuclear Waste Management XII*. **127**. Pittsburgh, PA: Materials Research Society. 389-396.

SKB (1993) *Project on alternative systems study (PASS) final report*. SKB 93-04, Stockholm: Svensk Karnbranslehantering AB.

SKB (2006a) *Long-term safety for KBS-3 repositories at Forsmark and Laxemar – a first evaluation. Main report of the SR-Can project*. SKB TR-06-09, Stockholm: Svensk Karnbranslehantering AB.

SKB (2006b) *Long-term safety for KBS-3 repositories at Forsmark and Laxemar – a first evaluation. Main Report of the SR-Can project.*, Stockholm: Swedish Nuclear Fuel and Waste Management Co. Co., S. N. F. a. W. M.

SKB (2010b) *Design, production and initial state of the canister*. SKB TR-10-14, Stockholm: Svensk Karnbranslehantering AB.

SKB (2011) *Long-term safety for the final repository for spent nuclear fuel at Forsmark: Main report of the SR-Site project. 3 Volumes*. SKB TR-11-01, Stockholm: Svensk Karnbranslehantering AB.

Smailos, E., Schwarzkopf, W., Köster, R., Fiehn, B. and Halm, G. (1990) *Corrosion testing of selected packaging materials for disposal of high-level waste glass in rock salt formations*. KfK-4723, Karlsruhe, Germany: Forschungszentrum Karlsruhe, Institut für Nukleare Entsorgungstechnik.

Smailos, E., Schwarzkopf, W., Gago, J. A. and Azkarate, I. (1992a) *Corrosion studies on selected packaging materials for disposal of heat-generating radioactive wastes in rock-salt formations*. KfK 5011, Karlsruhe, Germany: Forschungszentrum Karlsruhe, Institut für Nukleare Entsorgungstechnik.

Smailos, E. (1993) Corrosion of high-level waste packaging materials in disposal relevant brines. *Nuclear Technology* **104,** 343-350.

Smailos, E., Fiehn, B., Gago, J. A. and Azkarate, I. (1993) *General corrosion and stress corrosion cracking studies on carbon steels for application in nuclear waste disposal containers*. KfK-5166, Karlsruhe, Germany: Forschungszentrum Karlsruhe, Institut für Nukleare Entsorgungstechnik.

Smailos, E., Fiehn, B., Gago, J. A. and Azkarate, I. (1994a) *Corrosion studies on selected metallic materials for application in nuclear waste disposal containers*. KfK-5309, Karlsruhe, Germany: Forschungszentrum Karlsruhe, Institut für Nukleare Entsorgungstechnik.

Smailos, E., Gago, J. A., Azkarate, I. and Fiehn, B. (1994b) *Corrosion studies on selected packaging materials for disposal of heat-generating radioactive wastes in rock-salt formations, Final report to the EC for the period 1991-1994 (EC Contract No. FI2W CT90-0030)*. Report FZKA 5587, Karlsruhe, Germany: Forschungszentrum Karlsruhe, Institut für Nukleare Entsorgungstechnik.

Smailos, E., Schwarzkopf, W. and Köster, R. (1998a) *Corrosion behaviour of selected high-level waste packaging materials under gamma irradiation and in-situ disposal conditions in rock salt*. KfK-4426, Karlsruhe, Germany: Forschungszentrum Karlsruhe, Institut für Nukleare Entsorgungstechnik.

Smailos, E., Martinez-Esparza, A., Kursten, B., Marx, G. and Azkarate, I. (1999) *Corrosion evaluation of metallic materials for long-lived HLW/spent fuel disposal containers, Final report to the EC for the period 1996-1998, (EC Contract No. FI4W-CT95-0002)*. Report FZKA 6285, Karlsruhe, Germany: Forschungszentrum Karlsruhe, Institut für Nukleare Entsorgungstechnik.

Smailos, E. (2002) *Influence of gamma radiation on the corrosion of carbon steel, heat generating nuclear waste packages in salt brines*. IAEA-TECDOC-1316, pp. 131-140, Vienna, Austria: International Atomic Energy Agency.

Smailos, E., Cuñado, M. A., Azkarate, I., Kursten, B. and Marx, G. (2002) *Long-term performance of candidate materials for HLW/spent fuel disposal containers*. FZKA 6706, Karlsruhe, Germany: Forschungszentrum Karlsruhe, Institut für Nukleare Entsorgungstechnik.

Smailos, E., Schild, D. and Gompper, K. (1998b) Corrosion of Ti 99.8-Pd under gamma irradiation in MgCl2-rich brine. *In:* McKinley, I. G. and McCombie, C. (eds.) *Scientific Basis for Nuclear Waste Management XXI.* **506**. Warrendale, PA: Materials Research Society. 477-484.

Smailos, E., Schwarzkopf, W., Kienzler, B. and Köster, R. (1992b) Corrosion of carbon-steel containers for heat-generating nuclear waste in brine environments relevant for a rock-salt repository. *In:* Sombret, C. G. (ed.) *Scientific Basis for Nuclear Waste Management XV.* **257**. Pittsburgh, PA: Materials Research Society. 399-406.

Smart, N. R., Blackwood, D. J. and Werme, L. (2002a) Anaerobic corrosion of carbon steel and cast iron in artificial groundwaters: Part 1—electrochemical aspects. *Corrosion* **58**(7)**,** 547-559.

Smart, N. R., Blackwood, D. J. and Werme, L. (2002b) Anaerobic corrosion of carbon steel and cast iron in artificial groundwaters: Part 2—Gas Generation. *Corrosion* **58**(8)**,** 627-637.

Smart, N. R., Blackwood, D. J., Marsh, G. P., Naish, C. C., O'Brien, T. M., Rance, A. P. and Thomas, M. I. (2004) *The anaerobic corrosion of carbon and stainless steels in simulated cementitious repository*

environments: A summary review of NIREX research. AEAT/ERRA-0313, Harwell, England: AEA Technology.

Snider, A. C. (2003) *Verification of the definition of generic weep brine and the development of a recipe for this brine. Analysis report, April 8, 2003*. ERMS 527505, Carlsbad, NM: Sandia National Laboratories.

SNL (2006) *Technical work plan: Experimental work to support evaluation of dust-deliquescence-induced screening localized corrosion of Alloy 22*. TWP-MGR-PA-000040, Las Vegas, NV: Sandia National Laboratories.

SNL (2007a) *General corrosion and localized corrosion of the drip shield*. ANL-EBS-MD-000004 Rev 02 AD 01 Las Vegas, NV: Sandia National Laboratories.

SNL (2007b) *General and localized corrosion of the waste package outer barrier*. ANL-EBS-MD-000003, Albuquerque, NM: Sandia National Laboratories.

SNL (2007c) *Stress corrosion cracking of waste package outer barrier and drip shield materials*. ANL-EBS-MD-000033 Rev 0 Las Vegas, NV: Sandia National Laboratories.

SNL (2008a) *Cleaning corrosion resistant metals using a hydrochloric acid bath*. TST-PRO-T-008, Albuquerque, NM: Sandia National Laboratories.

SNL (2008b) *Technical work plan: General and localized corrosion testing of waste package and drip shield material*. TWP-WIS-MD-000022, Albuquerque, NM: Sandia National Laboratories.

SNL (2008c) *Multiscale Thermohydrologic Model*. ANL-EBS-MD-000049 Rev 03, Albuquerque, NM: Sandia National Laboratories.

SNL (2009) *General corrosion and localized corrosion of waste package outer barrier*. ANL-EBS-MD-000003 Rev 03 AD 01 Las Vegas, NV: Sandia National Laboratories.

SNL (2010) *Determination of seepage chemistry predicted by TSPA and P&CE and relationship to corrosion testing*. IAR-EBS-PA-000002, Albuquerque, NM: Sandia National Laboratories.

Sorensen, N. R. and Ruppen, J. R. (1985) The environmental cracking of Ticode-12 in aqueous chloride environments. *Corrosion* **41**(10)**,** 560-569.

Stenhouse, M., Apted, M. and Zhou, W. (2010) *EPRI review of geologic disposal for used fuel and high level radioactive waste Volume III — Review of national repository programs*. EPRI 1021614, Palo Alto, CA: Electric Power Research Institute.

StoreFUEL (2011) *StoreFUEL* **12**(153).

Swedish National Council for Nuclear Waste (2009) *Mechanisms of copper corrosion in aqueous environments*. Report 2009:4, Stockholm: Swedish Government Inquiries.

Swift, P. N., Arnold, B. W., Brady, P. V., Freeze, G., Hadgu, T., Lee, J. H. and Wang, Y. (2011) Preliminary Performance Assessment for Deep Borehole HLW Disposal. *Radwaste Solutions* **18**(3)**,** 60-65.

Szakalos, P., Hultquist, G. and Wikmark, G. (2007) Corrosion of copper by water. *Electrochemical and Solid State Letters* **10**(11)**,** C63-C67.

Szakalos, P., Hultquist, G. and Wikmark, G. (2008) Response to the comment on "Corrosion of copper by water" Electrochem. Solid-State Lett., 10, C63, (2007). *Electrochemical and Solid State Letters* **11**(4)**,** S2-S2.

Tani, J., Mayuzumi, M. and Hara, N. (2008) Stress corrosion cracking of stainless steel canister for concrete storage of spent fuel. *Journal of Nuclear Materials* **379,** 42-47.

Tani, J. I., Mayuzurmi, M. and Hara, N. (2009) Initiation and propagation of stress corrosion cracking of stainless steel canister for concrete cask storage of spent nuclear fuel. *Corrosion* **65**(3)**,** 187-194.

Taniguchi, N. and Kawasaki, M. (2008) Influence of sulfide concentration on the corrosion behavior of pure copper in synthetic seawater. *Journal of Nuclear Materials* **379**(1-3)**,** 154-161.

Telander, M. R. and Westerman, R. E. (1993) *Hydrogen generation by metal corrosion in simulated Waste Isolation Pilot Plant environments*. SAND92-7347, Albuquerque, NM: Sandia National Laboratories.

Telander, M. R. and Westerman, R. E. (1997) *Hydrogen generation by metal corrosion in simulated Waste Isolation Pilot Plant environments*. SAND96-2538, Albuquerque, NM: Sandia National Laboratories.

Thornton, E. C. and Seyfried, W. E. J. (1985) Sediment–sea-water interaction at 200 and 300 °C, 500 bars pressure: The role of sediment composition in diagenesis and low grade metamorphism of marine clay. *Geological Society of America Bulletin* **96**(10)**,** 1287-1295.

Transnuclear (2001) *Final safety analysis report for the standardized NUHOMS horizontal modular storage system for irradiated nuclear fuel*. NUH-003 Revision 6, Fremont, CA: Transnuclear West.

Turchi, P. E. A. (2001) *Delivery of property diagram (Phase fraction versus temperature) of Alloy 22 at its nominal composition. Memorandum from P.E.A. Turchi (BSC) to file, May 21, 2001, PROJ.05/01.051, with enclosure*. BSC.

Tyler, L. D., Matalucci, R. V., Molecke, M. A., Munson, D. E., Nowak, E. J. and Stormont, J. C. (1988) *Summary report for the WIPP technology development program for isolation of radioactive waste*. SAND88-0844, Albuquerque, NM: Sandia National Laboratories.

Van Humbeeck, H., Bastiaens, W., De Bock, C. and Van Cotthem, A. (2008) Experimental programme to demonstrate the viability of the supercontainer concept for HLW. *In: Underground Disposal Unit Design & Emplacement Processes for a Deep Geological Repository*, Prague. 4.11-14.10.

Volckaert, G., Bernier, F., Sillen, X., Van Geet, M., Mayor, J.-C., Göbel, I., Blümling, P., Frieg, B. and Su, K. (2004) Similarities and Differences in the Behaviour of Plastic and Indurated Clays. *In:* Davies, C., ed. *Proceedings of the Sixth European Commission Conference on the Management and Disposal of Radioactive Waste, Euradwaste '04*, 281-291. Luxembourg: European Commission.

Volzke, H. and Wolff, D. (2011) Safety aspects of long term dry interim cask storage of spent fuel in Germany. 10-14 April. *In: 13th International High-Level Radioactive Waste Management Conference (IHLRWMC)*, 712-719. American Nuclear Society.

Wall, F. D. and Brown, N. R. (2009) *Long-term corrosion testing plan*. SAND2009-0923:

Wall, N. A. and Enos, D. (2006b) *Iron and lead orrosion in WIPP-relevant conditions, TP 06 02, rev. 1. April 24, 2006*. ERMS 543238, Carlsbad, NM: Sandia National Laboratories.

Wang, Z. X., Moore, R. C., Felmy, A. R., Mason, M. J. and Kukkadapu, R. K. (2001) A study of the corrosion products of mild steel in high ionic strength brines. *Waste Management* **21,** 335-341.

Wenk, H. R., Voltolini, M., Mazurek, M., Van Loon, L. R. and Vinsot, A. (2008) Preferred orientations and anisotropy in shales: Callovo-Oxfordian shale (France) and Opalinus clay (Switzerland). *Clays and Clay Minerals* **56**(3)**,** 285-306.

Werme, L. O. and Korzhavyi, P. A. (2010) Comment on Hultquist et al. "Water Corrodes Copper" Catal. Lett. 132 (2009) 311. *Catalysis Letters* **135**(3-4)**,** 165-166.

Westerman, R. E. (1980) *Investigation of metallic, ceramic, and polymeric materials for engineered barrier applications in nuclear waste packages*. PNL-3484, Richland, WA: Pacific Northwest National Laboratory.

Westerman, R. E., Pitman, S. G. and Nelson, J. L. (1982) *General corrosion, irradiation corrosion, and environmental-mechanical evaluation of nuclear waste package structural barrier materials*. PNL-4364, Richland, WA: Pacific Northwest National Laboratory.

Westerman, R. E., Haberman, J. H., Pitman, S. G., Pulsipher, B. A. and Sigalla, L. A. (1986) *Annual report—FY 1984: Corrosion and environmental-mechanical characterization of iron-base nuclear waste package structural barrier materials*. PNL-5426, Richland, WA: Pacific Northwest National Laboratory.

Westerman, R. E., Haberman, J. H., Pitman, S. G., Pool, K. H., Rhoads, K. C. and Telander, M. R. (1988) *Salt repository project. Annual report–FY 1986. Corrosion behavior of A216 grade WCA mild steel and titanium grade 12 alloy in hydrothermal brines*. PNL/SRP-6221, Richland, WA: Pacific Northwest National Laboratory.

Westerman, R. E., Nelson, J. L., Pitman, S. G., Kuhn, W. L., Basham, S. J. and Moak, D. P. (1984) Evaluation of iron-base materials for waste package containers in a salt repository. *In:* McVay, G. L. (ed.) *Scientific Basis for Nuclear Waste Management VII, Symposium.* **26**. New York, NY: North Holland: Materials Research Society. 427-436.

Whitman, W. G. (1926) Elimination of salt from sea-water ice. *American Journal of Science* **11**(62)**,** 126-132.

Wilcox, W. L. (1969) Correspondence — anomalous gas-liquid inclusion movement. *Industrial and Engineering Chemistry* **61**(3)**,** 76-77.

Wilson, J., Cressey, G., Cressey, B., Cuadros, J., Ragnarsdottir, K. V., Savage, D. and Shibata, M. (2006a) The effect of iron on montmorillonite stability. (II) Experimental investigation. *Geochimica Et Cosmochimica Acta* **70**(2)**,** 323-336.

Wilson, J., Savage, D., Cuadros, J., Shibata, M. and Ragnarsdottir, K. V. (2006b) The effect of iron on montmorillonite stability. (I) Background and thermodynamic considerations. *Geochimica Et Cosmochimica Acta* **70**(2)**,** 306-322.

Winsley, R. J., Smart, N. R., Rance, A. P., Fennell, P. A. H., Reddy, B. and Kursten, B. (2011) Further studies on the effect of irradiation on the corrosion of carbon steel in alkaline media. *Corrosion Engineering Science and Technology* **46**(2)**,** 111-116.

Yagnik, S. K. (1983) Interfacial stability of migrating brine inclusions in alkali halide single crystals supporting a temperature gradient. *Journal of Crystal Growth* **62**(3)**,** 612-626.

Yih, C.-S. (1986) Movement of liquid inclusions in soluble solids: An inverse Stokes' Law. *Physics of Fluids* **29**(9)**,** 2785-2787.

Young, N. O., Goldstein, J. S. and Block, M. J. (1959) The motion of bubbles in a vertical temperature gradient. *Journal of Fluid Mechanics* **6**(3)**,** 350-356.

Appendix A

Preliminary Test Plan for Future Work

A-1. Preliminary Test Plan for Future work.

A-1.1   Introduction

The work planned for FY12 consists of the continuation and wrap-up of ongoing work initiated in previous years, as well as the initiation of new tasks aimed at addressing knowledge gaps identified in several gap analyses which were completed in FY11. The experimental work may be broadly classified as being either for dry storage conditions, repository conditions, or universally applicable. The work will be done both at Los Alamos National Laboratories and at Sandia National Laboratories, and different test plans will be written for the work at the different locations. These test plans will be completed as a L4 milestone on January 31, 2012.

A-1.2   New Experimental studies

A-1.2.1   Thermal Sensitization of Borated Stainless Steel (Storage and Repository)

Borated stainless steel (BSS) was one of the candidate materials to be used as a neutron moderator as the basket material within the waste package design for the proposed Yucca Mountain repository. One of the concerns with this material is that thermal sensitization of the steel would result in the precipitation of boron carbides, depleting the matrix phase of boron. If these carbides were electrochemically active, they may be removed due to corrosion, eliminating the boron thereby inhibiting the ability of the basket material to meet the criticality requirements of the waste package design.

Prior studies have been performed in an effort to determine if this effect was in fact a legitimate concern. However, the containment vessel in which the experiments were performed was a glass which itself was rich in boron. As a result, when the test was run, boron was leached from the glass vessel, masking any contribution from the dissolution of the borated stainless steel. Thus, there is a need to re-run these tests, this time taking precautions to prevent the accumulation of boron within the electrolyte due to sources other than the basket material.

Work will be performed on powder metallurgy borated stainless steel to determine if it is subject to sensitization (as is 304 Stainless Steel) under long term storage and/or disposal conditions. 304 SS and 304 BSS will be solutionized, and then subjected to range of temperatures and durations to establish time, temperature, transition (TTT) curves in an effort to determine the conditions under which sensitization may take place. Once thermally processed, samples will be characterized using electron microscopy and microindentation to determine the tendency for sensitization to occur under different thermal histories, as well as to quantify the extent of sensitization which might be anticipated following thermal processing.

Sensitized samples and as received material will be studied for corrosion resistance under in-package conditions, using long-term immersion testing as well as potentiodynamic polarization experiments. The fate of the boron during corrosion will be determined under accelerated corrosion testing.

The results of this task will benefit long term storage solutions as this will indicate if the BSS would have to be replaced prior to disposal, or if an alternate material (such as Ni-Gd) should be pursued. Disposal efforts will benefit due to reduced corrosion rate uncertainty and potential risk mitigation efforts.

This work will be done at Los Alamos National Laboratories, in accordance with the Fuel Cycle Technologies (FCT) Quality Assurance Program Document, the Los Alamos National Laboratory FCT Quality Assurance Program Plan, and the Los Alamos Quality Assurance Program (SD-330).

Summary:

Planned Experiment	Experimental Measurements	Additional Analyses
Thermal processing of 304BSS material	Phase structure	Combine experimental results from a variety of isothermal heat treatments to construct TTT curves
Thermal processing of 304 BSS using typical weld thermal profiles	Phase structure, microhardness	Combine results from multiple experiments to define thermal profiles likely to result in sensitization
Electrochemical testing of sensitized 304BSS	Potentiodynamic polarization curves, potentiostatic polarization, solution chemistry analyses	Combine experimental results to define the tendency for sensitization to result in potential boron loss from the stainless steel, and the magnitude of that loss as a function of environmental conditions

A-1.2.2   Copper Corrosion Under Reducing Conditions (Repository)

For repository designs in which the in-drift environment is anticipated to be saturated and reducing in nature (i.e., anoxic conditions), and the concentration of sulfide within the ground water is sufficiently low, copper is being considered as a potential material for the waste package outer barrier. Due to the thermodynamic stability of metallic copper under reducing conditions, it is anticipated that the dissolution rate of the waste package would become vanishingly small once the dissolved oxygen within the groundwater had been depleted.

Recently, there have been a number of researchers who have asserted that despite the traditional understanding of copper stability in deaerated water, that appreciable dissolution of the copper could still take place. These statements are based upon indirect measurements of what the researchers believe is active corrosion of the copper. There are two primary statements/observations which have been made. The first is the indirect measurement of gaseous hydrogen within the atmosphere over the copper (inundated in electrolyte). The theory is that the source of the hydrogen which they have observed is due to cathodic reduction of water at the copper surface. This cathodic reaction is in turn believed to support anodic dissolution of the copper. The second observation/theory is that there is a copper-oxy-hydroxide formed on the metal surface as a corrosion product. However, all attempts to experimentally observe this phase have failed. (Swedish National Council for Nuclear Waste 2009)

It is well known that if dissolved oxygen, or another cathodic reactant, such as sulfide, is present, that copper corrosion will take place. It is believed that neither of these two species is present in the experiments which generated the aforementioned results.

As a result, there is a significant experimental need to resolve this concern and to determine if copper is indeed an inappropriate choice as a waste package material as these researchers have asserted. A series of experimental studies will be performed in FY12 in an effort to meet these needs.

Experimental work will explore several potential artifacts which may explain the literature results as well as explore the corrosion behavior of copper in relevant aqueous environments.

1. Development and identification of potential corrosion products formed on a copper surface under anoxic conditions

2. Alternate production pathways for gaseous hydrogen observed in work of Hultquist et al. (2009; 2011) such as water reduction at the humid air/palladium foil interface

This work will be carried out at Sandia National Laboratories in accordance with the FCT Quality Assurance Program Document.

Summary:

Planned Experiment	Experimental Measurements	Additional Analyses
Potentiodynamic polarization in anoxic brines	Anodic and cathodic reaction rates as a function of potential	Evaluate results to determine the magnitude of anodic dissolution which might take place as a function of time
Potentiostatic polarization in anoxic brines	Reaction rate as a function of time; Cathodic reduction curves upon completion of experiment	Establish long term corrosion rates possible under anoxic conditions in relevant brines, then combine with cathodic reduction to aid with phase identification and corrosion product quantity.
Devanathan-Stachurski permeation measurements	Hydrogen permeation flux as a function of environmental conditions (i.e., T, RH) on the surface of a palladium foil	Evaluate steady state permeation flux and determine potential gas concentrations which might be achieved within a volume on the exit surface, then compare to results reported in the literature where anodic dissolution of the copper is reported as the source

A-1.2.3   Expansion/Continuation of Existing Tests

In general, continuation of existing tests will not require a new test plan. Moreover, small changes in experimental procedure or scope can be documented in experimental notebooks, and do not require an additional test plan. However, significant changes in planned work do require a new test plan. As noted below, both of the existing work scopes will be modified significantly to address potential corrosion of materials under long-term interim storage conditions.

Immersion testing of Alloy 22 (repository) and stainless steels (dry storage)

Numerous concerns exist as to the validity of the corrosion experiments performed in the long term corrosion test facility at LLNL used to determine both the general corrosion rate as well as the temperature dependence of the general corrosion rate, when exposed to repository relevant brines. In an effort to validate the results of that experimental program, a series of exposure tests were initiated in late FY10. In these tests, Alloy 22 samples were prepared and then placed in solutions identified in the General and Localized Corrosion of the Waste Package Outer Barrier AMR (SNL 2007b). These environments included 0.6M NaCl, simulated acidified water (SAW), and simulated concentrated water (SCW).

Specimens were to be removed after 3, 9, 18, and 24 months of exposure. The 3 month samples were added to the solution when the 9 month samples were removed. The 18 month samples are being removed at the beginning of FY12Q1, and the 24 month samples will be removed at the beginning of FY12Q3. Upon removal of each sample set, the total weight loss observed is determined via the methodologies defined in TST-PRO-T-008 (SNL 2008a). Once the 24 month coupons have been evaluated, this experimental program will then be concluded, and the results documented. A final report will be issued at the end of FY12Q3.

Upon completion of the Alloy 22 studies, additional work will be initiated to evaluate the performance of materials of relevance to dry storage (304SS, 316SS, etc.) to brine chemistries appropriate for either inland or coastal storage sites. The goal of these studies is to establish a reliable long term general corrosion rate as a function of temperature under conditions representative of dry storage such that predictive models can be utilized to accurately assess the corrosion performance of various container designs.

Summary:

Planned Experiment	Experimental Measurements	Additional Analyses
Complete exposure testing of Alloy 22 in SAW, SCW and 0.5M NaCl	Mass change as a function of time and temperature in each brine	Determine activation energy for the corrosion of Alloy 22 in each brine
Exposure testing of stainless steels of relevance to dry storage	Mass change and basic electrochemical properties in brines of relevance to storage sites in marine/coastal regions	Determine corrosion rate as a function of time and temperature for relevant materials

Dust deliquescence testing (repository and dry storage)

Any waste package or storage container which is exposed to the atmosphere will have particulates (i.e., dust) carried by the atmosphere deposited on its surface. A portion of most atmospheric dusts consists of various soluble salts. It has been suggested by several researchers that these salts may combine to form deliquescent brines on the surface of a waste package at temperatures well above the boiling point of water, and further, that these brines might be corrosive depending on the material used to construct the package. Other researchers have suggested that for highly corrosion resistant/passive materials, several factors will prevent extensive localized corrosion due to deliquescence, including electrochemical limitations (e.g., insufficient cathode reaction area) and physical (e.g., limited concentration of brine coupled with consumption or sequestration of aggressive species in the corrosion product).

In an effort to determine if there is indeed a potential for deliquescent brines to result in localized corrosion, a series of experiments have been (and continue to be) performed. Materials of interest have been decorated with thin layers of salt in the presence of an occluded geometry in an effort to establish if localized corrosion (i.e., crevice corrosion) could initiate and propagate under such conditions. In these experiments, no inert species were added, and as such physical sequestration of the brine by the dust layer due to capillary forces have been eliminated, allowing all of the material deposited on the metal surface to participate in the corrosion reaction.

The chemical composition of the brines which can form are a function of temperature, as well as the available constituent materials. At very high temperatures, brines must be very nitrate rich, whereas at lower temperatures, the composition can be dominated by other species, such as chloride. In terms of the corrosiveness of the brine, both the chemistry (e.g., concentration of aggressive species) and the exposure temperature have a strong impact on corrosion processes.

While experiments performed to date on Alloy 22 and other nickel based alloys have demonstrated that, consistent with the modeling performed to date, that localized corrosion cannot be supported, either in terms of initiation or propagation, with such a small volume of electrolyte. This was demonstrated to be true for multicomponent nitrate rich brines as well as chloride based brines at lower temperatures.

In addition, a series of experiments were performed on a more susceptible stainless steel, SS303 (a free-machining stainless steel which has an elevated sulfur concentration). In this case, localized corrosion was able to initiate and propagate into the material. This provides a definite material system which can be used to pursue experiments which could be used to bolster the argument that localized corrosion, if it were to initiate, would stifle due to consumption of the reactants.

In FY12, additional work is will be conducted to determine if the extent of attack is a function of the quantity of brine present on the metal surface.

1. 303 and 304SS samples have been loaded with the NaCl:KCl salt mixture at 50, 100, and 200 $\mu g\ cm^{-2}$ and placed again in an environment with a dewpoint of 94.5°C and a system temperature of 101°C. Upon completion of the exposure period (100 days, will complete in early FY12Q1), samples will be

evaluated and it will be determined if the degree of attack is indeed a function of the quantity of reactant present at the onset of the experiment.

2. Once acquired, data on the degree of attack as a function of contamination level will be combined with various literature models in order to develop a more technically sound explanation as to whether or not localized corrosion can take place at a sufficiently large magnitude so as to threaten the ability of a waste package or storage container to maintain waste confinement.

Summary:

Planned Experiment	Experimental Measurements	Additional Analyses
Localized corrosion initiation tests on 304 and 303SS as a function of contaminant loading	Extent of damage as a function of contaminant quantity and test conditions (temperature and dewpoint)	Evaluate tendency for localized corrosion to stifle once initiated on a susceptible material in the presence of a very limited quantity of reactant. Evaluate corrosion product to determine, if possible, manner in which chloride is sequestered.
Localized corrosion initiation tests for metal to metal crevices in presence of limited reactant	Extent of damage as a function of material combination	Establish resilience of metal seals presently in use for dry storage applications under relevant environmental conditions – compare potential extent of attack with the magnitude of damage required to breach a seal.